Université Pierre et Marie Curie

PARIS VI

Thèse de Doctorat

Présenté par Hadrien Demagny

2014

Ecole doctorale : Complexité du Vivant

Pour obtenir le titre de Docteur de l'Université PARIS VI

Titre :

Convergence des Voies de Signalisation Wnt, FGF et TGF-beta au Niveau des Facteurs de Transcription Smad1 et Smad4

Directeurs de thèse : Dr. Frédéric Rosa et Dr. Edward M. De Robertis

Je dédie cette thèse à mes deux fils, Leonardo et Alessandro, futurs experts en embryologie.

Remerciements:

Je tiens avant tout à remercier Frédéric Rosa sans qui il ne m'eut été possible de rejoindre le laboratoire d'Eddy De Robertis à UCLA. Pour son généreux soutien je lui suis très reconnaissant.

Eddy est passionné et passionne. My deepest gratitude is to my mentor Eddy De Robertis for his guidance, care, trust and friendship. I will never forget his passion and enthusiasm for Science. I would like to thank him for teaching me that a paper is first appreciated by the eyes and that the the background color for an *in situ hybridization* really *does* matter.

I also would like to thank my wife, Dasa, for her unconditional love, tender dedication, constant support and generosity that complete me and keep me afloat in the bad days. During my thesis, she gave birth to two adorable little boys who bring a new dimension to my life and remind me of the truly important things.

During all these years in Los Angeles, the following peole, among others, shared with me their scientific knowledge, experience, friendship and so much more. I would like to express my gratiture to Edward Eivers, Lucho Fuentealba, Veronika Sander, Radek, Philipp, Pancho, Fabio, Hyunjoon, Diego, Gabrielle, Yi, Yuki, Doug, Lise, Tatsuya, Brian, Josh and many more.

Sommaire:

Résumé 1

Summary 3

CHAPTER 1 INTRODUCTION 4

1.1 The Transforming Growth Factor-beta signaling pathway 8

1.1.1 Overview of the TGF-beta pathway 8

1.1.2 TGF-beta Ligands and Receptors 11

1.2 The Smad transcription factors 13

1.2.1 The Smad family of transcription factors 13

1.2.2 Structure of the Smad proteins 16

1.2.3 Activation of R-Smads 17

1.2.4 Dephosphorylation of Smad C-terminal motifs by phosphatases 19

1.2.5 Proteasomal degradation of Smad proteins 21

1.2.4 R-Smads oligomerization with Smad4 25

1.2.5 Smad nucleocytoplasmic shuttling 27

1.2.6 DNA recognition by Smad proteins 30

1.2.7 Negative regulation of R-Smads through linker phosphorylation 31

1.3 The canonical Wnt signaling pathway 33

1.3.1 Overview of the Wnt signaling pathway 33

1.3.2 The Wnt pathway regulates proteins stability 37

1.4 The FGF/EGF pathway 37

1.5 Conclusions 40

CHAPTER 2

Smad1/5/8 Linker Phosphorylations Integrate the BMP and Wnt Signaling Pathways 41

2.1 Introduction: embryonic axis formation and the double gradient model 44

2.2 Dorsal–ventral patterning: a morphogenetic gradient of BMP ligands 46

2.3 Intracellular transduction of the BMP signal 48

2.4 Anterior–posterior patterning and Wnt signaling 51

2.5 Regulation of Smad1 via linker phosphorylations downstream of BMP 53

2.5.1 Inhibitory Smad1 linker phosphorylations by MAPK 53

2.5.2 GSK3/Wnt regulates BMP/Smad1 signal termination 56

2.6 Asymmetric inheritance of Smad1 57

2.7 Smad1 signal duration: phenotypic similarities between BMP and Wnt antagonists in the developing embryo 61

2.8 Linker regulation of Drosophila Mad 63

2.8.1 Mad linker phosphorylations: BMP dependent or independent? 64

2.8.2 Phospho-resistant Mad mutants display Wg-like phenotypes 65

2.8.3 Mad and Smad1 are required for segment formation 68

2.8.4 The ancestry of segmentation 69

2.9 Conclusions 72

CHAPTER 3

Phosphorylation of Mad Controls Competition Between Wingless and BMP Signaling 74

3.1 Introduction 78

3.2 Results 81

3.2.1 GSK3 phosphorylation of Mad inhibits both BMP and Wg signaling 81

3.2.2 Mad activates Wg target genes independently of phosphorylation of its C terminus 86

3.2.3 Mad and Medea are required for Wg signal transduction 91
3.2.4 Mad binds to Pangolin in the absence of phosphorylation of its C terminus 95
3.2.5 The Pangolin-Mad-Armadillo complex binds to Tcf DNA binding sites 99
3.3 Discussion 101
3.4 Experimental Procedures 105

CHAPTER 4

The Tumor Suppressor Smad4/DPC4 is Regulated by Phosphorylations that Integrate FGF, Wnt and TGF-beta Signaling 128
4.1 Summary 131
4.2 Introduction 132
4.3 Results 134
4.3.1 Wnt and FGF regulate phosphorylation of Smad4 linker region 134
4.3.2 Wnt/GSK3 regulates the polyubiquitination and degradation of Smad4. 138
4.3.3 Wnt/GSK3 regulates a Smad4 beta-TrCP phosphodegron 143
4.3.4 Wnt and TGF-beta signaling cross-talk via Smad4 146
4.3.5 The Smad4 linker contains a growth-factor regulated transcriptional activation domain 152
4.3.6 Phosphorylation by MAPK/Erk promotes Smad4 peak activity 156
4.3.7 Smad4 regulation by GSK3 determines germ layer specification 160
4.4 Discussion 164
4.4.1 Smad4 activity is regulated by growth factors 164
4.4.2 beta-TrCP binds to the Smad4 phosphodegron 166
4.4.3 Signalling insulation and crosstalk 167
4.4.4 Smad4 linker phosphorylation and tumor suppression 169
4.5 Experimental Procedures 170

CHAPTER 5

CONCLUSIONS AND PERSPECTIVES 195

5.1 One transcription factor, two signaling pathways: Mad as a transducer of Dpp and Wg. 197

5.2 One structure, two functions: Smad4 activity and stability are co-regulated. 202

5.3 Is Smad4 phosphorylated by GSK3 after TGF-beta stimulation? 208

5.4 Is Smad4 degraded in the Wnt destruction complex? 211

5.5 Smad4 and cancer: the loss-of-Smad4 and the progression of cancer 214

5.6 Smad4 degradation by beta-TrCP in pancreatic carcinoma. 216

5.7 Concluding remarks. 222

References: 223

Résumé

Mon projet de thèse s'inscrit dans le cadre des études visant à comprendre comment les cellules embryonnaires intègrent les différents signaux auxquels elles sont exposées pour s'engager dans une voie de différenciation définie. Il est plus particulièrement centré sur le rôle des protéines Smad dans ces processus et peut se diviser en deux axes de recherche.

Le premier a trait au rôle de Mad (Smad1) dans les interactions entre signaux Wnt (Wg) et BMP chez la drosophile. Le travail a d'abord été orienté vers une analyse des phosphorylations de Mad par la kinase GSK3 et leurs éventuelles implication dans la dégradation de ce facteur de transcription par le protéasome. L'hypothèse initiale était que Wnt, en inhibant GSK3, stabilise Mad et prolonge la durée du signal BMP. Nous avons observé que l'expression dans les discs imaginaux d'aile d'une forme mutante de Mad non phosphorylable par GSK3 produit des phénotypes semblables à un gain de fonction Wg, et qu'inversement l'inactivation de Mad phénocopie la perte de fonction de Wg. Cette observation nous a permis de mettre en évidence le rôle de Mad dans la transduction du signal Wg. Nous avons pu démontrer que la forme non phosphorylée par le récepteur BMP se lie au complexe transcriptionnel ß-catenin/dTCF et est requise pour le signal Wnt canonique. La phosphorylation de Mad par le récepteur BMP dirige Mad vers la voie BMP, créant la possibilité d'une compétition entre les deux classes de signaux. Ces données ouvrent des perspectives majeures pour l'analyse de l'intégration des signaux BMP et Wnt au cours du développement.

Le second axe de recherche concerne le facteur de transcription Smad4 qui est requis pour la transduction des signaux TGF-ß et BMP. En arrivant dans le laboratoire d'Eddy De Robertis, j'ai pu identifier trois sites potentiels de phosphorylation par GSK3 dans la séquence primaire de Smad4. Après avoir développé un anticorps phospho-spécifique dirigé contre les deux premiers sites GSK3 de Smad4, j'ai obtenu de nombreux résultats qui nous permettent de comprendre comment la stabilité de Smad4 est contrôlée par les voies Wnt et FGF. En utilisant de nombreuses techniques de biochimie, j'ai pu montrer que Smad4 est

phosphorylé par la kinase Erk, puis par GSK-3 en réponse à un signal FGF. Lorsque Smad4 est doublement phosphorylé, il est reconnu par une E3-ligase, beta-TrCP, ce qui entraine sa polyubiquitination et sa dégradation. La voie Wnt étant capable d'inhiber GSK-3, j'ai pu montrer que Smad4 est stabilisé par des signaux Wnt. Ce résultat était extrêmement important car il ouvrait la possibilité d'une régulation de la voie TGF-beta par la voie Wnt. En effet, en utilisant des techniques de RT-PCR quantitative et de gènes rapporteurs, j'ai pu démontrer que lorsque les cellules reçoivent un signal Wnt, leur sensitivité aux signaux TGF-beta s'en trouve extrêmement augmentée. Ces résultats apportent des réponses moléculaires à différentes expériences d'embryologie durant lesquelles il fût observé que la compétence des cellules embryonnaires aux signaux Nodal est stimulée par la voie Wnt.

Summary

During my PhD I focused on understanding how cells receive and integrate multiple signals from the extracellular milieu. I focused on Smad proteins and my project can be divided into two parts.

My first project was centered on the transcription factor Mad (Smad1) and its requirement for the BMP and Wg pathways. Using a combination of genetic and biochemistry experiments, we showed that Mad is required for Wg signaling both in Tcf reporter gene assays and in vivo in *Drosophila*. We found that the choice for Mad to transduce Dpp or Wg signals is controlled by C-terminal phosphorylations so that Mad binds to Pangolin and participates in Wg target genes transcription only when not phosphorylated at its C-terminus. This results in a competition between Dpp and Wg controlled by the phosphorylation state of Mad.

My second project was focused on the tumor suppressor Smad4. When I first joined the lab, I identified three new potential GSK3 phosphorylation sites in Smad4 primary sequence. I used a home-made phospho-specific antibody to demonstrate that FGF or EGF stimulation trigger Erk-mediated phosphorylation of Smad4 which primes subsequent GSK3 phosphorylations. These phosphorylations regulate a transcription activation domain located in Smad4 linker domain and generate a Wnt-regulated phosphodegron recognized by the E3 ligase beta-TrCP. This mechanism provides a means of integrating distinct pathways which would otherwise remain insulated, allowing cells to sense FGF and Wnt inputs and adapt TGF-beta outcome to their context. It provides a molecular explanation of the long-standing mystery of the "competence modifier" effect of Wnt on Nodal signals discovered 20 years ago.

CHAPTER 1

INTRODUCTION

When I first arrived in the lab, Lucho Fuentealba, a last year graduate student, had just demonstrated that the Wnt and BMP signaling pathways where connected during *Xenopus* development through GSK3 linker phosphorylation of the transcription factor Smad1 (Fuentealba et al., 2007). I was given a project in collaboration with Edward Eivers to demonstrate that the same mechanism also applied during *Drosophila* early development. My mentor, Eddy De Robertis, wanted to know whether this regulation of the BMP pathway by linker phosphorylations had been conserved across evolution. Not only did we find that Mad – the Drosophila homologue of Smad1 – was also phosphorylated by GSK3 in its linker region but we also discovered a yet unrecognized role for Mad as part of the core Wnt transcriptional complex (Chapter 3).

My second project in the De Robertis lab was to solve the long-standing mystery of "competence modifier" during *Xenopus* mesoderm induction. Twenty years ago, D. Melton and R. Moon discovered that *xWnt8* mRNA did not induce mesoderm by itself, yet greatly increased the competence of *Xenopus* ectoderm to respond to mesoderm induction by Activin/TGF-beta (Sokol and Melton, 1992; Moon and Christian, 1992). We hypothesized that a mechanism similar to the GSK3 phosphorylation of Smad1 might also exist for the TGF-beta/Activin transducer Smad2/3. Initial work identified new linker phosphorylation sites in Smad2/3 but none of them seemed to be regulated by the Wnt pathway. Instead, it

quickly became evident that the co-Smad Smad4, with three putative GSK3 phosphorylation sites in its linker region, was the platform of integration that connected the TGF-beta signal to other pathways. Subsequently, I devoted four full years to demonstrate that Smad4 was phosphorylated by GSK3 and that its activity and stability were controlled by the FGF and Wnt pathway (Chapter 4).

I believe that this work will be of great interest to the cell-signaling research community as it shows that three major signaling pathways critical in development and cancer are integrated at the level of Smad4. In this first chapter, I will provide a brief introduction to the TGF-beta, Wnt and FGF pathways. In the Chapter 2, I present a review about cross-talk between Smads, FGF and the Wnt pathway which reflects the level of knowledge that was ours when I joined the lab.

Understanding how cells receive and integrate multiple signals from the extracellular milieu is a major challenge in cell and developmental biology. Nowhere is this more apparent than in a rapidly dividing embryo, which has to undergo cell fate decisions in response to a multitude of growth factor signals over narrow periods of time. Communication systems have evolved with the purpose of controlling the ability of cells to migrate, differentiate, die, and organize into tissues. Growth factors represent one of the most widely used forms of extracellular communication among which the Transforming Growth Factor-beta (TGF-beta) superfamily is the most studied. Members of this group include TGF-beta, Nodals, Activins, Bone Morphogenetic Proteins (BMPs), myostatins and anti-Muellerian hormone (AMH). They control a plethora of biological processes including cell differentiation, proliferation, migration, apoptosis, extracellular matrix (ECM) remodeling and are conserved in species ranging from flies to mammals (Massague, 2000).

1.1 The Transforming Growth Factor-beta signaling pathway

1.1.1 Overview of the TGF-beta pathway

The TGF-beta family of cytokines signal through receptor Serine/Threonine kinases to control a broad spectrum of biological processes such as cell differentiation, proliferation, migration, apoptosis and extracellular matrix remodeling. Despite these diverse roles, the canonical TGF-beta signaling pathway is surprisingly simple. First, the TGF-beta ligand bind on the serine/threonine receptors type I and type II (TbetaRI, TbetaRII) on the surface of the cell. Following ligand binding, type I and type II receptors are brought in close proximately and the constitutively active type II receptor can use its kinase domain to phosphorylate and activate the type I receptor. Once the type I receptor is activated, it can phosphorylate receptor-regulated Smads (R-Smads) transcription factors to propagate the signal (Massague, 2000). The phosphorylated R-Smad then form a complex with the common partner Smad, Smad4, and this heteromeric Smad complex becomes concentrated in the nucleus to regulate the expression of many target genes (Figure 1.1).

There are three functional classes of Smad proteins: the receptor regulated Smad (R-Smad) which include Smad1, 2, 3, 5 and 8, the common partner Smad (Co-Smad) Smad4, and the inhibitory Smads (I-Smad) represented by Smad6 and

7. The R-Smads can be subdivided into two groups: Smad1, 5 and 8 which act downstream of the BMP pathway and Smad2 and 3 which propagate the TGF-beta/Activin signal. The I-Smads negatively regulate TGF-beta signaling by competing with R-Smads for binding to the receptor or to the co-Smad (Moren et al., 2005) as well as targeting the receptor or Smad4 for proteasomal degradation (Ebisawa et al., 2001; Kavsak et al., 2000).

As can be seen in Figure 1.1, the TGF-beta pathway can seem surprisingly simple with a direct transmission of the signal from the receptor to the nucleus via Smad proteins. However many questions remain to be answered, one of them is how TGF-beta signaling is connected to other pathways. This thesis will attempt to answer some of these questions by showing that the co-Smad, Smad4, connects TGF-beta, FGF and Wnt via its linker phosphorylation sites.

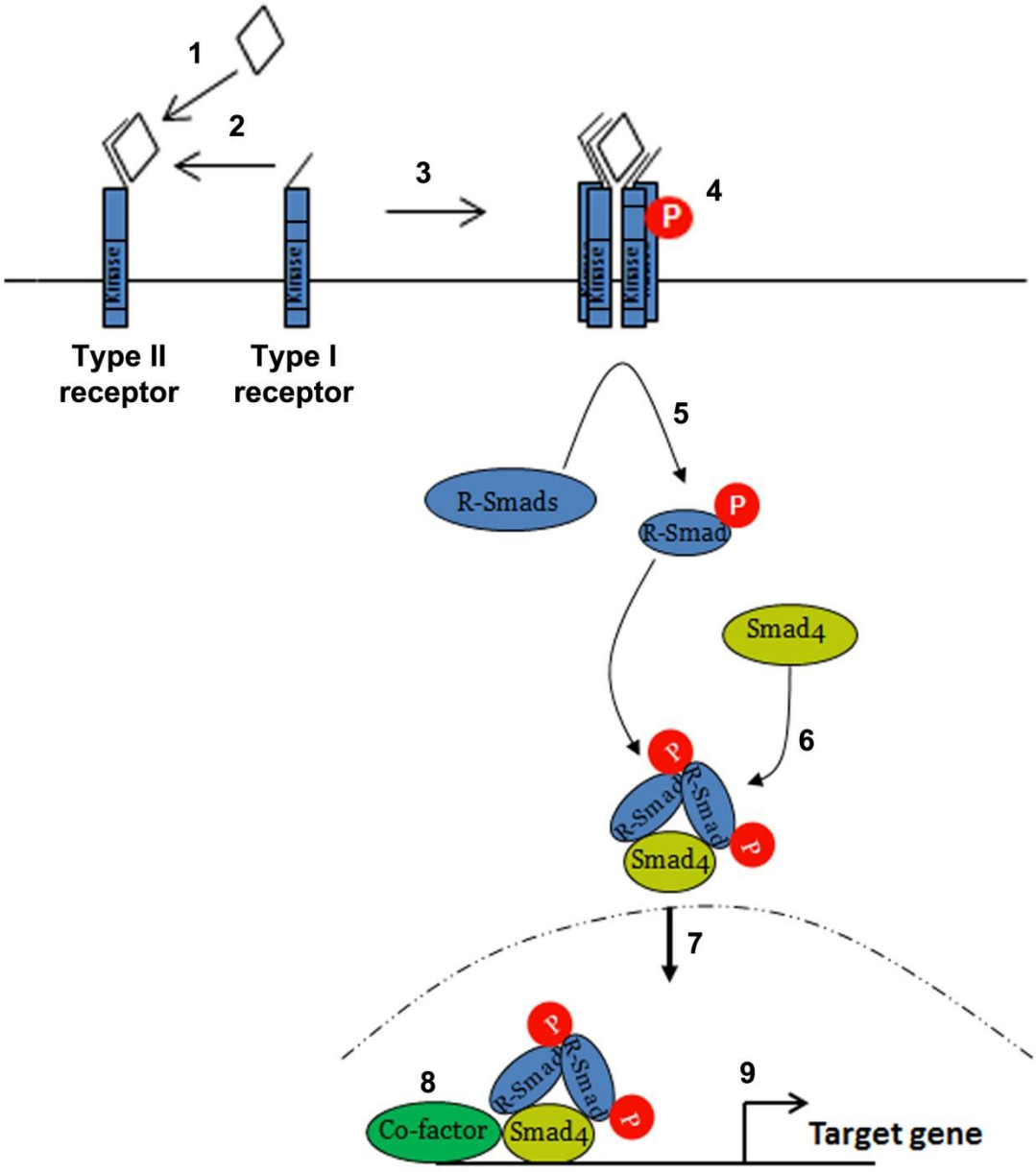

Figure 1.1: The transforming growth factor beta (TGF-beta)/SMAD pathway.

TGF-beta family member binds to the type II receptor (1) and recruits the type I receptor (2) leading to the formation of a receptor complex (3) and phosphorylation of the type I receptor (4). After activation, the type I receptor phosphorylates receptor-regulated SMADs (R-Smads) (5), allowing these proteins to associate with Smad4 (6) and translocate to the nucleus (7). In the nucleus, the SMAD complex associates with co-factors (8), and this complex binds to specific enhancers in targets genes, activating transcription (9). Adapted from Massagué, 1998

1.1.2 TGF-beta Ligands and Receptors

The TGF-beta family of cytokines contains two subfamilies: the TGF-beta/Activin/Nodal subfamily and the BMP/GDF (Growth and Differentiation Factor)/MIS (Muellerian Inhibiting Substance) subfamily. This classification is mainly based on sequence similarities (Figure 1.2). The TGF-beta ligands use two types of receptors to signal: the type II and the type I receptors. Both types of receptors are transmembrane serine/threonine kinases with extracellular ligand binding domain, transmembrane domain, and the intracellular kinase domain. The type II receptor is thought to be constitutively active, while the type I receptor's activity is regulated through phosphorylation. After ligand binding, type I and type II receptors are brought together and the type II receptor can phosphorylate a TTSGSGSG motif termed the "GS" domain within the type I receptor. This leads to type I receptor activation (Massague, 1998). There are 5 type II receptors (TbetaRII, ActRII, ActRIIB, BMPRII, MISRII) and 7 types I receptors (TbetaRI, ActRI, ActRIB, BMPRIA, BMPRIB, ALK1, and ALK7). The type I receptor plays an important role in determining signaling specificity. BMP ligands bind to BMP type I receptors (ALK1, ActRI, BMPRIA, BMPRIB), while TGF-beta/activin signals through TGF-beta or activin type I receptors (TbetaRI, ActRIB, ALK7)

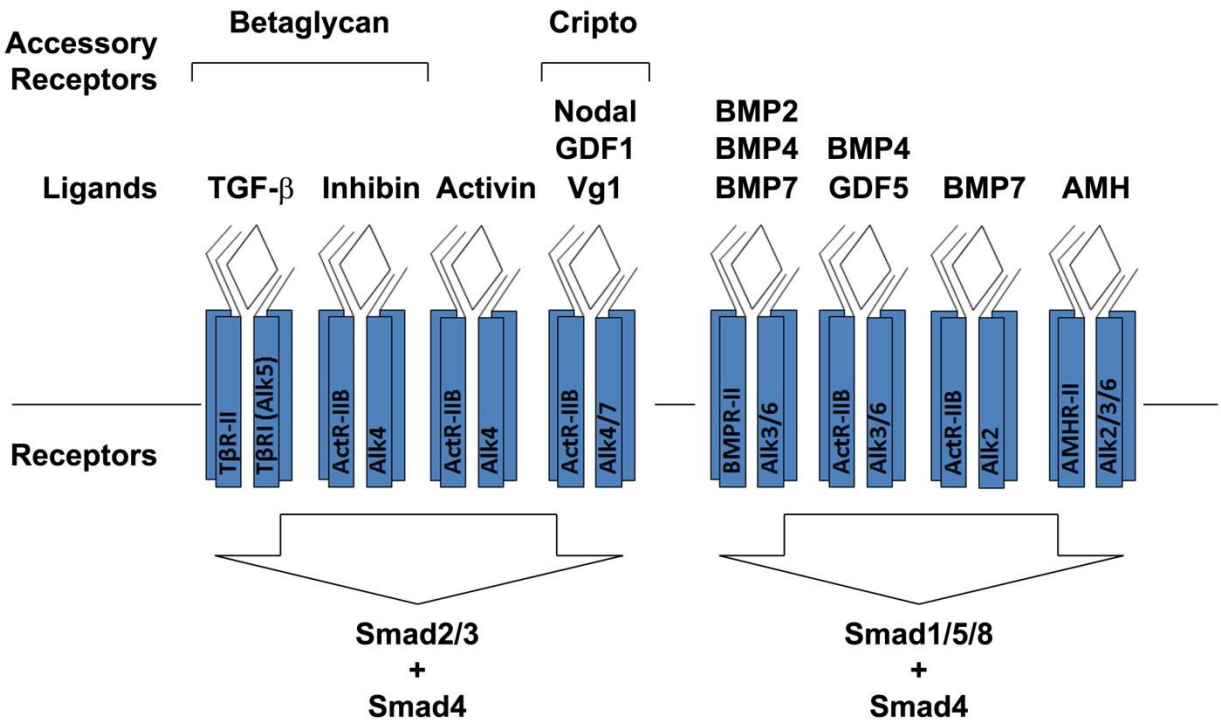

Figure 1.2: Schematic relationship describing TGF-beta ligands, accessory receptors and the combination of type I, type II receptors used in vertebrates

The downstream Smad2/3 and Smad1/5/8 are grouped based on their signaling specificities (adapted from Shi and Massague, 2003)

1.2 The Smad transcription factors

1.2.1 The Smad family of transcription factors

The *Drosophila* homolog of vertebrate BMP-2 and BMP-4 is encoded by the gene *decapentaplegic* (*dpp*), which is crucial for dorso-ventral axis formation as well as imaginal disc patterning. The protein Mad (Mothers against Dpp) was first identified in a genetic screen for modifiers of the *Drosophila* Decapentaplegic (Dpp) pathway (Raftery et al., 1995). Shortly after, the sma-2, sma-3 and sma-4 genes responsible for the *C.elegans* "*Small"* phenotype were identified as components of the TGF-beta pathway (Savage et al., 1996). The vertebrate Smad name comes from a combination of "Sma" and "Mad" funding members of this family of transcription factors. Receptor-regulated Smads (R-Smad) are substrates of the activated type I receptor kinase (Hoodless et al., 1996; Kretzschmar et al., 1997; Macias-Silva et al., 1996; Liu et al., 1997). Interaction between the L3 loop of Smads and L45 loop in the kinase domain of type I receptor determines signaling specificity. Smad1, 5, 8 interact with and are phosphorylated by BMP type I receptors to transduce BMP signals (Kretzschmar et al., 1997; Liu et al., 1996; Yamamoto et al., 1997; Kawabata et al., 1998; Nakayama et al., 1998; Nishimura et al., 1998), whereas Smad2 and Smad3 are phosphorylated by TGF-beta or activin type I receptors to relay TGF-beta/activin signals (Macias-Silva et

al., 1996; Liu et al., 1997; Souchelnytskyi et al., 1997; Abdollah et al., 1997) (Figure 1.3).

Another Smad, called Co-Smad, associates with R-Smads upon their carboxy-terminal phosphorylation and is essential for downstream function of R-Smads (Zhang et al., 1997; Lagna et al., 1996). The only mammalian Co-Smad is Smad4. Co-Smad is shared by both the BMP branch and the TGF-beta/Activin branch of signaling (Lagna et al., 1996).

A third class of Smad are inhibitory Smads (I-Smads) which include Smad6 and Smad7 (Casellas and Brivanlou, 1998; Takase et al., 1998; Hata et al., 1998; Nakao et al., 1997; Imamura et al., 1997; Hayashi et al., 1997). Smad7 inhibits the TGF-beta/Activin and BMP pathway (Hayashi et al., 1997; Nakao et al., 1997), whereas Smad6 seems to specifically inhibit the BMP pathway (Hata et al., 1998; Imamura et al., 1997). They function as inactive decoys to bind to type I receptor and competitively repress R-Smad phosphorylation. Smad6 can also interact with Smad1 to form an inactive Smad1/Smad6 complex, thereby suppressing the formation of the functional Smad1/4 complex (Hata et al., 1998).

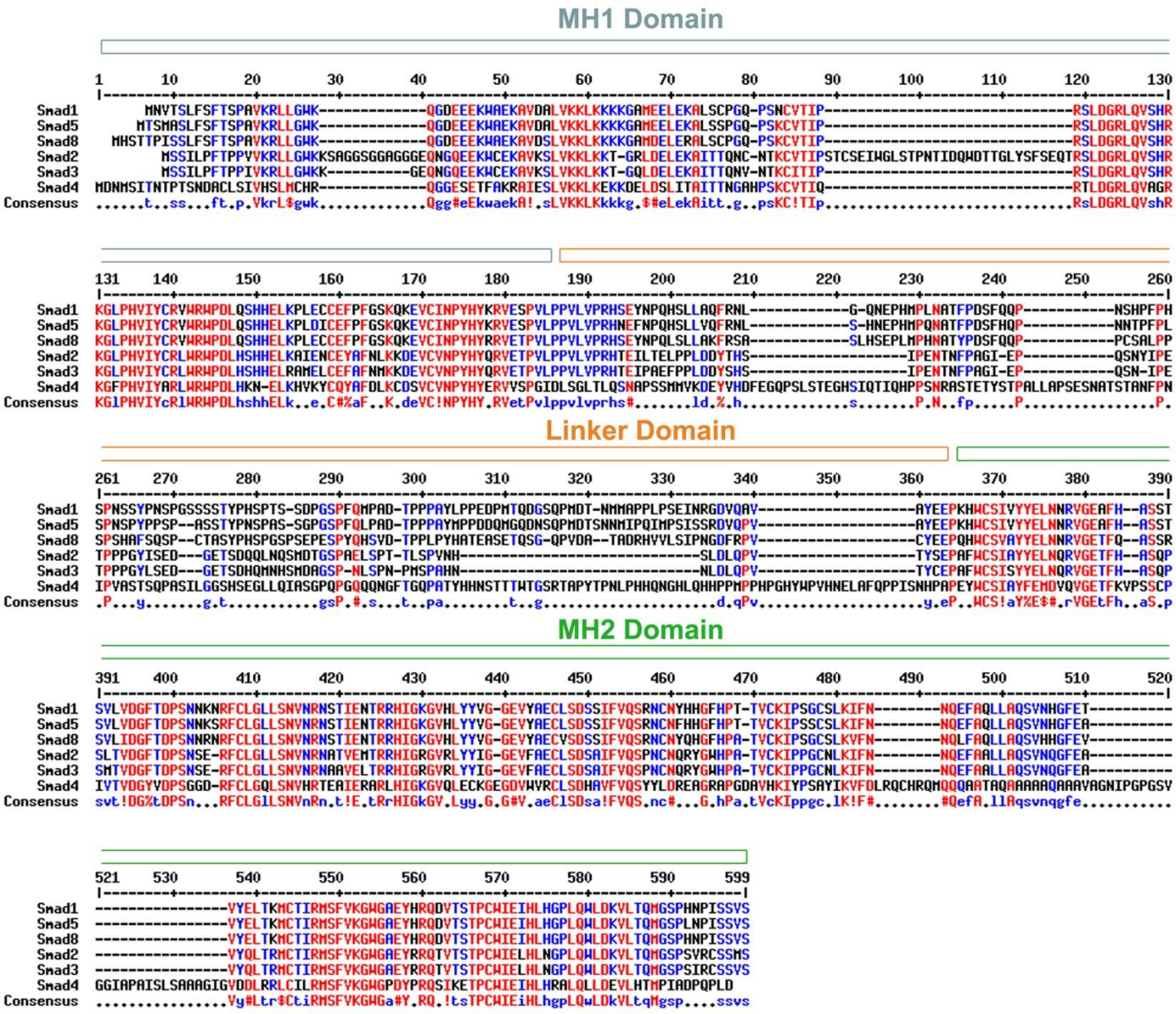

Figure 1.3: Sequence alignment between human Smad1, 2, 3, 4, 5 and 8.

Please note the high level of similarities in the MH1 domain (DNA binding domain) and the MH2 domain (protein-protein interaction domain). In contrast, the linker region is more divergent.

1.2.2 Structure of the Smad proteins

Smads proteins are about 500 amino acids in length and contain two conserved domains, the N-terminal MH1 (Mad Homology 1) domain and the C-terminal MH2 (Mad homology 2) domain. MH1 and MH2 domains are joined together by a less conserved linker region. The MH1 domains of R-Smad and Co-Smad contains the DNA binding domain (Shi et al., 1998; Zawel et al., 1998) and may also play a role in nuclear import and negatively regulate the function of the MH2 domain. The N-terminal domain of I-Smad shows only weak sequence homology to the MH1 region of R-Smads and does not bind to DNA.

The MH2 domain is highly conserved among all Smad proteins and mediates protein-protein interactions. Together with part of the linker region it can associate with transcriptional coactivators and can transactivate reporter gene when fused to GAL4 DNA binding domain (Pearson et al., 1999; de Caestecker et al., 2000; Shen et al., 1998; Pouponnot et al., 1998; Feng et al., 1998; Janknecht et al., 1998). The L3 loop of the MH2 domain bears determinants for pathway specificity (Persson et al., 1998; Chen et al., 1998; Lo et al., 1998), whereas phosphorylation of the C-terminal two serine residues (SxS) by the type I receptor drives activation of the R-Smads (Kretzschmar et al., 1997; Liu et al., 1997; Souchelnytskyi et al., 1997; Abdollah et al., 1997).

The MH1 and MH2 domains are connected by a more divergent linker region whose function is not yet fully understood. The linker region of R-Smad contains demonstrated phosphorylation sites for multiple kinases such as MAPK (Mitogen-Activated Protein Kinase), CDK (Cyclin-Dependant Kinase), GSK-3 (Glycogen Synthase Kinase-3) and CamKII (Ca2+/calmodulin-dependent protein kinase II) (Pera et al., 2003; Grimm and Gurdon, 2002; Sapkota et al., 2007; Fuentealba et al., 2007; Kretzschmar et al., 1997; Kretzschmar et al., 1999; de Caestecker et al., 1998; Matsuura et al., 2004; Alarcon et al., 2009). The linker region of R-Smad and I-Smad also contains a PPxY motif than can be bound by the WW domains of E3 ubiquitin ligases or transcriptional co-activators. How those phosphorylation sites regulate the active cycle of Smads and how do they connect them to other pathways will be discussed later in this chapter.

1.2.3 Activation of R-Smads

R-Smad are phosphorylated are their C-terminus by the type I receptor. This interaction is mediated by the R-Smad L3 loop and the type I receptor L45 loop (Chen et al., 1998; Lo et al., 1998). Additionally, it has been shown that a highly basic surface region near the L3 loop on R-Smad can interact with the phosphorylated GS domain of the type I receptor (Kavsak et al., 2000). In the

absence of ligand stimulation, the protein FKBP12 (FK506 binding protein 12) binds the unphosphorylated GS domain, locking the kinase domain in an inactive and inaccessible conformation. Upon ligand binding, the GS domain is phosphorylated and FKBP12 dissociates. This mechanism ensures that FKBP12 prevents opportunistic activation of R-Smads by type I receptor in the absence of ligand (Huse et al., 2001; Huse et al., 1999).

Smad2/3 are presented to the TGF-beta type I receptor by Smad Anchor for Receptor Activation (SARA) (Wu et al., 2000; Tsukazaki et al., 1998). SARA is a FYVE domain containing protein that is localized to endosomes and interacts with both Smad2/3 and type I receptor, bringing the two together to facilitate the phosphorylation and activation. Once activated, C-terminal phosphorylation destabilizes the Smad2/3-SARA interaction allowing R-Smads to be released and to translocate to the nucleus, where they fulfill their transcription function (Hoodless et al., 1996; Kretzschmar et al., 1997). Mutation analyses have demonstrated that C-tail phosphorylation is required for R-Smad dissociation from the receptor. Indeed, wild type Smad2 can stably associate with a kinase inactive type I receptor, but only transiently interacts with kinase active type I receptor (Souchelnytskyi et al., 1997).

It is thought that in the basal state the MH2 domain interacts with the MH1 region and inhibits its DNA binding property (Hata et al., 1997). Similarly, the

MH1 domain is thought to inhibit the MH2 domain transcriptional activity. Phosphorylation of the C-terminal SxS motif of R-Smad induces a Smad conformational change and relieves the mutual inhibition of Smad MH1 and MH2 domains. This phosphorylation event also allows R-Smad-Smad4 trimer formation.

1.2.4 Dephosphorylation of Smad C-terminal motifs by phosphatases

The TGF-beta/Smad signaling pathway is triggered by C-terminal phosphorylation of R-Smads, resulting in the accumulation of R-Smad and Smad4 in the nucleus, where they regulate gene transcription. TGF-beta signaling is eventually "switched off" in the nucleus. Although a significant portion of Smad proteins are irreversibly terminated by proteosomal degradation, another set of phospho-Smad is dephosphorylated in the nucleus. This dephosphorylation leads to the dissociation of R-Smad from Smad4. Dephosphorylated R-Smads have also lower affinity for other transcription factors, co-activators, and co-repressors. Finally, dephosphorylation of R-Smads restores their affinity for cytoplasmic retention factors such as SARA in the case of Smad2/3. Since un-phosphorylated R-Smads have a higher rate of nuclear export and a lower rate of nuclear import (Xu et al., 2004). Therefore, dephosphorylation of R-Smads terminates their nuclear function and transports them back into the cytoplasm. Recently, several groups have

identified phosphatases responsible for R-Smads Ctail dephosphorylation (Sapkota et al., 2006; Duan et al., 2006; Knockaert et al., 2006; Chen et al., 2006; Wrighton et al., 2006; Lin et al., 2006).

Two approaches were used to identify R-Smads phosphatases. With an overexpression strategy, Lin et al. created expression plasmids for the catalytic subunit of 39 protein serine/threonine phosphatases and dual-specific phosphatases (DUSP). When co-expressed with Flag-tagged Smad2/3 and the constitutively active TGF-beta type I receptor, only Protein phosphatase 1A (PPM1A) significantly reduced the level of Smad2/3 phosphorylation (Lin et al., 2006). Conversely, in PPM1A knock-down cells, TGF-beta induced a more robust nuclear accumulation of Smad2 and Smad3 and a global enhancement of TGF-beta signaling was observed. TGF-beta-induced expression of the CDK inhibitors p15 and p21, the extracellular matrix regulator plasminogen activator inhibitor (PAI-1) and fibronectin (FN), was more pronounced in PPM1A-depleted cells (Lin et al., 2006).

In similar overexpression experiments, PPM1A was also able to dephosphorylate the BMP-specific Smad1, 5 and 8 (Duan et al., 2006). Unlike Smad2/3, which only appeared to be dephosphorylated by PPM1A, among the 39 phosphatases tested, Smad1/5/8 could be dephosphorylated by several additional phosphatases such as small C-terminal domain phosphatases 1, 2 and 3 (SCP1/2/3).

In an another approach, Chen et al. used a loss-of-function, RNAi based, screen to identify phosphatases that affect the phosphorylation level of Mad, the *Drosophila* homologue of Smad1 (Chen et al., 2006). Among the 44 protein phosphatases tested, only pyruvate dehydrogenase phosphatase (PDP) had a significant impact on Mad phosphorylation. There are two homologues of PDP in mammals (PDP1 and PDP2) and knock down of both proteins in HeLa cells led to enhanced C-terminal phosphorylation of Smad1 in response to BMP4 treatment.

In conclusion PPM1A is the only phosphatase demonstrated to date to dephosphorylate the C-terminal domain of Smad2 and Smad3. However, several phosphatases, including PPM1A, SCPs and PDPs can dephosphorylate the C-terminal domain of the BMP specific Smad1.

1.2.5 Proteasomal degradation of Smad proteins

The first attempt to identify a Smad specific E3 ligase was carried by Zhu et al. by using a yeast two-hybrid screen with *Xenopus* Smad1 as the bait (Zhu et al., 1999). This work led to the identification of Smurf1 as a Smad1-interacting protein. Smurf1 belongs to the HECT subclass of E3 ubiquitin ligases. Smurf1 contains two WW domains that can bind PY motifs in partner proteins, and a C-terminal HECT domain involved in the ubiquitin transfer reaction. Overexpressed Smurf1 was

found to specifically reduce the steady state level of Smad1. In *Xenopus* embryos, the overexpression of Smurf1 in ventral marginal zone (VMZ) dorsalizes the embryos and can induce ectopic axis formation. The authors concluded that Smurf1 selectively targets the BMP specific R-Smad Smad1/5 for proteasome mediated degradation, and inhibits the activity of the BMP pathway (Zhu et al., 1999). Interestingly, the interaction of Smurf1 and Smad1 requires the PPAY motif in Smad1 linker region. Deletion of the PPAY residues from the Smad1 sequence abolishes its interaction with Smurf1. The Smad1 linker region also contains four Px(S/T)P motifs that are consensus sites for mitogen activated protein kinase (MAPK) and can be phosphorylated by many kinases according to the cellular context. Those Px(S/T)P site can prime additional phosphorylation by GSK3. It was later found that the binding between Smad1 and Smurf1 require phosphorylation of both Px(S/T)P and GSK3 sites (Sapkota et al., 2007; Fuentealba et al., 2007). How these phosphorylations regulate Smad1 turnover and connect the BMP pathway to Wnt signaling will be discussed later in this chapter.

The ubiquitin E3 ligases that control Smad1 stability are not limited to Smurf1. CHIP (carboxyl-terminus of Hsc70 interacting protein), a U-box dependent E3 ubiquitin ligase, was also found to interact with the MH2 domain of Smad1. The steady state level of Smad1 and Smad4 was significantly reduced by CHIP overexpression as well as the activation of the BMP specific (GCCG)12-Luc

reporter (Li et al., 2004). On the contrary, knock-down of CHIP by RNAi greatly potentiated BMP signaling. These results demonstrated that CHIP is another E3-ligase involved in Smad1/4 proteasomal degradation.

Several groups have identified Smad2/3 specific E3-ligases that can regulate the level of TGF-beta signaling. In a genome-wide search, Smurf2 was identified as a Smad1,2 and 3 interacting E3-ligase (Zhang et al., 2001; Lin et al., 2000). Smurf2 is highly similar to Smurf1 with an N-terminal C2 domain, three WW domains and a C-terminal HECT domain responsible for the ubiquitilation reaction. Although Smurf2 can interact with Smad1, 2 and 3, it only appears to polyubiquitinate and downregulate Smad1 and 2. Similar to Smurf1, the association of Smurf2 with Smads also depends on the presence of the PPxY motifs in the linker region of R-Smads. Smad2 and Smad3 also contain Px(S/T)P motifs that can be phosphorylated by many kinases. Given that the Smurf1-Smad1 association is regulated by these phosphorylation events, it is tempting to speculate that the same mechanism is involved in regulating the Smad2-Smurf2 interaction but, to date, this has not been investigated and remains an hypothesis. Instead, another WW domain containing E3-ligase has been shown to interact with Smad2 and Smad3. Gao et al. demonstrated that NEDD4-L (Neuronal precursor cell Expressed, Developmentally Downregulated 4-like) utilizes its four WW domain

to specifically recognize phosphorylated SP sites as well as a PPxY motif in Smad2/3 sequence (Gao et al., 2009).

Given its main role as a tumor suppressor, many efforts have focused on identifying a Smad4 ubiquitin E3-ligase. Smad4 can also be targeted by WW domain containing E3 ligases such as Smurf1/2 through its interaction with R-Smads and I-Smads that act as adaptors between Smad4 and Smurf proteins (Moren et al., 2005). In addition, Smad4 was found to interact with the F-box protein beta-TrCP1 (Wan et al., 2004). Expression of SCF-betaTrCP1 components reduced the half-life of co-transfected Smad4, whereas down-regulation of beta-TrCP1 with siRNA increased the level of endogenous Smad4. beta-$TrCP_1$ is an E3-ligase that specifically recognizes "phosphodegrons" on target proteins and we found that its binding to Smad4 is regulated by three GSK3 phosphorylation sites located in Smad4 linker region, as will be shown in the chapter 4 of this thesis.

Another RING type E3 ubiquitin ligase, Ectodermin, was identified in a functional screen for *Xenopus* ectoderm determinants (Dupont et al., 2005). Ectodermin, also known as Trim33, is a maternal determinant of *Xenopus* ectoderm that directly binds and ubiquitinates Smad4. In *Xenopus* embryonic development, Ectodermin antagonizes the mesoderm inducing activity of TGF-beta/Activin and promotes ectoderm development. Interestingly, the knock down of endogenous Ectodermin attenuates the degradation of cancer derived, unstable

Smad4 mutant R100T. It was later found that Ectodermin acts as a monoubiquitin E3-ligase whose effect can be reverted by the deubiquitinating enzyme FAM/USP9x (Dupont et al., 2009). This work by the Piccolo lab showed that Smad4 inhibition is a major regulator of ectoderm differentiation in *Xenopus* embryos; this view was further supported by our own work presented in Chapter 4 of this thesis where we find that GSK3 linker phosphorylations mediate Smad4 inhibition and allow ectodermal development.

In summary, Smad proteins can be targeted by three classes of E3 ubiquitin ligases, namely WW domain and HECT domain containing E3 ligases (Smurf1, Smurf2, NEDD4-L), SCF-ubiquitin E3 ligases (SCF-beta-TrCP1/2), and Ring finger type E3 ligases (Ectodermin).

1.2.6 R-Smads oligomerization with Smad4

The main effect of C-terminal R-Smad phosphorylation is to allow these proteins to interact with the L3 loop of another R-Smad or Smad4 (Wu et al., 2001; Qin et al., 2001). Interaction of the phosphorylated C-tail of one R-Smad with the MH2 domain of another R-Smad or Smad4 results in Smad homo- or hetero-oligomerization. Biochemical fractionation studies revealed that R-Smads preferentially exist as monomers in the basal state (Kawabata et al., 1998). It has

also been found that Smad1 and Smad3 have the ability to trimerize when protein concentration increases. This was especially the case when the C-terminal serine cluster (SxS) is mutated into a phospho-mimetic amino acid (Qin et al., 2002; Correia et al., 2001). These observations suggest that R-Smads undergo phosphorylation-dependent monomer to trimer transition upon activation. The Smad4 MH2 domain plus part of the linker region forms trimers in crystal structures (Qin et al., 1999) and many tumor-derived mutations map to the trimer interface residues that mediate subunit-subunit interaction (Shi et al., 1997). However, on size exclusion chromatography, the Smad4 MH2 domain elutes as a monomer.

The formation of R-Smad-Smad4 hetero-complexes is essential for TGF-beta ligand signaling. R-Smad-Smad4 hetero-oligomerization is mediated through similar trimer interfaces as those used in their homo-oligomerization (Correia et al., 2001). A key interaction is between the phospho-C-tail of an R-Smad and the L3 loop region of Smad4 or another R-Smad. Size exclusion fractionation of a mixture of Smad4 and pseudo-phosphorylated Smad1 or Smad3 demonstrated that Smad4-Smad1/3 form 1:2 ratio complex (Correia et al., 2001). However, the phospho-Smad2-Smad4 complex has been reported in various studies as either an heterodimer or an heterotrimer (Chacko et al., 2004; Shi et al., 1997; Qin et al., 1999; Chacko et al., 2001; Jayaraman and Massague, 2000; Wu et al., 2001). The

ratio of the complex will likely depend on R-Smads vs Smad4 protein concentrations. One important study analysed the ratio of the active Smad2/3-4 complex when bound to the DNA (Inman and Hill, 2002). In this study, the authors used differently tagged Smad2/3 and Smad4 proteins in an electrophoresis mobility shift assay (EMSA) using the Activin response element (ARE) from the Mix.2 promoter or a Smad-binding element (SBE) in the c-Jun promoter as probes. The stoichiometry of Smad/DNA complex was investigated by supershift assay using antibodies against different tags. It was demonstrated that the complex assembled on Mix.2 ARE contained two Smad2, one Smad4, and one Forkhead Activin signal transducer (Fast) 1/3, whereas one Smad3, one Smad4 and two additional components were bound to c-Jun SBE. From this result, the authors suggested that the stoichiometry of Smad complexes may depend on individual promoter contexts.

1.2.7 Smad nucleocytoplasmic shuttling

The transport of proteins between cytoplasm and nucleus is mediated by the nuclear pore complex (NPC). Nuclear import of transcription factors can occur through direct interaction with the nucleoporins of the NPC or via adaptor proteins such as Importin alpha and Importin beta (Xu et al., 2004).

Both R-Smad and Smad4 translocate into the nucleus upon ligand stimulation, but through different mechanisms. All R-Smads contain a conserved lysine-rich helix (KKLKK) located in the MH1 domain next to the DNA-binding motif. Phosphorylation of the C-terminal tail of R-Smads exposes this helix which was demonstrated to act as an NLS (Nuclear Localization Signal) for Smad1 and Smad3 and to mediate their nuclear translocation in an Importin beta-dependent way (Xiao et al., 2001; Xiao et al., 2000). In an *in vitro* nuclear import assay using digitonin permeabilized cells, the MH2, but not the MH1 domain of Smad2 was shown to be imported into the nucleus in a cytosol-independent manner (Xu et al., 2002). It was demonstrated that the Smad2 MH2 domain interacts with the Phenylalanine-Glycine (FG)-repeats of the nucleoporins Nup214 and Nup153 directly via a hydrophobic corridor. The MH2 region of Smad1 and Smad3 can also mediate nuclear import via a similar hydrophobic surface (Xu et al., 2003). Interestingly, it was later demonstrated that the Smad1-Nup214 interaction is prevented by Smurf1 binding to the Smad1 linker region (Sapkota et al., 2007).

The translocation of R-Smads and Smad4 to the nucleus following ligand stimulation is only transient and several reports suggest that Smad proteins are actively exported out of the nucleus (Xiao et al., 2001; Xiao et al., 2000; Inman et al., 2002; Watanabe et al., 2000). When the kinase activity of the TGF-beta type I receptor is blocked, Smad2/3 and 4 that have already accumulated in the nucleus

gradually start to distribute throughout the cytoplasm, accompanied by a decrease of C-tail phosphorylation. This observation suggests the dephosphorylation of R-Smads in the nucleus by specific phosphatases allows the recycling of activated Smads and their continuous shuttling between the cytoplasm and the nucleus. This mechanism allows R-Smads to constantly sense the activation status of the TGF-beta receptor (Inman et al., 2002).

Smad4 shuttles continuously in and out of the nucleus independently of signal activation (Inman et al., 2002). Smad4 however, accumulates in the nucleus after ligand stimulation by interacting with activated nuclear R-Smads. Interestingly, the R-Smads NLS is only partially conserved in Smad4 due to a lysine to glutamate substitution and as a result, the Smad4 NLS is not functional by itself. Instead, this motif together with other basic residues in Smad4 MH1 domain, mediate Smad4 nuclear import via interaction with Importin alpha (Xiao et al., 2003). The nuclear accumulation upon ligand stimulation is thought to be caused by a nuclear export signal in the linker region of Smad4 that is masked through the formation of the complex with R-Smads (Inman et al., 2002; Watanabe et al., 2000; Xiao et al., 2001).

Recently, Smad4 has been proposed to be a central regulator of TGF-beta transcriptional time window (Warmflash et al., 2012). The authors demonstrated that although R-Smads stably translocate to the nucleus under continuous TGF-

beta pathway stimulation, transcription of direct target genes was transient. Surprisingly, Smad4 nuclear localization was confined to short pulses that coincided with transcriptional activity. Conducting several experiments in cultured cells and *Xenopus* embryos, Warmflash et al. concluded that R-Smads relay graded information about extracellular ligand levels that is integrated with an intrinsic temporal control reflected in Smad4 into the active signaling complex.

1.2.8 DNA recognition by Smad proteins

All R-Smad and Co-Smad with the exception of Smad2 bind to the DNA in sequence specific manner. The MH1 domain of Smad3 and Smad4 selectively bind to the Smad Binding Element (SBE) sequence which only contains five base pairs, 5'-CAGAC-3' (Dennler et al., 1998; Song et al., 1998). Structural studies of the Smad3 MH1 domain bound to an SBE revealed that each MH1 domain binds to one CAGA sequence using a conserved beta-hairpin structure (Shi et al., 1998). The main spliced form of Smad2 MH1 domain cannot bind to the DNA because of the insertion of an exon 3 sequence that disrupts the hairpin structure. Independently, the sequence repeats of CAGAC in the PAI-1 promoter was identified to be essential for Smad binding and TGF-beta responsibility (Dennler et al., 1998; Song et al., 1998). In addition to the CAGA sequence, Smad1 can also

bind GC rich motifs in the promoters of *goosecoid*, *brinker*, and *vestigial* (Gao and Laughon, 2007; Kim et al., 1997).

1.2.9 Negative regulation of R-Smads through linker phosphorylation

Although activation of the Ras/ mitogen activated protein kinase (MAPK) pathway has been described to have synergistic actions with Smad signaling (Derynck and Zhang, 2003), many studies have also reported a negative effect of MAPK activation on TGF-beta and BMP actions.

This antagonist effect is well documented in many developmental processes, for instance, neural differentiation (De Robertis and Kuroda, 2004), limb development (Niswander and Martin, 2003) and bone and tooth development (Neubuser et al., 1997). The R-Smad linker region contains multiple serine and threonine consensus sites for Erk/MAPK (PxS/TP sites) or for proline-directed kinases. Several studies have shown that MAPK phosphorylation reduces Smad signaling using cell lines (Kretzschmar et al., 1997a), *Xenopus* embryo (Pera et al., 2003; Fuentealba et al., 2007) or transgenic mice (Aubin et al., 2004). Initial works suggested that phosphorylation of the linker region by MAPK/Erk attenuated the nuclear localization of Smad1 (Kretzschmar et al., 1997a) as well as Smad2 (Kretzschmar et al., 1999; Grimm and Gurdon, 2002). Interestingly the level of

nuclear exclusion was dramatically different among the different system tested, ranging from imperceptible in some mammalian cells (Lehmann et al., 2000) to extensive in *Xenopus* embryos (Grimm and Gurdon, 2002). Smad3 was also shown to be a substrate of the G1 cyclin-dependent kinases Cdk2 and Cdk4 (Matsuura et al., 2004). The CDK phosphorylation sites in Smad3 overlap with the ones used by Erk/MAPK and, as in the case of Erk-mediated phosphorylation, CDK-mediated phosphorylation correlates with a decrease in Smad3 activity (Matsuura et al., 2004).

Subsequent studies revealed a number of potential GSK3 phosphorylation sites within the linker region of Smad1 (Sapkota et al., 2007; Fuentealba et al., 2007). GSK3 phosphorylation requires a pre-phosphorylated phosphate located four amino acids upstream of a phosphorylated Serine or Threonine (S/TXXXS/T[PO3)] (Cohen and Frame, 2001). In Smad1, GSK3 is primed by MAPK sites that provide the priming phosphate (Sapkota et al., 2007; Fuentealba et al., 2007). Once Smad1 is phosphorylated in the linker region by both kinases Smurf1, an E3-ubiquitin protein ligase of the WW-Hect family polyubiquitinates and causes Smad1 degradation in the proteasome. Linker phosphorylations of Smad1 are essential for Smurf1 binding to its recognition motif, PPXY, which is located near the linker phosphorylation sites.

In an intriguing parallel, the TGF-beta transducer, Smad3 was also shown to be phosphorylated by MAPK and to prime a single GSK3 phosphorylation site (Gao et al., 2009; Millet et al., 2009; Aragón et al., 2011). When dually phosphorylated, Smad3 is recognized by its own specific E3-ligase, NEDD-4L, and targeted for degradation (Gao et al., 2009; Aragón et al., 2011). Interestingly, the unique Smad3 GSK3 phosphorylation site (Ser. 204) is also a proline directed kinase phosphorylation site (S/TP) and is directly phosphorylated by MAPK under FGF stimulation (Browne et al., 2013). In our initial attempts to determine if Smad3 was a node of integration between the TGF-beta and Wnt pathway, we tested whether the phosphorylation of Ser 204 in Smad3 was controlled by Wnt signals but instead found that the cross-talk was entirely mediated by the co-Smad, Smad4, as will be extensively discussed in the Chapter 4 of this thesis.

1.3 The canonical Wnt signaling pathway

1.3.1 Overview of the Wnt signaling pathway

Wnt signaling, like the TGF-beta pathway, plays a critical role in both embryonic development and mature tissue homeostasis regulating a variety of biological processes such as axis specification, neural development, cell proliferation and

differentiation. The signaling cascade and the functions of the Wnt pathway have been conserved across evolution (Cadigan and Nusse, 1997).

The canonical Wnt pathway is mediated by beta-catenin, which is both a structural protein and a transcription activator. There are three pools of beta-catenin in every cell: a plasma membrane associated pool, a cytoplasmic pool and a nuclear pool (Clevers and Nusse, 2012). Wnt signaling regulates and signals through the cytoplasmic pool. In the absence of Wnt ligand, the cytosolic beta-catenin is trapped in a multimeric protein complex called the destruction complex. The destruction complex is composed of Axin, Adenomatous Polyposis Coli (APC), GSK3 and casein kinase I alpha (CKIalpha). The collaborative work of proteins in this complex leads to beta-catenin phosphorylation by CKIalpha which primes subsequent GSK3 phosphorylations. Once phosphorylated by GSK3, beta-catenin is quickly polyubiquitinated by the E3 ligase beta-TrCP and degraded by the proteasome (Clevers and Nusse, 2012). This system ensures that the Wnt/beta-catenin pathway remains in an "off" state.

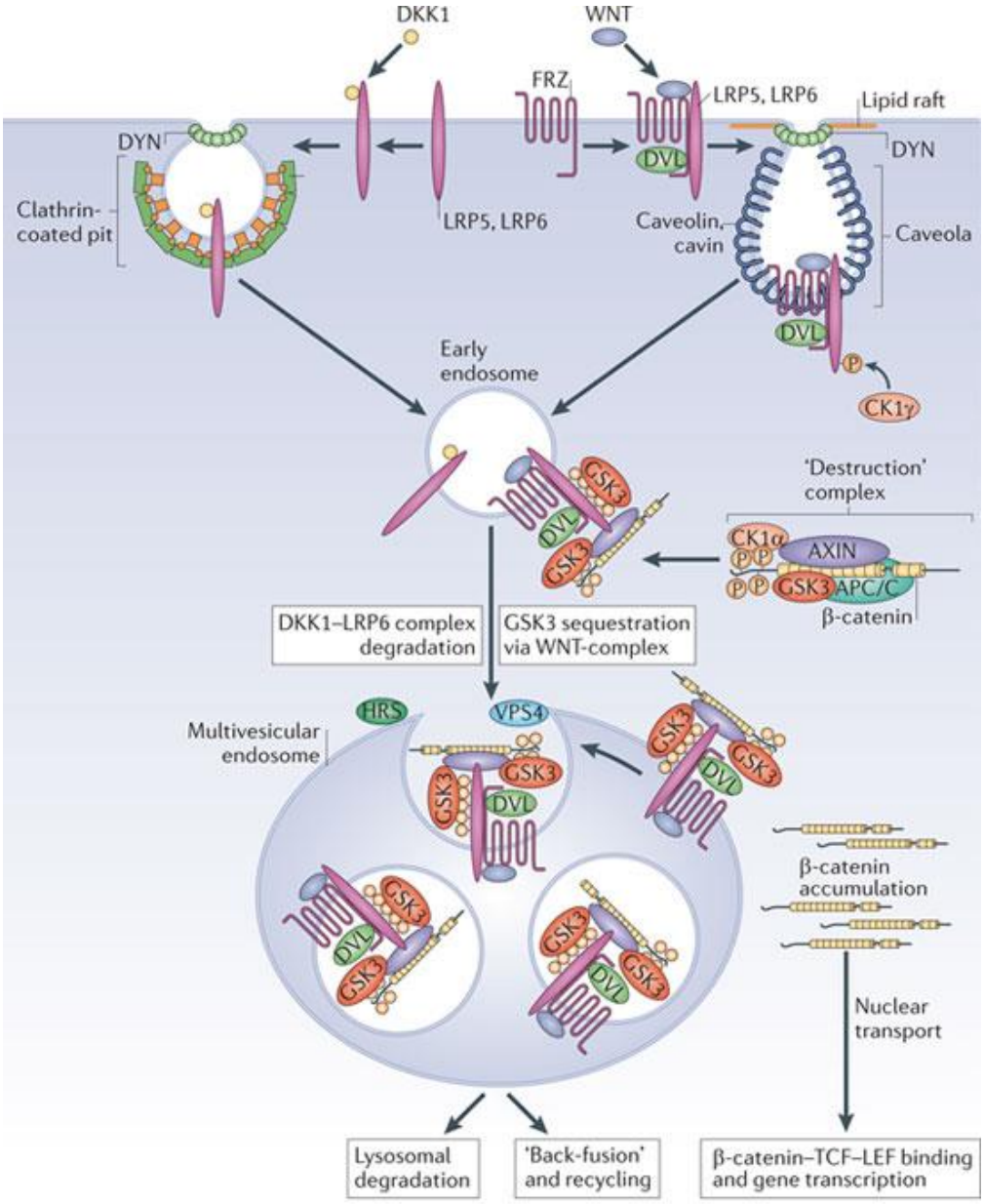

Figure 1.4: Model of Canonical Wnt Signaling through the Sequestration of GSK3 inside Multivesicular Endosomes

Binding of GSK3 (in red) to the Wnt receptor complex (including phospho-LRP6, phospho-beta-Catenin, and other GSK3 substrates such as Dvl, Axin, and APC) sequesters GSK3 inside small intralumenal MVB vesicles, causing its cytosolic substrates such as beta-Catenin (in blue) and many other proteins to become stabilized (see text). The initial GSK3 molecules are recruited to the receptor complex bound to Axin, ensuring that the GSK3 fraction bound to the destruction complex is depleted first. From Dobrowolski and De Robertis, 2011.

During Wnt signalling, Wnt ligands bind two co-receptors, Frizzled and low-density lipoprotein receptor-related 5 (LRP5) or LRP6. This directs the localization of LRP6 into caveolin-containing vesicles for endocytosis. The cytoplasmic tail of LRP6 is phosphorylated by two enzymes, casein kinase 1 (CK1) and later GSK3, which are recruited together with Axin from the cytosolic 'destruction' complex. This triggers the polymerization of Dishevelled (Dvl) and LRP6 on the plasma membrane and endocytosis of the Wnt receptor complex (Bilic et al., 2007; Zeng et al., 2008; Metcalfe et al., 2010). Dvl, Axin and beta-catenin are required for this endocytosis (Taelman et al., 2010; Bilic et al., 2007) and are all also GSK3 substrates.

The initial phosphorylation of LRP6 by GSK3 is required for the subsequent sequestration of this enzyme in MultiVesicular Bodies (MVBs) (Figure 1.4). Sustained activation of the Wnt pathway is achieved when the ESCRT machinery sequesters sufficient amounts of GSK3 inside Intra Luminal Vesicules (ILVs) of MVBs, protecting its many cytosolic substrates from phosphorylation (Taelman et al., 2010). Newly translated beta-catenin protein is not phosphorylated by GSK3, becomes stabilized and translocates to the nucleus, where it activates the transcription of Wnt target genes.

1.3.2 The Wnt pathway regulates proteins stability

GSK3 recognizes pre-phosphorylated residues in its many substrates, and phosphorylates upstream Ser or Thr residues spaced by four amino acids (Cohen and Frame, 2001). When proteins become heavily phosphorylated on several residues, it generates a phosphodegron that can be targeted by specific E3 ligases for polyubiquitination and subsequent proteasomal degradation. Taelman et al. found that when GSK3 is sequestered into MVBs in the presence of Wnt, many cellular proteins were protected from GSK3-mediated phosphorylation and became stabilized (Taelman et al., 2010; Vinyoles et al., 2014; Acebron et al., 2014). One of these proteins was Smad4 and this led us to investigate the phosphorylation of Smad4 by GSK3 which will be presented in the chapter 3 of this thesis.

1.4 The FGF/EGF pathway

The fibroblast growth factors (FGFs), together with TGF-beta and Wnt, represent another families of extracellular signalling peptides that are key regulators of metazoan development. FGFs are required for multiple processes in both protostome and deuterostome groups. Misregulation of this signalling pathway has been implicated in a number of human diseases in particular in cancer.

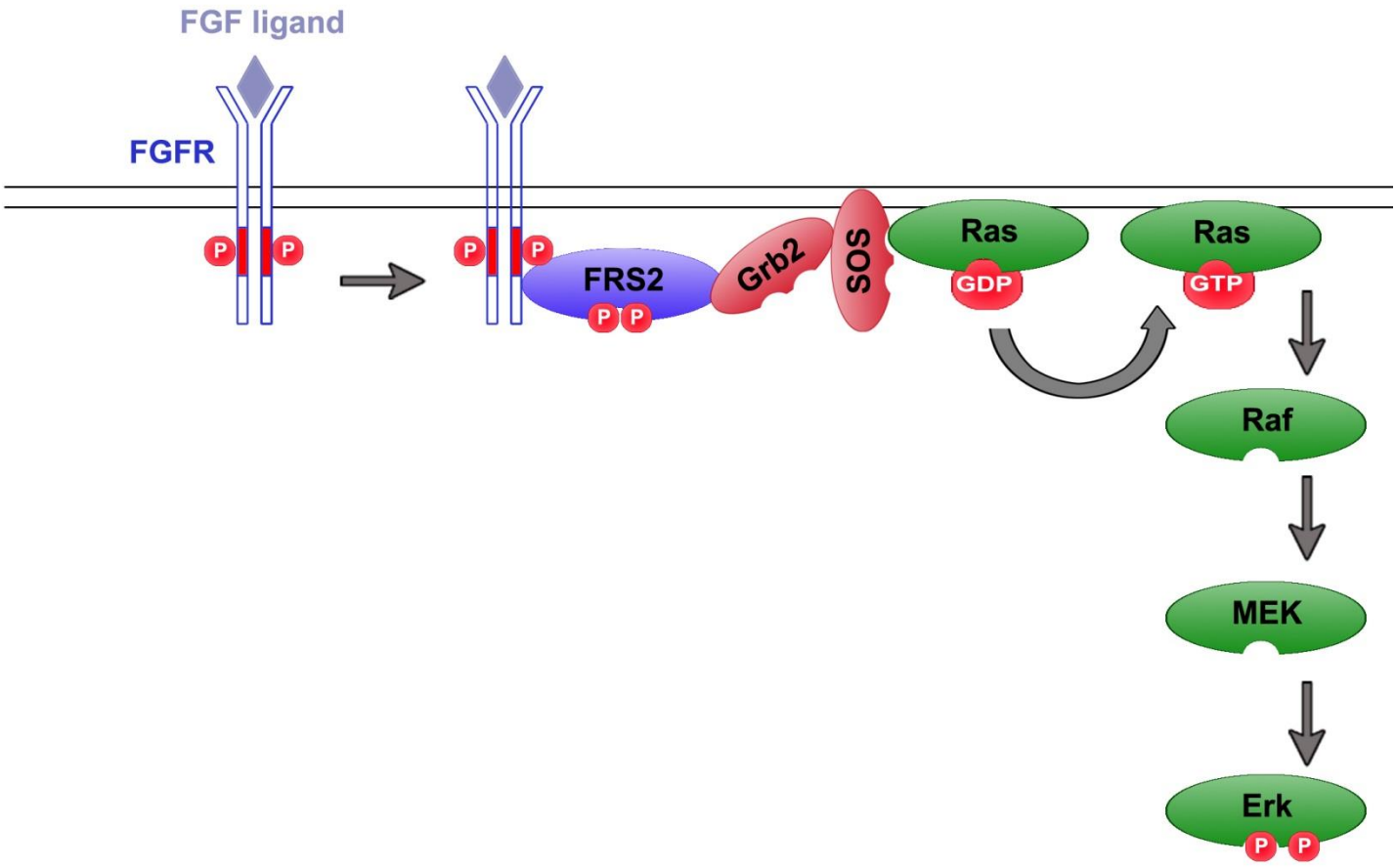

Figure 1.5: Schematic diagram of the FGF/Erk pathway.

Binding of fibroblast growth factor (FGF) to the FGF receptor (FGFR) induces FGFR dimerization, which brings in close proximity intracellular Tyr kinase domains of the receptors so that kinase activation by transphosphorylation can occur. Activated FGFR kinase in turn activates its intracellular substrates by phosphorylation. Major substrates of FGFR kinase are FGFR substrate 2 (FRS2), which is constitutively associated with the receptor kinase. Activated FRS2 binds the adaptor protein growth factor receptor-bound 2 (GRB2). GRB2 then recruits the guanine nucleotide exchange factor son of sevenless (SOS)) to the signalling complex. Recruited SOS activates RAS GTPase, which initiates activation of the MAPK cascade. Activated MAPK translocates from the cytoplasm to the nucleus, where it phosphorylates and hence activates immediate early gene transcription factors.

Assembly of the FGF signalling complex results in dimerisation of the receptor and activation of intracellular signal transduction pathways (Beenken and Mohammadi, 2009). Activation of FGF signalling leads to phosphorylation of a number of conserved Tyrosine residues in the intracellular domain of the FGF Receptor (FGFR) (Figure 1.5). One of the main target of FGFR phosphorylation is the FGFR substrate 2 (FRS2) (Kouhara et al., 1997) which associates with the receptor and in turn allows the recruitment of the Grb2 adaptor protein and the associated nucleotide exchange factor son of sevenless (SOS) (Ong et al., 2000). Grb2/SOS then activates the small GTP binding protein Ras by stimulating the transition from its inactive GDP bound to its active GTP bound form. Activation of Ras leads to the stimulation of a cascade of phosphorylation events involving Raf (a MAPK kinase kinase) and Mek (MAPK kinase), ultimately leading the activation and phosphorylation of MAPK ERK.

Phosphorylated MAPK, a serine/threonine kinase, is then able to phosphorylate and modify the activity of many transcription factors. Notable among the transcription factors activated by MAPK are ETS proteins (Randi et al., 2009) that use a winged helix-turn-helix protein fold as a DNA binding domain and have been shown to be key effectors of FGF signalling, regulating gene expression downstream of the MAPK pathway (Nentwich et al., 2009). The genes

transcribed in response to ETS proteins and other transcription factors activated by this pathway are considered FGF target genes.

1.5 Conclusions

During my PhD studies, I discovered how these three main signaling pathways converge at the level of two transcription factors, Mad/Smad1 and Smad4, whose linker phosphorylations integrate FGF and Wnt signals with the TGF-beta/BMP pathways. These findings will be discussed respectively in Chapter 3 and 4. In the next Chapter, I present a review that I wrote with Edward Eivers when I first arrived in the lab. This paper represents the state of our knowledge on Smad signaling and their integration with the FGF and Wnt pathways when I first joined the lab.

CHAPTER 2

Smad1/5/8 Linker Phosphorylations Integrate the BMP and Wnt Signaling Pathways

This Chapter contains text and figures as published in

Cytokine & Growth Factor Reviews *20*, 357-365. (2009)

Edward Eivers, **Hadrien Demagny**, and Edward M. De Robertis

When I first joined the lab, my advisor told me that the most important thing for a graduate student was to study in details every paper related to his/her project. I took this advice very seriously and quickly, my desk became covered with papers about Smad proteins structure, BMP signaling and *Xenopus* early development. Since we learn 10% of what we read but 95% of what we write, I asked Edward Eivers, a post-doctoral trainee in our lab, to join him in the writing of a review that was requested by the journal *Cytokine & Growth Factor Reviews*. In this process, I learnt how to assemble figures, a key skill for any young scientist. This chapter contains text and figure from this first review and reflects the level of knowledge that we had when I joined the De Robertis group.

ABSTRACT

BMPs pattern the dorsal–ventral axis of vertebrate embryos. Smad1/5/8 transduces the BMP signal, and receives phosphorylation inputs from both MAPK and GSK3. Phosphorylation of Smad1 by MAPK and GSK3 result in its polyubiquitination and transport to the centrosome where it is degraded by the proteasome. These linker phosphorylations inhibit BMP/Smad1signaling by shortening its duration. Wnt, which negatively regulates GSK3 activity, prolongs the BMP/Smad1 signal. Remarkably, linker-phosphorylated Smad1 has been shown to be inherited asymmetrically during cell division. Drosophila contains a single Smad1/5/8 homologue, Mad, and is stabilized by phosphorylation-resistant mutations at GSK3 sites, causing Wingless-like effects. We summarize here the significance of linker-phosphorylated Smad1/Mad in relation to signal intensity and duration, and how this integrates the Wnt and BMP pathways during cell differentiation.

2.1 Introduction: embryonic axis formation and the double gradient model

Understanding how cells receive and integrate multiple signals is a major challenge in cell and developmental biology. Nowhere is this more apparent than in a rapidly dividing embryo, which has to undergo cell fate decisions in response to a multitude of growth factor signals over narrow periods of time. These extracellular signals are critically regulated both in time and space and are fine-tuned by a vast network of inhibitors and activators. Two major morphogens exist in developing Xenopus embryos, the BMP (bone morphogenetic protein) and the Wnt gradients (Figure 2.1). These gradients are perpendicular to each other and are responsible for tissue position and determination along these axes, patterning the embryo from dorsal to ventral (D–V) and anterior to posterior (A–P) (Niehrs, 2004). Both these signals are seamlessly integrated and this can be demonstrated experimentally in Xenopus embryos. When a blastula embryo is equally cut in half, with each half containing a dorsal and ventral part, the embryo can self-regulate, forming perfectly identical twins (De Robertis, 2006). Below we discuss signaling by the BMP and Wnt morphogens and analyze recent advances in our understanding of signal integration along the D–V and A–P gradients at the level of Smad1/5/8 linker phosphorylations (Fuentealba et al., 2007; De Robertis, 2008; Eivers et al., 2008).

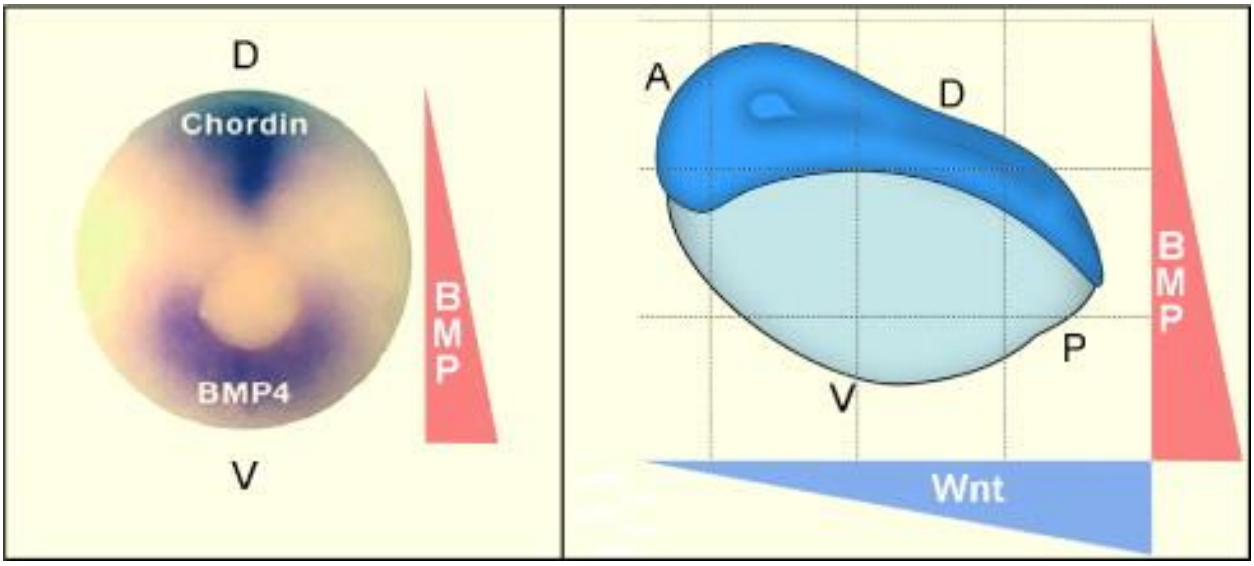

Figure 2.1: Dorsal to ventral (D–V) and anterior to posterior (A–P) gradients of the *Xenopus* embryo

(**Left**) Expression of Chordin and BMP4 on opposite centers of a Xenopus embryo. (**Right**) Model illustrating the two perpendicular morphogenetic gradients of BMP and Wnt. Cells sense their position within these Cartesian-coordinates, which specify their fate in the body plan (De Robertis, 2008).

2.2 Dorsal–ventral patterning: a morphogenetic gradient of BMP ligands

The earliest requirement for BMP signaling in an embryo is during the patterning of cell fates along its D–V axis. Formation of a D–V gradient of BMP signals has been evolutionary conserved and is utilized by both vertebrates and invertebrates (De Robertis, 2006; De Robertis, 2008; De Robertis and Sasai, 1996; O'Connor et al., 2006). In vertebrate embryos like Xenopus and zebrafish, BMPs pattern ventral cell fates, while BMP repression determines dorsal cell fate (Figure 2.1); this D–V polarity is reversed in invertebrate embryos such as Drosophila. The gradient of BMP signals subdivides the Xenopus ectoderm from ventral to dorsal into epidermis, neural crest, and central nervous system, while the mesoderm is subdivided into blood island, lateral plate mesoderm (kidney), somite, and notochord. Thus, a ventral gradient of extracellular BMPs regulates the initial tissue-type differentiations of the vertebrate embryo.

The main BMPs involved in D–V patterning in the Xenopus embryo are the ventrally expressed BMP4 and BMP7 and the dorsally expressed BMP2 and ADMP. Depletion of all four BMPs using injected antisense morpholino oligo nucleotides causes this robust morphogenetic field to collapse, resulting in complete neuralization of the developing embryo (Reversade and De Robertis, 2005). This is a spectacular transformation of the embryo, because the entire

ectoderm becomes covered by central nervous system (CNS), in particular brain tissue. If any one of the four BMPs is not depleted, the embryo retains some D–V patterning. This indicates that both the dorsal and the ventral poles of the embryo serve as sources of BMP signals. In zebrafish embryos, mutation of bmp2b or bmp7 result in strong dorsalization or neuralization of the embryo (Kishimoto et al., 1997; Nguyen et al., 1997; Schmid et al., 2000), demonstrating that the requirement for BMPs in the specification of ventral fates has been evolutionary conserved (Little and Mullins, 2009).

The main extracellular regulators of BMP ligands are Chordin and Noggin, two BMP antagonists secreted by the dorsal Spemann organizer at the onset of gastrulation (Smith and Harland, 1992; Sasai et al., 1994). Chordin and Noggin help create and maintain a D–V gradient of BMP and induce dorsal cell fates. Anti-BMPs do not directly signal dorsal fate, but the antagonism of BMP signaling by extracellular binding causes dorsal cell differentiation by decreasing BMP signaling levels (Piccolo et al., 1996; Zimmerman et al., 1996) and (Holley et al., 1996). The requirement for BMP inhibition was demonstrated by knockdown of Chordin, Noggin and a third BMP antagonist, Follistatin, in Xenopus tropicalis embryos. This resulted in severe loss of neural tissue and massive expansion of ventral cell fates (Khokha et al., 2005). Two opposing ventral and dorsal signaling centers of the gastrula embryo provide the initial basis for D–V patterning, and an

elaborate biochemical pathway of extracellular protein–protein interactions has been found to be required to maintain a well-regulated BMP morphogenetic field (De Robertis, 2008; Plouhinec and De Robertis, 2009).

2.3 Intracellular transduction of the BMP signal

BMPs transduce their intracellular signal via BMPR (BMP receptor) activation followed by transcription factor phosphorylation. BMPs first bind to and activate their transmembrane serine/threonine kinase receptors, which in turn phosphorylate the transcription factors Smad1/5/8 at its two C-terminal serines (SVS). Phosphorylated Smad1^{Cter} binds to Smad4 (co-Smad) and translocates and accumulates in the nucleus, activating BMP-responsive genes (Figure 2.2) (Shi and Massague, 2003; Feng and Derynck, 2005), such as BMP4/7 and others. A dynamic D–V nuclear gradient of pSmad1Cter has been shown in a number of model organisms such as Drosophila (Dorfman and Shilo, 2001; Sutherland et al., 2003), zebrafish (Tucker et al., 2008) and Xenopus (Plouhinec and De Robertis, 2009). At very low levels of pSmad1^{Cter}, caused by the extracellular inhibitory activity of Chordin and Noggin on BMP ligands, dorsally expressed genes are transcribed. Ventral genes are activated by BMP signals. The dorsal and ventral centers of the gastrula express molecules of similar biochemical activities but

under reciprocal transcriptional control. This explains how a self-regulating field is maintained in the early embryo (Reversade and De Robertis, 2005). When the amount of one molecule is lowered in the dorsal side, the gradient can be restored by the expression of ventral counterparts (Reversade and De Robertis, 2005; Plouhinec and De Robertis, 2009). For example, the dorsal organizer expresses Chordin, while the ventral center expresses a Chordin-related BMP-binding molecule called CV2 (Crossveinless-2) (Coffinier et al., 2002; Conley et al., 2000). When Chordin and CV2 are depleted simultaneously, the embryo reaches very high BMP levels, indicating that CV2 in the ventral side can compensate for loss-of Chordin in the dorsal signaling center (Ambrosio et al., 2008).

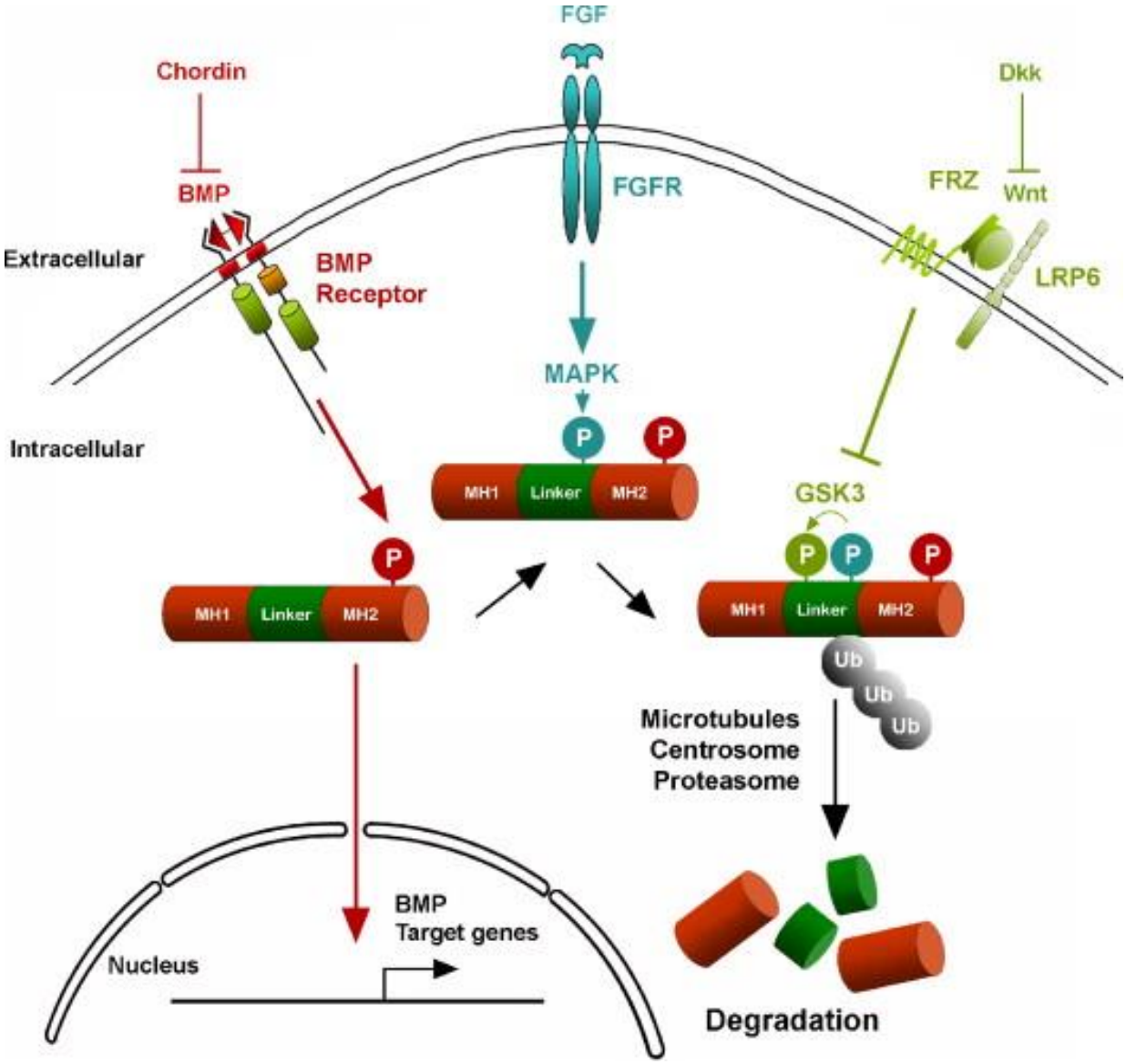

Figure 2.2: Integration of multiple extracellular signaling pathways at the level of Smad1/5/8 phosphorylations.

BMP-dependent C-terminal phosphorylation of Smad1, activates target gene expression whereas, MAPK and GSK3 linker-phosphorylations promote degradation terminating the BMP/Smad1 signal. Wnt prolongs BMP signals by inhibiting GSK3 phosphorylation.

2.4 Anterior–posterior patterning and Wnt signaling

The main determinant of the A–P axis in the early embryo is provided by Wnt signaling (Niehrs, 2004; Kiecker and Niehrs, 2001). A Wnt morphogen gradient is generated by a number of extracellular Wnt ligands, which are modulated by a diverse group of secreted Wnt antagonists such as Dkk-1 (Dickkopf-1) and sFRPs (secreted Frizzled-related proteins) (Logan and Nusse, 2004). In Xenopus and amphioxious embryos, the Wnt signaling gradient is maximal at the posterior blastopore (Niehrs, 2004; Christian and Moon, 1993; Yu et al., 2007), and its signal becomes lower in anterior regions (Figure 2.1). When neuralized Xenopus ectodermal explants are microinjected with varying doses of Wnt DNA, posterior markers are induced (McGrew et al., 1997). In planarians, A–P specification is also regulated by Wnt signaling, since inhibition of the canonical Wnt pathway by RNAi causes ectopic regeneration of head structures (Gurley et al., 2008; Reddien, 2008). A–P patterning by a Wnt gradient appears to be a universal property of animal development. At later stages, the A–P axis becomes subdivided into segments in many organisms. The A–P patterning within each segment also requires Wnt signals (De Robertis, 2008).

The organizer region of the frog embryo not only secretes BMP antagonists, but a cocktail of Wnt inhibitors, which include Frzb-1, sFRP-2, Crescent, and Dkk-

1 (Fedi et al., 1999; Glinka et al., 1997; Glinka et al., 1998; Piccolo et al., 1999; Hashimoto et al., 2000). Inhibition of the Wnt signaling pathway at early gastrula stage plays a vital role in head induction. When Dkk is overexpressed in Xenopus embryos it has potent head-inducing activity, resulting in an expanded anterior neural plate at the expense of epidermal tissues (Glinka et al., 1998). However, the anterior neural inducing activity of anti-Wnts also requires inhibition of BMP signaling to generate head structures (Niehrs, 2004; Glinka et al., 1997).

Wnt signaling involves ligand binding to its Frizzled/ lipoprotein receptor-related protein 6 (LRP6) co-receptor complex on the extracellular cell surface. These receptors then transduce an intracellular signal through a number of proteins which include Dishevelled, GSK-3 (glycogen synthase kinase-3), Axin, APC (adenomatous polyposis coli), and the transcriptional regulator beta-catenin. In the absence of Wnt signaling, beta-catenin levels in the cytoplasm are normally kept low by continuous proteasome-mediated degradation, involving a complex containing GSK-3/APC/Axin (Logan and Nusse, 2004). When a cell receives a Wnt signal this degradation pathway is inhibited, resulting in nuclear accumulation of beta-catenin. Nuclear beta-catenin then interacts with other transcription factors such as LEF/TCF (lymphoid enhancer-binding factor1/T cell-specific transcription factor) to initiate transcription of Wnt responsive genes (Logan and Nusse, 2004).

2.5 Regulation of Smad1 via linker phosphorylations downstream of BMP

The BMP transcription factor Smad1 is further regulated by inhibitory "linker" phosphorylations. The linker region of Smads lies between its MH1 (Mad homology domain, DNA binding) and MH2 (protein interaction) domains with a large number of potential phosphorylatable Serines and Threonines.

2.5.1 Inhibitory Smad1 linker phosphorylations by MAPK

Smad1 was first shown to be a target of growth factor signaling through the mitogen-activated protein kinase (MAPK) pathway in human cultured cell lines (Kretzschmar et al., 1997a). MAPK phosphorylations activated by epidermal growth factor receptor (EGFR) occur at four specific MAPK/Erk recognition consensus sites (PxS[PO3]P) within the linker region of Smad1. MAPK phosphorylation prevents nuclear accumulation of Smad1, and therefore inhibits its intracellular transcriptional activity (Kretzschmar et al., 1997a). Mutation of the Serines at the four MAPK sites into Alanines rendered Smad1 resistant to EGFR-induced phosphorylation and inhibition (Kretzschmar et al., 1997a). This discovery provided the first evidence of the antagonistic action of MAPK linker phosphorylation on the BMP signaling pathway.

The opposing BMP and EGFR/MAPK inputs on Smad1 suggested an explanation for the long-standing question of how fibroblast growth factors (FGFs) and insulin-like growth factors (IGFs) induce neural tissue (Streit et al., 2000; Wilson et al., 2000; Pera et al., 2001; Richard-Parpaillon et al., 2002; Eivers et al., 2004). This was a puzzle, because BMP antagonists such as Chordin and Noggin cause neural differentiations similar to those of FGF and IGF (De Robertis, 2006) and (Pera et al., 2003). Microinjection experiments and biochemical assays using Xenopus embryos demonstrated that MAPK/Erk is activated by both FGF and IGF causing an inhibitory phosphorylation in Smad1 that induces ectoderm to differentiate as neural tissue instead of epidermis (Pera et al., 2003). In gain-of-function experiments microinjection of phosphorylation-resistant Smad1 mRNA induced ectodermal cells to become epidermal tissue at the expense of neural fates. These data demonstrated that the epidermal-inducing activity of Smad1 requires low BMP antagonists, high BMP, and low levels of MAPK signals activated by receptor tyrosine kinases (Pera et al., 2003; Sater et al., 2003; Kuroda et al., 2005). During organ development, there are many situations in which FGF and BMP signals have opposing functions. Examples include: limb development, lung branching morphogenesis, cranial suture fusion, and tooth development (Pera et al., 2003). These opposing effects may also involve the integration of FGF/MAPK signals and BMP signals at the level of Smad1/5/8 phosphorylations.

The regulatory cross-talk between the BMP and MAPK pathways was demonstrated in knock-in mice containing Smad1 forms that are resistant to phosphorylation by MAPK in the Smad1 linker region. These studies indicated a requirement for linker phosphorylation in gastrointestinal and reproductive tract development (Aubin et al., 2005). Using embryonic fibroblasts from these knock-in mice, Sapkota et al. used a BMP reporter gene to show that FGF inhibits signaling by BMP (Sapkota et al., 2007). Importantly, exogenous FGF failed to inhibit BMP signaling in Smad1 linker phosphorylation-resistant knock-in mutant mouse embryonic fibroblasts. In addition, FGF inhibition of BMP signaling has also been reported in rat embryonic dorsal spinal cord precursor cultures, in which FGF2 addition prevents nuclear accumulation of $pSmad1^{Cter}$, sequestering it in the cytoplasm in a MAPK-dependent manner (Bilican et al., 2008).

Phosphorylation by MAPK has been shown not to be solely restricted to the linker domain. Drosophila Mad, which is the homolog of vertebrate Smad1/5/8, is phosphorylated by a MAPK-related kinase called Nlk (Nemo-like kinase) (Zeng et al., 2007). Nlk, an enzyme known to be involved in the Wingless/Wnt pathway, phosphorylates Mad at a conserved serine residue in its MH1 DNA binding domain. This phosphorylation inhibits BMP signaling by preventing nuclear accumulation of pMadCter, thus inhibiting the activation of BMP-responsive genes (Zeng et al., 2007).

2.5.2 GSK3/Wnt regulates BMP/Smad1 signal termination

Extensive sequence analysis within the linker region of Smad1 revealed a number of potential GSK3 phosphorylation sites (Fuentealba et al., 2007; Sapkota et al., 2007). GSK3 phosphorylation requires a pre-phosphorylated phosphate located four amino acids downstream of a Serine or Threonine (S/TXXXS/T[PO3)] (Cohen and Frame, 2001) (Figure 2.2). In Smad1, GSK3 is primed by MAPK sites that provide the priming phosphate (Fuentealba et al., 2007; Sapkota et al., 2007). Linker phosphorylation by GSK3 had an inhibitory effect on BMP signal transduction. Mutation of the GSK3 sites into Alanines resulted in strongly ventralized phenotypes (high BMP signaling) in injected Xenopus embryos (Fuentealba et al., 2007).

Pulse-chase experiments demonstrated that BMP signaling triggered three successive phosphorylations of Smad1 in cultured cell assays (Fuentealba et al., 2007). The first phosphorylation caused by BMPR activation, occurs in the C-terminal region of Smad1 (Figure 2.2). BMP determines the intensity or amplitude of the BMP signal. The two next phosphorylations in the linker region provided first by MAPK and then by GSK3, determine the duration of the BMP/pSmad1Cter signal. We deduce that the duration of the signal is a key regulatory step, because

inhibition of MAPK or GSK3 in cell culture prolongs the Smad1 C-terminal signal (Fuentealba et al., 2007).

Once Smad1 is phosphorylated in the linker region by both kinases, signal termination is set in motion. Smurf1 is an E3-ubiquitin protein ligase (of the WW-Hect family), which restricts BMP signaling and is required for the degradation of Smad1 (Podos et al., 2001; Murakami et al., 2006; Shi et al., 2004). Linker phosphorylation of Smad1 is essential for Smurf1 binding to its recognition motif, PPXY, which is located near the linker phosphorylation sites (Fuentealba et al., 2007; Sapkota et al., 2007). Smad1 is then polyubiquitinated and degraded in proteasomes (Figure 2.2) (Fuentealba et al., 2007). Thus, the inhibitory phosphorylations of the MAPK and GSK3 sites regulate the duration of the Smad1/5/8 signal. At high FGF levels the BMP signal will be shorter. Wnt signaling inhibits GSK3 and therefore at high Wnt levels the BMP signal is of longer duration. In this way, BMP determines the intensity of the Smad1/5/8 response, while FGF decreases and Wnt increases its duration (Figure 2.2).

2.6 Asymmetric inheritance of Smad1

Termination of the Smad1/5/8 signal involves linker phosphorylations at the MAPK and GSK3 sites and polyubquitinylation. Smad1 targeted for degradation

also requires transport along microtubules to be degraded by the proteasomal machinery in the pericentrosomal region of the cell (Fuentealba et al., 2008). Inhibition of the proteasomal enzymatic machinery using Lactacystin, a chemical inhibitor, caused accumulation of pSmad1 marked for degradation in the centrosomal region (Figure 2.3 A).

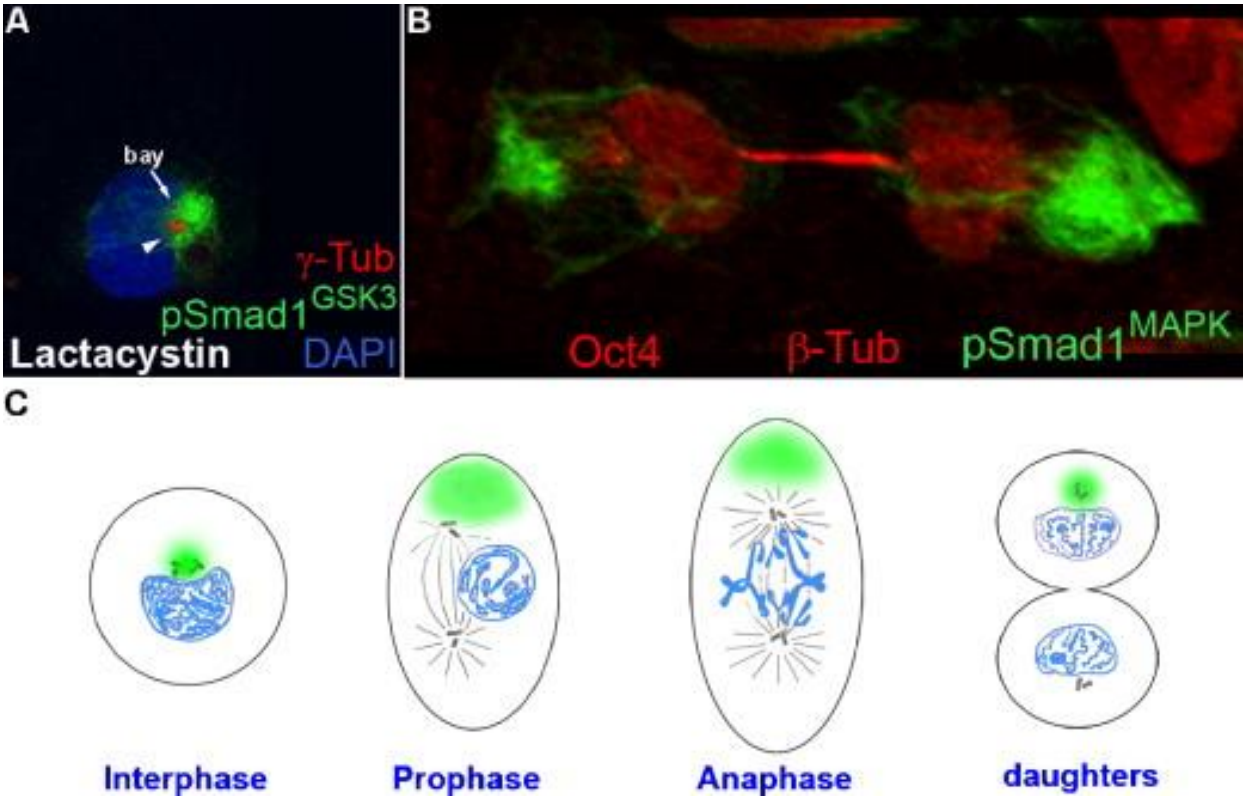

Figure 2.3: Asymmetric inheritance of Smad1

(**A**) Asymmetric distribution of pSmad1 targeted for degradation in self-renewing human embryonic stem cells.
(**B**) When the proteosomal machinery is inhibited pSmad1GSK3 accumulates in a pericentrosomal nuclear bay.
(**C**) Model illustrating asymmetric inheritance of pericentrosomal material (green) during mitosis (Fuentealba et al., 2008).

Unexpectedly, in cultured cells, particularly in human embryonic stem cells, we observed that linker-phosphorylated Smad1 was asymmetrically distributed during mitosis (Fuentealba et al., 2008) (Figure 2.3 B). This asymmetry took place in stem cells undergoing self-renewal, which were supposed to be equal divisions. Analysis of Cos7 cells showed a similar tendency to segregate pSmad1MAPK or pSmad1GSK3 asymmetrically, with one of the dividing daughter cells retaining the linker-phosphorylated Smad1 (Fuentealba et al., 2008). The asymmetric segregation is not a unique property of Smad1, for other proteins targeted for degradation, such as phospho-beta-catenin and total polyubiquitinated proteins (which include hundreds of cellular proteins) are also unequally segregated between daughter cells.

This asymmetry appears to be a general property of cell division as shown in the model in Figure 2.3 C. When the centrioles separate before mitosis to occupy opposite cell poles, the pericentrosomal material is inherited preferentially by one of the daughter cells. This simple cellular mechanism can explain the mitotic asymmetries. To investigate if this remarkable phenomenon occurred in vivo, an antibody was raised against the single MAPK phosphorylation site present in the linker region of Drosophila Mad. The pMadMAPK antibody stained a single bright spot in every blastoderm cell and co-localized close to one of the two centrosomes (Fuentealba et al., 2008).

The asymmetric distribution of phosphorylated proteins targeted for degradation uncovered an interesting phenomenon and raises many questions. Is it a cleansing mechanism so one daughter remains pristine; simply a case of garbage the cell wants to get rid of? Or are the asymmetric proteins targeted for degradation junk the cell might want to reuse? Is this asymmetry regulated by extracellular signals? These and other questions are under active investigation. Since the first description of mitosis by Flemming in 1882, studies on somatic cell division had focused on the equal partition of cellular materials. The new phospho-specific Smad1 MAPK and GSK3 antibodies were of very high titer and marked proteins destined for degradation. These new reagents made possible the discovery of inequalities in many mitoses, which we hope will advance the cell biology of signaling.

2.7 Smad1 signal duration: phenotypic similarities between BMP and Wnt antagonists in the developing embryo

With the advent of modern molecular embryology it became clear that D–V or A–P pattern formation were intertwined. For example, overexpression of BMP or Wnt antagonists in embryos, such as Chordin or Dkk-1 respectively, generated almost indistinguishable dorsalized phenotypes (Fuentealba et al., 2007). These and other

experiments suggested some type of cross-talk between the BMP and Wnt pathways. The node of interaction has now been shown to reside at the level of Smad1GSK3 linker phosphorylations. Wnt was shown to inhibit phosphorylation of Smad1 by GSK3 (Fuentealba et al., 2007). This stabilizes the Smad1 transcription factor, allowing it to extend the duration of the BMP signal.

The intensity of the BMP signal can be lengthened or shortened via linker phosphorylations (Fuentealba et al., 2007). The pSmad1Cter signal intensity will be highest in the ventral region of the gastrula embryo, where BMP is highest. The Wnt pathway, which is strongest in the posterior region of the embryo, provides an extracellular signal that prolongs the duration of the pSmad1Cter signal by inhibiting GSK3 phosphorylation of Smad1, preventing its degradation in the cell (Figure 2.2). The implications of these experiments go beyond a simple point of signal convergence. These studies help explain how an embryo reads, processes, and integrates the BMP and Wnt morphogenetic gradients in an embryo, thus determining the overall positional information that determines where the future organs or appendages will develop within the body plan (Figure 2.1).

2.8 Linker regulation of Drosophila Mad

Drosophila Mad, like its vertebrate counterparts Smad1/5/8, contains both MAPK and GSK3 phosphorylation sites within its linker domain. However, unlike the vertebrate BMP-Smads, Mad contains just a single canonical MAPK phosphorylation site and two upstream GSK3 sites. With a reduced number of phosphorylation sites and just one gene, Drosophila provided an ideal developmental model to study cross-talk between Wg (Wingless) and BMP signaling (Eivers et al., 2009). We mutated Mad MAPK (MMM) or GSK3 (MGM) Serine phosphorylation sites into Alanines. Expression of these constructs was driven in wing imaginal discs using the UAS-Gal4 system (Brand and Perrimon, 1993). Large amounts of ectopic vein and crossvein-like tissue were induced in adult wings (Eivers et al., 2009), a sign of increased Dpp (Decapentaplegic, a homologue of BMP2/4) signaling. MGM overexpression also increased expression of Dpp target genes Spalt and Optomotor-blind in wing discs, without increasing Dpp expression levels. Mutation of either phosphorylation site prevented Smurf-induced ubiquitination and degradation of Mad (Eivers et al., 2009), explaining how point mutations in Mad result in a hyperactive transcription factor.

2.8.1 Mad linker phosphorylations: BMP dependent or independent?

To determine whether the Mad linker phosphorylations were always BMP-dependent, polyclonal phospho-specific antibodies were raised against both the MAPK and GSK3 phosphorylation sites. Whole-mount immunostaining of blastoderm embryos was carried out to detect in vivo localization of the pMadMAPK and pMadGSK3. A narrow dorsal stripe was present containing strong nuclear accumulation of linker-phosphorylated forms of pMad. These MAPK and GSK3 phospho-stainings tracked pMadCter and were Dpp-dependent, as they were absent in Dpp null embryos. However, pMadMAPK and pMadGSK3 remained in the rest of the blastoderm embryo and therefore appear to be also Dpp-independent. pMadMAPK stained a single bright cytoplasmic spot of antigen usually adjoining one of the cellular centrosomes, where its degradation takes place (Fuentealba et al., 2008; Eivers et al., 2009). The persistence of the asymmetric centrosome-associated spots in Dpp null embryos indicates that MAPK and GSK3 phosphorylations can occur independently of Dpp.

The Dpp-independent in vivo staining was also supported by Drosophila S2 cell culture experiments using the Mad "null" mutant alleles, Mad10 and Mad12. Both these mutants contain point mutations in the MH2 domain of the transcription factor that prevent BMPR phosphorylation of Mad and are described in the

literature as nulls. cDNAs encoding MWT, Mad10 or Mad12 were expressed in Drosophila S2 cells, and it was found that MWT had phospho-MadCter (as expected), while both mutants did not have any C-terminal phosphorylation. However, the pMadMAPK and pMadGSK3 sites were phosphorylated normally in the mutant proteins. These data showed that Mad10 and Mad12 proteins were stably translated and were nulls for Dpp C-terminal phosphorylation, but were still regulated by MAPK and GSK3 linker phosphorylations, further supporting a Dpp-independent regulation of the linker domain of Mad (Eivers et al., 2009).

In microinjected Xenopus embryos, Mad12 mRNA reduced forebrain structures. When the GSK3 sites of Mad12 were mutated (mimicking a protein receiving a maximal Wnt signal), the head region was almost eliminated. These results suggest that Mad linker phosphorylations can be BMP-dependent or BMP-independent, and that Mad can still function in A–P axis patterning in the absence of C-terminal phosphorylation (Eivers et al., 2009).

2.8.2 Phospho-resistant Mad mutants display Wg-like phenotypes

The Drosophila studies revealed that Wg cannot only determine the stability of Mad by inhibiting GSK3 phosphorylation, as in the vertebrates (Fuentealba et al., 2007), but that Mad stabilized by Wg is involved in canonical Wg signaling. This

is a notable discovery, which places Mad as transducer of both the Dpp and Wg pathways (Eivers et al., 2009).

When Mad resistant to GSK3 phosphorylation (MGM) was driven in wing imaginal discs, additional Wg-dependent sensory bristles were formed along the anterior wing margin, whereas overexpression of MWT had little effect. Analysis of senseless, a Wg target gene required for sensory bristle formation, revealed a marked expansion of the number of cells overexpressing MGM.

MGM cell clones (marked by yellow (Struhl and Basler, 1993)) induced ectopic wing margins (Figure 2.4 A), while MWT clones had no effect on the wing margin. In knockdown experiments, UAS-Mad RNAi clones resulted in loss of wing margin tissue (Figure 2.4 B), a reliable readout for Wg loss-of-function. Thus, overexpression of Mad GSK3 phosphorylation-resistant mutant protein, which mimics Mad receiving a maximal possible dose of Wg, caused Wg-like phenotypes (in the absence of increased Wg signals). Conversely, Mad depletion caused Wg loss-of-function phenotypes. Mad, a protein that is phosphorylated by GSK3 in a Wg-regulated manner appears to be a component of the Wg signal transduction pathway.

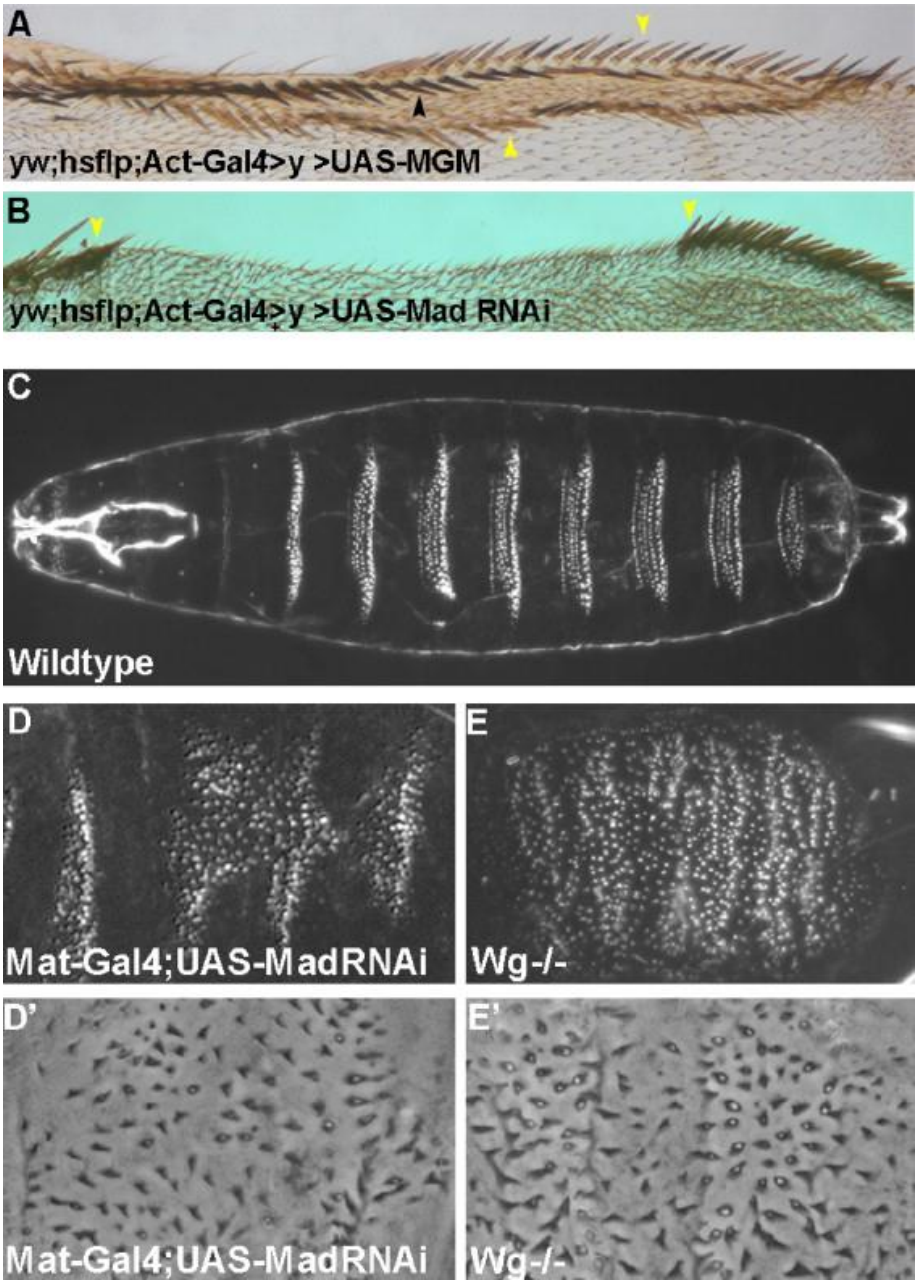

Figure 2.4: Drosophila Mad transduces Wg signals.

(**A-B**) Overexpression of MGM in clones induces duplications, and Mad depletion resulted in loss-of the margin.
(**C**) Wild-type cuticle.
(**D–D′ and E–E′**) Lawns of row 5 denticles in Mad RNAi or Wg null cuticles (Eivers et al., 2009).

2.8.3 Mad and Smad1 are required for segment formation

A remarkable finding from the study of linker phosphorylation regulation of Drosophila Mad was its involvement in segmental patterning. Maternal depletion of Mad using a pUASp-Mad RNAi (which can be expressed in the oocyte) caused denticle belt fusions at larval stages (Eivers et al., 2009). These fusions replaced regions of naked cuticle with lawns of large denticles of the same type (row 5) as those seen in Wg null cuticles (Figure 2.4 C and D) (Bejsovec and Wieschaus, 1993). In gain-of-function experiments, overexpression of Mad GSK3 mutant caused denticle belts to be replaced by regions of naked cuticle, mimicking Wg overexpression (Eivers et al., 2009). Thus, depletion or overexpression of Mad generated Wg-like phenotypes, indicating that Mad functions in the Wg signaling pathway during segmental patterning.

Finding a role for Mad in segmentation was surprising, since the segmentation process had previously been extensively studied in classical Drosophila genetic screens (Nüsslein-Volhard and Wieschaus, 1980; Sekelsky et al., 1995) and Mad had not been implicated as part of the segmentation machinery. The discovery of this new role for Mad after so many years, may be explained by the fact that Mad appears to also function independently of Dpp, and that the

Mad10 and Mad12 null alleles are nulls only for the BMP pathway, retaining linker regulation.

2.8.4 The ancestry of segmentation

The role of Mad in segmentation appears to be evolutionary conserved, as it was found that Smads have a role in somite border formation in Xenopus embryos. When the main maternally expressed Smad, Smad8 (Miyanaga et al., 2002), was depleted in the C3 blastomere (using a specific morpholino oligonucleotide), segmental somite borders were erased in the injected side at the tadpole stage (Figure 2.5 A–C). The Smad8 transcription factor designated as Smad8 in Xenopus probably corresponds to Smad5 of other vertebrates (Tucker et al., 2008; Miyanaga et al., 2002). Thus, the Mad/Smad5/8 transcription factors are required for segmentation both in *Drosophila* and *Xenopus*. These results are of considerable evolutionary interest.

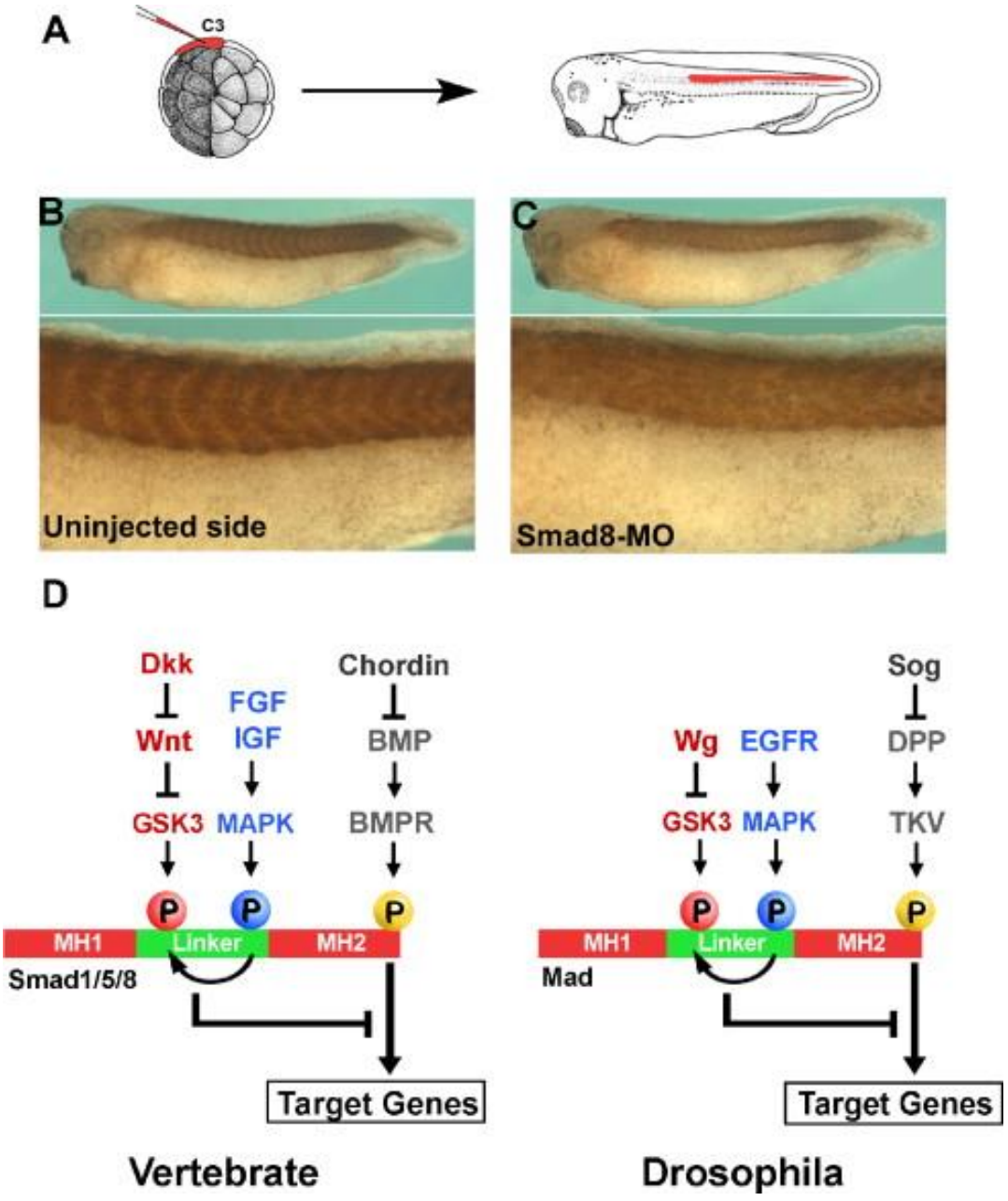

Figure 2.5: The ancestry of segmentation

(**A**) C3 *Xenopus* blastomere injection targets somites in *Xenopus*.
(**B**) Normal somite border pattern on injected side.
(**C**) Microinjection of Smad8-MO erase segmental somite borders (Eivers et al., 2009).
(**D**) Comparison of Smad/Mad linker regulation in vertebrate and *Drosophila*.

Many developmental mechanisms have been shown to be conserved throughout evolution (De Robertis, 2008). However, no common genes required for segment formation have been found between vertebrates and *Drosophila*. Segmentation in vertebrates depends on the cyclic oscillation of Notch pathway transcripts in the posterior paraxial mesoderm of the embryo (Pourquié, 2006). Given that BMP/Smad signals have a duration of 1–2 h in cultured cells (Fuentealba et al., 2007), and are regulated by GSK3 phosphorylations, Smad1/5/8 could be a potential regulator of the segmentation clock. Wnt pathway genes cycle rhythmically during segmentation in vertebrates (Pourquié, 2006), offering an interesting possibility for regulating Smad5/8 activity by modulating GSK3 activity. Notch, which is involved in spider and cockroach segmentation (Damen, 2007; Pueyo et al., 2008), is not required for Drosophila segmental formation. We have now found that Smad5/8 is required for the formation of segmental boundaries in *Xenopus* somites and that Mad is required for *Drosophila* segment patterning. This unexpected conserved role for Mad/Smad is important from an Evo-Devo perspective because it suggests that the last common ancestor shared between Drosophila and vertebrates, Urbilateria, might have been segmented (De Robertis, 2008b).

2.9 Conclusions

Finding new nodes of integration is essential to understanding how the multitude of signals received by each cell is read and interpreted in embryos and adult tissues. The discovery that Smad1/5/8 and Drosophila Mad receive negative linker phosphorylations from both MAPK and GSK3 not only explains how the BMP signal is terminated, but also uncovered a novel cell biological pathway of how Smad1/Mad is transported to and degraded in the centrosomal region of a cell. Linker-phosphorylated forms of Smad1 are asymmetrically distributed in dividing cells and inherited unequally by daughter cells after cell division. The demonstration that active Wnt signals, which inhibit GSK3 activity, prolong the duration of the BMP/pSmad1Cter signal helps explain the similarities between the dorsalizing phenotypes of anti-BMPs and anti-Wnts when overexpressed in Xenopus embryos. The intensity of the BMP signal is transduced by Smad1/5/8 in the form of C-terminal phosphorylations that determine the D–V axis. The duration of the BMP signal (De Robertis, 2008) is regulated by the Wnt morphogenetic gradient that specifies the A–P axis. The finding that three major signaling pathways – MAPK, Wnt/GSK3 and BMP – are integrated at the level of Mad/Smad1/5/8 both in the vertebrates and Drosophila (Figure 2.5 D) has interesting implications for the evolution of animal forms through variations on an

ancestral gene tool-kit (Figure 2.5 D) (De Robertis, 2008). Although much has been learned about the role of Smad1/Mad as a mode of signaling integration, many open questions remain to be answered before we understand the function of these remarkable transcription factors.

Acknowledgements

We thank members of our laboratory for critical readings of this manuscript. Our work is supported by the NIH (HD21502-23) and the Howard Hughes Medical Institute.

CHAPTER 3

Phosphorylation of Mad Controls Competition Between Wingless and BMP Signaling

This Chapter contains text and figures as published in

Science Signaling, 194: p. ra68 (2011)

Edward Eivers*, Hadrien Demagny*, Renee H. Choi, and Edward M. De Robertis

* These authors contributed equally to this work.

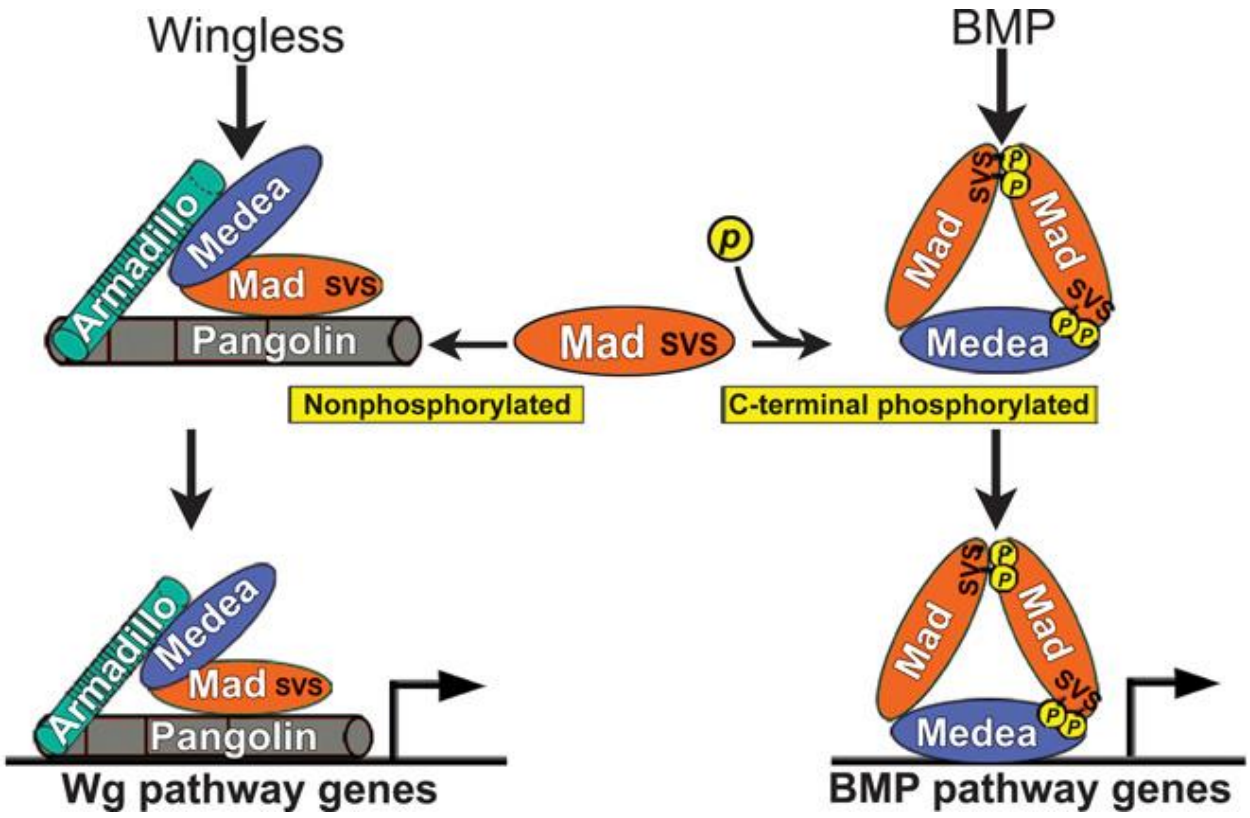

When I joined the lab, a post-doctoral trainee Edward Eivers had just observed that loss-of-function or overexpression of the Dpp transducer Mad could produce striking Wg-like phenotypes (Eivers et al., 2009). However it was not clear if these Wg phenotypes resulted from an indirect induction of Dpp target genes or from a direct implication of Mad in the Wnt transcriptional complex. This study was initiated to answer these questions. Using a combination of biochemistry and genetic experiments, we found that Mad was part of the core Wnt transcriptional machinery but could only participate in the transcription of Wg target genes when not phosphorylated at its C-terminus and not phosphorylated by GSK3. This

mechanism helped us explain observations by our lab (Eivers et al., 2009) and others (Zeng et al., 2008) who reported clear evidences of a competition between Dpp and Wg pathways in the *Drosophila* wing imaginal disc. I contributed to about half of the data presented in this chapter focusing on the biochemistry experiments to demonstrate that the binding between Mad and Pangolin was regulated by phosphorylation.

ABSTRACT

Bone morphogenetic proteins (BMPs) and Wnts are growth factors that provide essential patterning signals for cell proliferation and differentiation. Here, we describe a molecular mechanism by which the phosphorylation state of the Drosophila transcription factor Mad determines its ability to transduce either BMP or Wingless (Wg) signals. Previously, Mad was thought to function in gene transcription only when phosphorylated by BMP receptors. We found that the unphosphorylated form of Mad was required for canonical Wg signaling by interacting with the Pangolin-Armadillo transcriptional complex. Phosphorylation of the carboxyl terminus of Mad by BMP receptor directed Mad toward BMP signaling, thereby preventing Mad from functioning in the Wg pathway. The results show that Mad has distinct signal transduction roles in the BMP and Wnt pathways depending on its phosphorylation state.

3.1 Introduction

Wnts and bone morphogenetic proteins (BMPs) are crucial morphogens that instruct cells when to divide, differentiate, or die (Schwank et al., 2010). Both signaling pathways use a distinct repertoire of molecules to carry out their specific intracellular functions. Binding of Wingless (Wg, the *Drosophila* homolog of Wnt) to its receptors causes the stabilization and nuclear accumulation of the protein Armadillo (called beta-catenin in vertebrates), which forms a transcriptional complex with the DNA-binding HMG (high-mobility group) protein Pangolin [called T cell factor (Tcf) in vertebrates] (Logan and Nusse, 2004). Decapentaplegic (Dpp, a BMP ligand in *Drosophila*) signals by binding to its serine-threonine kinase transmembrane receptors, causing the phosphorylation of two C-terminal serine residues in the transcription factor Mad (the *Drosophila* homolog of vertebrate Smad1). Mad then interacts with the co-Smad Medea (called Smad4 in vertebrates), accumulates in the nucleus, and activates target genes. Although both cascades can function independently of each other, an increasing number of interactions have been described between these two pathways. During development, the BMP and Wnt pathways can synergize positively (through separate binding sites in enhancer elements in the genome) (Takaesu et al., 2008; Estella et al., 2008), or negatively by mutual antagonism at

the level of growth factor transcription (Theisen et al., 1996; Morimura et al., 1996; Dominguez et al., 1997). In addition, we have previously described a positive node of integration between BMP and Wnt signals at the level of phosphorylation of Mad and Smad1 (Fuentealba et al., 2007; Eivers et al., 2009).

Mad has three distinct structural domains: MH1 (Mad homology 1), which contains the DNA binding domain; MH2, which mediates protein-protein interactions; and the linker domain, which controls protein stability. Mad is phosphorylated by BMP receptors at the C terminus (Ser-Val-Ser) and by mitogen-activated protein kinase (MAPK) or cyclin-dependent kinases 8 and 9 (CDK8 and CDK9) in the linker region (Kretzschmar et al., 1997b; Pera et al., 2003; Alarcon et al., 2009; Aragon et al., 2011). These latter phosphorylation events prime for phosphorylation by glycogen synthase kinase 3 (GSK3), which triggers the polyubiquitinylation and degradation of Mad or Smad1, terminating the BMP signal (Fuentealba et al., 2007; Eivers et al., 2009). Wnt regulates this step by sequestering GSK3 inside multivesicular bodies (MVBs) (Taelman et al., 2010), preventing GSK3-mediated phosphorylation of Mad or Smad1 and therefore prolonging the BMP signal (Eivers et al., 2008). Here, we unexpectedly found a function for Mad in Wg signaling that is independent of phosphorylation of the C terminus of Mad. Genetic and molecular experiments show that unphosphorylated Mad binds to the Wnt transcriptional complex to activate a Wnt reporter gene,

independently of its well-known role in the BMP pathway. The choice between these two distinct functions is controlled by phosphorylation, so that Mad signals in the Wg Pangolin-Armadillo pathway only when not phosphorylated by BMP receptor and GSK3.

3.2 Results

3.2.1 GSK3 phosphorylation of Mad inhibits both BMP and Wg signaling

We noticed that the linker region of Mad contains more putative phosphorylation sites than previously reported (Eivers et al., 2009), with at least 11 potential phosphorylation sites in its linker region (Figures 3.1A and 3.S1A). Three are putative MAPK, CDK8, and CDK9 phosphorylation sites, which can serve as priming phosphates for a total of eight GSK3 phosphorylations (Figure 3.S1A). Mad was stabilized by treating *Drosophila* S2R+ cells with Wg-conditioned medium (Figures 3.S1, B and C). In addition, a form of Mad in which all eight GSK3 phosphorylation sites in the linker region were mutated into alanines (referred to as Mad-GM8) was no longer stabilized by Wg (Figures 3.S1, B and C), indicating that the stabilization of Mad by Wg requires intact GSK3 phosphorylation sites in its linker region. As expected for a transcription factor involved in the BMP pathway (Fuentealba et al., 2007; Eivers et al., 2009), the stabilized Mad mutant (Mad-GM8) increased the activity of a BMP reporter gene containing a BMP response element driving luciferase expression (Figures 3.1B and 3.S1D), and inhibition of GSK3 by lithium chloride (LiCl) prolonged the duration of BMP signaling after a short BMP pulse (Figure 3.S1E). In the wing

imaginal disc, Brinker acts as a transcriptional repressor of genes activated by Dpp, and one of the functions of Dpp-activated Mad is to inhibit *Brinker* transcription (Muller et al., 2003). In vivo, expression of stabilized Mad (Mad-GM8) increased BMP signaling in wing imaginal discs as demonstrated by reduced expression of *Brinker* (Figure 3.1 C to E). Mad-GM8 also induced ectopic wing vein formation, a phenotype typical of excess BMP signaling, to a greater extent than caused by the previously described form of Mad with mutations in two GSK3 sites (Mad-GM2) (Eivers et al., 2009) (Figure 3.S1, F to O). We conclude that GSK3 phosphorylation regulates the duration of the BMP signal through Mad (Fuentealba et al., 2007; Eivers et al., 2009).

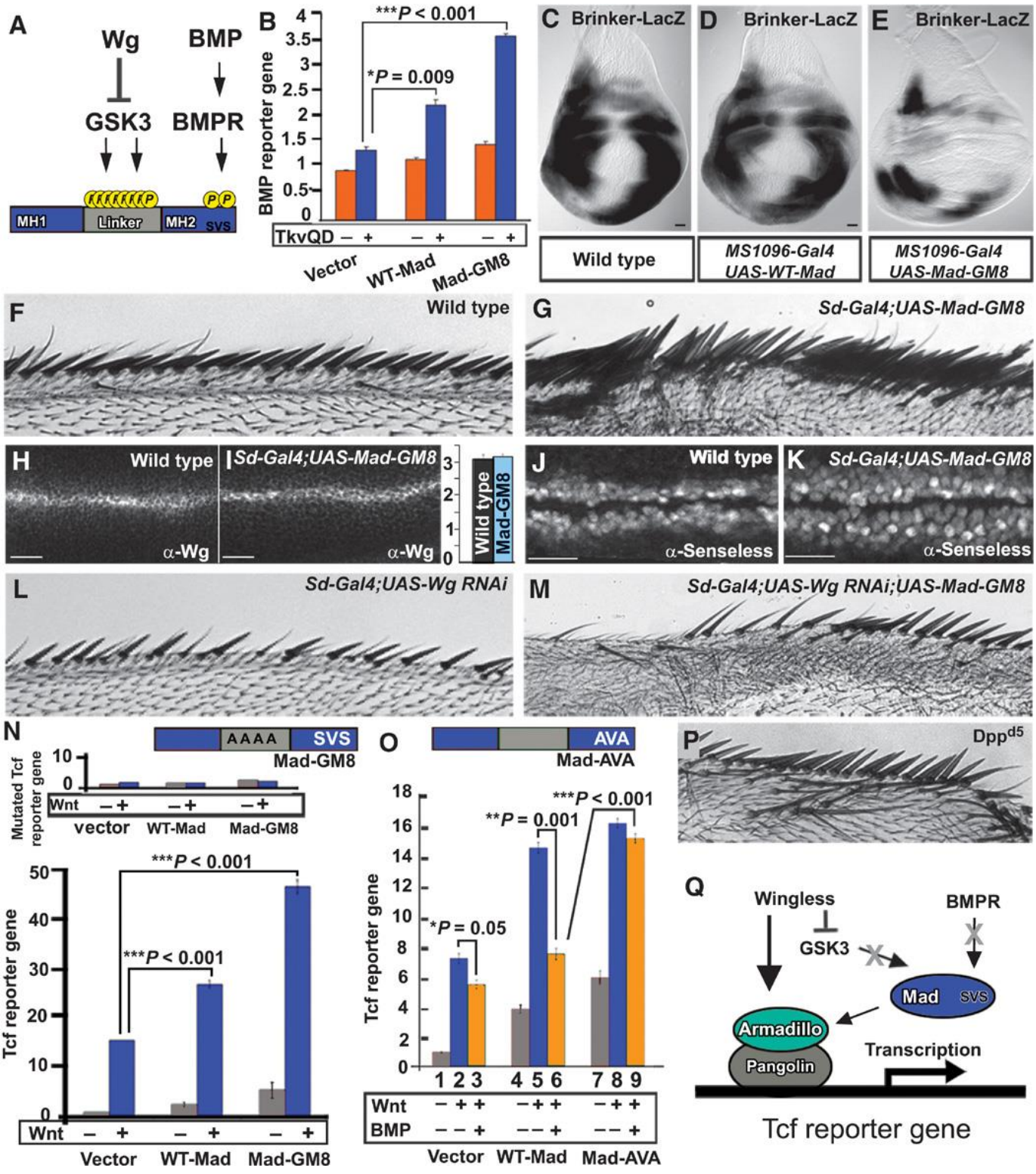

Figure 3.1: The phosphorylation state of Mad determines whether it signals through the BMP or the Wg pathway.

(**A**) GSK3 and BMP receptor (BMPR) phosphorylation sites in Mad.
(**B**) Wild-type Mad (WT-Mad) and Mad-GM8 increased the activity of the BMP reporter gene [**P* = 0.009; ****P* = 0.001, two-way analysis of variance (ANOVA) with Tukey's post test]. The BMP pathway was stimulated with an activated BMP receptor, activated Thickveins (TkvQD), in *Drosophila* S2 cells.
(**C** to **E**) Mad-GM8 increased BMP signaling as indicated by repressed *Brinker* expression in wing discs. *n* = 16 (C), *n* = 8 (D), and *n* = 7 (E).
(**F** and **G**) WT (*n* = 31) and ectopic wing margin bristles induced by Mad-GM8 overexpression (*n* = 40).
(**H** to **K**) Mad-GM8 did not alter endogenous Wg amounts (*P* > 0.66, *n* = 20 intensity measurements) but did increase the area of the Wnt target Senseless (*P* = 0.0086, *n* = 20 intensity measurements; Mann-Whitney Wilcoxon test). Numbers of wing discs examined were *n* = 40 (H), *n* = 10 (I), *n* = 16 (J), and *n* = 12 (K).
(**L** and **M**) Sensory bristle induction by Mad-GM8 required endogenous Wg. *n* = 16 (L) and *n* = 17 (M).
(**N**) WT-Mad and Mad-GM8 increased Tcf reporter gene activity in HEK293T cells, effects that were abolished by mutating the Tcf DNA binding sites (inset) (****P* < 0.001, two-way ANOVA with Tukey's post test; *n* = 6 experiments).
(**O**) Tcf reporter gene induction by WT-Mad, but not by phosphorylation-resistant Mad-AVA, is repressed by treating cells with BMP4 (**P* = 0.05; ***P* = 0.001; ****P* < 0.001, two-way ANOVA with Tukey's post test; *n* = 3 independent experiments).
(**P**) Ectopic bristles in Dpp^{d5} (Zeng et al., 2008) mutant wings (*n* = 12, 7 wings with extra bristles).
(**Q**) Proposed model in which Mad interacts with the Wg transcriptional complex. Scale bars, 20 μm.

In addition to the phenotypes noted above indicative of high BMP signaling, the stabilized form of Mad (Mad-GM8) caused induction of sensory bristles along the margin of the wing (Figure 3.1, F and G). This phenotype is typically associated with increased Wg signaling (Couso et al., 1997), prompting us to investigate the molecular mechanism by which Mad functions in the Wg pathway. The induction of bristles by stabilized Mad took place without changes in Wg protein abundance (Figure 3.1, H and I). However, the area of Wg targets such as Senseless (Figure 3.1, J and K) and Distalless (Figure 3.S2) was expanded by expression of Mad-GM8. This bristle induction required endogenous Wg (Figure 3.1, G, L, and M, and Figure 3.S3). Furthermore, Mad-GM8 overexpression induced phenotypes in eye imaginal discs reminiscent of those caused by gain-of-function mutations for Wg, such as transdetermination of adult eye cells into antenna-like tissue (Figure 3.S4) (Duong et al., 2008, Schubiger et al., 2010).

We next investigated whether Mad could activate a Tcf reporter gene (Super 7x TOPFLASH luciferase). Tcf reporter activity after Wnt3a treatment was increased by expression of wild-type Mad and to a greater extent by expression of stabilized Mad-GM8 (Figure 3.1N). As a control, we used a mutated Tcf reporter gene (Super 7x FOPFLASH luciferase) that cannot bind Tcf, and, as expected, this reporter gene failed to respond to wild-type or stabilized Mad transfection (inset in Figure 3.1N), demonstrating that Mad requires Tcf binding sites to activate Wnt

signaling. Together, these data indicated that inhibition of the GSK3-mediated phosphorylations of Mad enhances cellular responsiveness not only to BMP but also to Wnt.

3.2.2 Mad activates Wg target genes independently of phosphorylation of its C terminus

To rule out the possibility that Mad caused ectopic margin bristles by increasing BMP signals, we carried out three experiments. First, Dpp misexpression in wing discs caused loss of margin bristles (Figure 3.S1J). Second, addition of BMP4 inhibited stimulation of Wnt signaling in cells transfected with empty vector (Figure 3.1O); inhibition by BMP4 was more marked in cells transfected with wild-type Mad (Figure 3.1O). Third, a mutant with a partial Dpp loss of function (Dpp^{d5}) (Bryant, 1988) developed ectopic anterior margin bristles (Figure 3.1P), a phenotype indicative of increased Wg signaling. We conclude from these results that Dpp signaling normally inhibits canonical Wg signaling and that Mad may therefore induce Wg signaling through a Dpp-independent pathway.

To investigate this BMP-independent function further, we constructed a C-terminal phosphorylation-resistant mutant Mad by mutating the serine residues phosphorylated by BMP receptor (Ser-Val-Ser) into alanine residues (Ala-Val-Ala)

(Mad-AVA) (Figure 3.1O). This mutant form of Mad was inactive in the BMP pathway when compared to wild-type Mad (Figure 3.S1D), but activated Tcf reporter gene assays (Figure 3.1O, bar 8). In addition, the effect of Mad-AVA expression on Tcf reporter gene activity was no longer inhibited by BMP addition (Figure 3.1O, bars 6 and 9, and Figure 3.S5).

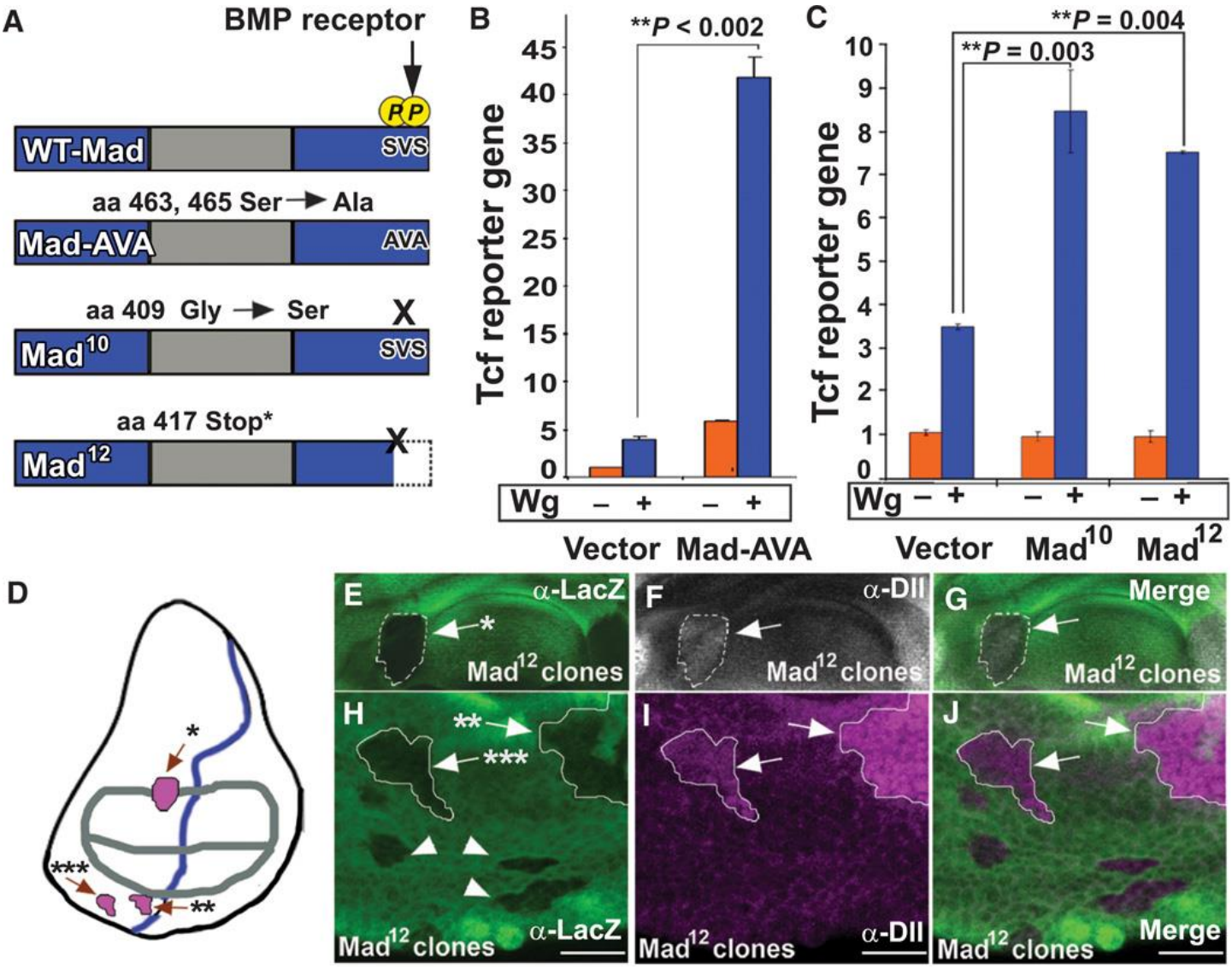

Figure 3.2: Mad transduces Wg signals independently of BMP activity.

(**A**) Diagrams of WT-Mad and phosphorylation-resistant C-terminal Mad mutant proteins.
(**B** and **C**) Mad C-terminal phosphorylation-resistant mutants increase Wg signaling, as measured by Tcf reporter gene activity in *Drosophila* S2R+ cells (***P* = 0.002; ***P*= 0.004; ***P* = 0.003, two-way ANOVA with Tukey's post test; *n*= 3 experiments).
(**D**) Diagram of third instar wing imaginal disc with the location of clones shown indicated by arrows and asterisks; regions of Wg (gray) and Dpp (blue) sources are outlined.
(**E** to **J**) Mitotic Mad^{12} clones in the wing imaginal disc activate the downstream Wg target Distalless near Wg sources. Clones distant to sources of Wg do not

activate Distalless and are indicated by arrowheads. This induction of the Wg target occurred at endogenous amounts of Mad (n = 15 clones from seven wing discs with ectopic Distalless). Scale bars, 20 μm.

These results suggested a molecular mechanism by which Mad interacts with the Wnt transcriptional complex in the absence of active BMP signaling (Figure 3.1Q).

To demonstrate that non-phosphorylated Mad functions in Wg signaling in *Drosophila*, we tested two C-terminal mutant forms of Mad, Mad^{10} (Hoodless et al., 1996) and Mad^{12} (Sekelsky et al., 1995), which lack C-terminal but retain linker phosphorylation sites (Figure 3.2A) (Eivers et al., 2009). *Drosophila* S2R+ cells transfected with phosphorylation-resistant Mad-AVA, Mad^{10}, or Mad^{12} showed increased Tcf reporter gene activity in response to Wg (Figure 3.2, B and C). In wing discs, Mad^{12} clones showed ectopic distribution of Distalless (arrows) close to sources of Wg protein production (Figure 3.2, D to J). Distalless is a specific reporter for Wg signaling in the wing disc (Neumann et al., 1997). Mad^{10} clones can also induce ectopic distribution of Distalless in wing imaginal discs (Zeng et al., 2008). However, Mad^{12} clones distant from Wg sources failed to induce ectopic production of Distalless (Figure 3.2H, arrowheads), suggesting that the induction of Wg signaling by Mad requires additional components, such as stabilized Armadillo, which is only found close to sources of Wg. These data demonstrate that the function of Mad in Wnt signaling occurs independently of BMP-induced phosphorylation of the C terminus of Mad. Increased abundance of the Wg target Distalless in Mad^{12} mutant clones (Figure 3.2I) indicates that

phosphorylation of the C terminus of Mad normally inhibits Wnt signaling at endogenous amounts of this transcription factor in vivo.

3.2.3 Mad and Medea are required for Wg signal transduction

We next examined the requirement of full-length Mad in Wg signal transduction. Because deletion alleles of Mad are not available, we used Mad RNA interference (RNAi) clones (Eivers et al., 2009). Wing discs with Mad RNAi clones lacked Distalless (Figure 3.3, A to D), whereas endogenous Wg was unaffected (Figure 3.3, E and F). The phenotype caused by this Mad RNAi was specific because it was rescued in the whole adult wing with a UAS-Smad1 transgene expressing the human homolog of Mad (Figure 3.S6). Mad knockdown throughout the developing wing pouch reduced the abundance of Wnt target Senseless (Figure 3.3, G and H) and prevented Dishevelled overexpression from inducing ectopic Senseless in the wing pouch (Figure 3.3, compare I to J, and Figure 3.S7, A to D). This epistatic experiment showed that Mad is required downstream of Dishevelled in the Wnt pathway. Similarly, formation of increased numbers of sensory bristles by Dishevelled overexpression was inhibited by Mad RNAi (Figure 3.S7, E to L). Furthermore, Tcf reporter gene activity in S2R+ cells was reduced by Mad RNAi

(Figure 3.3K), an inhibitory effect that was rescued by overexpression of human Smad1 (Figure 3.S7M).

In addition, we found a requirement for Armadillo (Noordermeer et al., 1994) and Medea in Wg signaling in Drosophila S2R+ cells and for Smad4 and beta-catenin in human embryonic kidney (HEK) 293T cells (Figure 3.3, L and M, and Figure 3.S7, N to P).

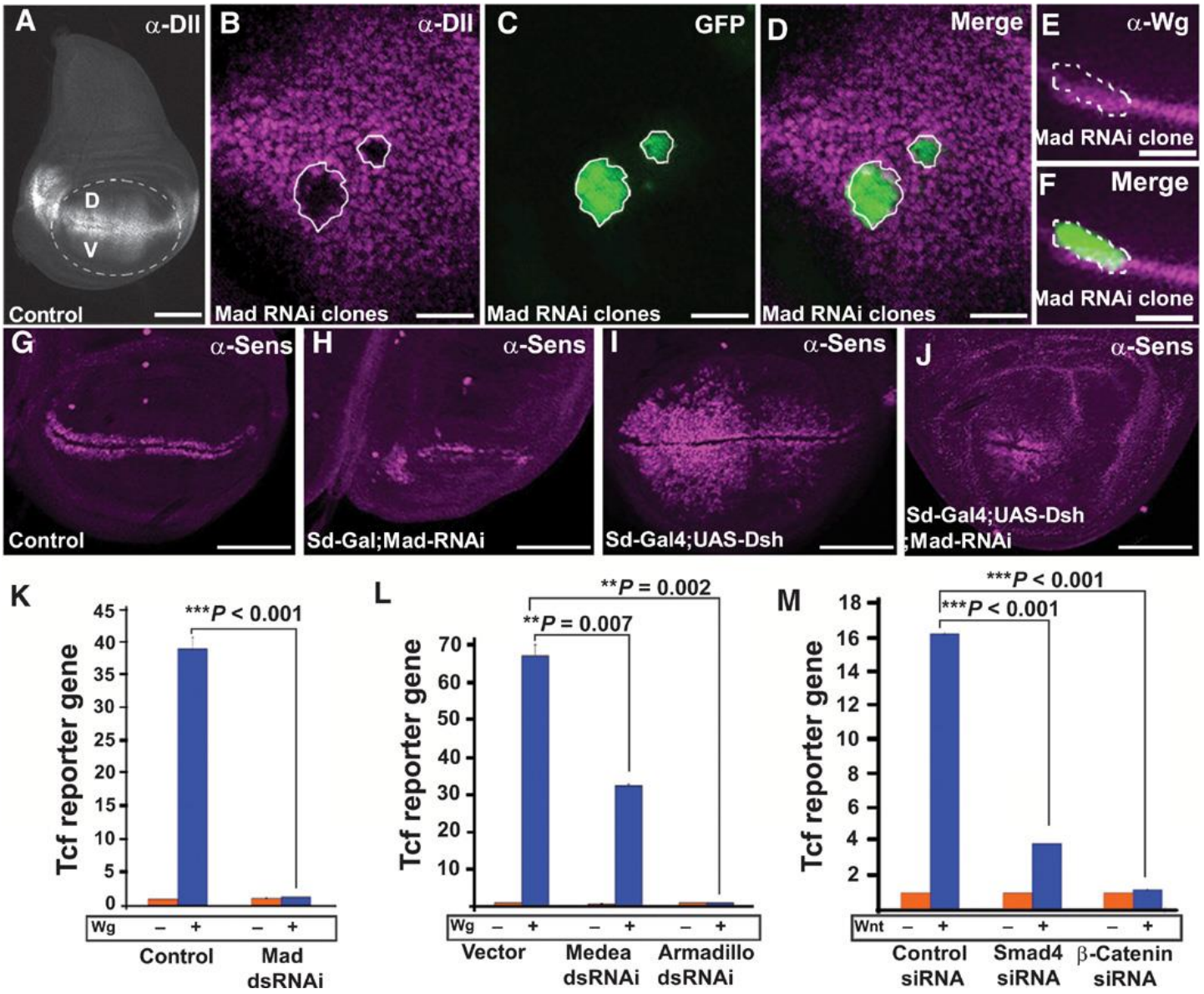

Figure 3.3: Mad and Medea are required for Wg signal transduction.

(**A**) Wild-type distribution of Distalless in a wing imaginal disc. Scale bar, 100 μm. (**B** to **D**) Decreased abundance of the Wnt target Distalless in Mad RNAi clones in the ventral (V) wing pouch. *n* = 10 clones in the region where Distalless is normally found, all showing decreased Distalless abundance. Scale bar, 20 μm.
(**E** and **F**) Wg production was maintained in Mad RNAi clones (*n* = 14 clones; scale bar, 50 μm).
(**G** to **J**) The area of Senseless in wing imaginal discs was reduced in clones expressing Mad RNAi or those expressing both UAS-Mad RNAi and UAS-

Dishevelled. At least 12 discs per genotype were analyzed, with similar results. Scale bars, 100 μm.

(**K**) Knockdown of Mad by dsRNA inhibited the activity of the Tcf reporter gene in *Drosophila* S2R+ cells (***$P < 0.001$, two-way ANOVA with Tukey's post test, $n = 6$ experiments).

(**L**) Knockdown of Medea or Armadillo by dsRNA blocked Wg signaling in S2R+ cells (**$P = 0.007$; **$P = 0.002$, two-way ANOVA with Tukey's post test, $n = 3$ experiments).

(**M**) siRNAs against Smad4 or beta-catenin inhibited Wnt reporter responses in HEK293T cells (***$P < 0.001$, two-way ANOVA with Tukey's post test, $n = 3$ experiments).

These observations are consistent with previous reports that Smad4 interacts with beta-catenin in the activation of Xenopus homeobox genes (Nishita et al., 2000; Labbe et al., 2000). We conclude that Mad and Medea are required for Wg signaling, both in Tcf reporter assays of Wg activity and in vivo in Drosophila.

3.2.4 Mad binds to Pangolin in the absence of phosphorylation of its C terminus

Next, we examined whether Mad could bind to the Pangolin-Armadillo complex. A previous report had described that the mammalian Mad homolog Smad1 interacted with beta-catenin and Tcf to activate Myc transcription (Hu and Rosenblum, 2005). Mad-Flag, Armadillo–HA (hemagglutinin), and Pangolin-Myc were transfected separately into HEK293T cells and cell lysates were prepared. To stabilize Mad and Armadillo, we treated all cultures with the GSK3 inhibitor 6-bromoindirubin-3′-oxime (BIO) (Meijer et al., 2003). We later found that preventing GSK3 phosphorylation of Mad increased binding efficiency (Figure 3.S8, A and B). Less Mad bound to Pangolin in lysates from transfected cells treated with a pharmacologically inactive form of BIO, 1-methyl BIO (Meijer et al., 2003) (Figure 3.S8C).

Mad and Armadillo failed to bind to each other (Figure 3.4A). However, in the presence of Pangolin, Mad-Flag pulled down Pangolin and Armadillo (Figure 3.4B). Thus, Pangolin mediates the binding of both Mad and Armadillo. Moreover, Mad-AVA bound Pangolin to a similar extent as wild-type Mad (Figure 3.4B, compare lanes 2 and 3), suggesting that phosphorylation of the C terminus of Mad is not required for binding of Pangolin. Binding of Mad to Pangolin was previously reported, but it was suggested that the binding of Mad inhibited the interaction between Armadillo and Pangolin (Zeng et al., 2008). The different findings might be due to our use of a GSK3 inhibitor, which stabilizes Mad and Armadillo. As described previously, Mad10 mitotic clones show increased abundance of the Wg target Distalless in wing discs (Zeng et al., 2008). Therefore, we propose that because Mad10 or Mad12 cannot be phosphorylated by BMP receptors, more Mad protein is available to signal through the Wg pathway. We conclude from these biochemical experiments that Mad, Pangolin, and Armadillo can form protein complexes in cell extracts, independently of the phosphorylation of the C terminus of Mad.

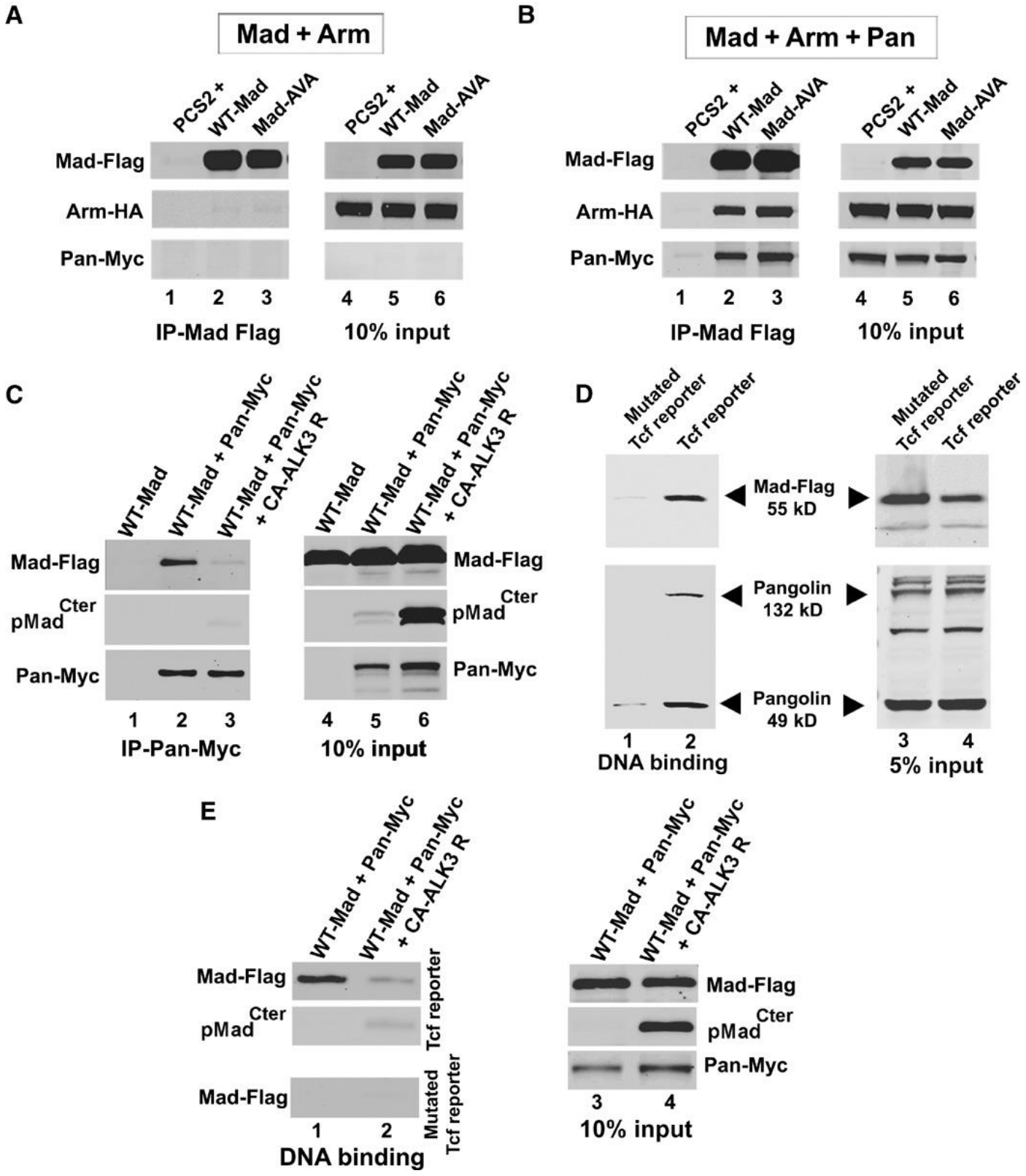

Figure 3.4: Mad is a component of the Wnt transcriptional complex bound to DNA.

(**A**) Mad-Flag did not immunoprecipitate with Armadillo in the absence of Pangolin ($n = 4$ experiments).
(**B**) Mad-Flag bound Pangolin, which also coimmunoprecipitated with Armadillo ($n = 3$ independent experiments).
(**C**) Pangolin-Myc immunoprecipitated unphosphorylated Mad-Flag (lane 2). Less Mad-Flag bound to Pangolin-Myc (lane 3) in cells expressing a constitutively activated BMP receptor (CA-ALK3 receptor) (which would be expected to trigger phosphorylation of sites in the C-terminal domain). Binding of Mad to Pangolin was significantly reduced ($P = 0.0014$, *t* test; $n = 3$ independent experiments).
(**D**) Biotin-labeled PCR products containing Tcf binding sites bound both Pangolin and Mad-Flag proteins (lane 2) from S2R+ cell lysates in a DNA affinity precipitation assay. Pangolin was detected by immunoblotting. PCR products containing mutated Tcf binding sites failed to bind Pangolin or Mad proteins (lane 1) ($n = 3$ experiments).
(**E**) Pangolin-Myc and Mad-Flag bound to PCR products containing Tcf binding sites (lane 1, top panel) but not to those containing mutated Tcf binding fragments (lane 1, bottom panel). C-terminally phosphorylated Mad-Flag extracts did not bind to the PCR products containing Tcf binding sites (lane 2, top panel). Inputs are shown in lanes 3 and 4.

Next, we asked whether binding of Mad to Pangolin was inhibited by phosphorylation of its C terminus. We cotransfected HEK293T cells with Mad-Flag and Pangolin-Myc, with or without a constitutively active Alk3 BMP receptor (CA-Alk3). As expected, expression of CA-Alk3 resulted in phosphorylation of the two C-terminal serine residues of Mad (Figure 3.4C, compare lanes 5 and 6). Pangolin-Myc immunoprecipitated Mad-Flag only in cells lacking the constitutively active Alk3 receptor (Figure 3.4C, compare lanes 2 and 3). Activation of BMP signaling with expression of the constitutively active Alk3 receptor significantly reduced binding of Mad to Pangolin. These experiments indicate that the phosphorylation of the C terminus of Mad has an inhibitory effect on the formation of complexes with Pangolin.

3.2.5 The Pangolin-Mad-Armadillo complex binds to Tcf DNA binding sites

Using a DNA affinity precipitation assay (Lei et al., 2004), we asked whether the protein complex of Pangolin and Mad could interact with Tcf DNA binding sites. A 5′ biotin-labeled and a 3′ unlabeled primer were used to amplify by polymerase chain reaction (PCR) the seven Tcf binding repeats (table 2.S1) of the Tcf reporter gene (SuperTOPFLASH) or its mutated counterpart (SuperFOPFLASH), in which

all seven specific binding sites for Tcf are mutated. Biotin-labeled PCR products were then bound to streptavidin-agarose beads and lysates from Wg-treated Drosophila S2R+ cells transfected with Mad-Flag were incubated with streptavidin-biotin-DNA beads. We found that Mad-Flag and two isoforms of endogenous Pangolin bound to Tcf reporter gene DNA (Figure 3.4D, lane 2). Mad binding to the mutated Tcf reporter gene product was barely detectable (Figure 3.4D, lane 1). In addition, extracts containing C-terminally phosphorylated Mad displayed decreased association with DNA containing Tcf binding sites (Figure 3.4E). In conclusion, these biochemical experiments suggest that Mad preferentially binds to the Pangolin-Armadillo complex on Tcf binding sites in DNA in the absence of phosphorylation of the C terminus by BMP receptor. The results uncover a role for nonphosphorylated Mad in Wg signaling transduction.

3.3 Discussion

We investigated how the phosphorylation state of the transcription factor Mad can determine its ability to transduce a BMP or a Wnt signal in the cell. The molecular mechanism depicted in Figure 3.5 proposes a new layer of regulation in canonical Wg signaling. Mad is required for Wg signaling both in Tcf reporter gene assays and in vivo in Drosophila. This aspect of Mad activity is inhibited by phosphorylation by BMP receptor resulting from activation of the BMP pathway. Wnt signaling sequesters GSK3 from the cytosol into MVBs (Taelman et al., 2010), causing stabilization of Armadillo and Mad, which then binds to Pangolin. This protein complex can bind to Tcf binding sites in DNA to control the transcription of Wnt target genes. The proteins encoded by the Drosophila Mad10 and Mad12 genetic mutants have lost the BMP receptor branch of their function, but retain their ability to engage in Wg signaling (Figure 3.2).

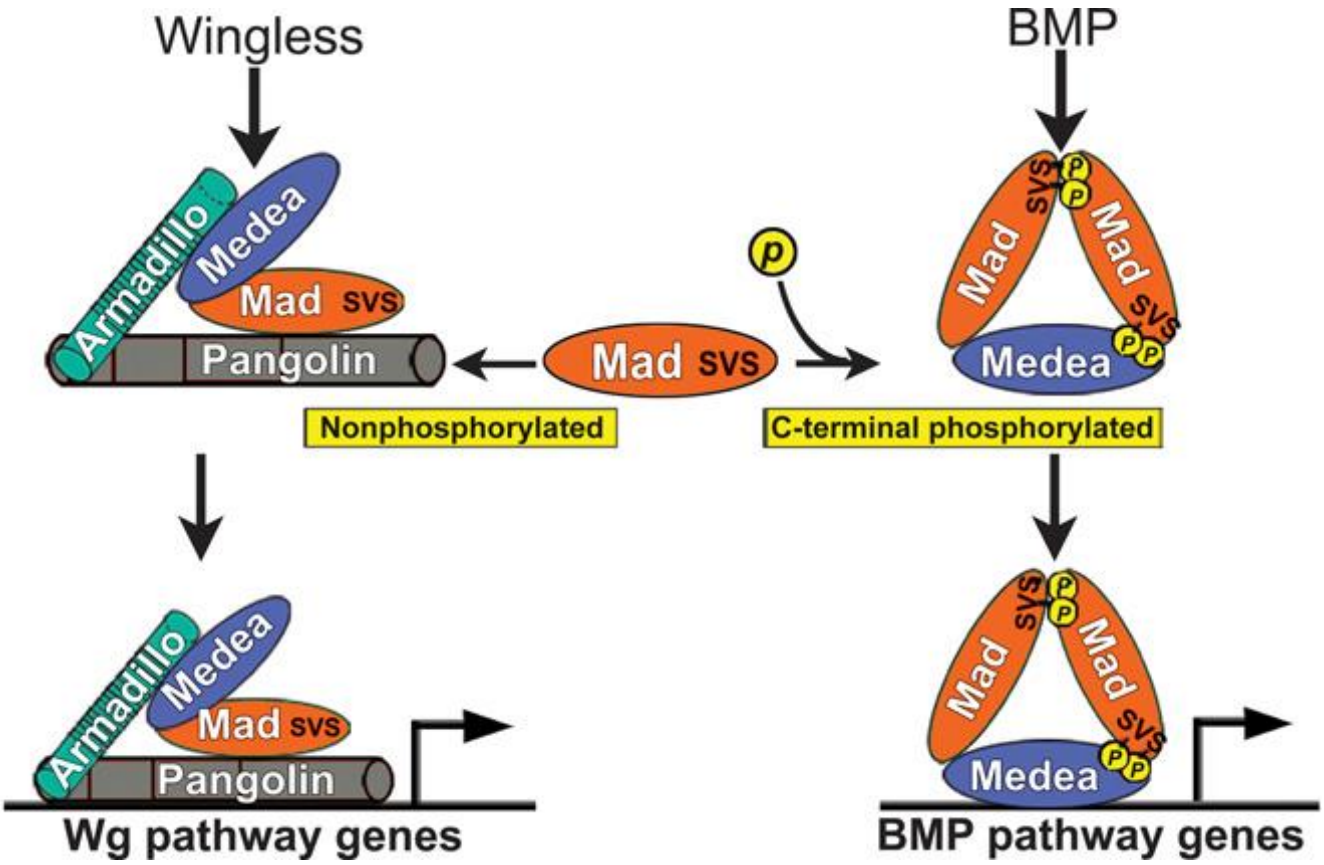

Figure 3.5: Proposed model in which Mad and Medea bind to the Wg Pangolin-Armadillo transcriptional complex in the absence of BMP signals

Previously, Mad was believed to be transcriptionally active only when phosphorylated at its C terminus by BMP receptor. In this model, Mad promotes activation of Wg pathway target genes when not phosphorylated. In the presence of BMP, Wg serves to prolong the signal from Mad phosphorylated in the C-terminal domain by inhibiting GSK3-mediated phosphorylation of the linker region of Mad (Fuentealba et al., 2007; Eivers et al., 2009). In addition, BMP signaling also diverts Mad or Medea from the Wg pathway to promote activation of BMP target genes, thereby causing competition between the BMP and the Wingless pathway.

Interactions between Dpp and Wg signaling, both positive (Takaesu et al., 2008; Estella et al., 2008) and negative (Theisen et al., 1996; Morimura et al., 1996; Dominguez et al., 1997), have been reported in Drosophila. We propose that the BMP pathway would have positive interactions with Wg only for genes with both BMP and Wg response elements in their promoters (Takaesu et al., 2008; Estella et al., 2008). In most other cases, we suggest that the BMP and Wg pathways compete for the available pool of Mad (Figure 3.5). Our findings suggest that Dpp signaling can generate an inverse gradient of Wnt activity because high BMP activity competes for Mad and Medea, reducing their availability to signal in the Wg pathway. Unphosphorylated Mad can participate in Wg signaling when only Pangolin binding sites are present in an enhancer. When BMP receptor phosphorylates Mad, a trimer with Medea would be formed that would direct Mad to BMP responsive promoters (Figure 3.5). It has been proposed that Smad4 is the limiting component in cells transducing BMP and transforming growth factor–beta (TGF-beta) signals (Candia et al., 1997). In a cell receiving both BMP and Wnt signals, Mad phosphorylated at the C terminus would compete with unphosphorylated Mad for limited amounts of Medea. Moreover, most cellular Smad1 has been reported to enter the nucleus in response to BMP2 treatment (Schwappacher et al., 2009), suggesting that the competition between BMP and Wnt signaling could occur directly at the level of Mad as well.

This study advances our understanding of signaling crosstalk between the Wg and the BMP pathways in several ways. First, it shows that Mad, a transcription factor classically associated with the BMP pathway, is also an effector of canonical Wnt signaling. Second, BMP receptor–mediated phosphorylation of Mad is not required for activity in the Wnt pathway. Instead, mutations such as Mad12 that truncate the C terminus increase Wnt signaling at endogenous protein amounts. Third, phosphorylation of the linker region of Mad by GSK3 has an inhibitory effect on Wnt signaling. This previously unknown phosphorylation-independent function of Mad has implications for cell differentiation and cancer.

3.4 Experimental Procedures

Drosophila stocks

Drosophila strains used in this work were as follows: UAS-WT-Mad, UAS-Mad-GM8/Cyo, UAS-Mad-GM2, UAS-human-Smad1, UAS-Dishevelled (#9453), UAS-DN-GSK3, UAS-ArmS10 (#4782), hsflp;UAS-Mad RNAi;UAS-Mad-RNAi, UAS-Wg-RNAi (Vienna Drosophila RNAi Center, VDRC #13352). Gal4 drivers used (Bloomington stock number in parentheses) were as follows: MS1096-Gal4, Scalloped-Gal4 (#8609), Engrailed-Gal4 (#6356), Eyeless-Gal4, and yw;Act>y+>Gal4;UAS-GFP. Other strains used in this study were Brinker-LacZ, Dpp[d5]/Cyo (#2071), and Canton S.

Clonal analysis

For random heat shock "flip-out" clones, we crossed females of the genotype yw;Act>y+>Gal4;UAS-GFP to males of the genotype ywhsflp;Mad-RNAi/Mad-RNAi. Flies laid eggs for 6 to 8 hours, and eggs were incubated for a further 16 to 20 hours at 25°C. Larvae at first instar were administered single heat shocks (37°C) ranging from 5 to 15 min. An RNAi approach was used because no complete loss-of-function Mad mutants exist at present; the most precisely defined deletion of

Mad Df(2L)C28 removes a number of other genes (Wisotzkey et al., 2003). The Mad RNAi construct used previously described Mad sequences (Eivers et al., 2009) placed in a Gal4-inducible pWiz vector (Lee and Carthew, 2003). Mitotic Mad12 clones were induced by crossing female ywhsflp;Arm-LacZM21FRT40/Cyo-GFP with ywhsflp;Mad12FRT40/Cyo males. Flies laid eggs for 8 hours, and eggs were incubated for a further 16 to 28 hours at 25°C. Larvae at the first instar were administered single heat shocks (37°C) ranging from 20 to 30 min. After heat shock, larvae were grown at 25°C for recovery and further development.

Mounting of adult wings

Wings were removed from adult flies and dehydrated in 100% ethanol for 5 min. The wings were placed on a slide with the dorsal side up, and the ethanol was allowed to evaporate. A small drop of Canada balsam was dropped onto the wing and a glass coverslip was placed on top. A 10-g weight was used to flatten the preparation.

Wing disc fixation and immunostaining

Wing discs were dissected from third instar larvae in cold 0.02% Triton X-100 phosphate-buffered saline (PBS) (PBST) solution. Discs were fixed in 4% formaldehyde for 20 min on ice and rinsed with PBST. Discs were then incubated in blocking solution (2.5% bovine serum albumin and 5% goat serum in PBS/0.02% Triton X-100) for 1 to 2 hours at room temperature. Primary antibodies - alpha-Senseless (1:10; gift of H. Bellen), alpha-Distalless (1:300; gift of I. Duncan) (Duncan et al., 1998), alpha-LacZ (1:1000), or alpha-Wg (1:200; Developmental Hybridoma Bank) - were incubated in blocking solution overnight at 4°C and washed 10 times for 2 hours in PBST. Discs were incubated for 1 to 2 hours in blocking solution and incubated for 1 hour in anti-mouse Cy3-conjugated secondary antibody (1:1000, Jackson Laboratory) at room temperature. Wing discs were placed in DAPI (4′,6-diamidino-2-phenylindole)–containing Vectashield (Vector) overnight and mounted on glass slides.

Reporter gene assays in Drosophila S2 and HEK293T cells

To test whether stabilized Mad linker mutants could activate a BMP reporter gene (BRE-luciferase) (Korchynskyi and ten Dijke, 2002) to a greater extent than wild-

type Mad, we cotransfected pAC-Mad (0.1 μg), BMP reporter gene (0.1 μg), and thymidine kinase (TK)–Renilla (0.01 μg) constructs with an activated form of the Thickveins receptor (pAC-TKVQD, 0.1 μg) (Inoue et al., 1998) into S2 cells. Luciferase readings were measured 48 hours after transfection with the Promega Dual-Luciferase Reporter Assay System. S2 cells produce the BMP ligands Dpp and Glass bottom boat (Gbb), and pMadCter is readily detected in nuclei. For this reason, we also used HEK293T cells, which have no detectable amounts of pSmad1Cter, to carry out Wnt reporter assays. HEK293 cells were cultured in 12-well plates and transiently transfected with Fugene (Roche). Renilla luciferase pRLCMV served as the internal control. Transfections contained 0.2 μg of SuperTOPFLASH Tcf reporter gene (Veeman et al., 2003), 0.02 μg of pRL-CMV, and 0.5 μg of the various pCS2-Mad constructs. pCMV empty vector was used to reach a total of 0.72 μg of DNA per well. Wg-conditioned medium from permanently transfected S2 cells (Drosophila Genomics Resource Center, stock #165; originally from R. Nusse) was used to treat Drosophila S2R+ cells. For 293T cells, Wnt3a-conditioned medium from permanently transfected L cells (gift of R. Nusse) was used.

Luciferase assays were performed with the Dual-Luciferase Reporter Assay System (Promega) according to the manufacturer's instructions, and the results were standardized against internal Renilla controls. To assess the duration of BMP

signals (Figure 3.S1E), we transfected cells with BMP reporter gene (BRE-luciferase) (Korchynskyi and ten Dijke, 2002) with wild-type Mad in a six-well plate. Twelve hours later, cells were starved in serum-free medium for 4 hours, and 5 nM BMP7 (R&D Systems) was added for 30 min. Cells were washed in serum-free medium and incubated with or without 30 mM LiCl to inhibit GSK3.

Gene silencing in Drosophila S2R+ cells and HEK293T cells

Double-stranded RNA was used to knock down Mad, Medea, and Armadillo in S2R+ cells. RNA design and treatment was based on the protocol by Clemens and co-workers (Clemens et al., 2000). Primer sequences are found in table S1. The Ambion MEGAscript kit was used for double-stranded RNA (dsRNA) amplification. Cells were treated with Mad, Medea, or Armadillo dsRNA for 4 days. Cells were transfected on day 3 with Tcf reporter gene (0.4 μg) (Veeman et al., 2003) and pTK-Renilla (0.04 μg) with Effectene (Qiagen). On day 4, cells were treated with Wg-conditioned medium or control medium for 8 hours.

To rescue Mad knockdown in S2R+ cells, we used a human Smad1 construct (in pAC 5.1 vector) transfected together with a copper-inducible pWiz-Mad RNAi construct (Lee and Carthew, 2003). Transfection of pWiz-Mad RNAi (0.1 μg), metallothionein-Gal4 (0.1 μg), SuperTOPFLASH luciferase (0.1 μg), and

pTK-Renilla (0.01 μg) was carried out with Qiagen Effectene. S2R+ cells were grown for a total of 4 days and then treated with either Wg-conditioned medium or control medium for 8 hours.

For small interfering RNAs (siRNAs) in HEK293T cells, siRNAs targeting human beta-catenin and Smad4 were ON-TARGETplus SMARTpool from Thermo Scientific (#L-003482 and #L-003902, respectively). Control siRNA was BLOCK-iT Fluorescent Oligo (Invitrogen, #44-2926). siRNAs were transfected with Lipofectamine 2000 by means of the reverse transfection protocol (Invitrogen) and analyzed after 48 hours. Cells were first transfected with siRNA and then with DNA 24 hours later.

Coimmunoprecipitation assays

HEK293T cells were cultured in six-well plates and transiently transfected with DNA using Fugene (Roche). pCMV-Pangolin-Myc, pCS2-Mad-Flag, and pCMV Armadillo-HA plasmid DNAs were transfected separately into HEK293T cells and treated with 5 μM GSK3 inhibitor BIO for 4 hours (Meijer et al., 2003). The use of BIO in this experiment was essential to ensure efficient binding, because GSK3 phosphorylations inhibit complex formation (Figure 3.S8). The Pangolin and Armadillo constructs were gifts of E. Verheyen (Zeng et al., 2008). Cells were

lysed with a standard lysis buffer [50 mM tris (pH 7.4), 150 mM NaCl, 1 mM EDTA, and 1% Triton X-100]. Usually, 250 µl of cell lysate containing Mad proteins was incubated with 250 µl of lysates containing tagged proteins at 4°C with end-over-end rotation for 1 hour. For the binding of Mad-Flag, Armadillo-HA, and Pangolin-Myc, 166 µl of each lysate was added. Immunoprecipitation of Mad-Flag was carried out with anti-Flag beads (Sigma). Beads were centrifuged at 1000g for 1 min. The bound proteins were washed three times with 1 ml of tris-buffered saline (TBS) and then eluted with 200 µl of TBS containing FLAG peptide (100 µg/ml; Sigma) with end-over-end rotation for 30 min at 4°C. The results were analyzed by Western blot. The antibodies used were anti-Flag mouse (Sigma), 1:1000; anti–c-Myc mouse (Santa Cruz), 1:1000; anti-Smad1Cter, 1:1000 (Persson et al., 1998); and anti-HA (Sigma), 1:1000. Pangolin-Myc, Mad-Flag, and CA-ALK3 receptor were cotransfected into HEK293T cells for experiments testing whether C-terminally phosphorylated Mad bound Pangolin. Cells transfected with or without CA-ALK3 were treated with the GSK3 inhibitor BIO for 6 hours before lysate preparation. Pangolin-Myc immunoprecipitation was carried out with anti-Myc beads (Covance AFC-150P) under conditions in which Mad was phosphorylated or not. Elution was performed with Myc peptide (100 µg/ml; Sigma).

DNA affinity precipitation assay

The sequence encoding the seven Tcf binding sites present in the SuperTOPFLASH luciferase reporter (Tcf reporter gene) plasmid was amplified by PCR (Veeman et al., 2003). The primers used were a forward biotin-labeled primer and a nonbiotinylated 3′ reverse primer (table 2.S1). As a negative control, the same primers were used to amplify the sequence of the SuperFOPFLASH luciferase reporter (mutated Tcf reporter gene) (Veeman et al., 2003). The biotinylated PCR products were incubated for 1 hour at 4°C with streptavidin-agarose beads (Sigma, S1638-5ML) (Lei et al., 2004). The beads were then washed three times with binding buffer [10% glycerol, 4 mM tris-Cl (pH 7.9), and 60 mM KCl] to remove unbound PCR products. DNA-biotin-avidin agarose beads were then added to S2R+ cell extracts overexpressing wild-type Mad-Flag. Transfected S2R+ cells were lysed with a modified lysis buffer: 10% glycerol, 4 mM tris-HCl (pH 7.9), 60 mM KCl, and 1% Triton X-100. Cell lysates and beads were incubated overnight at 4°C with end-over-end rotation to allow proteins to bind to DNA (Lei et al., 2004). The beads were then centrifuged at 1000g for 1 min. Bound proteins were washed three times with 1.5 ml of binding buffer [10% glycerol, 4 mM tris-HCl (pH 7.9), and 60 mM KCl] and then eluted by adding 12.5 µl of 5× SDS sample buffer and boiled for 5 min. Proteins were resolved on

polyacrylamide gels followed by immunoblotting with mouse anti-Flag (Sigma; 1:1000) and rabbit anti-Pangolin (1:700).

For the custom Pangolin antibody, a synthetic peptide ([H]-CK-Acp-MPHTHTRHGSSGDDL-[NH2]) was used to immunize two rabbits (8) (Covance). The antiserum recognized three different isoforms of Pangolin in S2 cells (isoform J, 132 kD; isoforms B and H, 85 kD; isoform I, 49 kD), two of which specifically bound to Tcf binding sites.

Mad stability assay

To demonstrate stabilization of wild-type Mad by GSK3 inhibition, we transfected UAS–wild-type Mad-Flag or UAS–Mad-GM8 Flag with a metallothionein-Gal4 plasmid into S2R+ cells. Twelve hours after transfection, cells were treated with 100 mM CuSO4 for 24 hours. Cells were then grown for a further 24 hours in the absence of CuSO4, incubated with Wg medium for 12 hours, and lysed with radioimmunoprecipitation assay (RIPA) buffer. Western blots were performed using standard protocols. A rabbit alpha-Flag antibody (Sigma) was used to detect total amounts of wild-type Mad and Mad-GM8. A mouse alpha-Armadillo antibody was obtained from Developmental Studies Hybridoma Bank.

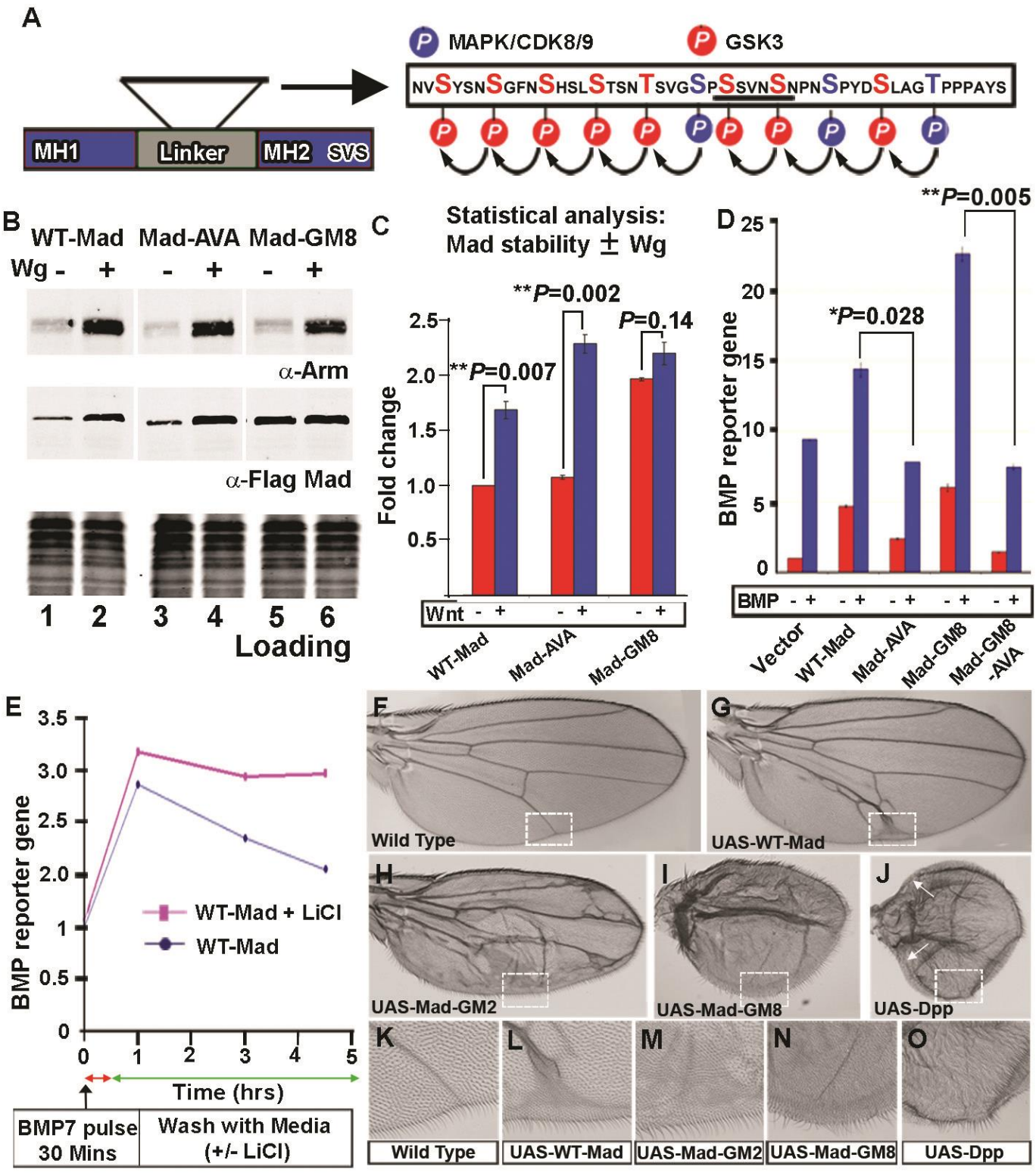

Figure 3.S1: Increased BMP signals generated by a stabilized Mad protein.

In the Mad GSK3 mutant 8 (Mad-GM8), the eight putative GSK3 sites were rendered resistant to phosphorylation by mutating Ser or Thr to Ala.

(A) Schematic diagram highlighting the putative phosphorylation sites in the linker region of Mad. Three potential MAPK or CDK8 and CDK9 priming phosphorylations (Ser-Pro) are highlighted in blue. The eight putative GSK3 phosphorylations in Mad are indicated in red.

(B) Flag-tagged WT-Mad is significantly stabilized in cells treated with Wg-conditioned medium compared to cells treated with conditioned medium from cells not transfected with Wg (compare lanes 1 and 2). Mad-AVA, which is resistant to C-terminal phosphorylation, is also stabilized by Wg protein (lanes 3 and 4). Mutation of all eight GSK3 phosphorylation sites in the linker region of Mad (Mad-GM8) causes stabilization of the protein even in the absence of Wg conditioned medium (lanes 5 and 6). Armadillo, a protein that is stabilized by Wg, is used to demonstrate activation of Wg signaling. Equal loading is shown in the coomassie blue image (n = 4 blots).

(C) Analysis by Mann-Whitney-Wilcoxon test of the stability of Mad from immunoblots quantified using the LI-COR Odyssey system.

(D) BMP reporter gene (BRE-luciferase) activity was increased when GSK3 phosphorylation sites in Mad (Mad-GM8) were mutated. BMP stimulation did not increase BMP reporter activity above basal values in cells expressing Mad-GM8-AVA ($P < 0.001$, brackets; 2-way ANOVA with Tukey's post-test). These experiments demonstrate that Mad-GM8 enhances the effects of BMP signaling by increasing the duration of the BMP signal, but only when C-terminal phosphorylation is possible (n = 3 experiments).

(E) A 30-minute incubation with BMP7 was performed at the beginning of this assay. The duration of the BMP signal was prolonged by inhibiting GSK3 phosphorylation with LiCl, a treatment that mimics the Wg signal.

(F) Wild-type adult wing, showing normal venation.

(G) A moderate increase in vein tissue in adult wings was seen when WT-Mad was driven with MS1096-Gal4 (n = 23).

(H) In adult wings with a form of Mad bearing two mutated GSK3 phosphorylation sites (Mad GSK3 mutant 2; Mad-GM2), vein formation was increased (n = 34) (1).

(I) Overexpression of Mad-GM8 protein resulted in increased venation (n = 45, all specimens showed similar phenotypes). The shape of the adult wing also adopted a more circular shape compared to wild-type wings.

(J) Dpp overexpression generated vein and wing shape phenotypes similar to those of Mad-GM8 overexpression (n = 20). Dpp overexpression causes loss of margin bristles (white arrows), a typical Wg loss-offunction phenotype (2).

(K) High magnification of boxed region in (B) showing the distal portion of vein 5. Note that vein cells were smaller than intervein cells.
(L) High magnification of longitudinal vein 5 showing that WT-Mad overexpression mildly increased distal venation forming a delta structure towards the margin.
(M) High magnification of Mad-GM2 overexpressing wings showing transformation of intervein tissue into vein tissue.
(N) High magnification of Mad-GM8 overexpressing wings showing that intervein tissue displayed the smaller cell phenotype characteristic of vein tissue.
(O) Dpp overexpression, like Mad-GM8 overexpression, transforms intervein tissue into vein tissue.

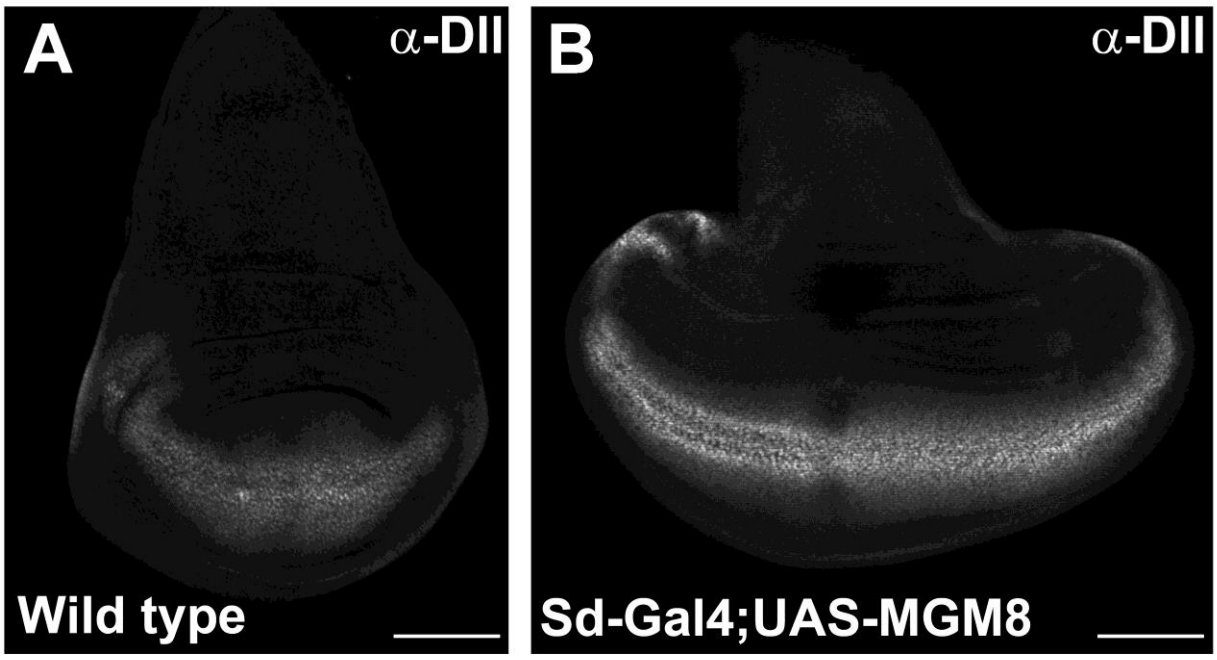

Figure 3.S2: Mad-GM8 expression increases the area of Distalless, a downstream target of Wg.

(A) Distribution of Distalless in a wild-type wing imaginal disc at 3rd instar larval stage (n = 24 discs). Distalless is strongest along the presumptive wing margin and weaker in other regions of the wing pouch (n = 14 discs).
(B) Overexpression of Mad-GM8 using Scalloped-Gal4 wing disc increases the area of Distalless in the wing pouch (n = 15). The shape of the wing disc is also extended along the anterior-posterior axis, and the overall size increased, as is typical of wing discs with increased Dpp signaling (3). Scale bars, 100 μm.

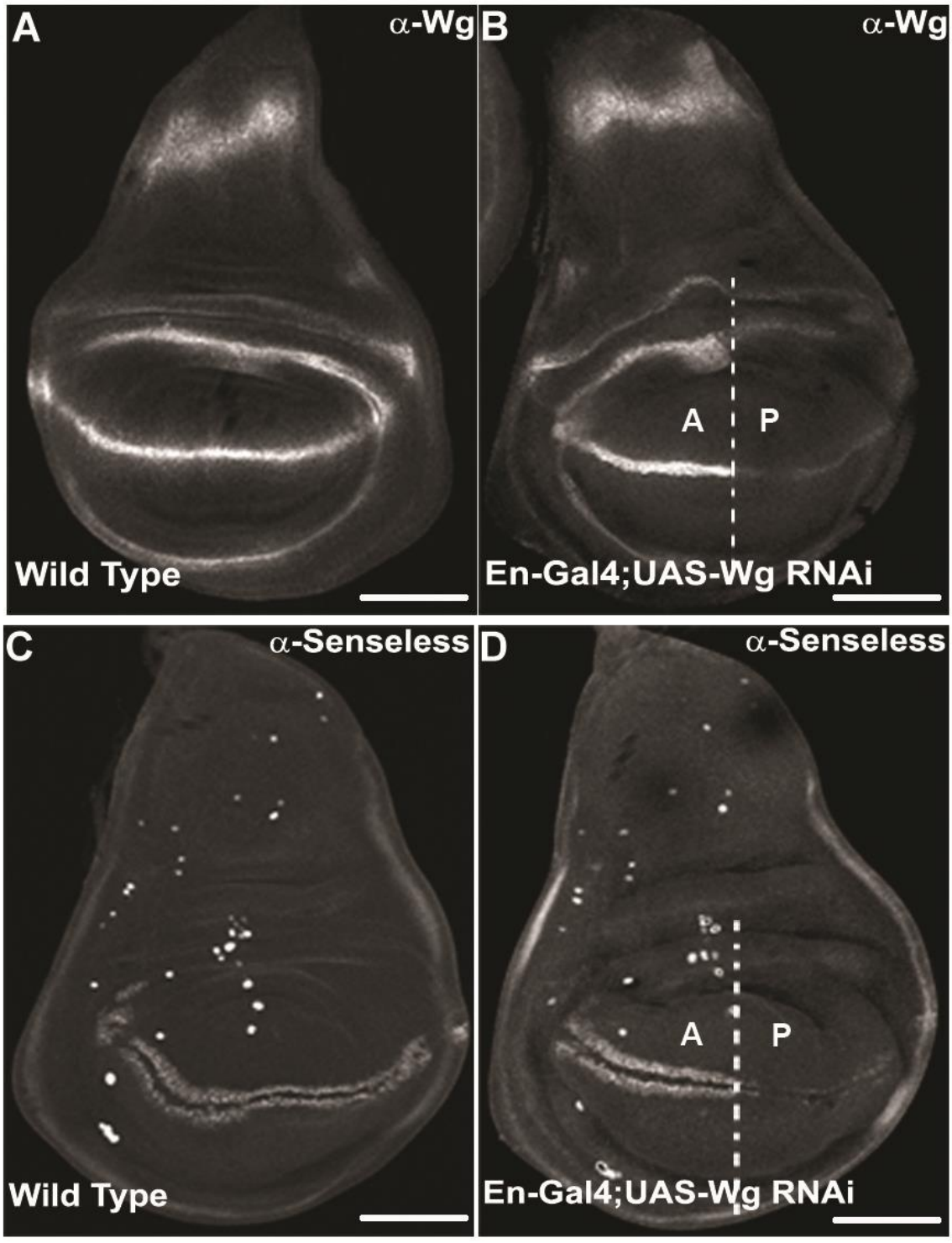

Figure 3.S3: Inducible RNAi directed against Wg depletes Wg protein and its downstream target Senseless.

(A) Wild-type distribution of Wg protein in 3rd instar larval wings imaginal discs (n = 20 discs).
(B) Wg RNAi in the posterior (P) wing compartment driven by Engrailed-Gal4 reduced Wg protein abundance (n = 18).
(C) Wild-type distribution of Senseless, a downstream target of Wg target (n = 40 discs).
(D) Senseless is lost in the posterior wing compartment when Wg is knocked down by RNAi driven by Engrailed-Gal4 (n = 23 discs). These results demonstrate that the Wg RNAi construct used (VDRC #13352) is effective in Drosophila. Scale bars, 100 μm.

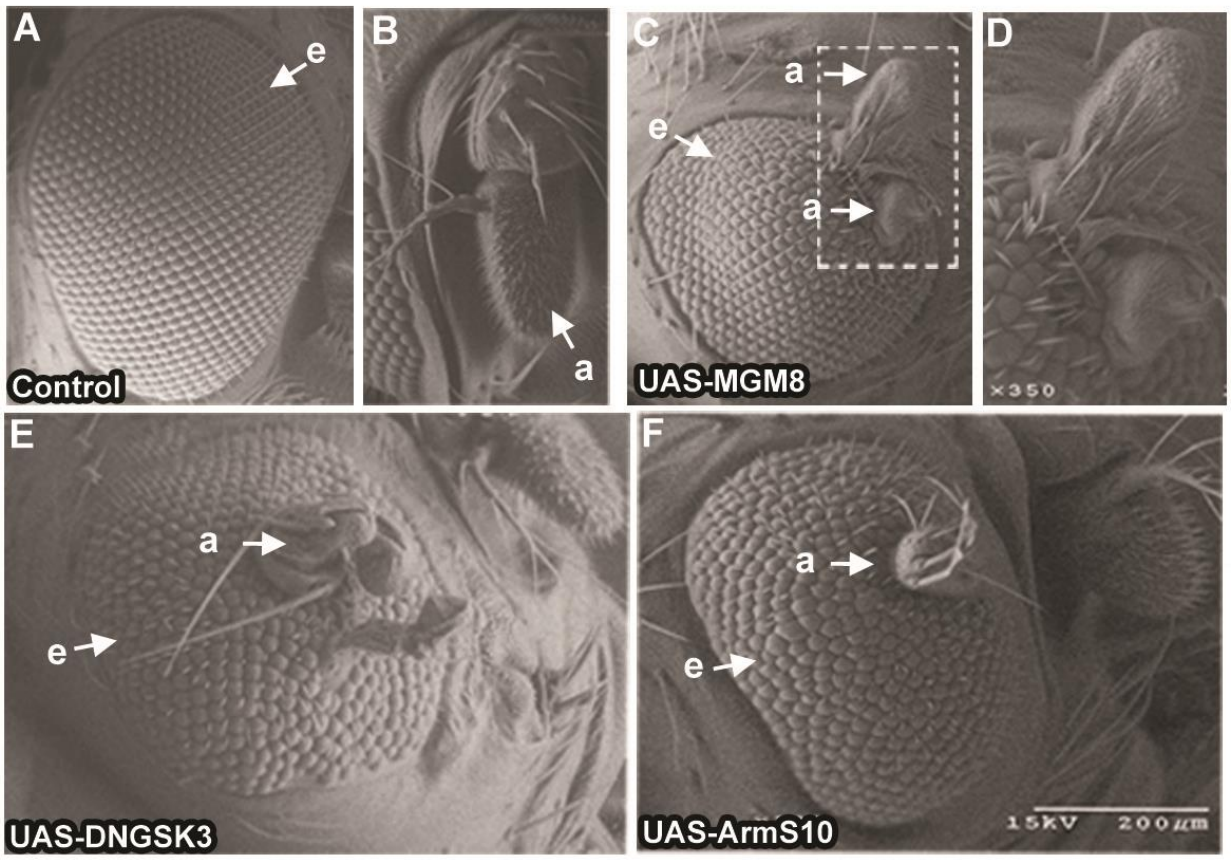

Figure 3.S4: Mad-GM8 expression in the eye imaginal disc produces phenotypes suggestive of high Wg signaling.

(A) Image of wild-type adult eye (e)
(B) Image of antenna (a) by scanning electron microscopy.
(C) Transformation of part of the Drosophila eye into antennal-like tissue when Mad-GM8 was driven by eyeless-Gal4 (n = 66 eyes with ectopic antennae or bulging structures out of 97 eyes).
(D) A high power image of two ectopic antennal-like growths induced by Mad-GM8 overexpression.
(E) Similar antennal-like structures were observed when Wg signaling was activated by dominant negative GSK3 (DNGSK3) (n = 24 eyes) or
(F) stabilized Armadillo (ArmS10) driven by eyeless-Gal4 (n = 13 eyes). This experiment shows that overexpression of the stabilized, GSK3 phosphorylation-resistant form of Mad elicits a canonical Wg signal.

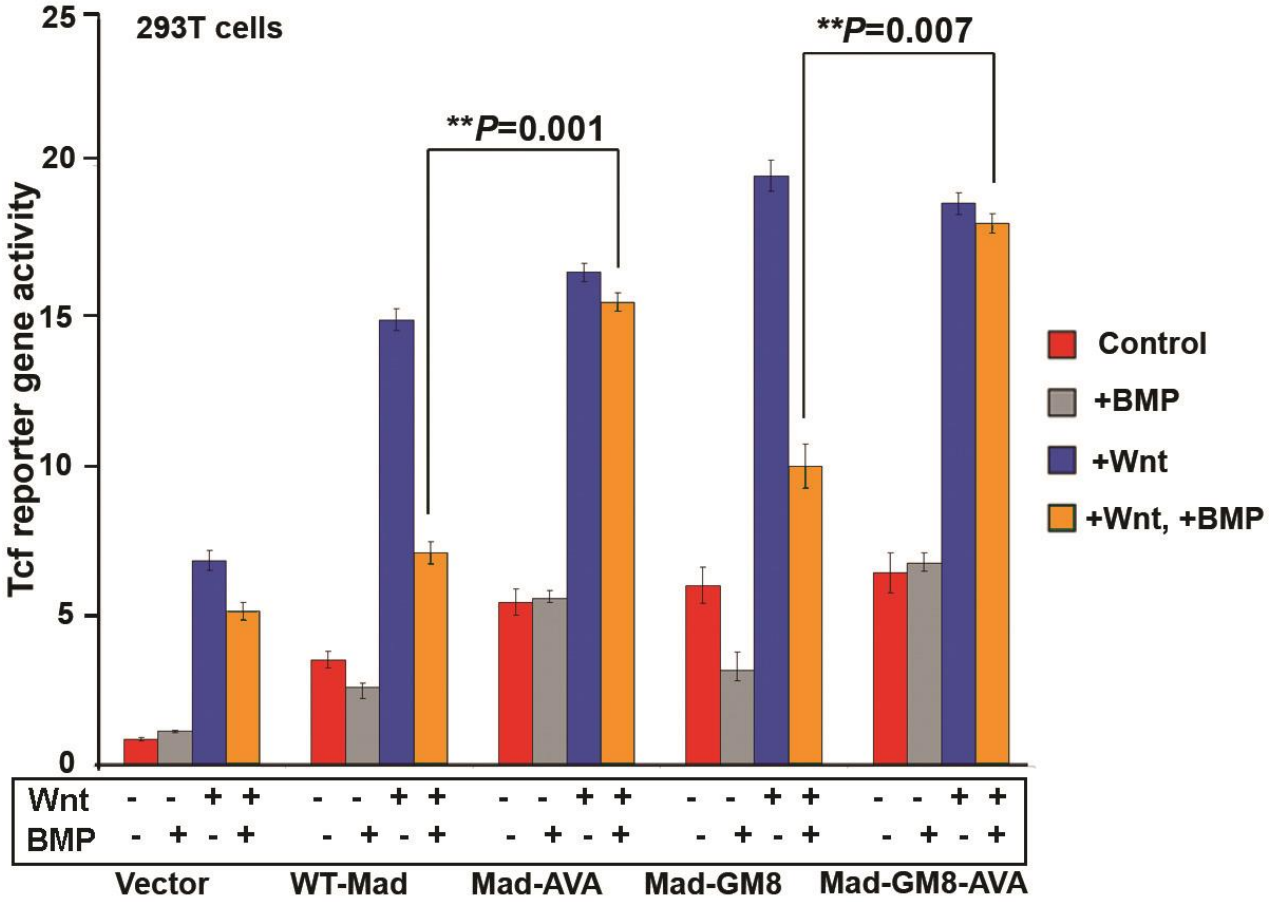

Figure 3.S5: C-terminal phosphorylation of Mad enables BMP4 to repress the Mad-induced increase in Tcf reporter gene activity.

Mad forms resistant to phosphorylation by BMP receptor are insensitive to inhibition of Wnt signaling by BMP4. W-Mad or Mad mutant proteins (Mad- AVA, Mad-GM8, or Mad-GM8-AVA) increased Wnt reporter activity compared to control cells. A comparable increase in Wnt activity was found when cells were transfected with WT-Mad or Mad-AVA (the C-terminal phosphorylation mutant), an effect that can be attributed to the lack of endogenous BMP signaling in HEK293T cells. In the case of Drosophila S2R+ cells, which have endogenous BMP signaling, Mad-AVA stimulated the activity Tcf reporter (Fig. 2B). Expression of a form of Mad with mutations in the 8 putative GSK3 phosphorylation sites in the linker region increased Wnt reporter activity compared to WT-Mad. Also, BMP4 treatment of cells failed to induce significant Tcf reporter activation (grey bars). Treating cells with both Wnt and BMP4 inhibited the ability of WT-Mad to increase Wnt-reporter activity, but not in cells expressing

C-terminal mutant forms of Mad (Mad-AVA and Mad-GM8-AVA; see brackets). We propose that phosphorylation of Mad by BMP receptor prevents Mad from signaling in the Wnt pathway (n = 3 experiments; statistical analysis was carried out with a 2-way ANOVA with Tukey's post-test).

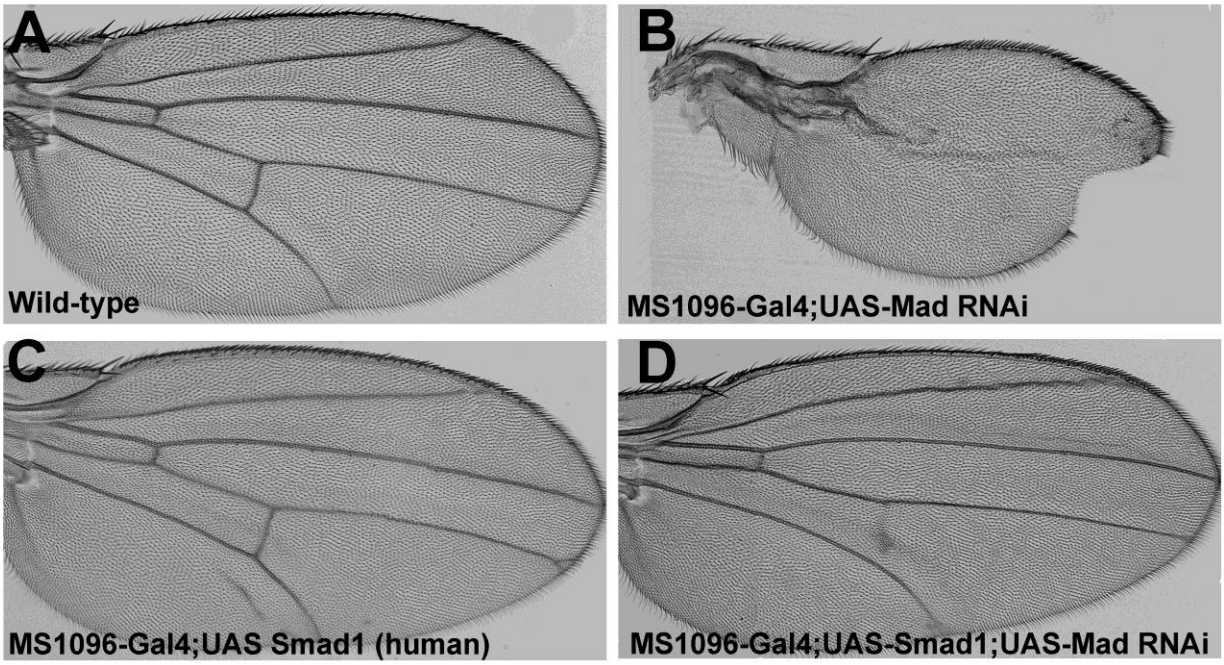

Figure 3.S6: The Mad RNAi phenotype is rescued by coexpression of a human Smad1 transgene.

(A) Wild-type adult wing, showing normal venation, which requires BMP signaling (n = 30 wings).
(B) Loss of vein tissue and margin notching in Mad-RNAi adult wings (n = 25).
(C) Overexpression of a UAS-Smad1 human produced some extra vein tissue, but the wing was largely normal (n=15).
(D) The Mad RNAi phenotype was rescued (except for the posterior crossvein) when a human Smad1 transgene was expressed (n=9).

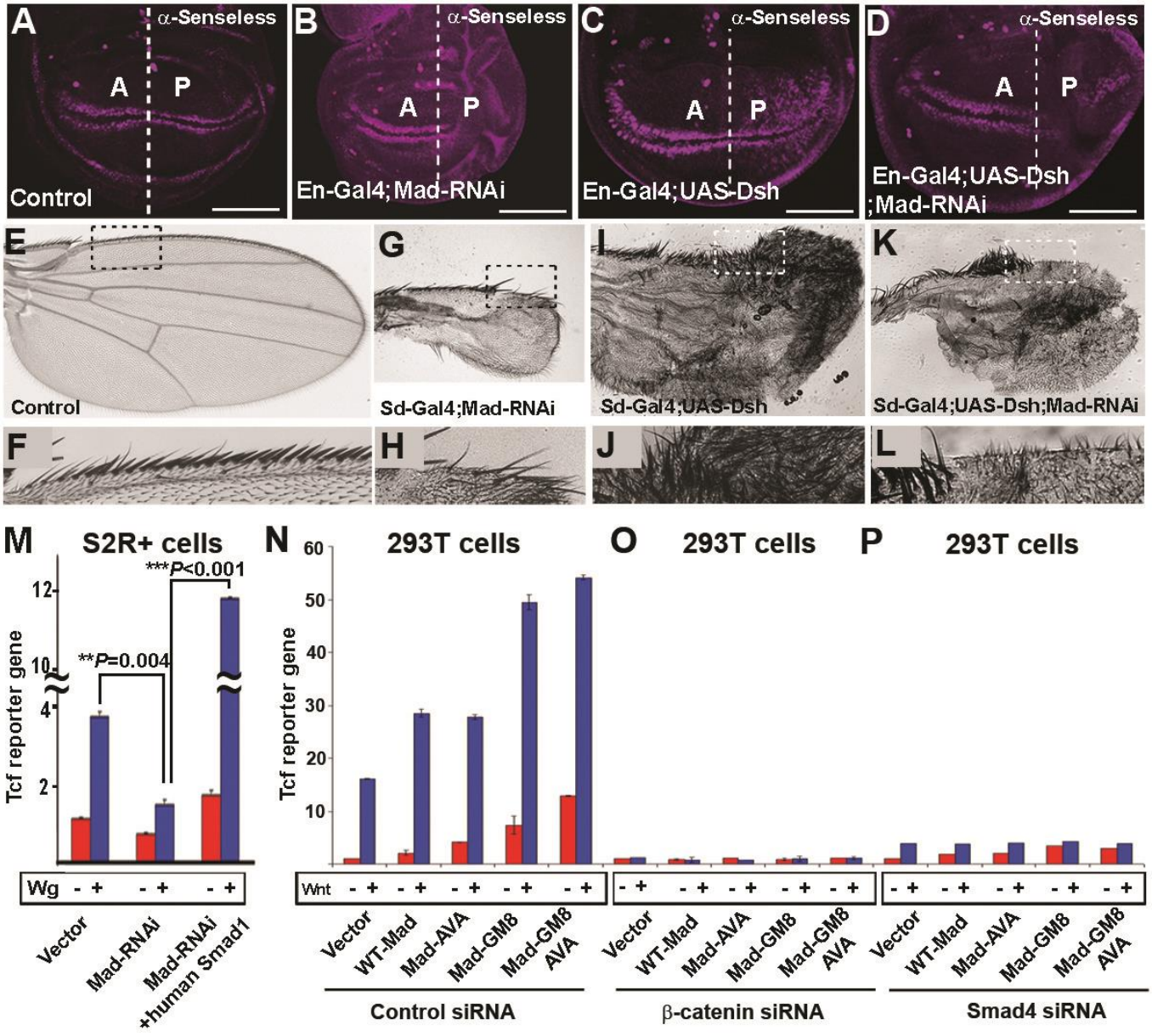

Figure 3.S7: Mad is required for Wg signal transduction during wing margin development.

(A) Distribution of Senseless in 3rd instar wild-type wing imaginal disc. Anterior-posterior axis of the wing disc is indicated as A and P.
(B) Mad knockdown using an RNAi driven by Engrailed-Gal4 specifically in the posterior wing compartment reduces the area of Senseless.
(C) Overexpression of Dishevelled in the posterior compartment causes ectopic areas of Senseless.

(D) Ectopic Senseless is blocked by Mad-RNAi expression in the posterior compartment. Mad RNAi is epistatic to Dishevelled, indicating that Mad is required downstream of Dishevelled in the Wnt pathway. At least 12 imaginal discs were analyzed for each genotype, all with similar phenotypes.
(E) Wild-type adult wing.
(F) High magnification of the anterior wing margin (highlighted as a boxed region in E).
(G and H) Mad RNAi driven with Scalloped-Gal4 results in a small veinless wing. This wing is deficient in margin bristles, which suggests loss of Wg signaling (n = 45 wings).
(I and J) Overexpression of Dishevelled caused increased bristle formation throughout the wing blade (n = 38 wings).
(K and L) Increased bristle formation in the wing blade caused by Dishevelled was inhibited when Mad was knocked down using RNAi (n = 24).
(M) Mad knockdown by Gal4-inducible RNAi inhibited Tcf reporter gene activation, which was rescued by transfection of human WT-Smad (n = 5 experiments, statistical analysis carried out using a 2-way ANOVA with Tukey's post-test).
(N to P) Activation of the Tcf reporter gene by Mad constructs in the presence of control siRNA, beta-catenin siRNA, or Smad4 siRNA in HEK293T cells. Treating cells with a control siRNA had no effect on Tcf reporter gene activation. siRNA-mediated depletion of beta-catenin blocked activation of the canonical Wnt pathway. Treatment of cells with Smad4 siRNA also efficiently blocked Wnt signaling. This shows that both Smad4 and beta-catenin are essential components of the Wnt signaling pathway (n = 3 experiments, statistical analysis carried out using a 2-way ANOVA with Tukey's post-test). Scale bars 100 μm.

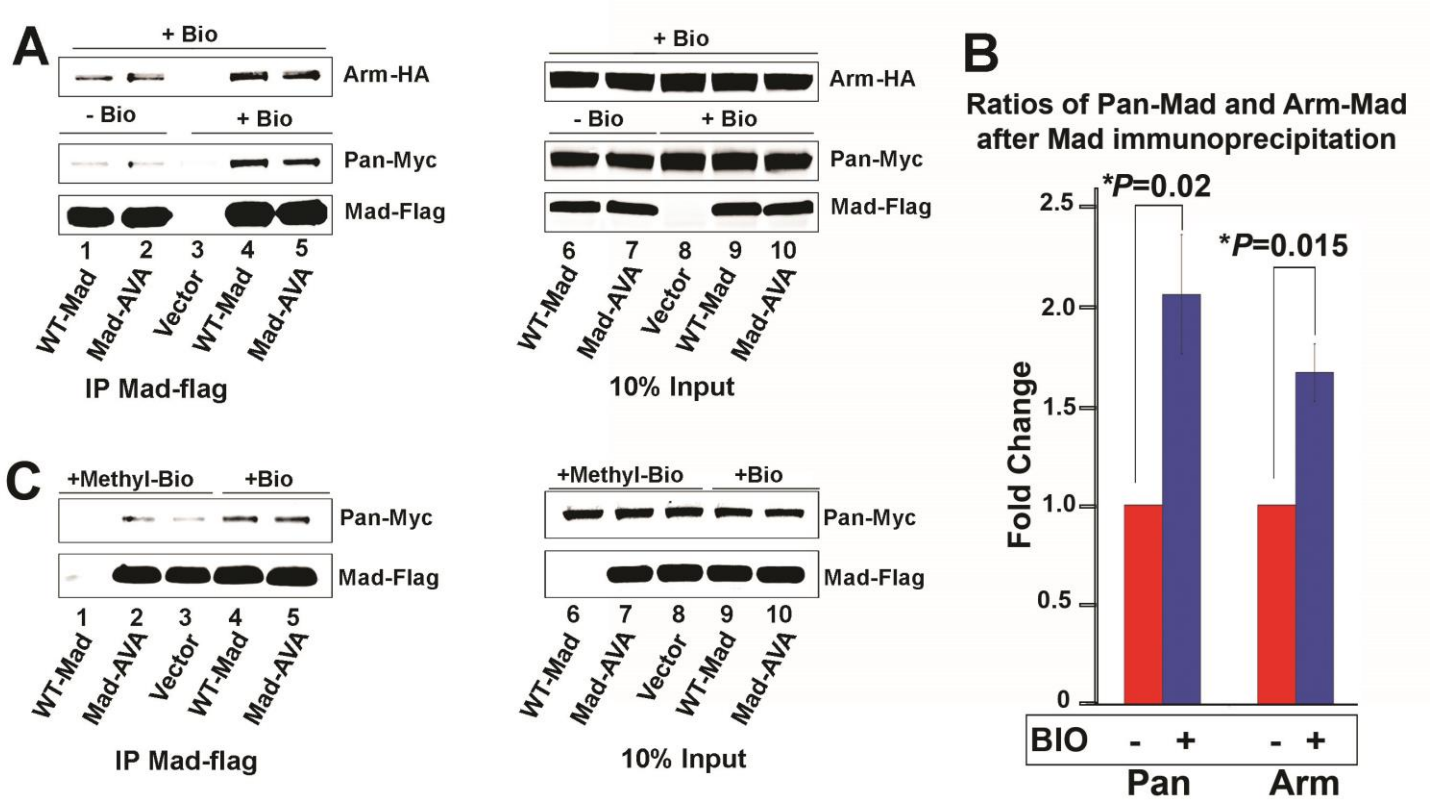

Figure 3.S8: Inhibition of GSK3 activity by BIO enhances the binding of Mad to Pangolin.

(A) Coimmunoprecipitation of Pangolin-Myc and Armadillo-HA through Mad-Flag or Mad-AVAFlag (lanes 1-5). Pangolin and Mad DNAs were transfected separately into HEK293T cells and treated with or without the GSK3 inhibitor BIO. Cells expressing Armadillo were subjected to BIO treatment under all conditions to ensure sufficient protein amounts. Input proteins (lanes 6- 10) shown are 10% of the amount used for the binding experiments. Cell lysates containing Mad proteins were incubated with separate lysates containing Pangolin and Armadillo proteins for one hour at 4oC to allow binding. In the absence of BIO, we observed only weak binding between Mad and Pangolin (lanes 1 and 2, minus BIO). Treating HEK293T transfected cells with BIO enhanced the binding of Mad to Pangolin (lanes 4 and 5, +BIO), indicating that the phosphorylation of Mad by GSK3 inhibits binding between Mad and Pangolin. Based on these findings, we propose that Wnt signaling promotes the binding of Mad to Pangolin by preventing GSK3 phosphorylations, in addition to stabilizing Armadillo (n = 3 experiments).
(B) Quantification of the ratio of immunoprecipitated Pangolin and Armadillo protein over Mad using a LI-COR Odyssey scanner system. Treatment with the

GSK3 inhibitor BIO caused a 2- fold increase in binding efficiency between Mad and Pangolin and a 1.5 -fold increase in binding efficiency to Armadillo in HEK293T cell extracts ($P = 0.0017$, $P = 0.008$, Mann-Whitney Wilcoxon test, $n = 3$).

(C) We also used an inactive form of this compound, methylated-BIO, to test whether BIO had non-specific off target effects. In cells treated with methylated-BIO, there was less binding of Mad to Pangolin (lanes 2 and 3) when compared to the active form of BIO (lanes 4 and 5).

CHAPTER 4

The Tumor Suppressor Smad4/DPC4 is Regulated by Phosphorylations that Integrate FGF, Wnt and TGF-beta Signaling

This Chapter contains text and figures as submitted to

Molecular Cell, (under review)

Hadrien Demagny, Tatsuya Araki, and Edward M. De Robertis

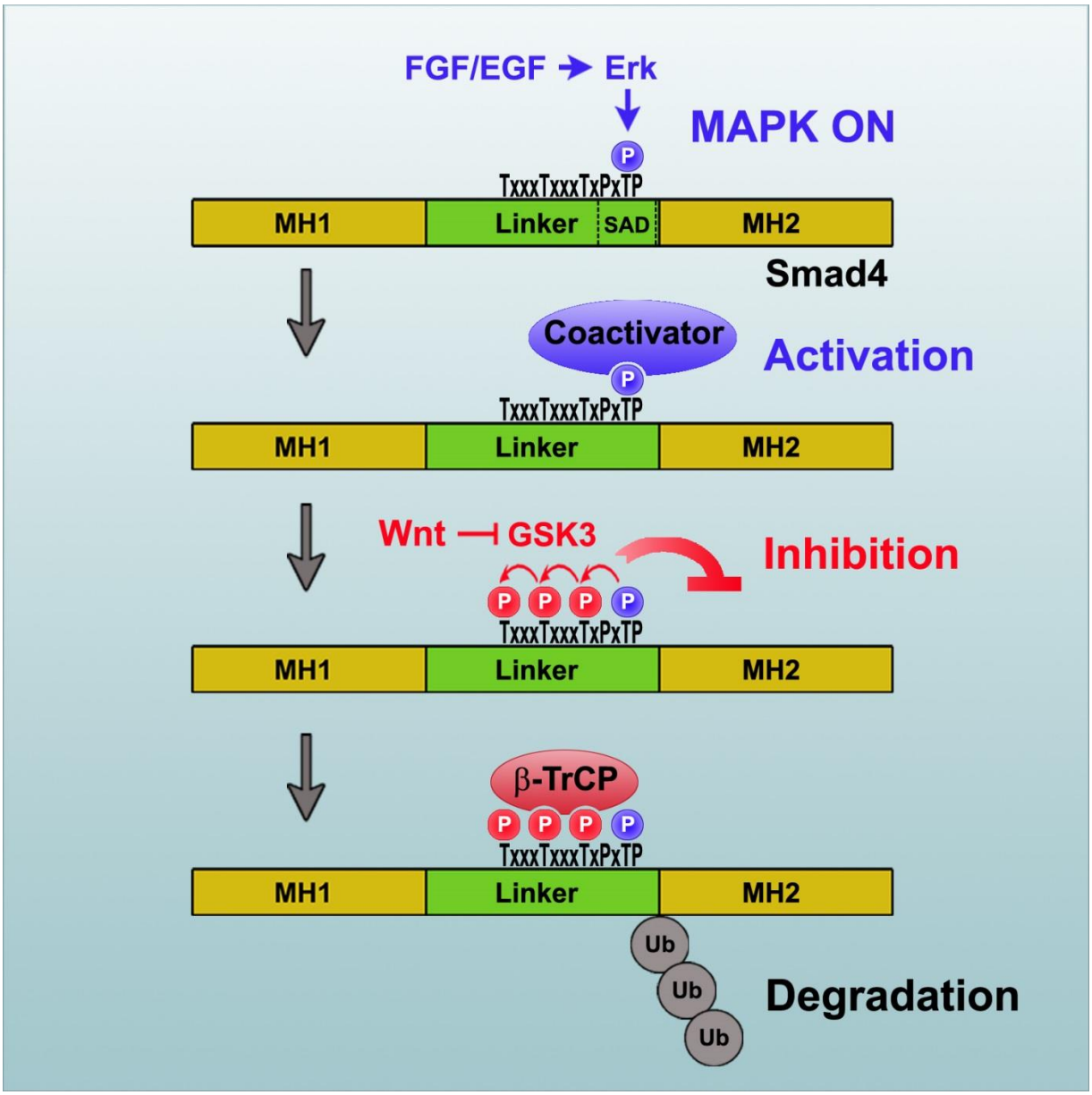

During a bioinformatic screen of the human proteome we noticed that Smad4 contains three putative GSK3 phosphorylation sites primed by a MAPK site (PxTP) (Taelman et al., 2010). The present chapter intends to study the possible convergence of FGF/MAPK, Wnt/GSK3 and TGF-beta signals at the level of

Smad4 phosphorylations. While Smad4 was long thought to be a silent partner in the TGF-beta pathway, we showed that conserved phosphorylation sites allowed its regulation by two main growth factors: FGF and Wnt. We showed that Smad4 phosphorylations by MAPK and GSK3 regulated the activity of an internal transcriptional activation domain located in Smad4 linker region. We also showed that Smad4 phosphorylation by GSK3 generated a phosphodegron recognized and bound by the ubiquitin E3-ligase beta-TrCP. In the context of the *Xenopus* embryo, we found that replacing endogenous Smad4 with a GSK3 phosphorylation-resistant mutant converted the entire ectoderm into mesoderm and expanded Spemann organizer formation, indicating that the growth factor-regulated Smad4 phosphorylations play an important role in animal development.

The findings presented in this study are the results of my principal involvement in most aspects of this project.

4.1 Summary

Smad4 is a major tumor suppressor currently thought to function constitutively in the TGF-beta signaling pathway. Here we report that Smad4 activity is directly regulated by the Wnt and FGF pathways through novel GSK3 and MAPK phosphorylations sites. FGF activates MAPK, which primes three sequential GSK3 phosphorylations that generate a Wnt-regulated phosphodegron bound by the Ubiquitin E3 ligase beta-TrCP. In the presence of FGF, Wnt potentiates TGF-beta signaling by preventing Smad4 GSK3 phosphorylations that inhibit a transcriptional activation domain located in the linker region. When MAPK is not activated, the Wnt and TGF-beta signaling pathways remain insulated from each other. In *Xenopus* embryos, these Smad4 phosphorylations regulate germ layer specification and Spemann organizer formation. The results show that three major signaling pathways critical in development and cancer are integrated at the level of Smad4.

4.2 Introduction

Smad4, also known as Deleted in Pancreatic Carcinoma 4 (DPC4), is a major tumor suppressor gene that constrains cancer growth. Pancreatic, colorectal and prostate carcinomas proliferate rapidly and progress toward metastases when Smad4 function is lost (Levy and Hill, 2006; Ding et al., 2011; Massague, 2012). Transforming Growth Factor-beta (TGF-beta) receptors signal by phosphorylating carboxy-terminal serines of the transcription factors Smad1/5/8 (for Bone Morphogenetic Proteins, BMPs) or Smad2/3 (for TGF-beta/Activin). These receptor-activated Smads (R-Smads) then undergo a second set of phosphorylations in the linker region catalyzed by the transcriptional cyclin-dependent kinases CDK8 and CDK9, allowing them to reach peak activity before being phosphorylated by Glycogen Synthase Kinase-3 (GSK3) and targeted for proteasomal degradation (Alarcón et al., 2009; Gao et al., 2009; Aragón et al., 2011). The linker region of R-Smads is also regulated by activation of Tyrosine kinase receptors such as those for fibroblast growth factor (FGF) and epidermal growth factor (EGF) that activate MAPK phosphorylations and prime subsequent GSK3 phosphorylations (Kretzschmar et al., 1997; Pera et al., 2003; Sapkota et al., 2007; Fuentealba et al., 2007; Millet et al., 2009; Aragón et al., 2011). The transcription factor Smad4 functions as a co-Smad that binds to R-Smads and was,

until now, considered a constitutively active component of the pathway (Massague, 2012).

The Wnt pathway is activated in the early stages of many tumors and its transcriptional effects are mediated by the stabilization of beta-Catenin (Clevers and Nusse, 2012). Canonical Wnt signaling causes the sequestration of cytosolic GSK3, Axin and Dishevelled (Dvl) in multivesicular bodies (MVBs) (Taelman et al., 2010; Vinyoles et al., 2014). In addition to beta-Catenin, other proteins may be regulated by Wnt signaling through the decrease in GSK3 phosphorylations that are normally recognized as phosphodegrons to be polyubiquitinated and degraded in the proteasome (Kim et al., 2009; Taelman at al., 2010; Vinyoles et al., 2014; Acebron et al., 2014). GSK3 is a kinase that prefers pre-phosphorylated substrates, introducing phosphorylations on Ser or Thr residues located four amino acids upstream (S/TxxxS/T[PO_3]) (Cohen and Frame, 2001). During a bioinformatic screen of the human proteome we noticed that Smad4 contains three putative GSK3 phosphorylation sites primed by a MAPK site (PxTP) (Taelman et al., 2010).

Here we report that Smad4 activity depends on Tyrosine kinase/MAPK- and Wnt/GSK3-regulated phosphorylations, revealing a novel node of signaling integration between these two main oncogenic pathways and the TGF-beta tumor suppressor signal. We show that when cells received an FGF signal, phosphorylation of the MAPK site promoted Smad4 peak transcriptional activity

before priming inhibitory GSK3 phosphorylations. Smad4 phosphorylation by GSK3 created a phosphodegron that lead to its subsequent polyubiquitination and degradation by the E3-ligase beta-TrCP. In the presence of Wnt, Smad4 GSK3 phosphorylations were inhibited and the TGF-beta signal was prolonged, particularly at low levels of TGF-beta ligands. Replacing Smad4 with a GSK3-resistant mutant showed that the cross-talk between TGF-beta and Wnt is mediated by Smad4. This new molecular mechanism, in which Wnt and MAPK activation enhance anti-proliferative TGF-beta signals, may help understand the role of Smad4 as a barrier to tumor progression. In the context of the *Xenopus* embryo, we found that replacing endogenous Smad4 with a GSK3 phosphorylation-resistant mutant converted the entire ectoderm into mesoderm and expanded Spemann organizer formation, indicating that the growth factor-regulated Smad4 phosphorylations play an important role in animal development.

4.3 Results

4.3.1 Wnt and FGF regulate phosphorylation of Smad4 linker region

The putative regulatory sites consisted of four threonines located in the linker (middle) region of Smad4 (Figure 4.1 A). To determine whether Smad4 was phosphorylated by GSK3, we generated an antibody raised against phospho-

threonines 273 and 269 (pSmad4^{GSK3} Ab). Because the priming site was a canonical MAPK/Erk site (PxTP), we treated 3T3 fibroblasts with FGF2, and found that a single band of endogenous pSmad4^{GSK3} antigen was increased (Figure 4.1 B, lanes 1 and 2). The pSmad4^{GSK3} signal was blocked by treatment with the MEK-specific inhibitor U0126, demonstrating a requirement for Erk/MAPK downstream of FGF stimulation (Figure 4.1 B, lane 3). FGF-induced pSmad4^{GSK3} phosphorylation was inhibited by pre-incubation with Wnt3a protein (Figure 4.1 C, lanes 2 and 3), and blocked by the GSK3 inhibitor BIO (Figure 4.1 C, lane 4). The specificity of the antibody was confirmed by Smad4 siRNA depletion and phosphatase treatment (Figure 4.S1).

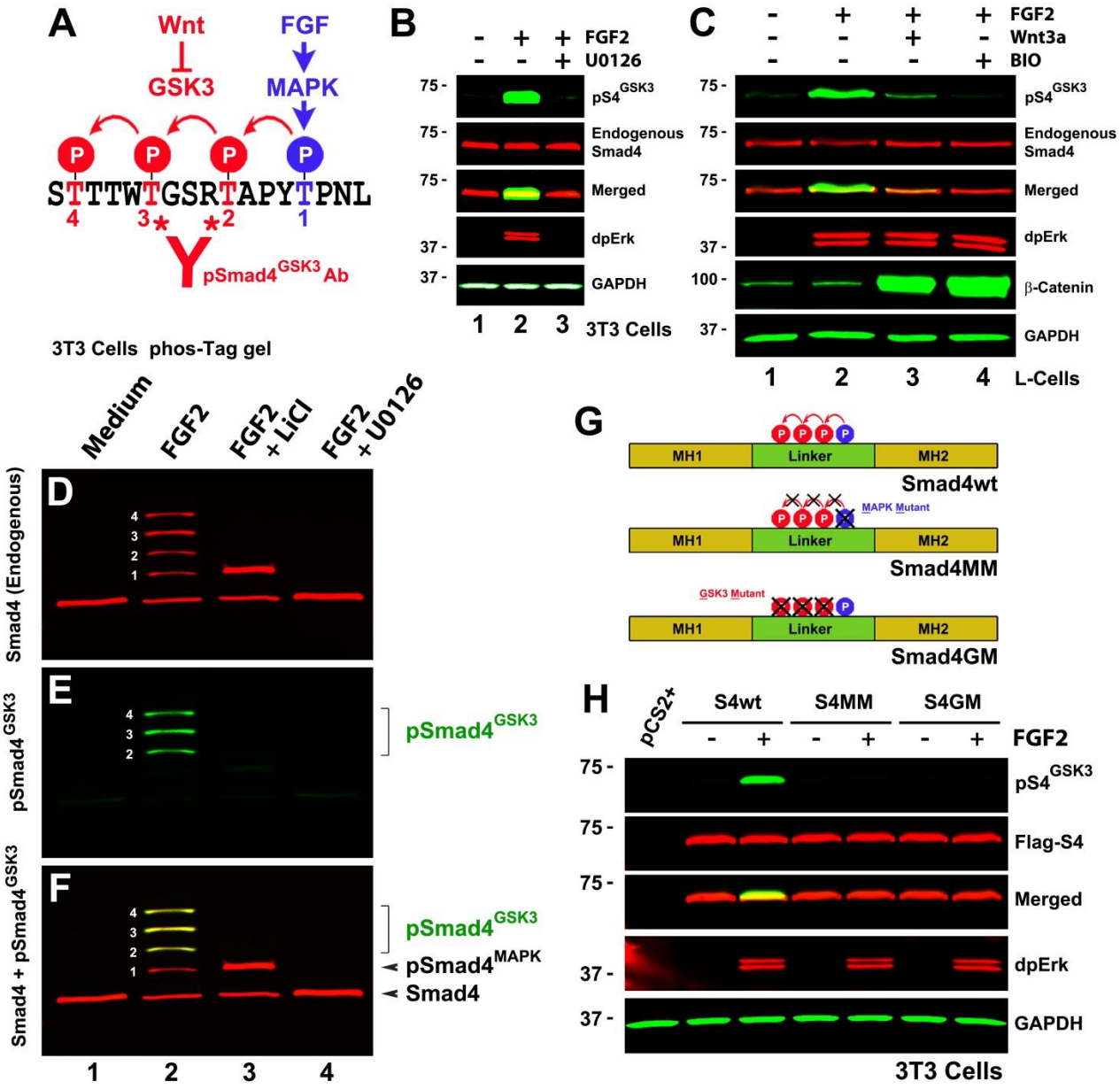

Figure 4.1: The Smad4 Linker Region is Phosphorylated by GSK3

(**A**) Smad4 contains MAPK (blue) and GSK3 (red) phosphorylation sites in its linker region.
(**B**) Endogenous FGF-induced pSmad4^{GSK3} phosphorylation requires Erk activity in serum-depleted NIH-3T3 cells stimulated with FGF2 for 1 hour.
(**C**) Endogenous pSmad4^{GSK3} antigen is induced by a 1 hour FGF2 treatment, inhibited by preincubation with Wnt3a for 5 hours, and blocked by the GSK3 inhibitor BIO.

(**D-F**) Mn^{2+}-Phos-tag analysis of endogenous Smad4 in NIH-3T3 cells cultured in the absence of serum.
(**G**) Diagrams of Smad4 constructs encoding Smad4 wild-type (Smad4-wt) or phosphorylation-resistant mutants (Thr to Val) for MAPK (Smad4-MM) and GSK3 (Smad4-GM) sites.
(**H**) GSK3 phosphorylations require an intact MAPK site in transfected 3T3 cells.

To determine the number of sites that were phosphorylated, we separated proteins from untransfected 3T3 cells in polyacrylamide SDS gels containing the phosphate-binding compound Mn^{2+}-Phos-tag (Kinoshita et al., 2006). In the absence of serum, a single band was detected by a Smad4 monoclonal antibody, while upon addition of FGF four additional bands were displayed (Figure 4.1 D, lanes 1 and 2). The three slower migrating bands were also positive for $pSmad4^{GSK3}$ antibody (Figure 4.1 E). GSK3 inhibition by LiCl resulted in the accumulation of the mono-phosphorylated form, while treatment with U0126 eliminated all Smad4 phosphorylations (Figure 4.1 F, lanes 3 and 4). Studies with transfected phosphorylation-resistant MAPK or GSK3 mutants (designated as Smad4-MM and Smad4-GM, respectively, Figure 4.1 G) showed that the priming site (Threonine 277) was required for GSK3 phosphorylations (Figure 4.1 H). Taken together, these results demonstrate that Smad4 is regulated by sequential phosphorylations as proposed in Figure 4.1 A.

4.3.2 Wnt/GSK3 regulates the polyubiquitination and degradation of Smad4.

Polyubiquitination of R-Smads is controlled by linker phosphorylations (Sapkota et al., 2007; Fuentealba et al., 2007; Gao et al., 2009), prompting us to investigate the

effects of GSK3 phosphorylations on Smad4 stability. In a first experiment, we treated HaCaT cells with a 20 min pulse of EGF and found that $pSmad4^{GSK3}$ was degraded over a period of 4 hours (Figure 4.2 A). Proteasomal inhibition by MG-132 greatly stabilized the phosphorylated form of Smad4 (Figure 4.2 A), indicating that $pSmad4^{GSK3}$ was preferentially degraded by the proteasome. Immunoprecipitation studies showed that endogenous Smad4 polyubiquitination was increased by FGF treatment and required GSK3 activity (Figure 4.2 B), as well as intact phosphorylation sites for GSK3 and MAPK (Figure 4.2 C). A dominant-negative form of GSK3 also inhibited the sustained polyubiquitination of Smad4 driven by transfection of an oncogenic form of Ras (G12V mutation) (Figure 4.S2 C and C').

Because GSK3 is Wnt-regulated kinase, we asked whether the Wnt growth factor could regulate Smad4 stability. In Cycloheximide time-course experiments, endogenous Smad4 was stabilized by Wnt3a addition or by the GSK3 inhibitor LiCl, in FGF-treated cells (Figure 4.2 D and D'). *Xenopus* animal caps explants microinjected with Flag-tagged *Smad4* mRNAs were also used to study the degradation of Smad4; since mRNAs were injected any differences in protein levels were expected to be post-transcriptional. In *Xenopus* ectodermal explants, a potent and sustained activation of the MAPK/Erk pathway is achieved by cell dissociation (Kuroda et al., 2005). We found that in dissociated animal cap cells

diphospho Erk was activated, the Smad4 GSK3 sites were strongly phosphorylated and, importantly, Flag-Smad4 was degraded (Figure 4.2 E, lane 6). The phosphorylation by GSK3 and the degradation of Smad4 were dependent on MAPK/Erk activity as they were blocked by U0126 treatment (Figure 4.2 E, lane 10). Co-injection of *Wnt8* mRNA inhibited Smad4 phosphorylation by GSK3 and prevented Flag-Smad4-wt degradation (Figure 4.2 E, compare lanes 6 and 7). Importantly, the GSK3 phosphorylation-resistant Smad4 mutant (Flag-Smad4-GM) was insensitive to stabilization by Wnt8 (Figure 4.2 E, 4.S2 D and 4.S2 D').

Taken together, these experiments show that linker phosphorylations regulated by FGF/MAPK and Wnt/GSK3 control Smad4 polyubiquitination and degradation.

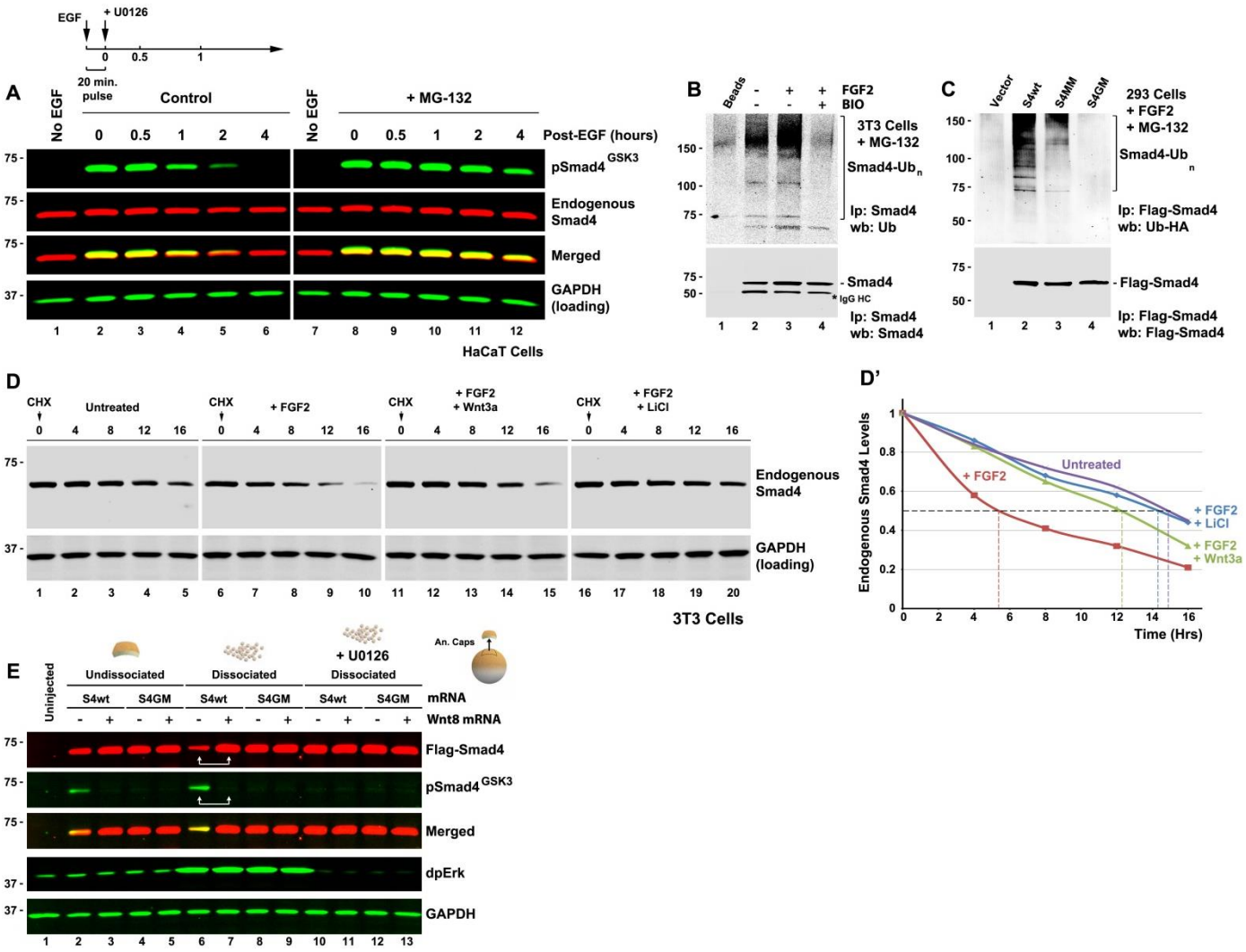

Figure 4.2: Wnt-regulated GSK3 Phosphorylations Control Smad4 Polyubiquitination and Degradation

(**A**) Time-course of pSmad4GSK3 phosphorylation primed by a 20 min pulse of EGF in HaCaT cells showing that the proteasome inhibitor MG-132 preferentially prolongs the half-life of pSmad4GSK3.
(**B**) Endogenous Smad4 polyubiquitination is increased by FGF and requires GSK3 activity (in the presence of the proteasome inhibitor MG132). Before immunoprecipitation with monoclonal Smad4 antibody, 0.2% SDS was added, samples heated at 95oC for 10 min to break protein-protein interactions, and diluted 10-fold with RIPA buffer to ensure that the polyubiquitinated bands detected were not ubiquitinated Smad4-interacting proteins (Zhu et al., 1999). For 5% input loading see Figure 4.S2A.

(**C**) Smad4 polyubiquitination requires intact MAPK and GSK3 sites; Flag-Smad4 or its phosphorylation-resistant mutants were co-transfected with HA-Ubiquitin into FGF-treated HEK293 cells and immunoprecipitated (Zhu et al., 1999) with anti-Flag antibodies. For 5% input loading see Figure 4.S2B.
(**D**) Wnt3a or LiCl treatment extended the half-life of endogenous Smad4 in FGF-treated 3T3 cells. In the absence of FGF, Smad4 is more stable.
(**D'**) Quantification of western results shown in panel D.
(**E**) Smad4 protein is stabilized by microinjection of xWnt8 mRNA in Xenopus dissociated animal cap cells. In dissociated cells dpErk is activated, causing increased pSmad4GSK3 and Flag-Smad4 degradation (lane 6). Both GSK3 phosphorylation and Flag-Smad4 degradation were blocked by co-injection of Wnt8 mRNA (lane 7). Smad4 degradation in microinjected embryos required intact GSK3 phosphorylation sites and was blocked by the Erk pathway inhibitor U0126 (40 μM). Cells were harvested at stage 10.5, early gastrula.

4.3.3 Wnt/GSK3 regulates a Smad4 beta-TrCP phosphodegron

We next analyzed the molecular mechanism by which Smad4 phosphorylations regulated its polyubiquitination. Smad4 proteolysis is mediated by interaction with the F-box E3 ubiquitin ligase beta-TrCP, but was not previously known to be regulated by growth factor signaling (Wan et al., 2004, 2005; Yang et al., 2006). Since beta-TrCP recognizes phosphodegrons (Fuchs et al., 2004), we investigated whether its binding to Smad4 was regulated rather than constitutive. Immunoprecipitation studies with endogenous proteins showed that beta-TrCP bound preferentially to Smad4 in the presence of FGF, and that Wnt3a treatment prevented this interaction in untransfected 3T3 cells (Figure 4.3 A, lanes 3 and 4). We also found that intact GSK3 phosphorylation sites in Smad4 were essential for the FGF-induced binding of beta-TrCP to Smad4 (Figure 4.3 B, lanes 3 and 5). Finally, a dominant-negative form of beta-TrCP (DN-beta-TrCP lacking the F-box domain; Orian et al., 2000) inhibited the polyubiquitination of Smad4 induced by RasG12V (Figure 4.3 C).

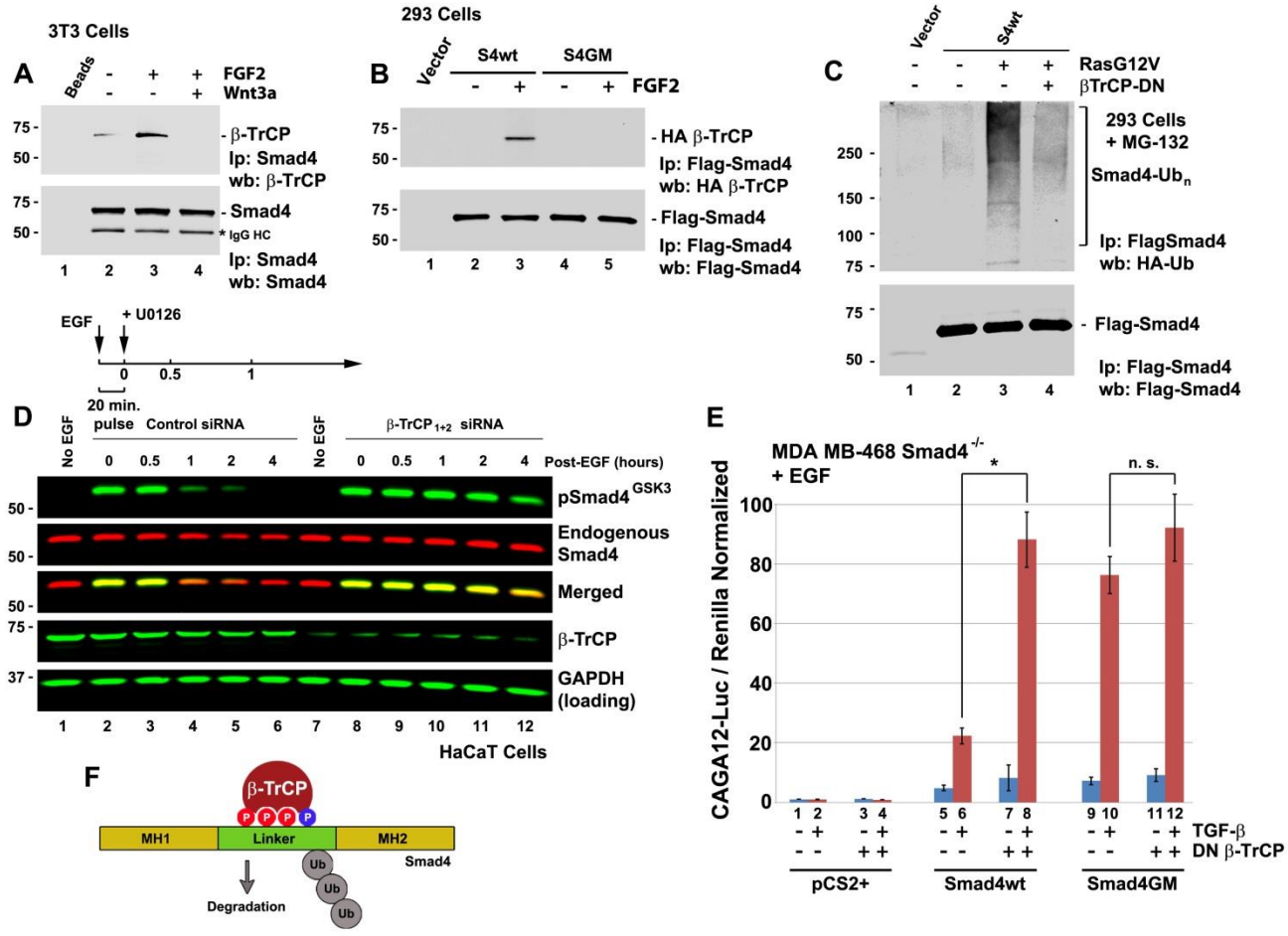

Figure 4.3: The Wnt-regulated Smad4 GSK3 phosphodegron is bound by the ubiquitin E3-ligase beta-TrCP and targeted for degradation.

(**A**) Endogenous binding between Smad4 and beta-TrCP is increased by FGF and blocked by Wnt3a treatment. Immunoprecipitation of endogenous Smad4 from untransfected 3T3 cells using a Smad4 monoclonal antibody bound to protein A/G agarose beads; 5% loading of initial lysate is shown in Figure 4.S3B.
(**B**) FGF-induced binding between Smad4 and beta-TrCP requires intact GSK3 phosphorylation sites in transfected 293 cells. Flag-tagged Smad4-wt bound HA-tagged beta-TrCP in the presence of FGF, but phosphorylation-resistant Smad4-GM was unable to co-precipitate with beta-TrCP; 5% loading is shown in Figure 4.S3C.
(**C**) Smad4 polyubiquitination induced by the oncogenic RasG12V protein is mediated by beta-TrCP, 5% loading is shown in Figure 4.S3D.
(**D**) beta-TrCP depletion with siRNA prolongs the half-life of pSmad4^{GSK3} induced by a 20 min pulse of EGF in HaCaT cells.

(**E**) Transfection of DN-beta-TrCP significantly increased TGF-beta signaling in Smad4$^{-/-}$ MB-468 cells transfected with hSmad4-wt. DN-beta-TrCP had no significant effect in Smad4-GM-expressing MB-468 cells. Note that beta-TrCP limits TGF-beta signaling and that this requires the Smad4 GSK3 phosphorylation sites.
(**F**) Diagram of the proposed Smad4 phosphodegron recognition by beta-TrCP.

To test whether beta-TrCP was the E3 ligase responsible for pSmad4^{GSK3} degradation, we depleted HaCaT cells of beta-TrCP with an siRNA that targets both beta-TrCP1 and 2 (Guardavaccaro et al., 2003). GSK3 phosphorylation of Smad4 was primed by a 20 min pulse of EGF, and we found that beta-TrCP depletion strongly stabilized the pSmad4^{GSK3} form (Figure 4.3 D). Finally, in a functional reporter gene assay, DN-beta-TrCP increased responsiveness to TGF-beta and this effect required intact Smad4 GSK3 sites (Figure 4.3 E).

Taken together, these experiments indicate that MAPK and GSK3 trigger the formation of a phosphodegron bound by the E3 ligase beta-TrCP, causing the polyubiquitination of Smad4 as indicated in the model in Figure 4.3 F.

4.3.4 Wnt and TGF-beta signaling cross-talk via Smad4

A central question is whether the TGF-beta, FGF and Wnt signaling pathways are insulated from each other or integrated via the Smad4 phosphorylation sites. To address this, HEK293 cells were transfected with the TGF-beta-specific reporter CAGA12-Luciferase (Dennler et al., 1998) and treated with or without Wnt3a. TGF-beta signaling was unaffected by Wnt3a (Figure 4.4 A, bars 2 and 4), as expected if the two pathways were distinct and insulated from each other. However, addition of FGF2 reduced TGF-beta signaling by two thirds (Figure 4.4 A, bar 6),

presumably by priming inhibitory GSK3 phosphorylations. Importantly, in the presence of FGF2, Wnt3a was able to stimulate TGF-beta signaling, reaching signaling levels higher than those of TGF-beta alone (Figure 4.4 A, see brackets). Wnt also potentiated expression levels of the endogenous TGF-beta target genes PAI-1 and Smad7 in HepG2 cells (Figures 4.4 B, 4.S4 A and B), and the stimulation of TGF-beta signaling by Wnt was mimicked by the GSK3 inhibitor LiCl (Figure 4.S 4C and D). A DN-Tcf3 construct (Molenaar et al., 1996) did not affect the cross-talk between TGF-beta, FGF and Wnt3a, indicating that this mechanism is independent of Tcf3/beta-Catenin mediated transcription (Figure 4.S4E). We note that the stimulation of TGF-beta signaling by Wnt was not observed in confluent cell cultures (Figure 4.S4F), as is the case with other TGF-beta effects (Varelas et al., 2010). Finally, a BMP reporter gene (BRE-Luc) (Korchynskyi and ten Dijke, 2002) was also regulated by Wnt in the presence of FGF (Figures 4.S4 G and H), indicating that the Smad4 regulatory mechanism described here applies to both the TGF-beta and BMP branches of the pathway. These experiments showed that Wnt enhances TGF-beta signaling, but only when MAPK/Erk is activated by FGF.

We then investigated the extent to which the observed cross-talk between TGF-beta and Wnt signaling was mediated by the linker GSK3 phosphorylations in Smad4. The receptor-regulated Smad2/3 contains linker SP sites as well as an

unprimed GSK3 site in the DNA binding domain of Smad3 (Guo et al., 2008; Millet et al., 2009, Abushahba et al., 2012). To assess specifically the role of Smad4, we used mammary carcinoma MDA MB-468 cells which lack endogenous Smad4 and TGF-beta responsiveness (de Caestecker et al., 2000). Transfection of Smad4-wt restored TGF-beta signaling which was potentiated by Wnt in the presence of EGF (Figure 4.4 C, bars 5 and 6). However, when cells were transfected with the GSK3 phosphorylation-resistant Smad4-GM, TGF-beta caused a strong signal but lost all regulation by Wnt3a (Figure 4.4 C, bars 8 and 9). Since replacing Smad4 by a GSK3-insensitive mutant eliminated Wnt potentiation, we conclude that the observed cross-talk between TGF-beta and Wnt is mediated through the GSK3 phosphorylation sites of Smad4 and not by other components of the signal transduction pathway.

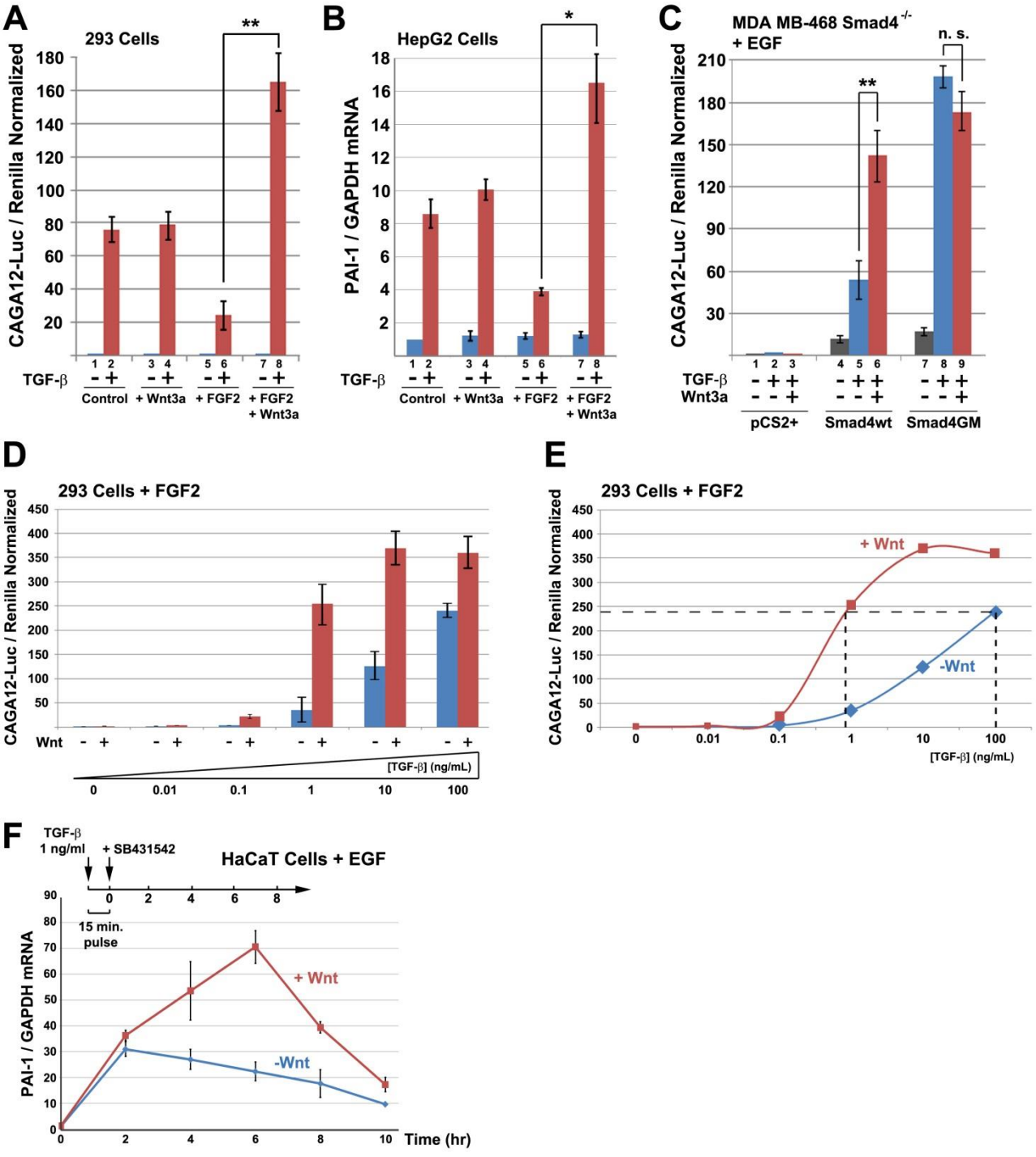

Figure 4.4: Wnt and TGF-beta Signaling Cross-talk via Smad4 GSK3 Phosphorylations

(**A**) TGF-beta CAGA12-Luc reporter gene assays in 293 cells showing that Wnt potentiated TGF-beta signaling, but only in the presence of FGF (brackets).

(**B**) The endogenous TGF-beta target gene PAI-1 was similarly regulated 3 hours after addition of TGF-beta and FGF (HepG2 cells).
(**C**) TGF-beta signaling was restored in MDA-MB-468 ($Smad4^{-/-}$) cells by Smad4-wt. Note that Wnt3a regulation was lost when Smad4-wt was replaced by the GSK3 phosphorylation-resistant mutant Smad4-GM.
(**D**) TGF-beta concentration-dependence of CAGA12-Luc expression in FGF2-treated 293 cells.
(**E**) Same data as in D displayed as curves showing that Wnt3a is a very potent activator at low concentrations of TGF-beta ligand.
(**F**) Time-course analysis of the TGF-beta transcriptional response after terminating a 15 min of a pulse of a low amount of TGF-beta with SB-431542. The induction of PAI-1 transcripts was prolonged by Wnt3a treatment (in EGF-treated HaCaT cells).

The potent stimulatory effect of Wnt on TGF-beta signaling was concentration-dependent, and best revealed in 293 cultured cells treated with FGF and variable amounts of TGF-beta (Figure 4.4 D). When the same data was displayed as shown in Figure 4E, it was observed that in the absence of Wnt3a (and presence of FGF) 100 ng/ml TGF-beta were required for a 240-fold induction of CAGA12-Luc, while in the presence of Wnt3a only 1 ng/ml TGF-beta was sufficient to reach a similar transcriptional activation.

We also examined how Wnt affected the time-course of the TGF-beta transcriptional response (Figure 4.4 F). HaCaT cells were treated with a 15 min pulse of 1 ng/ml TGF-beta, which was terminated by adding 2 µM of the type I TGF-beta receptor inhibitor SB-431542 (Halder et al., 2005). Analyses of transcripts for the TGF-beta target gene PAI-1 showed that Wnt significantly prolonged the TGF-beta transcriptional response (Figure 4.4 F).

From these functional experiments we conclude that, although TGF-beta and Wnt signaling are insulated in the absence of FGF, activation of the MAPK pathway causes a robust cross-talk in which canonical Wnt enhances and prolongs signaling by low, presumably the most physiologically relevant, levels of TGF-beta ligands.

4.3.5 The Smad4 linker contains a growth-factor regulated transcriptional activation domain

A short region of the linker has been identified as a Smad4 Activation Domain (SAD) (de Caestecker et al., 2000). This 48 amino acid sequence binds the transcriptional co-activator p300/CBP and contains the MAPK site, but not the GSK3 sites. We asked if a construct containing the entire linker domain (169 amino acids) could be regulated by FGF and Wnt. The Smad4 linker region was fused to the yeast Gal4 DNA Binding Domain (Gal4DBD) (Figure 4.5 A) and used in transcriptional assays with a UAS-Gal4-Luciferase reporter gene (de Caestecker et al., 2000). The linker region of Smad4 was both required and sufficient to drive transcriptional activity in a TGF-beta independent way (Figure 4.S5 A and B). Interestingly, the activity of the transcription activation domain contained in the linker region was repressed by FGF and significantly increased by Wnt3a (Figure 4.5 B, bars 2-4). When the GSK3 sites were mutated (Gal4DBD-S4linker-GM) Wnt lacked any significant effect (Figure 4.5 B, bars 6 and 7). Surprisingly, FGF stimulated the transcriptional activity of the S4linker-GM construct instead of inhibiting it (Figure 4.5 B, bars 5 and 6), indicating that MAPK phosphorylation has a positive effect on the Smad4 transcription factor (in the absence of GSK3 phosphorylations). In agreement with this, mutation of the MAPK priming site

(Gal4DBD-S4linker-MM) had very low levels of transcriptional activity (Figure 4.5 B bars 8 to 10).

An important feature of the Gal4DBD-S4linker constructs is that their stability was not affected by FGF or Wnt treatment (Figure 4.5 C). In RasG12V-transfected cells Gal4DBD-S4linker-wt was heavily phosphorylated by GSK3 but not degraded (Figure 4.5 D). In the same cells, endogenous Smad4 was destabilized by the sustained Ras activation and its steady-state levels were restored by a dominant-negative form of GSK3 (Figure 4.5 D, lanes 3 and 4). The Smad4 linker region lacks lysine residues, suggesting that the polyubiquitination and degradation of this artificial Gal4-DBD fusion protein might differ from Smad4-wt. In support of this view, DN-beta-TrCP did not affect the induction of the UAS-Luciferase reporter gene by Gal4DBD-S4linker regardless of FGF treatment (Figure 4.S5D), even though the same DN-beta-TrCP construct was able to significantly increase TGF-beta signaling by Smad4-wt (Figure 4.3 E). Because the stability of the Gal4-DBD construct was unchanged by phosphorylation of the linker sites, the induction of the UAS-Luciferase reporter allowed the measurement of transcriptional responses independently of changes in protein stability.

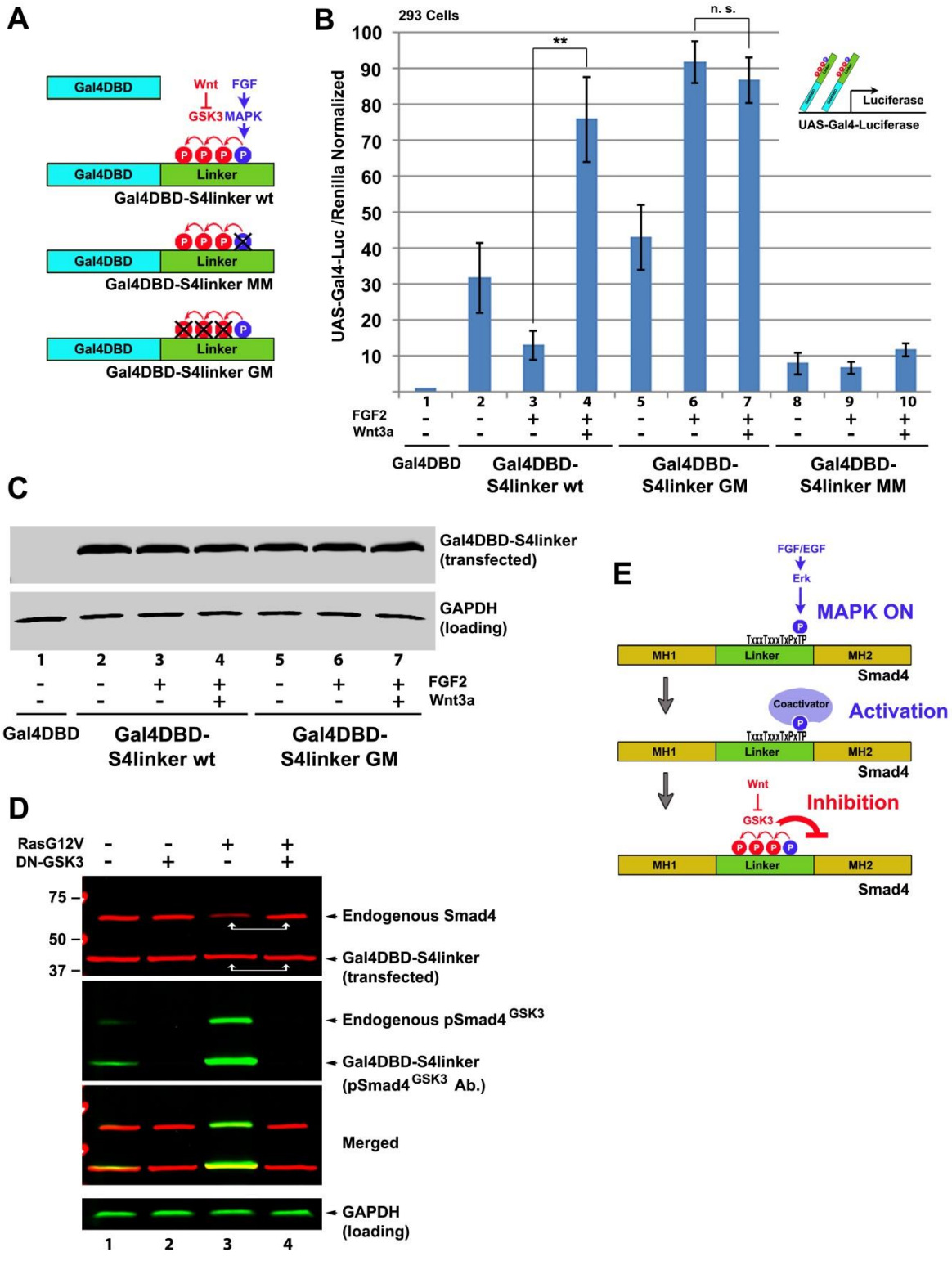

Figure 4.5: The Smad4 Linker Domain Contains a Growth Factor Regulated Transcriptional Activation Domain

(**A**) Diagram of the yeast Gal4 DNA Binding Domain (Gal4DBD) fused to Smad4 linker region and of the phosphorylation-resistant mutants used to test transcriptional activation.
(**B**) UAS-Gal4-Luciferase reporter gene assays in 293 cells showing that the linker transcriptional activation domain was regulated by FGF and Wnt.
(**C**) Western blot showing that Gal4DBD-S4linker protein levels remained unchanged by FGF and Wnt treatment despite the differences observed in transcriptional activity.
(**D**) Gal4DBD-S4linker was heavily phosphorylated by GSK3 when co-transfected with activated RasG12V, but its stability is not affected. In contrast, endogenous Smad4 was destabilized by the sustained MAPK activation driven by Ras, and this required GSK3 activity.
(**E**) Model of Smad4 transcriptional activity regulation by FGF and Wnt via the linker phosphorylation sites and binding of an as yet unknown coactivator.

These results indicate that MAPK and GSK3 phosphorylations regulate the activity of a transcriptional activation domain located in the Smad4 linker region (Figure 4.5 E). The phosphorylation of Smad4 linker region by MAPK and GSK3 initially regulates its transcriptional activation domain, and then facilitates its degradation via the E3-ligase beta-TrCP.

4.3.6 Phosphorylation by MAPK/Erk promotes Smad4 peak activity

To further investigate the function of the MAPK phosphorylation site, we constructed a series of Smad4 mutants mimicking different combinations of signaling events (Figure 4.6 A). The MAPK/Erk site (PxTP) located at position 277 was known to be important for Smad4 nuclear translocation in response to TGF-beta treatment (Roelen et al., 2003). Using EGF-stimulated MDA MB-468 Smad4$^{-/-}$ cells, we found that a MAPK phosphorylation-resistant mutant (Smad4-MM) had lower levels of TGF-beta signaling (Figure 4.6 B, compare bars 4 to 6). Smad4GM-MM, which differs by a single amino acid (T277V) from Smad4-GM, also had reduced activity (Figure 4.6 B, bars 8 and 10). These experiments indicated that Thr 277 phosphorylation is required for Smad4 peak activity.

In the absence of priming by EGF stimulation, the cross-talk between TGF-beta and Wnt3a was not observed in Smad4wt transfected MB-468 cells (Figure

4.6 C, compare bars 5 to 6). However, when a phospho-mimetic amino acid was introduced (T277D) at the MAPK site (MAPK phospho-Activated, Smad4-MA), the enhancement of TGF-beta signaling by Wnt was restored (Figure 4.6 C, compare bars 8 and 9). Wnt was without effect when the GSK3 sites were also mutated (Smad4GM-MA construct, Figure 4.6 C, bars 11 and 12).

A similar requirement for the Smad4 MAPK site was found in the *Xenopus* embryo using an assay in which a low dose of *beta-Catenin* mRNA (20 pg) was injected into a ventral blastomere to induce partial secondary axes (Figure 4.6 D). These axes were blocked by co-injection of Smad4 antisense morpholinos (MOs) (Dupont et al., 2009), but restored by hSmad4-wt mRNA (Figure 4.6 E and F). Smad4-GM induced complete secondary axes with heads, and this required a functional or phospho-mimetic 277 site (Figures 6 G-J and 4.S6).

From these experiments, and others shown in this study, we conclude that Smad4 phosphorylation at Thr 277 has a dual function. First, it allows Smad4 to reach peak transcriptional activity. Second, it primes Smad4 for GSK3 phosphorylations that cause transcriptional inhibition and generate a phosphodegron that serves as a docking site for the ubiquitin E3 ligase beta-TrCP. Thus, both the activity and the stability of Smad4 are regulated by FGF/EGF and Wnt.

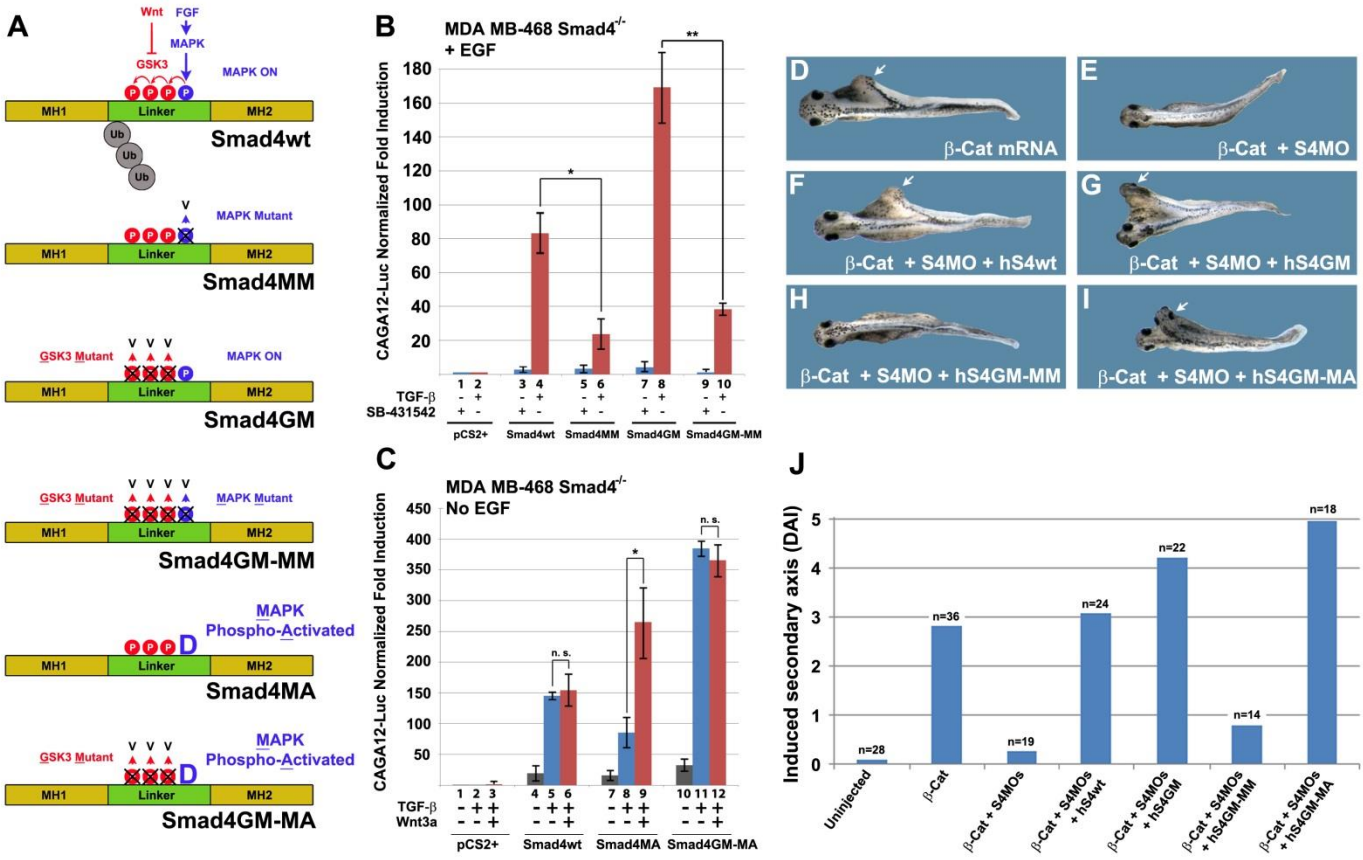

Figure 4.6: Phosphorylation of Threonine 277 is Required for Smad4 Peak Activity

(**A**) Schematic diagrams of Smad4 phospho-resistant and phospho-mimetic mutants.
(**B**) Phosphorylation of the MAPK site (Thr 277) was required for Smad4 maximal activity in the presence of EGF in Smad4$^{-/-}$ cells. Brackets indicate that Smad4-MM had decreased activity in the TGF-beta pathway. The TGF-beta receptor inhibitor SB-431542 (2 µM) was added in the indicated lanes to block autocrine TGF-beta derived from MDA-MB-468 cells; for results in the absence of SB-431542 see Figure 4.S6B.
(**C**) In the absence of an EGF signal, mutation of the MAPK priming site into a phospho-mimetic residue (T277D, Smad4-MA) restored the cross-talk between Wnt and TGF-beta in transfected Smad4$^{-/-}$ cells. Note also that Wnt potentiation of TGF-beta signaling required functional Smad4 GSK3 sites.
(**D**) 20 pg of beta-Catenin mRNA injected ventrally at the 4-cell stage is sufficient to induce a partial duplicated axis lacking head structures.
(**E**) Formation of beta-Catenin secondary axes required Smad4.

(**F**) Partial axes were rescued by 125 pg of hSmad4-wt mRNA co-injected together with beta-Catenin mRNA and Smad4 MOs.
(**G**) The same amount of mRNA encoding hSmad4-GM induced complete axis with eyes and cement gland (see arrow).
(**H**) 125 pg of hSmad4GM-MM mRNA in which the MAPK site was mutated (T277V) was completely inactive in this assay. Note that this construct differs from Smad4-GM by a single amino acid. This suggests that Smad4 activity requires an intact MAPK phosphorylation site in *Xenopus* embryos.
(**I**) hSmad4GM-MA in which the MAPK site was mutated into a phospho-mimetic Aspartic acid induced the strongest complete axes indicating a positive role for the PxTP site.
(**J**) Quantification of the embryos microinjection results using the Dorso-Anterior Index (DAI) (Kao et al., 1986) to measure the completeness of secondary axes; similar results were obtained in three independent experiments.

4.3.7 Smad4 regulation by GSK3 determines germ layer specification

The early *Xenopus* embryo provides an excellent system to study cell signaling. Using embryos depleted of endogenous Smad4 with MOs, we found that hSmad4-wt mRNA rescued expression of *xBrachyury* (a Nodal/TGF-beta mesodermal target), while the same amount of GSK3-resistant Smad4-GM showed a great increase in signaling (Figure 4.7 A-D). The replacement of endogenous Smad4 by Smad4-GM mRNA caused the entire embryonic ectoderm to become mesoderm (Figure 4.7D). This indicated that inhibition of Smad4 by GSK3 plays a crucial role in allowing ectodermal differentiation *in vivo*.

Smad4-GM also caused a strong increase in Spemann organizer tissue marked by *chordin* mRNA in embryos depleted of endogenous Smad4 (Figure 4.7 E-H). This suggested that GSK3 activity may normally limit the size of the organizer through Smad4. In *Xenopus*, Spemann organizer formation requires the combined action of the maternal Wnt/beta-Catenin pathway and of an early zygotic Nodal signal (Labbé et al., 2000; Reid et al., 2012) as indicated in Figure 4.7 I.

To test whether Wnt can directly regulate Smad4 through its GSK3 sites in the embryo, we developed a sensitive synthetic Smad4-Luciferase reporter derived from the mouse *chordin* promoter, described in Figure 4.S7. Smad4-depleted embryos were co-injected with the reporter and Smad4-wt or Smad4-GM, animal cap cells dissociated, and treated with Activin protein (Figure 4.7 J). Microinjected

Wnt8 mRNA potentiated Activin signaling, and this Wnt8 effect had a complete requirement for the GSK3 sites in Smad4 (Figure 4.7 J, brackets). Because the Smad4 reporter gene does not respond to Wnt or Siamois (Figure 4.S7E), this result shows that the enhanced sensitivity to Activin caused by Wnt is mediated, at least in part, through the GSK3 phosphorylation sites in Smad4. In the *Xenopus* early blastula, three signaling pathways - Wnt/beta–Catenin, Nodal/pSmad2, and FGF/MAPK – have been shown to be activated in the dorsal region (Schohl and Fagotto, 2002). The convergence of these three signals by the molecular mechanism identified here helps explain the peak Smad4 activity required for Spemann organizer induction (Figure 4.7 K).

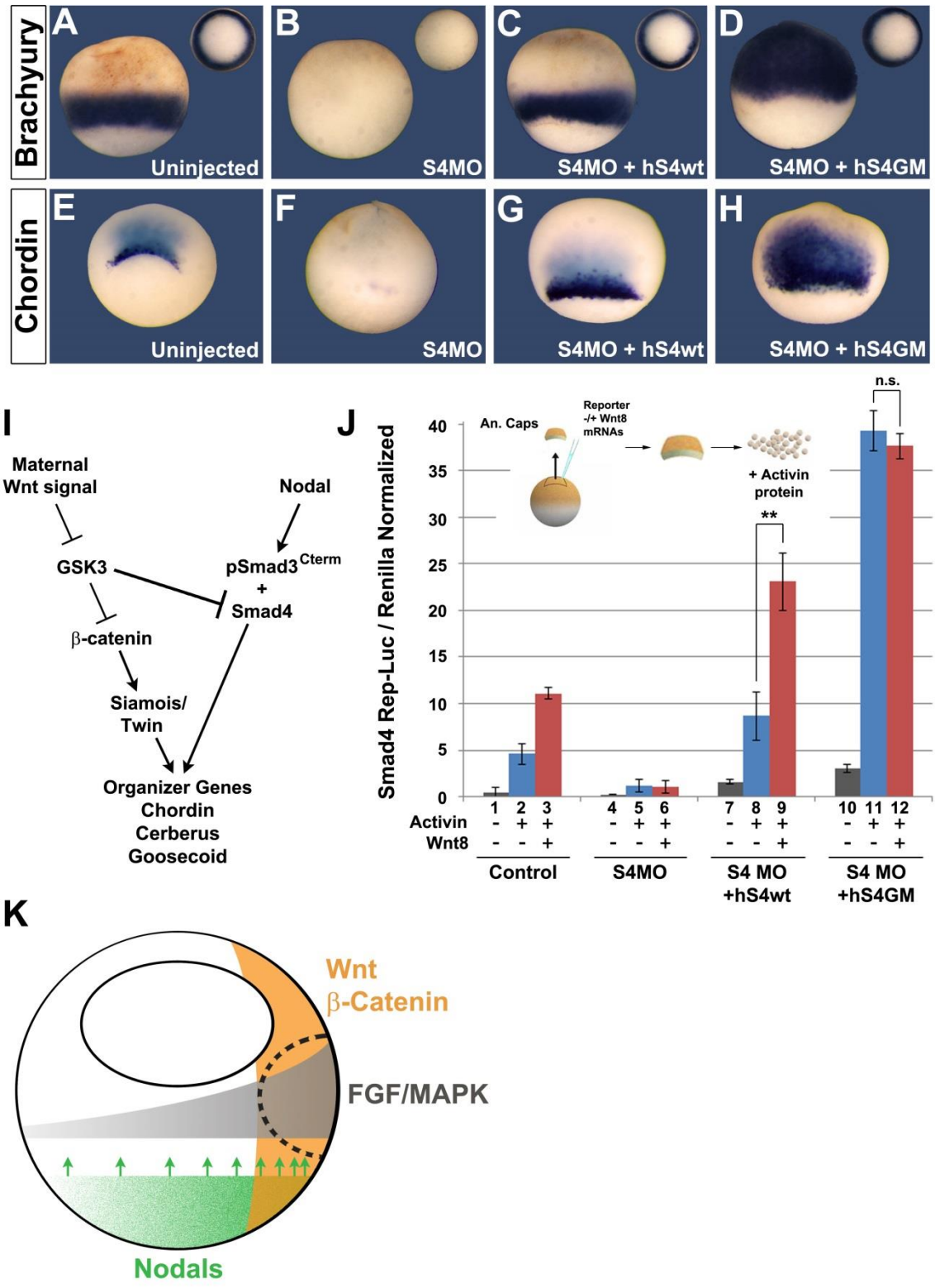

Figure 4.7: Smad4 Regulation by GSK3/Wnt is Involved in Germ-Layer Specification and organizer formation in *Xenopus*

(**A-D**) Endogenous Smad4 replacement by Smad4-GM showing that GSK3 phosphorylation was required for ectodermal specification in *Xenopus*. The mesodermal marker xBrachyury was greatly expanded when Smad4 GSK3 phosphorylations were prevented.
(**E-H**) The Spemann organizer gene Chordin is expanded by Smad4-GM injection.
(**I**) Diagram showing how maternal Wnt and zygotic Nodal/TGF-beta signals converge in early *Xenopus* embryo patterning. GSK3 is proposed to inhibit Nodal/Smad4 activity.
(**J**) In dissociated *Xenopus* animal cap cells, *xWnt8* mRNA potentiates signaling by 5 ng/ml Activin through the Smad4 GSK3 phosphorylation sites. This experiment used a novel Smad4-Luciferase reporter designed for *Xenopus* assays, and shows that Wnt modifies the competence of cells to Activin induction through Smad4. Cells were harvested when sibling embryos reached early gastrula (stage 10.5).
(**K**) Three signaling pathways – Wnt, FGF and Nodal – converge on the dorsal side of the *Xenopus* embryo (stippled line) during Spemann organizer formation.

4.4 Discussion

The experiments reported here show that Smad4, long thought to act as a constitutively active component of the TGF-beta and BMP pathways, is strongly regulated by growth factor signaling through novel phosphorylation sites in its linker region. We found that Smad4 is phosphorylated by GSK3 in response to FGF. These phosphorylations regulate a transcription activation domain located in the Smad4 linker domain and generate a Wnt-regulated phosphodegron recognized by the E3 ligase beta-TrCP. This mechanism provides a means of integrating distinct pathways which would otherwise remain insulated, allowing cells to sense FGF and Wnt inputs and adapt TGF-beta outcome to their context.

4.4.1 Smad4 activity is regulated by growth factors

Although the TGF-beta pathway has been extensively studied for more than two decades, many efforts have focused on R-Smads regulation and less is known about Smad4. In this study, we show that four phosphorylation sites located in the linker region of Smad4 control its activity and stability in response to growth factor stimulation. GSK3 phosphorylation is triggered by FGF or EGF through activation of the Erk pathway. Phosphorylation by MAPK at Thr 277 allows Smad4 to reach its peak of activity while priming it for subsequent inhibitory GSK3

phosphorylations. The switch operated by GSK3 phosphorylation provides a way of controlling the duration of the Smad4 signal by ensuring that degradation and turnover follow transcriptional activation. Our observations reconcile previous results in the literature that appeared to be contradictory: it had been proposed that activation of the MAPK pathway was required for Smad4 nuclear localization (Roelen et al., 2003) while also triggering its degradation (Saha et al., 2001). In addition, Smad4 had been proposed to be a central regulator of TGF-beta transcriptional timing (Warmflash et al., 2012).

Our findings that Wnt signals through Smad4 GSK3 sites and can prolong the duration of a TGF-beta pulse support the view that Smad4 is an active regulator of TGF-beta signaling rather than a silent partner. The stimulatory effects of Wnt on TGF-beta signaling were entirely lost when Smad4-wt was replaced by the GSK3 phosphorylation-resistant Smad4-GM, both in human cultured cells and in *Xenopus* embryos. This indicates that the cross-talk between Wnt and TGF-beta described here is mainly mediated by Smad4 GSK3 sites and not by other components of the TGF-beta signaling pathway. Perhaps the co-Smad Smad4 evolved a specialized role in the integration of multiple signaling pathways.

Wnt and FGF/EGF growth factors had striking effects on Smad4 transcriptional activity, particularly at low TGF-beta concentrations (Figure 4.4). They also had an effect on Smad4 stability by triggering the polyubiquitination and

proteasomal degradation of the fraction of Smad4 phosphorylated by MAPK and GSK3 (Figures 2 and 3). A short Smad4 Activation Domain (SAD) that contains the MAPK site (but not the GSK3 sites) had been described (de Caestecker et al., 2000). We now found that the linker domain of Smad4 acts as a Wnt-stimulated activation domain independently of protein degradation (Figure 4.5).

4.4.2 beta-TrCP binds to the Smad4 phosphodegron

Smad4 is polyubiquitinated and degraded by beta-TrCP (Wan et al., 2004; Wan et al., 2005; Yang et al., 2006). We now show that the binding of beta-TrCP to Smad4 is not constitutive, but finely regulated by GSK3 linker phosphorylations triggered by FGF and inhibited by Wnt. In *Drosophila* egg chambers, clonal analysis of *slmb* mutations (the beta-TrCP homolog) revealed high levels of Medea protein (the Smad4 homolog), together with a high-BMP phenotype (Muzzopappa and Wappner, 2005). The first two Smad4 GSK3 sites have been conserved in *Drosophila*, other insects, and even planarians (data not shown) suggesting that linker phosphorylations represent an ancient mechanism that regulates Smad4 activity during embryonic patterning.

The positive effect of Threonine 277 phosphorylation on Smad4 activity (Figure 4.6) and the presence of a transcriptional activation domain in Smad4

suggest that co-activators might bind to the mono-phosphorylated PxTP site to drive transcription. A prime candidate is p300, which has been shown to bind to the SAD domain of Smad4 (de Caestecker et al., 2000). Recently, it has been found that the mediator of the Hippo pathway YAP binds phosphorylated SP sites in the Smad1 sequence (Alarcón et al., 2009; Aragón et al., 2011) through its WW domain. The other mediator of the Hippo pathway, TAZ, has been shown to bind active Smad2/3/4 complexes and to connect TGF-beta signaling to cell density (Varelas et al., 2008, 2010). It is therefore tempting to speculate that TAZ or YAP may recognize the phosphorylated TP site in Smad4 acting as co-activators. Alternatively, the Smad4 linker region might recruit other co-activators depending on cellular context. Future studies will be required to identify Smad4 phospholinker interacting proteins.

4.4.3 Signalling insulation and crosstalk

Wnt signaling depletes active GSK3 from the cytosol, potentially affecting the phosphorylation of many proteins in addition to beta-Catenin (Taelman et al., 2010; Vinyoles et al., 2014, Acebron et al., 2014). This raises the general question of how signaling pathways are normally insulated from, or integrated with, each other. The regulation of Smad4 activity by Wnt, which is observed only in the presence

of MAPK activation (or by introducing a phospho-mimetic priming site) indicates that the choice between insulation or cross-talk depends on priming kinases regulated by growth factors.

In the *Xenopus* embryo, it has been determined that shortly after mid-blastula (stage 8.5), nuclear beta-Catenin, diphospho Erk, and C-terminal phospho-Smad2 are found in dorsal-marginal cells (Schohl and Fagotto, 2002). These protein distributions result from a maternal Wnt signal, a marginal zone gradient of FGF that starts on the dorsal side, and a Nodal/TGF-beta gradient emanating from the dorsal-vegetal pole (Figure 4.7K) (De Robertis and Kuroda, 2004). This may generate a perfect storm of growth factor signals that converge on the Smad4 protein to generate maximal transcriptional activation. In this view, the different territories of the embryo would be shaped and defined by Wnt/GSK3 and FGF/MAPK feeding on the Nodal/TGF-beta morphogen gradient. Other mechanisms including combinations of transcription factors, such as Siamois/Twin and activated Smad2/3/4 at the level of specific promoters will be important as well (Labbé et al., 2000; Reid et al., 2012).

Replacement of endogenous Smad4 with its GSK3 phosphorylation-resistant mutant in *Xenopus* embryos resulted in the entire ectoderm becoming mesoderm. This suggests that GSK3 inhibition of Smad4 plays an essential role in allowing ectodermal differentiation in vivo, and extends previous findings in the field

indicating a key role for Smad4 in ectoderm specification (Dupont et al., 2005; Dupont et al., 2009). In addition, phosphorylation of Smad4 by GSK3 serves to constrain the size of Spemann's organizer. The cross-talk between the Wnt and Nodal/TGF-beta pathways at the level of Smad4 could help explain in part the mysterious "competence modifier" effect observed in *Xenopus,* in which xWnt8 mRNA does not induce mesoderm by itself, yet greatly sensitizes the competence of ectoderm to respond to Activin/TGF-beta (Sokol and Melton, 1992; Moon and Christian, 1992).

4.4.4 Smad4 linker phosphorylation and tumor suppression

In cancer, Smad4/DPC4 acts as a barrier for tumor progression (Ding et al., 2011; Vogelstein et al., 2013). TGF-beta signaling has potent anti-proliferative effects in epithelia through the activation of Cyclin-Dependent Kinase (CDK) inhibitors such as $p14^{Ink4b}$ and $p21^{WAF1}$ (Hanahan and Weinberg, 2011). At early stages, many tumors are driven by activation of the Ras/Erk and the Wnt oncogenic pathways, which increase proliferation genes such as Cyclin D and c-Myc (Hanahan and Weinberg, 2011). In our proposed mechanism, these mitogenic effects will be counterbalanced by the increase in TGF-beta/Smad4 anti-proliferative activity mediated by MAPK and Wnt/GSK3 signaling. This barrier effect of TGF-beta is

lost when the Smad4 tumor suppressor is deleted or inhibited. The discovery that Smad4 activity is not constitutive but instead regulated by growth factors helps understand why its loss has such catastrophic consequences during progression of pancreatic, colorectal, and prostate cancers.

Smad4 is frequently deleted in metastatic tumors, but intragenic point mutations are also found (Levy and Hill, 2006; Xu and Attisano, 2000). Interestingly, several of these point mutations increase Smad4 degradation by facilitating binding to beta-TrCP (Wan et al., 2005; Yang et al., 2006). Our finding that beta-TrCP binding to Smad4 is regulated by GSK3 phosphorylations suggests that pharmacological GSK3 inhibitors may stabilize Smad4 and restore growth control in such tumors.

4.5 Experimental Procedures

Mammalian Cell Culture

NIH-3T3, CAGA12-HaCaT, HEK293 (lacking T antigen, which respond very well to TGF-beta), L-cells (ATCC #CRL-2648) as well as L-Wnt3a-cells (ATCC #CRL-2647) were cultured in DMEM supplemented with 10% fetal bovine serum (GIBCO) and cultured at 37°C in 5% CO_2. MDA-MB-468 cells (which lack Smad4) were cultured in DMEM:Ham's-F12 (1:1 vol:vol). L-cell control

conditioned medium and Wnt3a conditioned medium were prepared according to the ATCC protocol (Willert et al., 2003), with the exception that 2% serum was used. Wnt3a conditioned medium was further boosted by adding 200 ng/ml of recombinant murine Wnt3a protein (PeproTech). DNA constructs were transfected with BioT (Bioland) 24 hr after plating cells. siRNAs were transfected with Lipofectamine 2000 using the reverse transfection protocol (Invitrogen) and analyzed after 48 hr. Cycloheximide (Sigma #C-7698) was dissolved in ethanol and used at a final concentration of 20 mg/ml (Taelman et al., 2010).

Antibodies

The following antibodies were used in this study: alpha-Smad4 monoclonal (Santa Cruz Biotechnology B-8, 1:250), alpha-diphosphorylated ERK-1&2 monoclonal (Sigma, 1:500), alpha-GAPDH (Cell Signaling 14C10, 1:7,000), alpha-Flag mouse (Sigma, 1:3,000), rabbit alpha-ubiquitin (Santa Cruz Biotechnology FL-76, 1:200), alpha-HA (Sigma, 1:3,000), rabbit alpha-beta-TrCP (Cell Signaling D13F10, 1:800), mouse alpha-Gal4DBD (Santa Cruz RK5C1, 1:200). Secondary antibodies used were IRDye 800CW Donkey anti-Rabbit IgG (Li-Cor 926-32213, 1:5,000) and IRDye 680RD Donkey anti-Mouse IgG (Li-Cor 926-68072, 1:5,000). For custom pSmad4^{GSK3} antibody, a synthetic peptide ([H]-CKK-Acp-

NSTTTWT(PO3)GSRT(PO3)APY-[NH2]) was used to immunize two rabbits (Covance). The antiserum with the highest ELISA titer was positively affinity-purified and was used at a concentration of 1:5,000 for detection of endogenous Smad4 phosphorylations and at 1:25,000 for overexpressed proteins.

Statistical Analyses

Results are given as the mean ± standard error of the mean (SEM). Statistical analyses were performed with Excel (Microsoft Corp.) applying the two-tailed t test. Differences of means were considered significant at a significance level of 0.05. The following symbols are annotated: not significant, n.s. ($P > 0.05$); * ($P \leq 0.05$); ** ($P \leq 0.01$); *** ($P \leq 0.001$).

Western blot analyses

For western blot analyses, cells were cultured in 6-well plates and deprived of serum for 18 hours prior to treatment. Cells were treated with the indicated additions for 4 hours and then lysed in radioimmunoprecipitation assay buffer (RIPA lysis buffer, 0.1% NP40, 20 mM Tris/HCl pH 8, 10% Glycerol) supplemented with protease inhibitors (Roche #04693132001) and phosphatase inhibitors (Calbiochem 524629). Western blots were performed using standard

protocols. Odyssey™ Blocking Buffer (LI-COR) diluted in PBS (1:1 ratio) was used to block nitrocellulose membranes for one hour at room temperature. All antibodies were diluted in PBS:Odyssey™ Blocking Buffer supplemented with 0.1% Tween 20. Primary antibodies were incubated overnight at 4°C. Membranes were then washed extensively with Tris-buffered saline Tween 20 (TBST buffer) and incubated with secondary antibodies for one hour at room temperature. Images were acquired using an Odyssey 9120 infrared imaging system (LI-COR).

Phos-tag analyses

For each condition a 10 cm plate of near-confluent NIH-3T3 cells was used. Cells were washed with ice cold HBS (HEPES 20 mM, NaCl 150 mM) (note that it is important to avoid use of a phosphate-containing buffer such as PBS) before lysis with 1 ml of RIPA buffer. The phosphate-affinity polyacrylamide gel was prepared using a 9% polyacrylamide gel containing 75 µM Phos-tag and 100 µM $MnCl_2$. Samples were electrophoretically resolved at 10 mA. After electrophoresis, the gel was soaked in transfer buffer (25 mM Tris, 192 mM glycine, pH 8.3, 20% methanol and 0.1% SDS) containing 1 mM EDTA for 10 min (to remove Phos-tag), and washed in buffer without EDTA for 10 min at room temperature. Proteins were then transferred to a Protran BA 83 nitrocellulose membrane and probed with

mouse alpha-Smad4 monoclonal (Santa Cruz) and rabbit pSmad4^{GSK3} (custom-made).

Phosphatase treatment

Cells were deprived of serum for 18 hours and then treated for two hours with 10 ng/ml FGF2 (R&D Systems, 233-FB). Cells were washed extensively with HBS (note that PBS should not be used since it contains sodium phosphate which acts as a competitive inhibitor of the phosphatase) before being lysed with EDTA-free RIPA lysis buffer. Sample was divided into two, one for control and one for phosphatase treatment. Calf intestinal alkaline phosphatase, CIP, treatment was performed for 45 minutes at 37ºC according to manufacturer's instructions (New England Biolabs).

Plasmid Reagents

Flag-tagged human Smad4 in pCMV5 was obtained from Addgene (Addgene plasmid 14039) (Lagna et al., 1996) and subcloned into the ClaI and EcoRI sites of the *Xenopus* expression vector pCS2+. PCR-based site-directed mutagenesis (QuikChange II Site-Directed Mutagenesis, Stratagene) was employed to generate all Smad4 mutants used in this study. Primers used were as follows:

Smad4-MM (ggactgcaccatacgcacctaatttgc);

Smad4-GM (cataacagcgtaccacctgggctggaagtagggctgcaccatac);

Smad4-MA (ggactgcaccatacgaccctaatttgc).

Mutations were confirmed by sequencing. pCS2+ Smad4ΔMH1 was generated by PCR amplification and subcloning of amino acids 139-552 of pCMV5-Smad4 into pCS2+. pCS2+ Smad4Δlinker was generated by subcloning the isoform Smad4Δ4-7 (generous gift of C. Hill) from pEF-Flag into pCS2+. HA-tagged human beta-TrCP wt or ΔF-box (referred as DN-beta-TrCP in Figure 4.S2) were generous gifts from C. Carbone, and subcloned from pEF61 vector into pCS2+.

Polyubiquitination Assays

Ubiquitination assays were as described (Zhu et al., 1999). For polyubiquitination assays using endogenous Smad4, 10 cm plates were used. Briefly, cells were depleted of serum for 16 hours and then treated in the indicated conditions for 4 hours. Cells were lysed in 500 µl RIPA lysis buffer. Lysates were centrifuged at 16,000 × *g* at 4°C for 10 min, supernatants transferred to new tubes and 10 µl of 10% SDS was added. The samples were boiled at 95°C for 10 min to break protein-protein interactions and then diluted 10-fold with RIPA buffer. The diluted samples were then incubated with Smad4 monoclonal antibody (Santa Cruz Biotechnology B-8, 2 µg), protein A/G agarose beads (Santa Cruz Biotechnology sc-2003) and incubated using an end-over-end rotator overnight at 4°C. Lysates and beads were transferred to clean tubes and beads precipitated. Precipitates were

washed three times using RIPA buffer and finally denatured in SDS loading buffer at 95°C for 10 min. Rabbit anti-Ubiquitin (Santa Cruz Biotechnology FL-76, 1:200) was used to detect polyubiquitinated endogenous Smad4.

Quantitative RT-PCR

For expression analyses of endogenous genes, total RNA was extracted using Absolutely RNA Microprep Kit (Agilent Technologies). cDNA was synthesized and mRNA levels analysed using the SYBR green reagent. Relative levels were determined using the Comparative C_t method using the housekeeping gene *Gapdh* as loading control. Primers were as described (Varelas et al., 2010).

Reporter Gene Assays

For most Luciferase reporter gene assays 293 cells (lacking T antigen, which respond better to TGF-beta) were transiently transfected in 6-well plates at 80% confluency. The following day, cells were trypsinized and plated on 24-well plates with 2% serum medium. Serum contains growth factors, including FGF, that complicate analysis so using low serum is important. Cells were allowed to attach to the plastic surface and treated with control conditioned medium, FGF2 or Wnt3a for 16 hours. Growth factors were added when cells reached 60% or less confluency. This is important because we found that high confluency inhibits TGF-

beta signaling and the cross-talk between Wnt and TGF-beta (Figure 4.S3 E). In order to normalize the transfection efficiency, pCS2+ Renilla was co-transfected. The following amounts of plasmids were used per well: 1.2 µg CAGA12 reporter; 0.4 µg pCS2+ Renilla; 0.4 µg pCS2+ Smad4 in its wild type and mutant forms. DNA levels in each well were adjusted by adding empty pCS2+ vector, so that each well received a total of 2 µg of DNA. After treatment, cells were lysed with 180 µl of Passive Lysis Buffer (Promega) and Luciferase assays were performed with the Dual-Luciferase Reporter Assay System (Promega) according to the manufacturer's instructions, using a Glomax Luminometer (Promega).

Gal4DBD-Smad4 linker Transcriptional Activation Assay

Constructs for Gal4DBD-S4linker wt, MM or GM were generated by PCR amplification and subcloning of the linker region (amino acids 139-308) of Smad4-wt, MM or GM into pSG424 (de Caestecker et al., 2000). pG5-E1B-Luc was used as the UAS-Gal4 reporter gene (Prokova et al., 2005) and results were normalized over SV40-Renilla (because pSG424 uses a SV40 basal promoter). The following amounts of plasmid were transfected into 6-well plates: pG5-E1B-Luc (1.2 µg), SV40-Renilla (0.4 µg) and pSG424 constructs (0.4 µg).

Dissociation of Animal Caps Cells from *Xenopus* Embryos

Animal caps were excised at mid-blastula (stage 8) in Ca^{2+} Mg^{2+}-free Steinberg solution supplemented with 0.1% BSA. For each condition, twenty explants were transferred in 1.5 mL siliconized Eppendorf tubes (VWR #20170) and shaken at 1000 rpm in a Thermomixer (Eppendorf) until cells dissociated (this takes typically five minutes). Cells were allowed to settle, medium removed, and incubated in 100 µL of 10 ng/ml of recombinant human Activin A (R&D) until sibling embryos reached stage 10.5 (early gastrula). The supernatant was carefully removed and cells lysed in 50 µL of Passive lysis buffer (Promega) for Luciferase measurement.

Xenopus Embryo Assays

For *Xenopus* embryo microinjections, pCS2 plasmids were linearized with XhoI (therefore generating short mRNAs lacking the SV40 polyadenylation sequence) and mRNA synthesized with mMessage mMachine SP6 (Ambion). For embryo secondary axis induction, unless otherwise specified, the amount of mRNA injected into a ventral-vegetal cell at 4-8 cell stage was: 80 pg *GSK3-DN* mRNA, 100 pg *Siamois* mRNA, or 80 pg *beta-Catenin-Myc* mRNA (Yost et al., 1998). Ectodermal explants harvested for western blots (Figure 4.2H) were injected four times with 50 pg *Flag-Smad4* mRNA with or without 50 pg *xWnt8* mRNA. Animal

caps were excised at stage 9 and left intact or dissociated (see below). Animal caps were cultured until stage 10.5 and homogenized in lysis buffer (50 mM Tris pH 7.4, 150 mM NaCl, 1 mM EDTA, 1% Triton X-100, and Protease inhibitor #10863600 from Roche). For Luciferase reporter gene assays in *Xenopus* embryos, normalization was performed by co-injecting 5 pg of *Renilla* mRNA per cell (transcribed from the SP6 promoter of a $pCS2^{+}$ Renilla construct). This gives better results than injecting Renilla DNA, as it avoids squelching due to two different promoters and toxicity caused by DNA injections in *Xenopus* embryonic cells. In all experiments, the total amount of mRNA microinjected was adjusted by adding *GFP* mRNA, which is inert in signaling. Smad4 morpholinos were as described (Dupont et al., 2009; Chang et al., 2006):

XSmad4beta1-MO was GTAACAACAAGGGCAAAAGATGGCG;

XSmad4beta2-MO was GGGTCAGAGACATGGCCGGGATCTC;

XSmad4alpha-MO was TGTTTGTGATGGACATATTGTCGGT;

XSmad4 MOs were mixed and injected at 1:1:1 ratio (60 ng/embryo total). A total of 375 pg of *hSmad4-wt* mRNA injected four times at the 4-cell stage rescued the XSmad4 MO phenotype (Figure 4.6 A-H). A protocol for whole-mount *in situ* hybridization, can be found at www.hhmi.ucla.edu/derobertis/index.html.

Construction of a new Smad4-LucReporter for *Xenopus* experiments

In the course of this study we realized that, although excellent to study TGF-beta signaling in cultivated cells, the CAGA12-Luc reporter was suboptimal for *in vivo* assays in *Xenopus* embryos. We found that large DNA amounts of the reporter had to be injected in the embryo in order to detect a readable signal. This is particularly problematic in *Xenopus* because DNA injections are toxic and embryos will not tolerate more than 20 pg of DNA per injection. For this reason, we developed a new Smad4-Luciferase reporter derived from the mouse Chordin promoter containing multiple Smad Binding Elements (SBEs). This new reporter was found to respond very well to TGF-beta/Activin signals and moderately to BMP as well (Figure 4.S7). Most importantly, this new reporter produced strong signals with DNA injections as low as 5 pg, making it ideal for *Xenopus* studies.

The reporter was constructed (Figure 4.S7) as follows: oligonucleotides containing the mouse Chordin putative Smad4 binding sequence with 7 overlapping Smad binding element

(Fwd: 5'CAGACAGACAGACAGACAAACAGACAGACAGACAGgaattc3' and Rev: 5'CTGTCTGTCTGTCTGTTTGTCTGTCTGTCTGTCTGgaattc3') were annealed together. Oligos were ordered (ValueGene Inc.) with phosphates on the 5' end for subsequent ligation. An EcoRI sequence (gaattc) was added at the 3' end of

both oligonucleotides to generate a 3' overhang. The annealed oligos were then polymerized using the Takara DNA Ligation Kit. To terminate polymerization and prevent circularization of the DNA, we added pre-annealed flanking adapters (Fwd: 5' GGCGCAATACTCGAGgaattc 3'; Rev: 5' CTCGAGTATTGCGCC 3') with blunt ends on the 5' side and EcoRI overhangs on the 3' side. Oligonucleotides for the flanking adapters were ordered without a 5' phosphate end to prevent self-ligation. The optimal molar ratio to obtain multiple inserts was found to be 2:8 (adapter:SBEs). Ligated oligonucleotides were amplified by PCR using the primer sequences included in the termination adapter. The PCR product was ligated into the XhoI site of the pGL3-Basic Vector (Promega), and a minimal promoter (TATA box and initiator sequence of the adenovirus major late promoter MLP) was inserted between the BglII and HindIII sites.

AUTHORS CONTRIBUTION

H.D. and E.M.D.R. designed research. H.D. performed all biochemical experiments. T.A. generated the novel Smad4-luc reporter and carried out RT-PCR experiments. H.D. and E.M.D.R. performed the *Xenopus* experiments and wrote the manuscript.

ACKNOWLEDGMENTS

We thank C. Hill, S. Piccolo, J. Massague, M. de Caestecker, C. Carbone, R. Nusse, D. Kimelman, and D. Kardassis for materials, L.C. Fuentealba for help with antibodies, members of our laboratory, and three anonymous reviewers for improving the manuscript. T.A. was supported by the Undergraduate Research Scholars Program at UCLA. This work is in partial requirement for a Ph.D. degree for the Université Pierre et Marie Curie, Paris, France (H.D.). This work was supported by RO1 HD21502-25 and the Howard Hughes Medical Institute, of which E.M.D.R. is an Investigator.

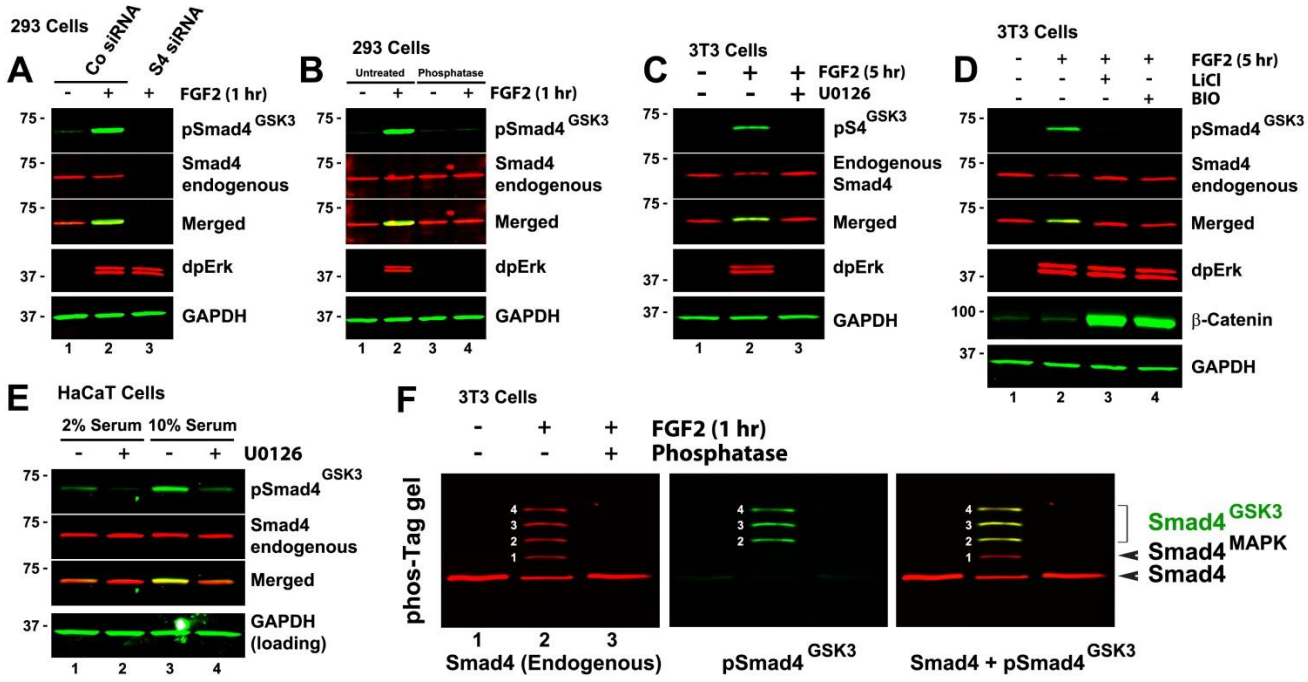

Figure 4.S1: The pSmad4^{GSK3} Antibody Is Highly Specific

These results extend those in Figure 4.1, showing that the custom-made pSmad4^{GSK3} antibody was specific for phosphorylated Smad4.

(A) The endogenous band recognized by pSmad4^{GSK3} antibody was eliminated after Smad4 siRNA knockdown, demonstrating that the antibody was specific for Smad4. Total endogenous Smad4 recognized by a mouse monoclonal antibody was also inhibited while diphospho Erk (dpErk, used to show that the FGF2 treatment was effective) and GAPDH were not affected.
(B) The endogenous FGF-induced band recognized by the pSmad4^{GSK3} antibody disappeared with phosphatase treatment, demonstrating the phospho-specificity of the antibody.
(C) Endogenous FGF-induced pSmad4GSK3 phosphorylation required Erk activity in serum-depleted NIH-3T3 cells stimulated with FGF2 for 5 hours. Note that endogenous Smad4 was partially decreased by FGF treatment. This decrease was blocked by U0126.
(D) FGF-induced Smad4 phosphorylation at threonines 269 and 273 was sensitive to GSK3 inhibitors. NIH-3T3 cells were deprived of serum for 18 hours and then treated for 5 hours with 10 mg/ml FGF2. The GSK3 inhibitors BIO (5 μM) or lithium chloride (30 mM) were added 15 minutes prior to FGF treatment. Note the moderate decrease in total Smad4 by FGF treatment that was be reversed by BIO.

This panel also shows that endogenous total Smad4 stability was less sensitive to stabilization by GSK3 inhibition than beta-Catenin.

(E) When grown in 2% serum, HaCaT cells showed a low basal level of $pSmad4^{GSK3}$ that was blocked by U0126. In 10% serum, a higher basal level of phosphorylation was found, which was also inhibited but not completely by U0126; this suggested that other kinases outside of the Erk pathway may also be able to phosphorylate Thr 277.

(F) Phos-tag western analysis of phosphatase-treated 3T3 cell extracts revealed that the upper bands detected after FGF treatment of NIH-3T3 cells represented phosphorylated forms of endogenous Smad4. NIH-3T3 cells were serum deprived for 18 hours and treated for one hour with 10 ng/ml FGF2. The extract was divided into two aliquots, one receiving phosphatase treatment while the other was incubated in the absence of the enzyme.

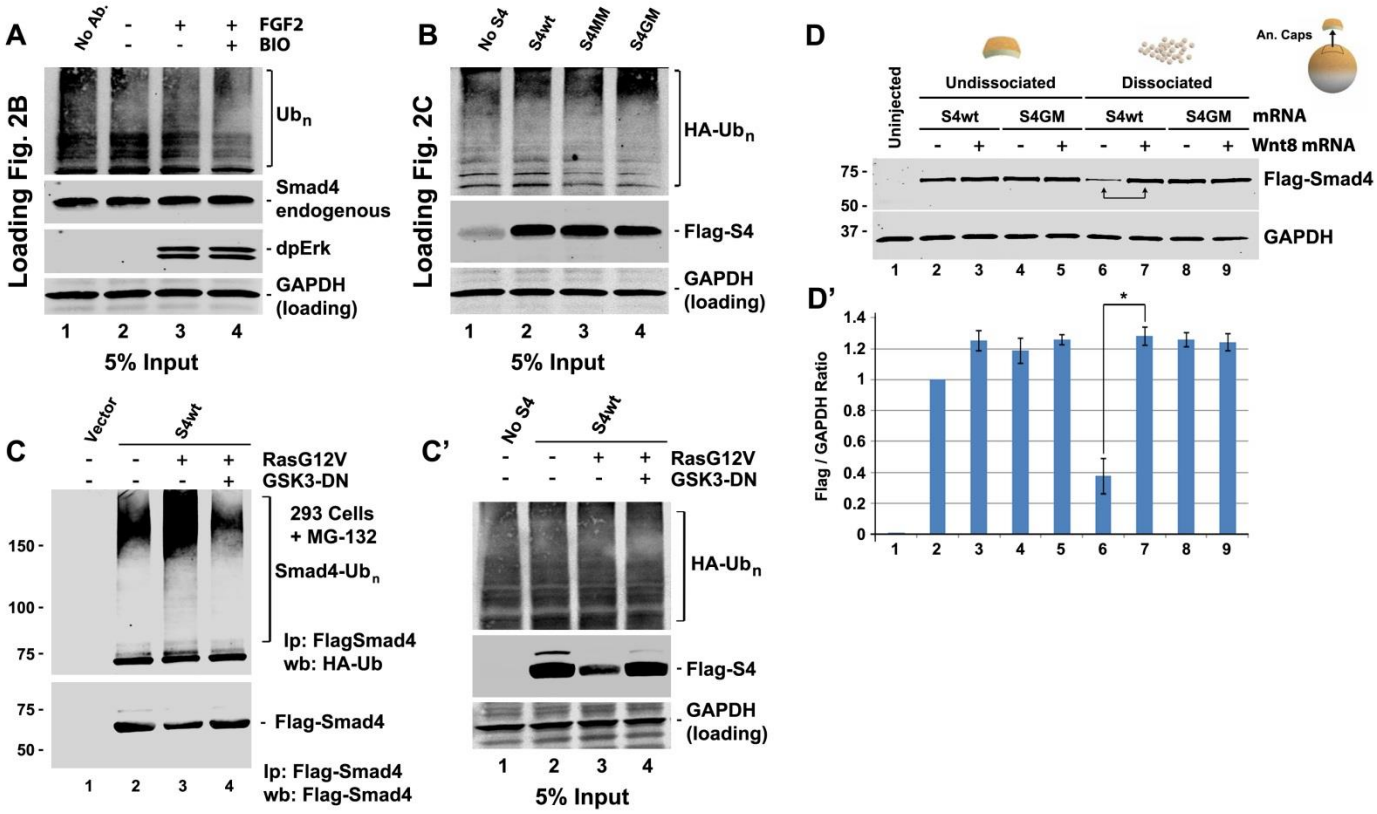

Figure 4.S2: Loading Controls of the Lysates Used for Immunoprecipitation Experiments and Quantification of Animal Cap Experiments.

(A) Western analysis of 5% of input used in the immunoprecipitation experiment shown in Figure 4.2B. Rabbit anti-ubiquitin antibody (Santa Cruz, FL-76) was used to detect endogenous polyubiquitinated ($Ub_{n)}$ proteins.
(B) 5% input of extracts used for the experiment in Figure 4.2C.
(C) Smad4 polyubiquitination induced by oncogenic RasG12V requires GSK3 activity.
(C') 5% of the lysate used as input in Figure 4.S2C. Please note that overexpression of RasG12V reduced the levels of Flag-Smad4 (compare lanes 2 to 3, middle panel). Smad4 degradation required GSK3 activity as it was blocked by GSK3-DN (compare lane 3 to 4). Steady-state degradation of Smad4 by MAPK was observed under strong and sustained activation conditions such as activated Ras or *Xenopus* animal caps dissociation.
(D) Flag-Smad4 protein was stabilized by microinjection of *xWnt8* mRNA in *Xenopus* dissociated animal cap cells and this required intact GSK3 phosphorylation sites.
(D') Quantification of Flag-Smad4 levels from the above western blot results.

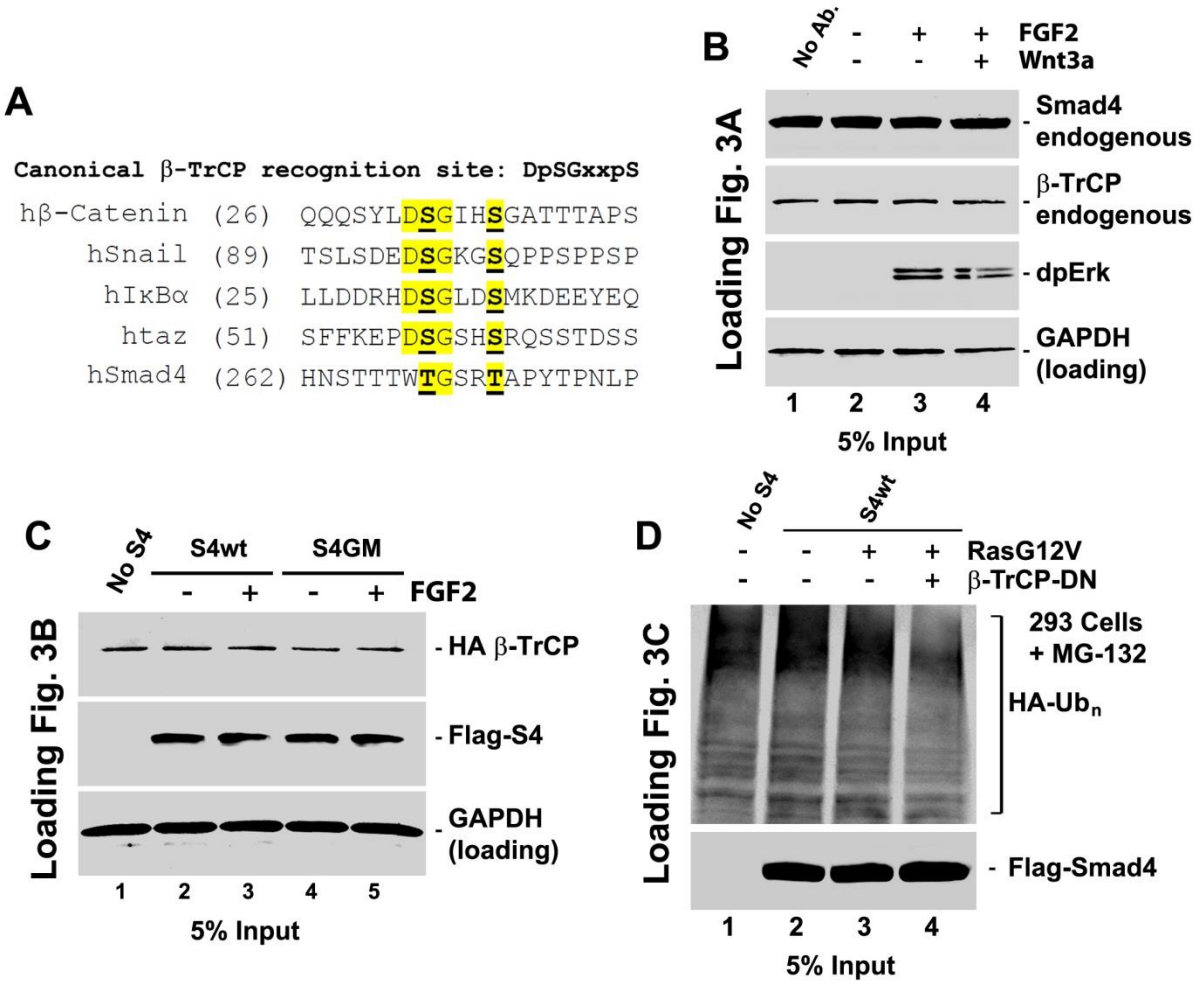

Figure 4.S3: Loading Controls of the Lysates Used for Immunoprecipitation Experiments

(A) Sequence alignment showing conserved recognition sequences within the phospho-degrons of several known beta-TrCP substrates.
(B) 5% of the lysate used as input in Figure 4.3A showing equal amounts of endogenous beta-TrCP in the conditions used for immunoprecipitations of endogenous proteins.
(C) 5% input of extracts used for the experiment in Figure 4.3B.
(D) 5% input of extracts used for the experiment in Figure 4.3C.

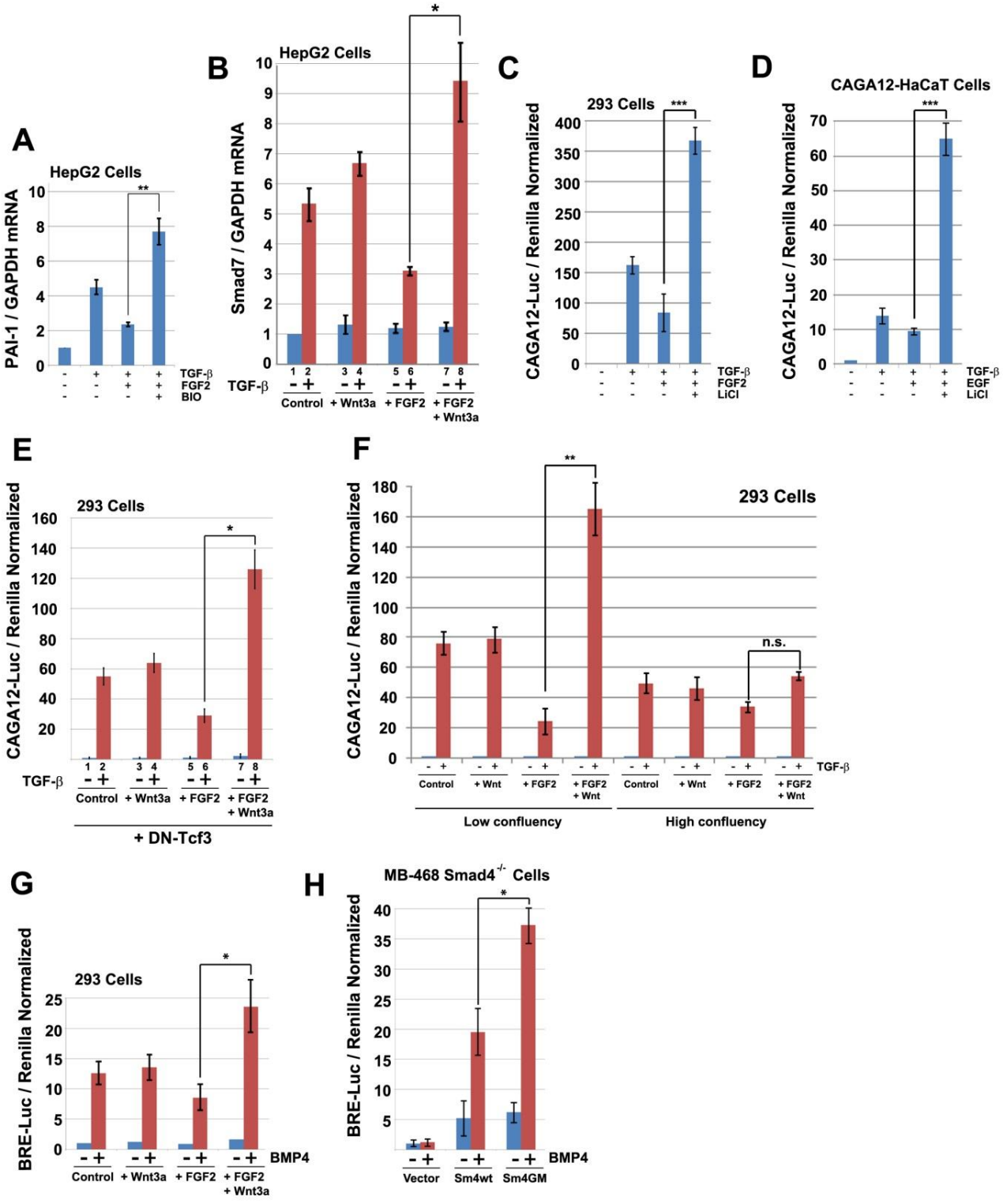

Figure 4.S4: GSK3 Inhibition by Wnt, LiCl, or BIO Potentiated TGF-beta and BMP Signaling in an FGF- or EGF-dependent Way

These experiments illustrate that the cross-talk between TGF-beta, FGF, and Wnt is a general mechanism that applies to multiple cell lines, endogenous TGF-beta target genes and also to the BMP pathway.
(A) In hepatoma HepG2 cells, the stimulatory effect of Wnt could be mimicked by chemical inhibition of GSK3; mRNA expression levels of the TGF-beta target gene PAI-1 (normalized for GAPDH transcripts) were inhibited by FGF2 treatment and stimulated by the GSK-3 inhibitor BIO.
(B) Smad7, a TGF-beta target gene, was activated by Wnt3a in the presence of FGF in HepG2 cells (brackets).
(C) In 293 cells, FGF2 had a dual effect on TGF-beta signaling. When GSK3 is active, FGF2 reduced the TGF-beta signal, but when GSK3 activity was blocked by the inhibitor LiCl, FGF2 potentiated TGF-beta signaling. These results are similar to those shown for Wnt in Figure 4.4A. Higher levels of CAGA12-Luc signaling were reached with LiCl (or Wnt) because Smad4 phosphorylated solely by MAPK constitutes the most active form.
(D) In human keratinocyte HaCaT cells (containing a stably integrated CAGA12-Luc reporter) GSK3 inhibition by LiCl strongly increased TGF-beta signaling (brackets); EGF was used instead of FGF2 because HaCaT cells do not respond to FGF while Erk is strongly stimulated by EGF.
(E) In 293 cells, the cross-talk between TGF-beta, FGF and Wnt was not affected by DN-Tcf3, an inhibitor of canonical Wnt transcriptional responses (for signaling in the absence of DN-Tcf3compare to Figure 4.4A).
(F) The potentiation of TGF-beta signaling by Wnt3a was only seen in non-confluent cells (brackets) in 293 cells; this effect may be connected to the known link between TGF-beta signaling and cell confluency (Varelas et al., 2010).
(G) In 293 cells, the BMP response (measured by the BRE-Luc reporter gene) is stimulated by Wnt in the presence of FGF.
(H) In the Smad4$^{-/-}$ cell line MDA-MB-468, transfected Smad4-GM showed an enhanced BMP response when compared to Smad4-wt.

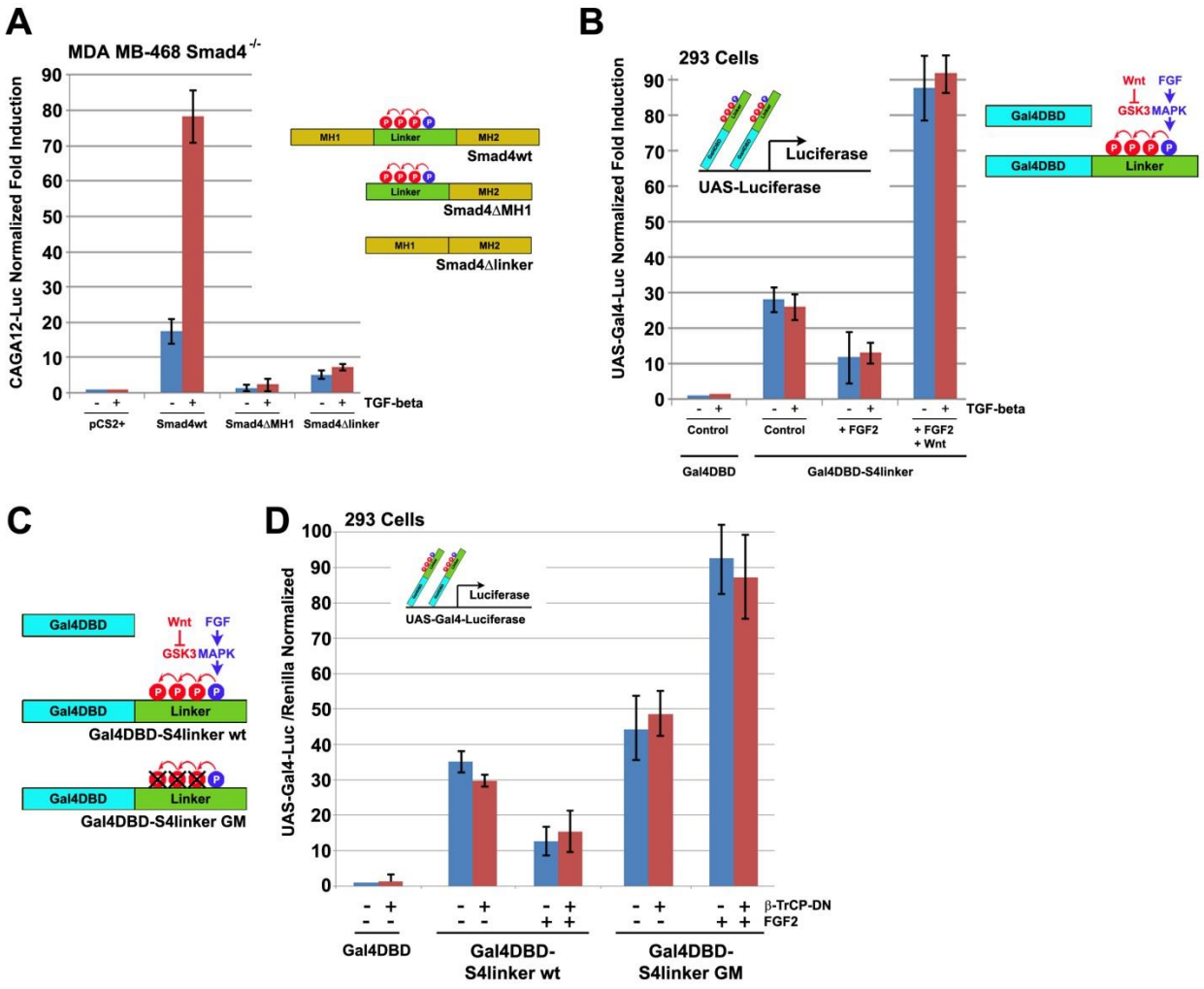

Figure 4.S5: Smad4 Linker Region Is Required for Smad4 Activity and Contains a Growth Factor-Regulated Transcription Activation Domain

These data provide the background for experiments showing that the linker domain of Smad4 (which is flanked by the more conserved Mad Homology domains MH1 and MH2) constitutes a growth factor-regulated transcriptional activation domain.

(A) The linker region was required for Smad4 transcriptional activity in Smad4$^{-/-}$ MB-468 cells.
(B) Fusion of the Smad4 Linker region to a yeast Gal4 DNA binding domain showed that a UASGal4-Luciferase reporter gene could be transactivated by this domain. The Smad4 linker transcriptional activation domain was independent of TGF-beta signaling but could still be inhibited by FGF and stimulated by the addition of FGF2 and Wnt3a.

(C) Diagram of the yeast Gal4 DNA Binding Domain (Gal4DBD) fused to Smad4 linker region and of the phosphorylation-resistant mutant used to test transcriptional activation.
(D) In 293 cells, induction of the UAS-Gal4-Luc reporter by Gal4DBD-S4linker was not affected by co-transfection of DN-beta-TrCP even when the MAPK pathway was activated by FGF stimulation. The same DN-beta-TrCP construct potentiated TGF-beta signaling by the wild type Smad4 protein (Figure 4.3E), suggesting that Gal4DBD-S4linker and full-length Smad4-wt differ in their polyubiquitination regulation.

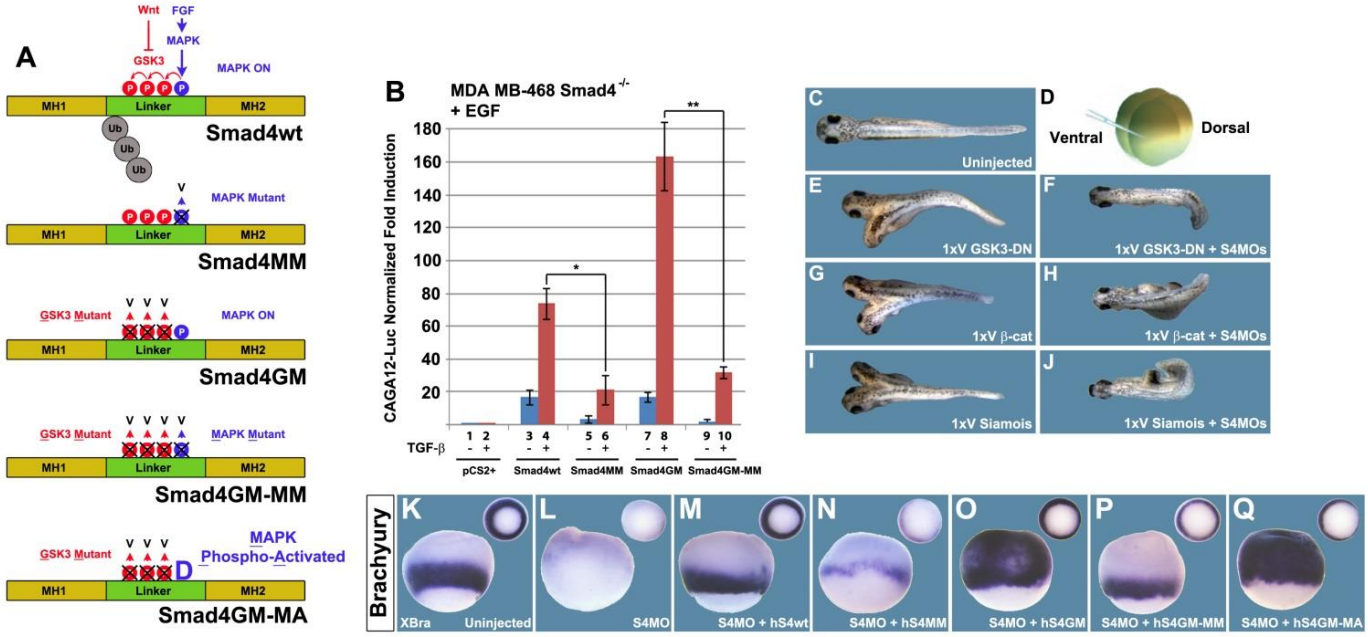

Figure 4.S6: Phosphorylation of Threonine 277 Is Required for Smad4 Peak Activity in *Xenopus* Embryos; a MAPK phospho-Activated (MA mutant, T277D) Circumvents the Need for MAPK Phosphorylation

The experiments in this supplementary figure show that the MAPK site at position 277 is critical for maximal Smad4 transcriptional activity.

(A) Schematic diagrams of Smad4 phospho-resistant and phospho-mimetic mutants. Smad4-MM cannot be phosphorylated by MAPK and thus cannot be primed for GSK3 phosphorylations; Smad4-GM is a mutant that mimics Smad4 receiving a maximum amount of Wnt in which the MAPK site can still be phosphorylated; Smad4GM-MM has all MAPK and GSK3 sites mutated into phosphorylation resistant residues; Smad4GM-MA mimics Smad4 receiving a maximal amount of Wnt (because GSK3 phosphorylation is prevented) and a maximal MAPK signal (because Thr 277 has been mutated into the acidic residue Asp that mimics the MAPK phosphorylated form).
(B) Phosphorylation of the MAPK site was required for Smad4 peak activity in the presence of EGF in Smad4$^{-/-}$ cells. Note that the effect of mutating the MAPK site was best appreciated when the GSK3 sites were also mutated (compare bar 8 to 10)
(C-J) Experiments showing that secondary axis development required Smad4/TGF-beta activity in *Xenopus* embryos. Ventral injection of mRNAs encoding *dominant-negative GSK3*, *beta-catenin*, or *Siamois* induced duplicated axes that were blocked by co-injection of Smad4 MOs.

(K-Q) x*Brachyury* expression, which marks mesoderm induction by TGF-beta growth factors, showed that an intact MAPK site was required for maximal Smad4 activity. Note that Smad4MOs eliminated X*Brachyury* expression, which was restored by Smad4-wt but much less by Smad4-MM (compare M and N). This difference is very marked when the GSK3 phosphorylation-resistant form Smad4-GM is used to replace Smad4 (panels O to Q).

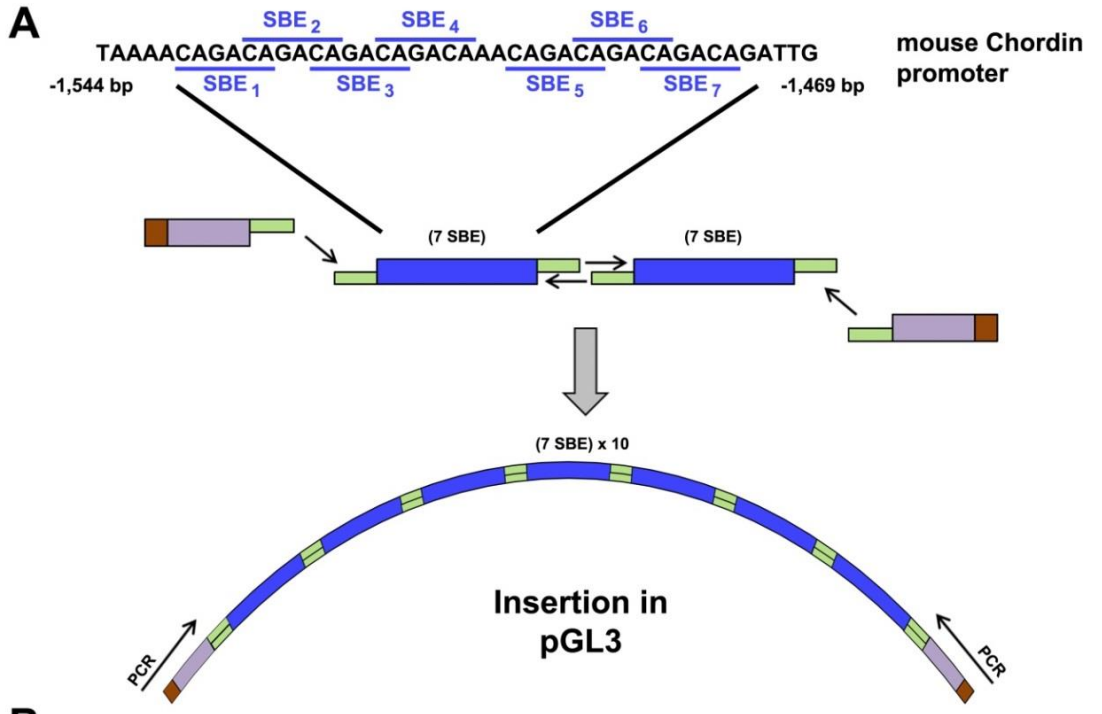

B

GGTACCGAGCTCTTACGCGTGCTAGCCCGGGCTCGAGGAATTCCAGACAGACAGACAGACAAACAGACAGACAGACAG
GAATTCCAGACAGACAGACAGACAAACAGACAGACAGACAGGAATTCCAGACAGACAGACAGACAAACAGACAGACAG
ACAGGAATTCCAGACAGACAGACAGACAAACAGACAGACAGACAGGAATTCCAGACAGACAGACAGACAAACAGACAG
ACAGACAGGAATTCCTGTCTGTCTGTCTAATCACTAGTCGAGGAATTCCAGACAGACAGACAGACAAACAGACAGACA
GACAGGAATTCCAGACAGACAGACAGACAAACAGACAGACAGACAGGAATTCCAGACAGACAGACAGACAAACAGACA
GACAGACAGGAATTCCAGACAGACAGACAGACAAACAGACAGACAGACAGGAATTCCAGACAGACAGACAGACAAACA
GACAGACAGACAGGAATTCCTGTCTGTCTGTCTAATCACTAGAGCTTGGGCTCGAGATCTGGGCTATAAAAGGGGGTG
GGGGCGCGTTCGTCCTCACTCTCTTCCAAGCTT

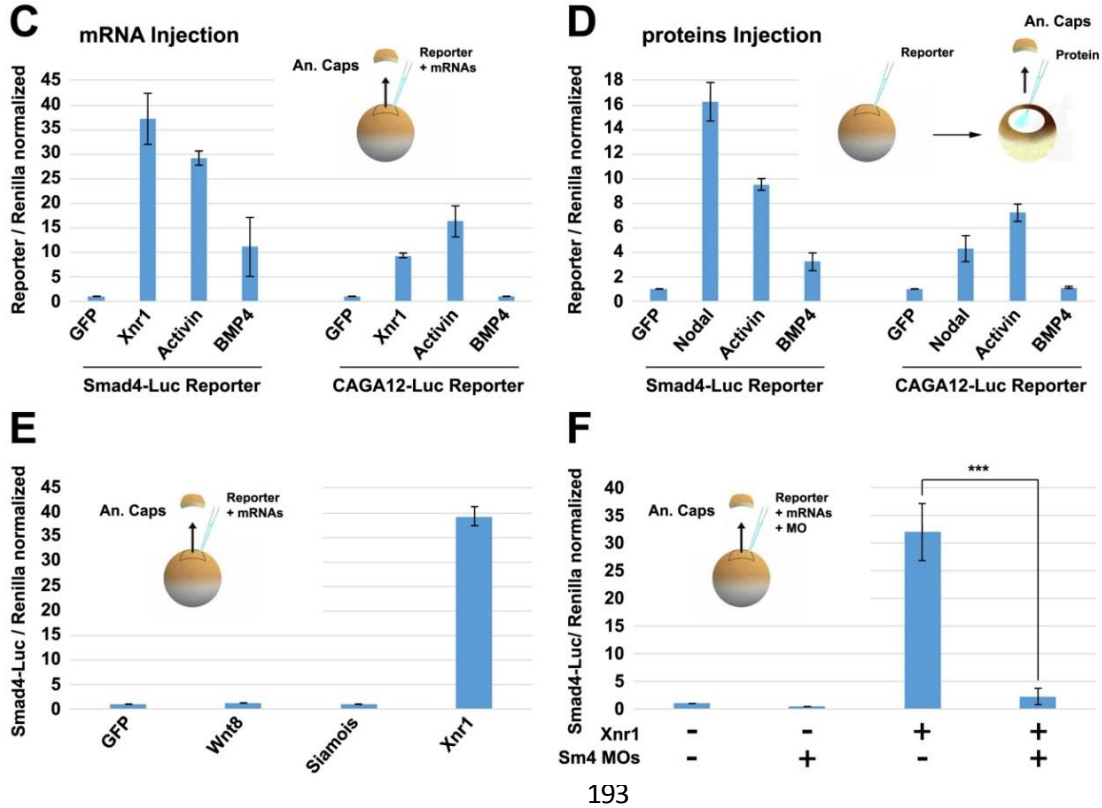

Figure 4.S7: Generation and Characterization of a New Smad4-Luciferase Reporter Particularly Suitable for Experiments in *Xenopus* Embryos

A Smad4-Luciferase reporter was generated by multimerizing a sequence of the mouse *chordin* promoter consisting of seven overlapping CAGACA Smad4 binding sites. This Smad4 reporter has the advantage that it generates strong Luciferase signals at low (5 pg) amounts of microinjected DNA, while other reporters require higher DNA amounts per injection that are toxic for embryos. However, it has the disadvantage of being stimulated both by TGF-beta and BMP, but is useful for studying the effects of Activin/Nodal signaling in naïve ectodermal explants.

(A) A sequence 1,469 nucleotides upstream of the mouse Chordin initiator Methionine containing seven overlapping Smad4 Binding Elements (SBE). Synthetic oligos with added 3' overhang EcoRI sites were ligated and the polymerization terminated by adding a lower amount of terminator oligo sequences including primer regions for PCR amplification (see Supplemental Experimental Procedures). A clone containing 10 oligomerized sequences was used for subsequent analyses.
(B) Sequence of the Smad4-Luciferase reporter inserted upstream of the firefly Luciferase gene in the pGL3 vector (Promega); 70 SBEs are present in this construct.
(C) In animal cap cells, microinjection of only 5 pg of Smad4Chd-Luc reporter (normalized by injection of *Renilla* mRNA) caused a strong induction by *Xenopus* Nodal-related 1 (Xnr1; Nodal) (100 pg) and Activin (80 pg), as well as a moderate response to mouse *BMP4* mRNA (400 pg). 75 pg per injection of CAGA12 DNA generated weaker Luciferase signals (but did not respond to BMP4). No signal was detected when 5 pg of CAGA12 DNA were injected. This indicates that the Smad4-luciferase reporter is well suited for reporter gene experiments in *Xenopus* embryos, in which amounts of DNA in excess of 20 pg per injection usually have toxic effects.
(D) Experiment similar to that of the previous panel, except that reporters were activated by microinjection of recombinant proteins into the blastula cavity; Smad4Chd-Luc performed better than CAGA12 in this assay as well.
(E) The Smad4Chd-luc reporter was not induced by co-injection of *xWnt8* or *Siamois* mRNA and was activated by Xnr1.
(F) Activation of the Smad4-Luc reporter by *Xnr1* mRNA required Smad4, since its induction was blocked by co-injection of Smad4MOs.

CHAPTER 5

CONCLUSIONS

AND

PERSPECTIVES

Understanding how cells integrate multiple signaling pathways to achieve specific cell differentiations is one of the major challenges in cell and developmental biology. Patterning in the *Xenopus* embryo, or the wing imaginal disc in *Drosophila*, is regulated by gradients of growth factors and their antagonists. This positional information must be tightly integrated, for when a *Xenopus* blastula is cut in half, the embryo can self-regulate, forming perfect identical twins (De Robertis, 2006). In this thesis, I have described two new nodes of signal integration. In a first approach, using a combination of genetic and biochemistry experiments, we showed that the *Drosophila* Dpp transducer Mad is also part of the core Wnt transcriptional complex. In a second approach, I showed that the activity of a single transcription factor, Smad4, previously thought to function constitutively in TGF-beta signaling is strongly regulated by two major signaling pathways, RTK/MAPK and Wnt/GSK3. The molecular, cellular and potentially therapeutic significance of these signal integrations and other questions are examined below. I also provide some unpublished experiments that points to new research avenues opened by this thesis.

5.1 One transcription factor, two signaling pathways: Mad as a transducer of Dpp and Wg.

In the chapter 3 of this thesis, we showed a previously unrecognized role for Mad as part of the Wg transcriptional complex. Mad also transduces the Dpp signal and this raises the question on how those two pathways cross-talk to each other. We found that the choice for Mad to transduce Dpp or Wg signals is controlled by C-terminal phosphorylations so that Mad binds to Pangolin and participates in Wg target genes transcription only when not phosphorylated at its C-terminus. This results in a competition between Dpp and Wg controlled by the phosphorylation state of Mad (Figure 2.5).

One important question raised by this study is whether this mechanism is specific to the development of the wing imaginal disc of *Drosophila melanogaster* or whether it has been conserved across evolution. Unpublished, preliminary data in *Xenopus* embryos shows that overexpression of mutant mRNAs mimicking different phospho-isoforms of Mad give rise to typical BMP or Wnt phenotypes in the early embryo (Figure 5.1 A). The late Wnt phenotype obtained by injection of Wnt8 DNA is a loss of anterior structure (head) in *Xenopus* embryos (Niehrs, 2004). Strikingly, Mad-GM8-AVA which mimics Mad receiving a maximal amount of Wnt without being able to participate in the BMP pathway gave a phenotype similar to the one of Wnt8 DNA injection with loss of head structures

marked by *Rx2A* and *XAG* (Figure 5.1 A). It is interesting to note that AVA mutations prevent Mad from affecting the dorso-ventral axis (marked by *Sizzled* expression) whereas linker (GSK3) phosphorylations affect both the patterning of the dorso-ventral (D-V) and antero-posterior (A-P) axes. Further experiment will be required to confirm these findings but if this model is correct, a single transcription factor Smad1/Mad, would be able to read positional information along the dorso-ventral axis (BMP) through its C-terminal phosphorylation and along the antero-posterior axis (Wnt) through its linker GSK3 phosphorylation sites (Figure 5.1 C). The implication of Mad in both BMP and Wnt transcriptional complexes through a pattern of phosphorylation sites encoded in its primary sequence might be one of the mechanisms explaining the integration of D-V and A-P axes in the morphogenetic field formed by the *Xenopus* blastula embryo (De Robertis, 2006).

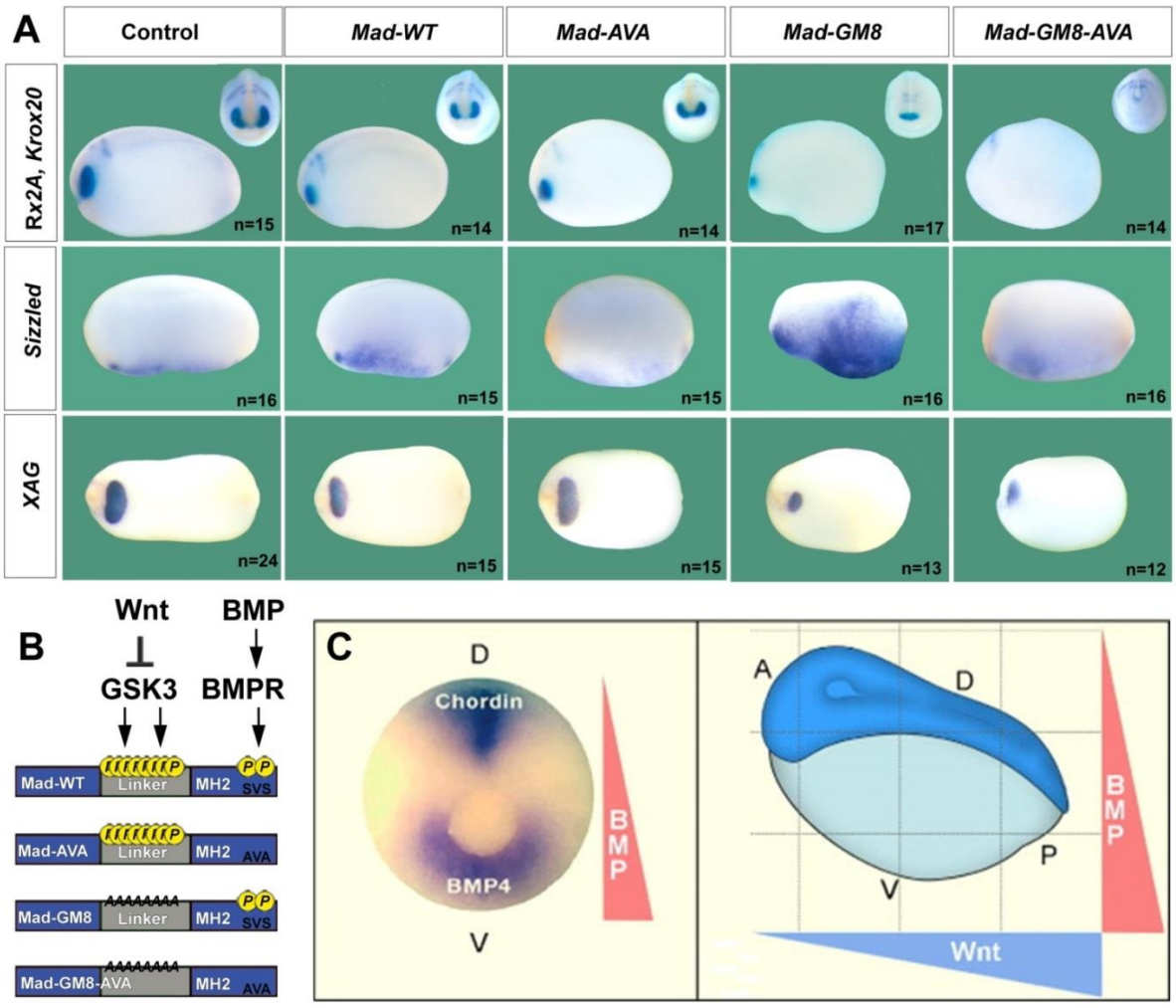

Figure 5.1: Overexpression of mutants mimicking different phospho-isoforms of Mad produce Wnt and BMP phenotypes in *Xenopus* embryo.

(**A**) Results of in situ hybridization for the eye marker *Rx2A*;, the hindbrain marker *Krox20*; the ventral BMP target *Sizzled* and the cement gland marker *XAG* for injection of 400pg of different mutants of Mad (Unpublished results).
(**B**) Schematic of the different Mad mutants injected in *Xenopus* embryos. Mad AVA cannot be phosphorylated by the BMP Receptor (BMPR) and is therefore inactive in the BMP pathway. Mad-GM8 cannot be phosphorylated by GSK3 in its linker region and mimics Mad receiving a maximal amount of Wnt.
(**C**) (Left) Expression of Chordin and BMP4 on opposite centers of a Xenopus embryo. (Right) Model illustrating the two perpendicular morphogenetic gradients of BMP and Wnt. Cells sense their position within these Cartesian-coordinates, which specify their fate in the body plan (from De Robertis, 2008).

Another interesting area of research opened by our finding that Mad participates in Wg signaling is an explanation of the mysterious "helper site" found in the promoter of nearly all known Wg target genes (Chang et al., 2008; Hoverter et al., 2012). It has been known for a long time that the T cell factor (TCF)/Pangolin uses its high mobility group (HMG) domain to bind specific DNA sequences (SCTTTGWWS) named the TCF Binding Site (van de Wetering et al., 1997; van Beest et al., 2000). However, it was recently found that another DNA sequence, named the Helper site, found in all Wg target genes in *Drosophila* was as at least as important as the main TCF binding site (Chang et al., 2008). While it has been suggested that the Helper site can be bound by another domain of TCF (the C-clamp domain), the Helper site sequence (GCCGCCA) and the DNA sequence bound by the Mad MH1 domain (GCCG*n*CGC) (Kim et al., 1997) are highly similar. One tempting hypothesis in line with our findings is that Mad, as part of the Wnt core transcriptional machinery, would be the protein that binds the Helper site *in vivo*. This theory could explain the great inconsistency in the spacing and orientation of functional helper sites when the entire *Drosophila* genome is searched. The helper site can be found in nearly any possible orientation or spacing with regard to the TCF binding site (Chang et al., 2008). If the helper site were bound by the c-clamp domain of TCF and the TCF site by the HMG domain, this raises the question on how this transcriptional repressor can be so "flexible". As

indicated in the model in Figure 5.2, it would seem more intuitive that the two sites are bound by two distinct proteins (respectively Mad and TCF) that cooperate with Armadillo to drive the transcription of Wnt target genes. This will be an interesting area of investigation in the future.

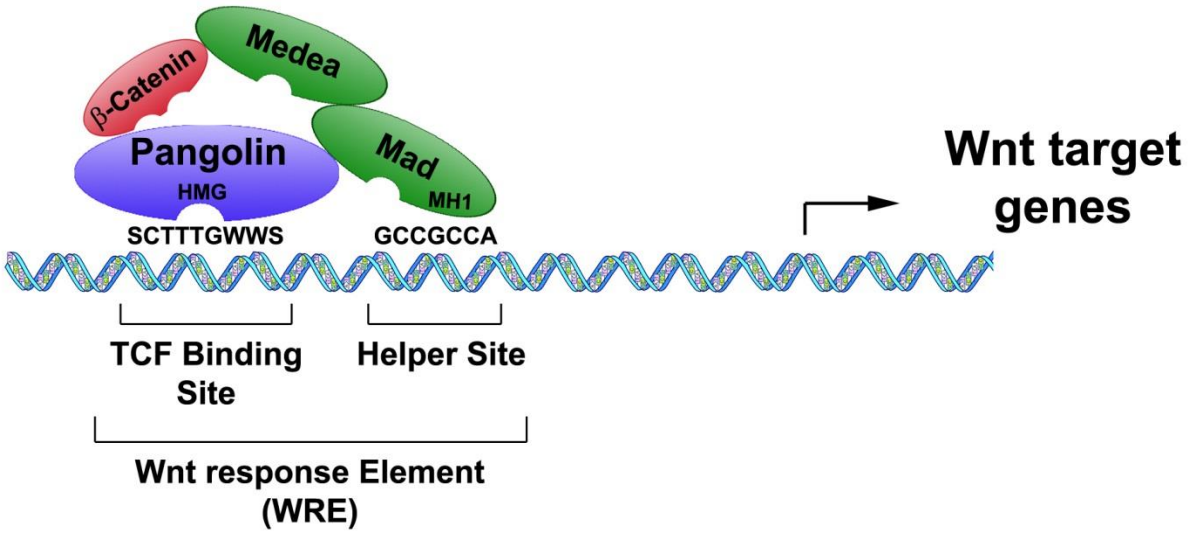

Figure 5.2: Proposed model where the MH1 domain of Mad binds the helper site.

The helper site found in the Wnt response element (WRE) of nearly all known Wnt target genes has been proposed to be bound by the c-clamp domain of Pangolin. However the helper site can be found in any possible orientation or spacing with regard to the TCF binding site (Chang et al., 2008). We proposed that Mad, as part of the Wnt transcriptional machinery, binds to the helper site *in vivo*. This model remains to be proven

5.2 One structure, two functions: Smad4 activity and stability are co-regulated.

Chapter 4 of this thesis was entirely dedicated to the study of four new phosphorylation sites in the Smad4 sequence. We found that activation of the MAPK pathway by FGF or EGF lead to Smad4 phosphorylation at Threonine 277. This event allows Smad4 to reach its peak of transcriptional activity while priming it for subsequent degradation. Thus, a common structure, the linker region, fulfills two opposite functions: Smad4 transcriptional action and turnover. This mechanism is most likely mediated by the recruitment of different proteins: an as yet-unidentified transcriptional co-activator and an E3-ligase (Figure 5.3). We propose that the unknown co-activator binds mono-phosphorylated Smad4 at Thr277 while the E3-ligase beta-TrCP binds the two first phosphorylated GSK3 sites in Smad4 linker. In this model, GSK3 switches the phosphorylation code in the Smad4 linker region from one that favors Smad4 action to one that favors Smad4 destruction. This mechanism provides a way of controlling the duration of the Smad4 signal by ensuring that degradation and turnover follow transcriptional activation. In the cruel world of signal transduction, degradation is a price that Smad4 molecules have to pay to participate in transcription. This model reconciles previous results in the literature that appeared to be contradictory: it had been

proposed that activation of the MAPK pathway was required for Smad4 activity (Roelen et al., 2003) while also triggering its degradation (Saha et al., 2001).

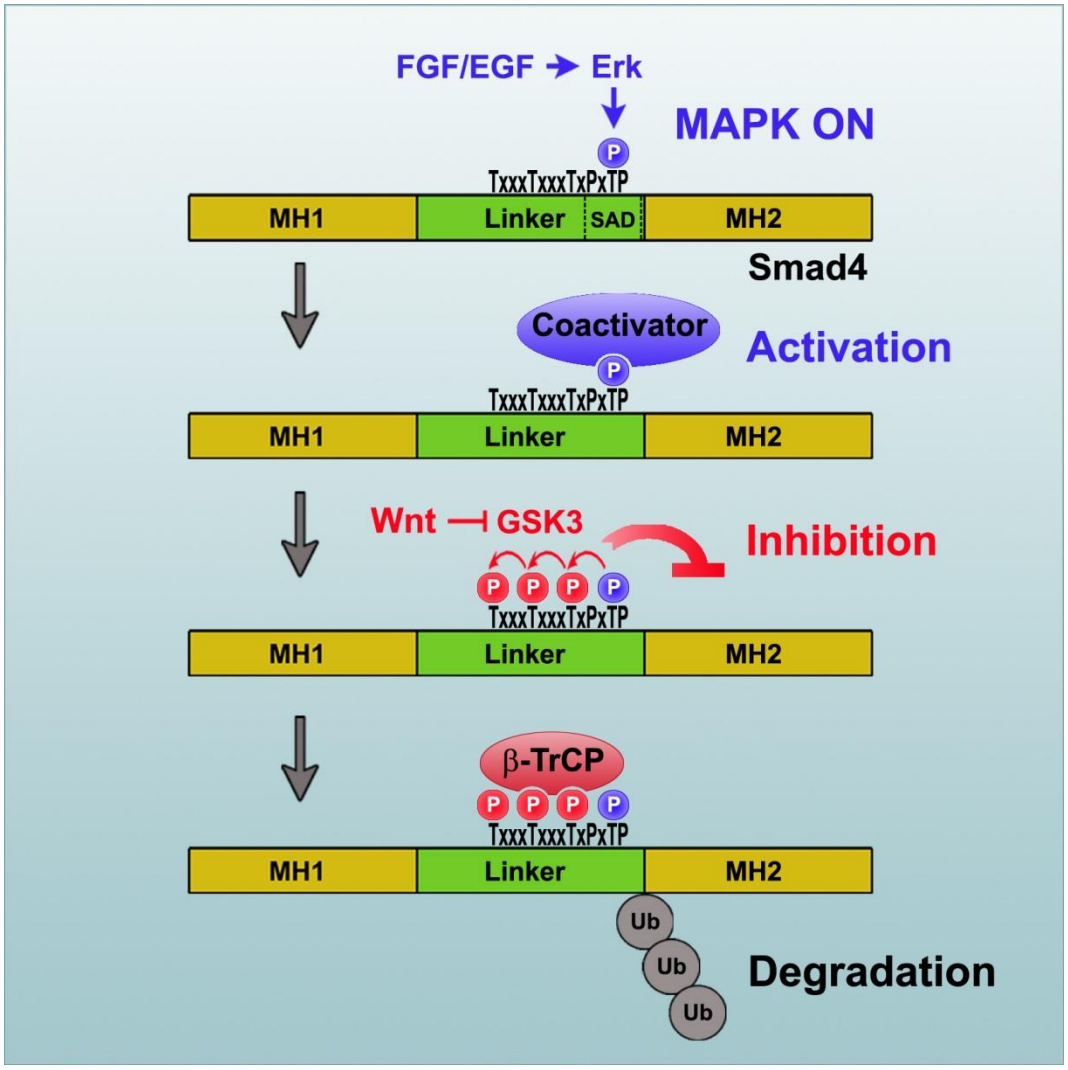

Figure 5.3: The cyclic recruitment and continuous turnover of Smad4.

Smad4 phosphorylation at Thr 277 has a dual function. First, it allows Smad4 to reach peak transcriptional activity. Second, it primes Smad4 for GSK3 phosphorylations that cause transcriptional inhibition and generate a phosphodegron that serves as a docking site for the ubiquitin E3 ligase beta-TrCP. Thus, both the activity and the stability of Smad4 are regulated by FGF/EGF and Wnt.

Future studies will be required to identify the Smad4 linker co-activator. A prime candidate is p300, which has been shown to bind to the SAD domain of Smad4 (de Caestecker et al., 2000). Recently, it has been found that the mediator of the Hippo pathway YAP binds phosphorylated SP sites in the Smad1 sequence (Alarcón et al., 2009; Aragón et al., 2011) through its WW domain. The other mediator of the Hippo pathway, TAZ, has been shown to bind active Smad2/3/4 complexes and to connect TGF-beta signaling to cell density (Varelas et al., 2008, 2010). It is therefore tempting to speculate that TAZ or YAP may recognize the phosphorylated 277 TP site in Smad4 acting as co-activators. Alternatively, the Smad4 linker region might recruit other co-activators depending on cellular context. In order to identify Smad4 phospho-linker interacting factors, we suggest to conduct a functional screening where co-activators known to contain a pS/TP binding domain (such as class IV WW domain; WD40 domains; Yaffe and Elia, 2001) will be tested in our Gal4DBD-Smad4-linker transcriptional assay (Figure 4.5). The Gal4-Smad4-linker-GM construct in which the GSK3 sites are mutated but the MAPK was left intact is ideal to identify the Smad4 linker co-activator. Indeed, FGF has confounding effects on the wt-linker because it induces phosphorylation of Thr277 but also primes GSK3 inhibitory phosphorylations (Figure 4.5). In the GM-linker, phosphorylation of the GSK3 sites is impossible and the activity is maximal. We propose to permanently infect HaCaT cells with

the Gal4DBD-Smad4-linker-GM construct together with the UAS-Gal4-luciferase and SV40-Renilla for normalization (Figure 5.4). Once this stable cell line is established functional screening with siRNAs against different candidates co-activator will become possible (Figure 5.4).

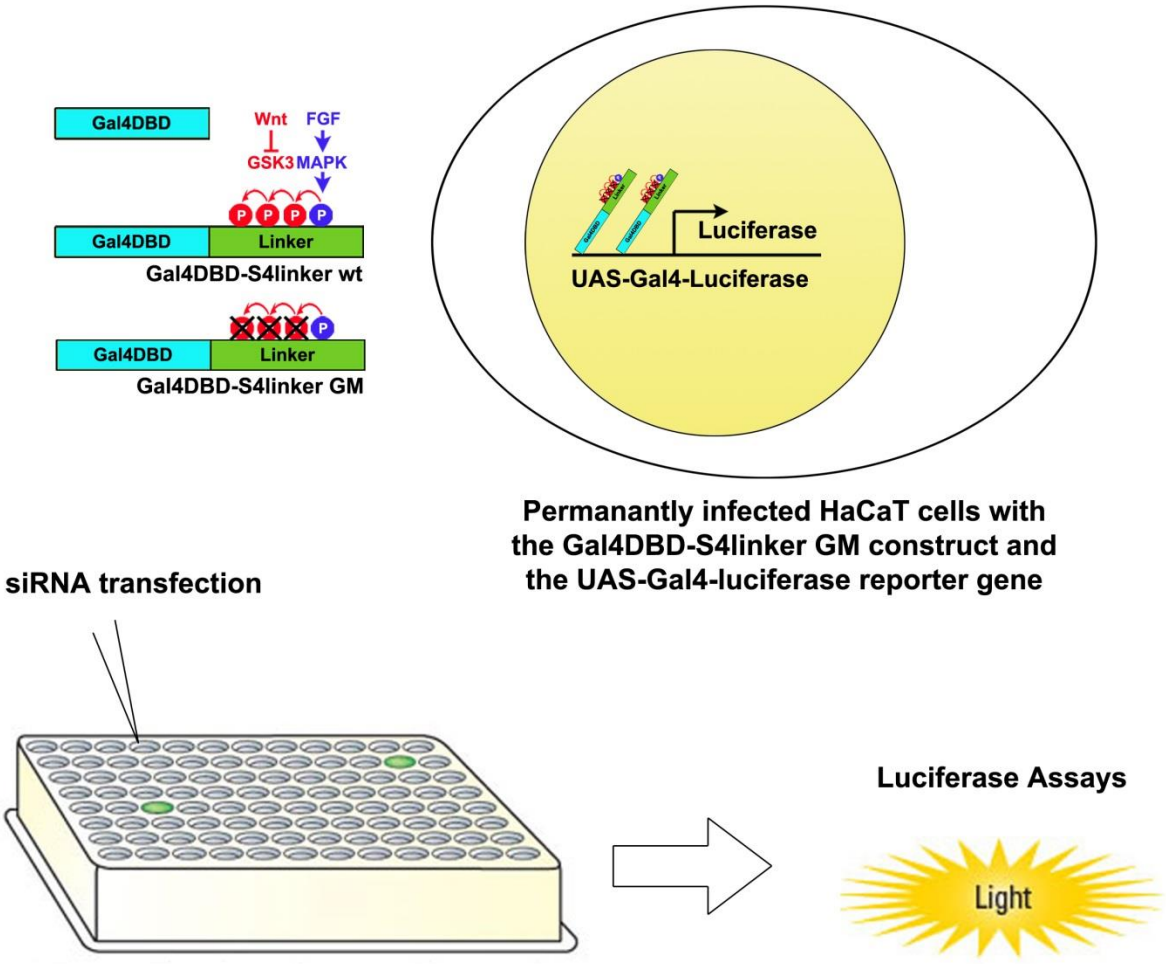

Figure 5.4: Proposed functional screening to identify Smad4 phospho-linker associated co-activator.

HaCaT cells will be permanently infected with the Gal4DBD-S4linker GM construct together with the UAS-Gal4-Luciferase reporter and a Renilla construct for normalization. siRNA transfection against transcriptional co-activators known to contain a pS/TP interacting domain and luciferase based screen should help identify the Smad4 co-activator.

5.3 Is Smad4 phosphorylated by GSK3 after TGF-beta stimulation?

In Chapter 4 of this thesis we described GSK3 phosphorylation of Smad4 when primed by MAPK after FGF or EGF stimulation. However, numerous kinases (the so-called proline-directed kinases) can phosphorylate PxS/TP sites. In the course of this study we made the unexpected observation that linker phosphorylation of Smad4 could also be triggered by TGF-beta or BMP stimulation of HaCaT cells (Figure 5.5 A.). Interestingly, these phosphorylations induced by TGF-beta, while completely inhibited by the GSK3 inhibitor LiCl, were unaffected by the Erk inhibitor U0126 suggesting the involvement of a kinase different from Erk in the priming of the GSK3 sites (Figure 5.5 B, compare lanes 2 to 3). This observation calls for investigation in order to identify the kinase acting downstream of TGF-beta activation.

A prime candidate would be a kinase belonging to the family of nuclear CDKs associated with transcription such as CDK8/9. Indeed, the linker region of R-Smads was shown to be phosphorylated by nuclear CDKs in response to TGF-beta or BMP stimulations (Alarcón et al., 2009; Aragón et al., 2011). To test this, HaCaT cells will have to be depleted of endogenous CDK8 and 9 by siRNA and the involvement of these kinases downstream of TGF-beta will then be tested with our pSmad4^{GSK3} antibody in cell culture immuno-staining and western-blotting.

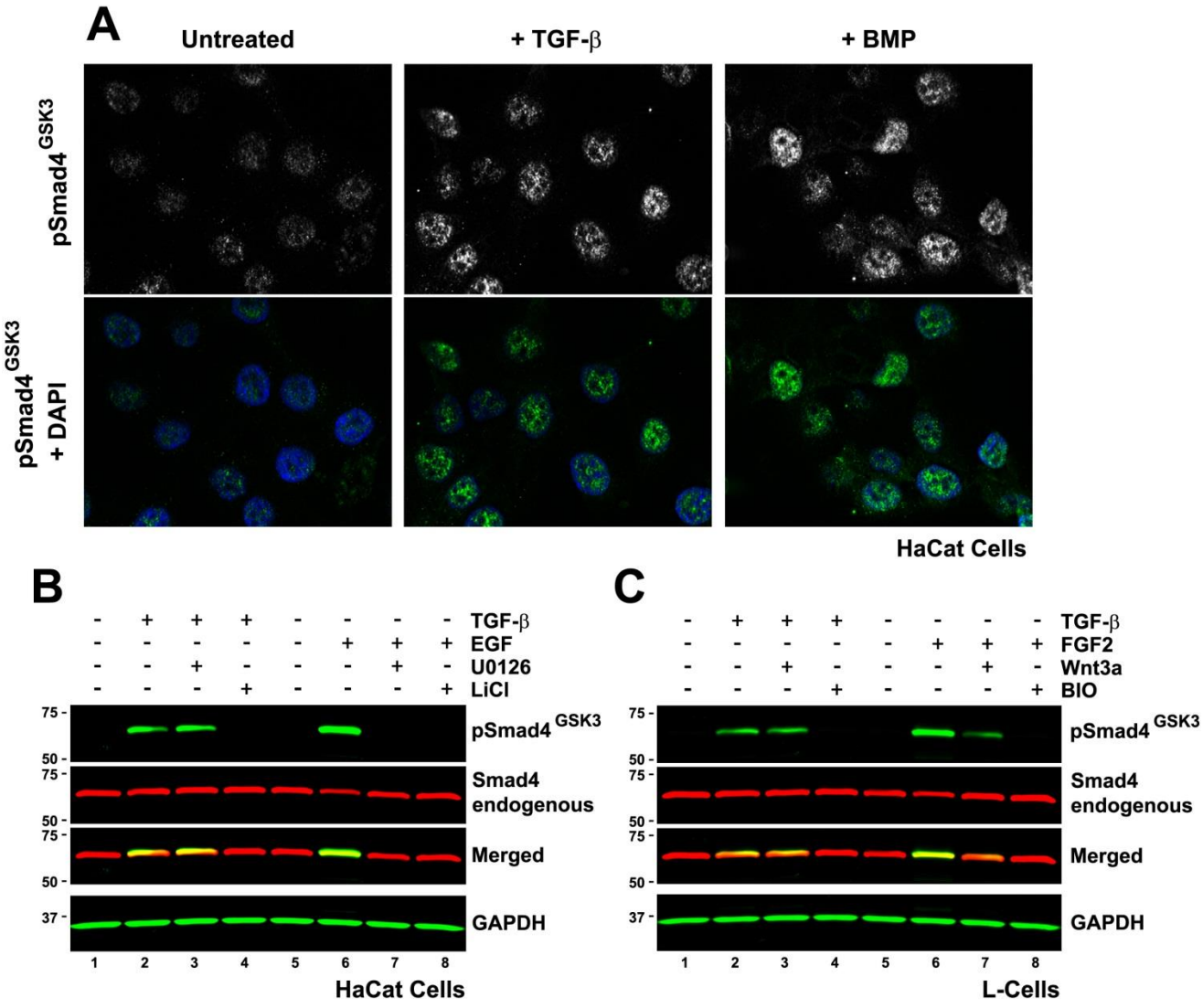

Figure 5.5: Linker phosphorylation of Smad4 can be induced by TGF-beta in an Erk-independent mechanism.

(A) pSmad4GSK3 staining is increased in HaCaT cells stimulated with TGF-beta or BMP4 (unpublished result)
(B) Western-blot showing that GSK3 phosphorylation of Smad4 linker region can be induced by EGF through an Erk dependent mechanism or TGF-beta through a different, Erk-independent mechanism (unpublished result).
(C) GSK3 linker phosphorylation of Smad4 are inhibited by Wnt3a when induced by FGF. However, the TGF-beta induced linker phosphorylations were unaffected by Wnt3a (unpublished result).

The GSK3 linker phosphorylations induced by TGF-beta seem to differ in more than one way from the ones induced by FGF. Indeed, we found that pSmad4^{GSK3} phosphorylations are greatly inhibited by Wnt3a but only when primed by FGF. When the pSmad4^{GSK3} phosphorylation was triggered by TGF-beta, Wnt3a treatment had no effect (Figure 5.5 C, compare lanes 2 to 3 and 6 to 7). This suggests that the two signaling pathways use different cellular mechanisms to trigger the phosphorylation of Smad4 by GSK3. One possible explanation for this observation is that the FGF-induced GSK3 phosphorylations of Smad4 take place in the cytoplasm and require other components of the Wnt destruction complex such as Axin and APC (see below) whereas TGF-beta induced GSK3 phosphorylation of Smad4 takes place in the nucleus while Smad4 is engaged in transcription and are independent of the Wnt-destruction complex. This hypothesis is in line with the proposed cycle of activation that R-Smad proteins undergo (Alarcón et al., 2009; Aragón et al., 2011). To clarify this, the requirement for Axin or APC in TGF-beta- or FGF-induced phosphorylation of Smad4 will be tested with new Axin and APC inducible shRNAs cell lines as described in the next paragraph of this chapter.

5.4 Is Smad4 degraded in the Wnt destruction complex?

A key question raised by our study on Smad4 is whether other components of the Wnt destruction complex such as Axin and APC are involved in the GSK3-mediated phosphorylation of Smad4 linker region. To test this, I collaborated with Dr. Hyunjoon Kim, a post-doctoral trainee in our lab, who had just developed new and highly effective shRNAs against Axin and APC. We permanently infected 293T cells with lentivirus carrying a doxycyclin-inducible shRNA against Axin or APC. In the presence of FGF, we found that Wnt treatment stabilized Smad4 (Figure 5.6 A compare lanes 1 to 2 and 7 to 8) as predicted by our model (Figure 5.3). Interestingly, when endogenous Axin or APC proteins were depleted by inducing their respective shRNA, Smad4 became more stable and was no longer affected by Wnt treatment (Figure 5.6 A, lanes 4 to 6 and 10 to 12). This result suggests that the FGF-induced phosphorylations of Smad4 by GSK3 and subsequent proteasomal degradation require at least two key components of the Wnt destruction complex, namely Axin and APC. The Wnt-destruction complex can be concentrated in "signalosomes-MVBs" by transfection of a truncated LRP6 Wnt-receptor named CA-LRP6 (Bilic et al., 2007). When we looked at the sub-cellular distribution of $pSmad4^{GSK3}$ in cells transfected with CA-LRP6, we found

that the GSK3-phosphorylated form of Smad4 accumulated in signalosomes/MVBs that were also positive for the destruction complex protein Axin (Figure 5.6 B). Similar results were obtained in functional reporter genes assays. In 293T cells, depletion of endogenous APC or Axin significantly stimulated the TGF-beta response (Figure 5.6 C). If confirmed, the involvement of the Wnt destruction complex in the GSK3-mediated phosphorylation and subsequent proteasomal degradation of Smad4 will have important consequences on cancer progression as discussed later in this chapter.

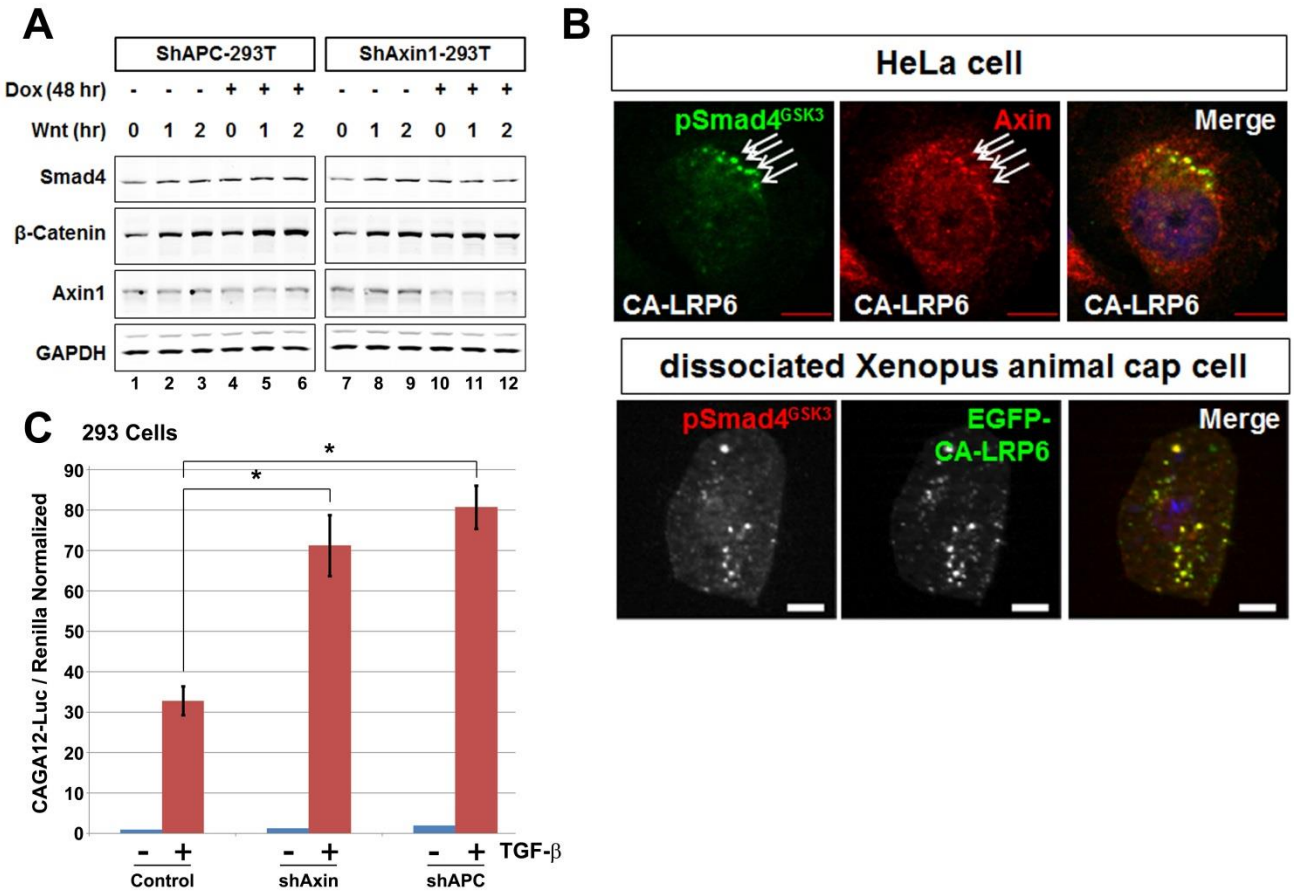

Figure 5.6: Axin and APC regulate Smad4 stability and colocalize with pSmad4^{GSK3}

(**A**) Wnt stimulation stabilizes Smad4 protein in 293T cells treated with FGF. Depletion of Axin or APC with specific inducible shRNA also stabilizes Smad4 and prevents any effect of Wnt on Smad4 stability (unpublished results).
(**B**) CA-LRP6 transfection concentrates the Wnt destruction complex in Axin-positive particles called signalosome. pSmad4^{GSK3} colocalizes with Axin in CA-LRP6 transfected HeLa Cells (unpublished results).
(**C**) In 293T cells, depletion of endogenous APC or Axin greatly stimulated the TGF-beta response (unpublished results).

5.5 Smad4 and cancer: the loss-of-Smad4 and the progression of cancer

At early stages, many tumors are driven by activation of the Ras/Erk and the Wnt oncogenic pathways, which increase proliferation genes such as Cyclin D and c-Myc (Hanahan and Weinberg, 2011). Somatic, gain-of-function mutations in Ras genes are known to activate the MAPK/Erk pathway and to promote tumor development (Schubbert et al., 2007). Mutations in the Wnt pathway, generally affecting components of the Wnt destruction complex such as APC, lead to an increase in beta-catenin levels which also drive proliferation. In many of these tumors, Smad4/DPC4 acts as a barrier for tumor progression (Ding et al., 2011; Vogelstein et al., 2013). These effects are most likely mediated by the TGF-beta pathway which has potent anti-proliferative effects through the activation of Cyclin-Dependent Kinase (CDK) inhibitors such as $p14^{Ink4b}$ and $p21^{WAF1}$ (Hanahan and Weinberg, 2011).

In our proposed model (Figure 5.3), activation of the Ras/Erk and Wnt pathways should lead to an accumulation of activated, stable Smad4 whose anti-proliferative effect could compensate the mitogenic Wnt and Ras mutations (Figure 5.7). This barrier effect of TGF-beta will be lost when the Smad4 tumor suppressor is deleted or inhibited, providing a molecular explanation for the "barrier" effect of Smad4 during cancer progression.

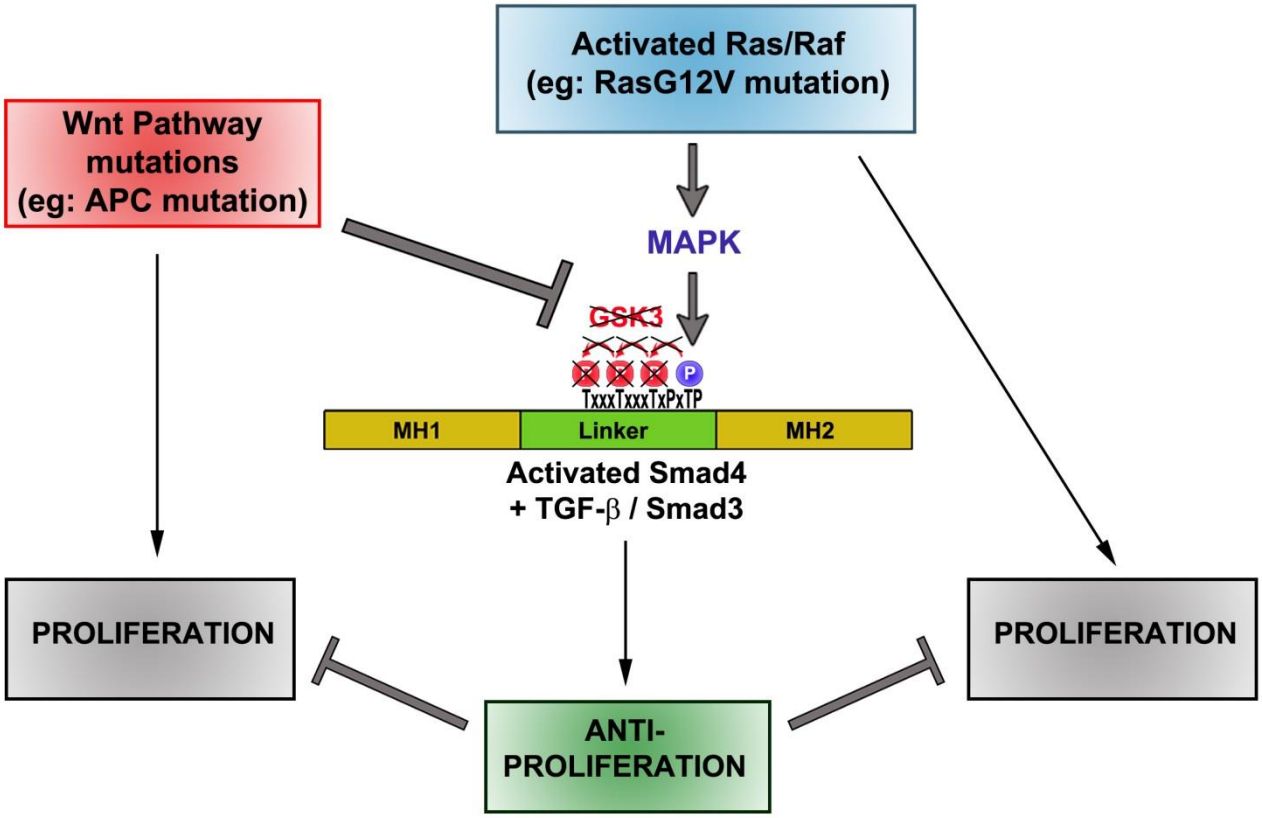

Figure 5.7: Proposed model for the "barrier" effect of Smad4 during cancer progression.

In our proposed model, tumors harboring Ras and Wnt mutations (for example loss of APC) will see an increase in Smad4 activity and stability through the described mechanism (Figure 5.3). The gain in Smad4 activity will increase the anti-proliferative effects of TGF-beta compensating or restraining the proliferation driven by the above mentioned mutations. When Smad4 is lost, as is the case for many tumors, the barrier protective effect of Smad4 will be lost.

This mechanism could explain why the loss of Smad4 has such dramatic effect in mice already harboring an APC truncation (Takaku et al., 1998). In this landmark paper, the authors showed that *Apc$^{\Delta}$716* knockout mice, a model for human familial adenomatous polyposis, display few polyps that usually do not progress toward metastasis. However, in double *Apc$^{\Delta}$716/Smad4$^{-/-}$* knockout mice, intestinal polyps developed into more malignant tumors, showing an extensive stromal cell proliferation, submucosal invasion, and in vivo transplantability (Takaku et al., 1998). The authors concluded that Smad4/DPC4 plays a significant role in the malignant progression of colorectal tumors that could be explained by our new molecular mechanism.

5.6 Smad4 degradation by beta-TrCP in pancreatic carcinoma.

Another exciting area of research opened by our discovery that Smad4 linker is subject to regulation by GSK3 phosphorylations is a possible molecular explanation for the great instability of some Smad4 proteins harboring point mutations in the MH1 or MH2 domains. Indeed, Smad4 is frequently deleted in metastatic tumors, but intragenic point mutations are also quite common (Levy and Hill, 2006; Xu and Attisano, 2000).

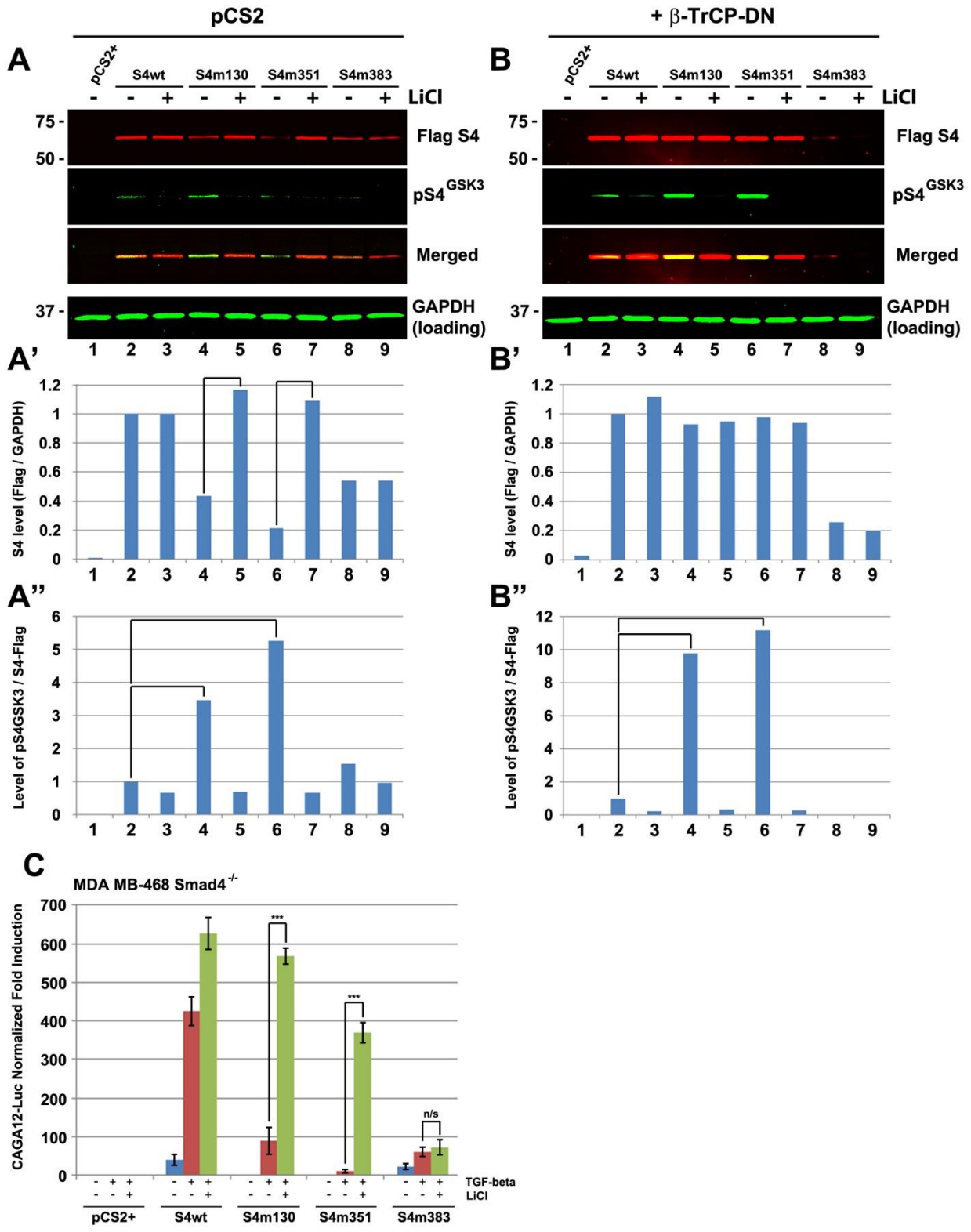

Figure 5.8: Smad4 proteins harboring m130 and m351 mutations are hyperphosphorylated by GSK3.

(**A**) Western-blot showing that Smad4 proteins harboring point mutations are less stable than their wt counterpart. Mutations m130 and m351 increase phosphorylation by GSK3 as marked by $pSmad4^{GSK3}$ antibody. LiCl treatment block GSK3 phosphorylation and increase protein stability
(**A'**) Quantification of proteins stability showed in western-blot (A)
(**A"**) Quantification of proteins phosphorylation by GSK3 from western-blot (A)
(**B**) In cells transfected with DN-beta-TrCP, Smad4 m130 and m351 are strongly phosphorylated by GSK3 but are more stable.
(**B'**) Quantification of proteins stability showed in western-blot (B)
(**B"**) Quantification of proteins phosphorylation by GSK3 from western-blot (B)
(**C**) In MB468 cells (Smad4-/-) Smad4m130 and m351 are less active than Smad4wt. TGF-beta signaling can be restored in those cells by LiCl treatment.

Interestingly, several of these point mutations increase Smad4 degradation by facilitating binding to beta-TrCP (Wan et al., 2005; Yang et al., 2006). Our finding that beta-TrCP binding to Smad4 is regulated by GSK3 phosphorylations suggests in cells harboring those intragenic point mutations, Smad4 protein, possibly misfolded, could be recognized by chaperone proteins associated with a yet-unidentified kinase that could lead to the phosphorylation of threonine 277. This priming site will then be used by GSK3 to generate a phosphodegron recognized and bound by the E3 ligase beta-TrCP. Preliminary results strongly support this model. I prepared mutants Smad4 proteins harboring mutations at codon 130 and 351 (Pro130Ser; Asn351His), two mutations that were shown to increase the binding between Smad4 and beta-TrCP (Wan et al., 2005), were found to be hyperphosphorylated by GSK3 whereas protein harboring mutation at codon 383 (Ile383Lys; a mutation not associated beta-TrCP-mediated degradation) did not show any increase in GSK3 phosphorylation (Figure 5.8 A). These GSK3 phosphorylations disappeared with LiCl and Smad4m130 and m351 became more stable (Figure 5.8 A' and A"). Smad4m383 stability was unaffected by LiCl treatment (Figure 5.8 A' and A"). The hyperphosphorylation of Smad4m130 and m351 was more pronounced in cells transfected with a DN-beta-TrCP construct confirming the involvement of this ubiquitin E3-ligase in the degradation of Smad4 mutated proteins Figure 5.8 B, B' and B"). Finally, in a functional reporter gene

assay using Smad4$^{-/-}$ cells transfected with the different mutant forms of Smad4, I found that the activity of Smad4 m130, m351 and m383 were strongly decreased compared to the wt protein. Interestingly, LiCl treatment restored TGF-beta signaling in cells harboring the m130 and m351 mutation but was without effect on Smad4m383.

This unpublished result is very promising as it suggests that some mutant proteins of Smad4 commonly found in pancreatic cancer retain their ability to transduce the TGF-beta pathway provided that their rapid degradation by beta-TrCP is blocked by GSK3 inhibitors. This suggests that pharmacological GSK3 inhibitors may stabilize Smad4 and restore growth control in tumors harboring such mutations (Figure 5.9).

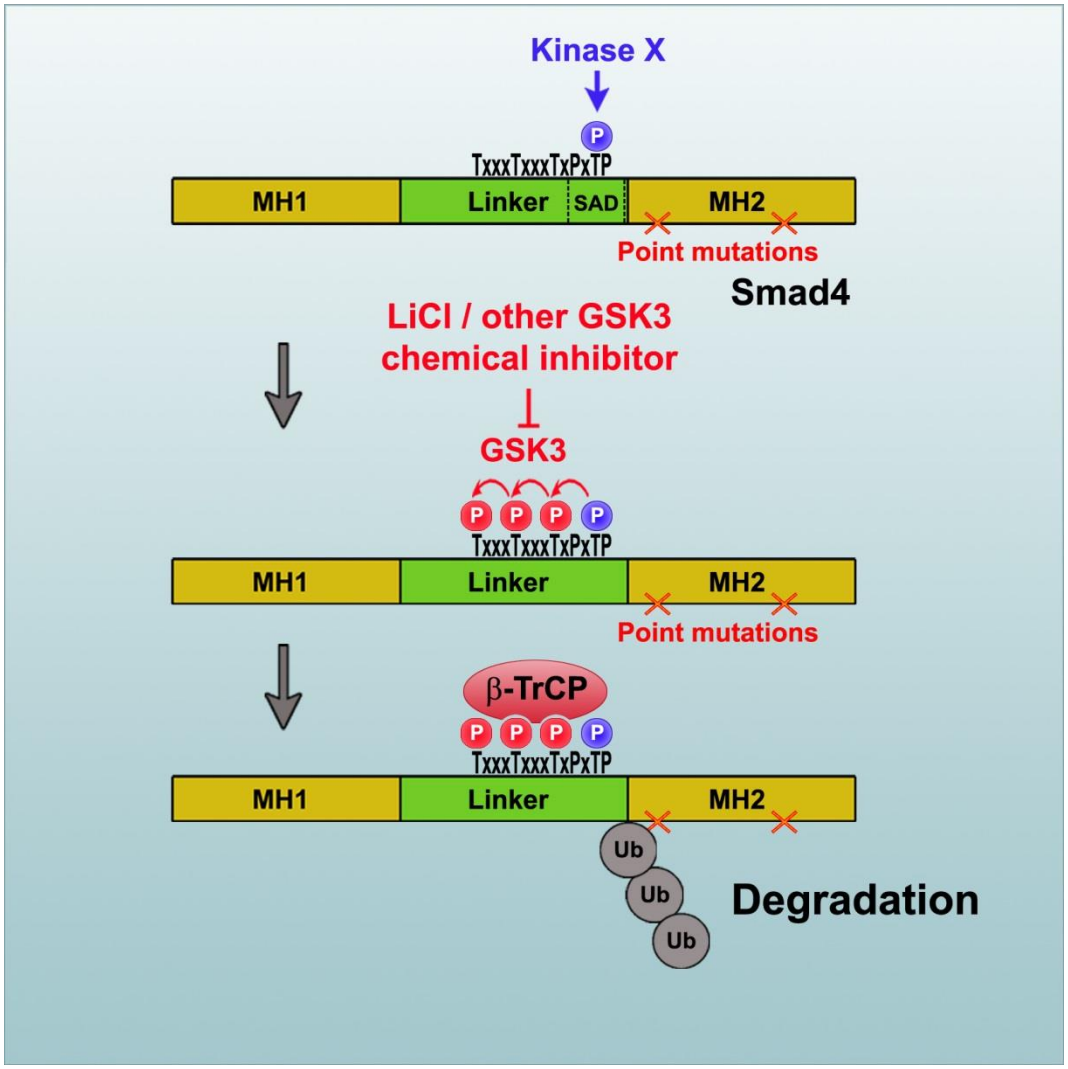

Figure 5.9: Proposed model where some point mutations found in Smad4 will increase its degradation via GSK3 phosphorylation.

We propose that some point mutations commonly found in human cancers will lead to the recutment of a yet-unknown kinase (kinase X) whose phosphorylation of Thr 277 will lead to subsequent GSK3 phosphorylations generating a phosphodegron recognized and bound by the E3 ligase beta-TrCP. In this model, chemical inhibitors of GSK3 should prevent Smad4 degradation and restore growth control by TGF-beta signaling.

5.7 Concluding remarks.

My thesis work has shown that the tumor suppressor Smad4 is not a silent partner in the TGF-beta pathway but rather that its activity and stability are tightly controlled by linker phosphorylation encoded in its primary sequence. These sequential phosphorylations regulate first the activity before priming the degradation of the transcription factor and are controlled by the FGF/MAPK and Wnt/GSK3 pathways providing a novel node of signal integrations between these two pathways and TGF-beta signaling. This work opens new perspectives in classic embryology by providing a molecular explanation to the long stading question of the “competence modifier” effect of Wnt on Nodal signaling and in cancer biology where the role of Smad4 has a “barrier” to tumor progression is explained by our new mechanism.

References:

Abdollah, S., MaciasSilva, M., Tsukazaki, T., Hayashi, H., Attisano, L., and Wrana, J. (1997). T beta RI phosphorylation of Smad2 on Ser(465) and Ser(467) is required for Smad2-Smad4 complex formation and signaling. Journal of Biological Chemistry 272, 27678-27685.

Abushahba, W., Olabisi, O., Jeong, B., Boregowda, R., Wen, Y., Liu, F., Goydos, J., Lasfar, A., and Cohen-Solal, K. (2012). Non-Canonical Smads Phosphorylation Induced by the Glutamate Release Inhibitor, Riluzole, through GSK3 Activation in Melanoma. Plos One 7.

Acebron, S., Karaulanov, E., Berger, B., Huang, Y., and Niehrs, C. (2014). Mitotic Wnt Signaling Promotes Protein Stabilization and Regulates Cell Size. Molecular Cell 54, 663-674.

Alarcon, C., Zaromytidou, A., Xi, Q., Gao, S., Yu, J., Fujisawa, S., Barlas, A., Miller, A., Manova-Todorova, K., Macias, M., et al. (2009). Nuclear CDKs Drive Smad Transcriptional Activation and Turnover in BMP and TGF-beta Pathways. Cell 139, 757-769.

Ambrosio, A., Taelman, V., Lee, H., Metzinger, C., Coffinier, C., and De Robertis, E. (2008). Crossveinless-2 is a BMP feedback inhibitor that binds Chordin/BMP to regulate Xenopus embryonic patterning. Developmental Cell 15, 248-260.

Aragon, E., Goerner, N., Zaromytidou, A., Xi, Q., Escobedo, A., Massague, J., and Macias, M. (2011). A Smad action turnover switch operated by WW domain readers of a phosphoserine code. Genes & Development 25, 1275-1288.

Aubin, J., Davy, A., and Soriano, P. (2004). In vivo convergence of BMP and MAPK signaling pathways: impact of differential Smad1 phosphorylation on development and homeostasis. Genes & Development 18, 1482-1494.

Azzolin, L., Zanconato, F., Bresolin, S., Forcato, M., Basso, G., Bicciato, S., Cordenonsi, M., and Piccolo, S. (2012). Role of TAZ as Mediator of Wnt Signaling. Cell 151, 1443-1456.

Beenken, A., and Mohammadi, M. (2009). The FGF family: biology, pathophysiology and therapy. Nature Reviews Drug Discovery 8, 235-253.

Bejsovec, A., and Wieschaus, E. (1993). Segment polarity gene interactions modulate epidermal patterning in Drosophila embryos. Development 119, 501-517.

Bilic, J., Huang, Y., Davidson, G., Zimmermann, T., Cruciat, C., Bienz, M., and Niehrs, C. (2007). Wnt induces LRP6 signalosomes and promotes dishevelled-dependent LRP6 phosphorylation. Science 316, 1619-1622.

Bilican, B., Fiore-Heriche, C., Compston, A., Allen, N., and Chandran, S. (2008). Induction of Olig2(+) Precursors by FGF Involves BMP Signalling Blockade at the Smad Level. Plos One 3.

Brand, A., and Perrimon, N. (1993). Targeted gene-expression as a means of altering cell fates and generating dominant phenotypes. Development 118, 401-415.

Browne, J., Liu, X., Schnaper, H., and Hayashida, T. (2013). Serine-204 in the linker region of Smad3 mediates the collagen-I response to TGF-beta in a cell phenotype-specific manner. Experimental Cell Research 319, 2928-2937.

Bryant, P. (1988). Localized cell-death caused by mutations in a Drosophila gene coding for a transforming growth factor-beta homolog. Developmental Biology 128, 386-395.

Cadigan, K., and Nusse, R. (1997). Wnt signaling: a common theme in animal development. Genes & Development 11, 3286-3305.

Candia, A., Watabe, T., Hawley, S., Onichtchouk, D., Zhang, Y., Derynck, R., Niehrs, C., and Cho, K. (1997). Cellular interpretation of multiple TGF-beta signals: intracellular antagonism between activin/BVg1 and BMP-2/4 signaling mediated by Smads. Development 124, 4467-4480.

Casellas, R., and Brivanlou, A. (1998). Xenopus Smad7 inhibits both the activin and BMP pathways and acts as a neural inducer. Developmental Biology 198, 1-12.

Chacko, B., Qin, B., Correia, J., Lam, S., de Caestecker, M., and Lin, K. (2001). The L3 loop and C-terminal phosphorylation jointly define Smad protein trimerization. Nature Structural Biology 8, 248-253.

Chang, C., Brivanlou, A., and Harland, R. (2006). Function of the two xenopus Smad4s in early frog development. Journal of Biological Chemistry 281, 30794-30803.

Chang, M., Chang, J., Gangopadhyay, A., Shearer, A., and Cadigan, K. (2008). Activation of Wingless Targets Requires Bipartite Recognition of DNA by TCF. Current Biology 18, 1877-1881.

Chen, H., Shen, J., Ip, Y., and Xu, L. (2006). Identification of phosphatases for Smad in the BMP/DPP pathway. Genes & Development 20, 648-653.

Chen, Y., Hata, A., Lo, R., Wotton, D., Shi, Y., Pavletich, N., and Massague, J. (1998). Determinants of specificity in TGF-beta signal transduction. Genes & Development 12, 2144-2152.

Christian, J., and Moon, R. (1993). Interactions between xwnt-8 and spemann organizer signaling pathways generate dorsoventral pattern in the embryonic mesoderm of Xenopus. Genes & Development 7, 13-28.

Clemens, J., Worby, C., Simonson-Leff, N., Muda, M., Maehama, T., Hemmings, B., and Dixon, J. (2000). Use of double-stranded RNA interference in Drosophila cell lines to dissect signal transduction pathways. Proceedings of the National Academy of Sciences of the United States of America 97, 6499-6503.

Clevers, H. (2006). Wnt/beta-catenin signaling in development and disease. Cell 127, 469-480.

Clevers, H., and Nusse, R. (2012). Wnt/beta-Catenin Signaling and Disease. Cell 149, 1192-1205.

Coffinier, C., Ketpura, N., Tran, U., Geissert, D., and De Robertis, E. (2002). Mouse Crossveinless-2 is the vertebrate homolog of a Drosophila extracellular regulator of BMP signaling. Mechanisms of Development 119, S179-S184.

Cohen, P., and Frame, S. (2001). The renaissance of GSK3. Nature Reviews Molecular Cell Biology 2, 769-776.

Conley, C., Silburn, R., Singer, M., Ralston, A., Rohwer-Nutter, D., Olson, D., Gelbart, W., and Blair, S. (2000). Crossveinless 2 contains cysteine-rich domains

and is required for high levels of BMP-like activity during the formation of the cross veins in Drosophila. Development 127, 3947-3959.

Correia, J., Chacko, B., Lam, S., and Lin, K. (2001). Sedimentation studies reveal a direct role of phosphorylation in Smad3 : Smad4 homo- and hetero-trimerization. Biochemistry 40, 1473-1482.

Couso, J., Bishop, S., and Arias, A. (1994). The wingless signaling pathway and the patterning of the wing margin in Drosophila. Development 120, 621-636.

Damen, W. (2007). Evolutionary conservation and divergence of the segmentation process in arthropods. Developmental Dynamics 236, 1379-1391.

de Caestecker, M., Parks, W., Frank, C., Castagnino, P., Bottaro, D., Roberts, A., and Lechleider, R. (1998). Smad2 transduces common signals from receptor serine-threonine and tyrosine kinases. Genes & Development 12, 1587-1592.

de Caestecker, M., Yahata, T., Wang, D., Parks, W., Huang, S., Hill, C., Shioda, T., Roberts, A., and Lechleider, R. (2000). The Smad4 activation domain (SAD) is a proline-rich, p300-dependent transcriptional activation domain. Journal of Biological Chemistry 275, 2115-2122.

De Robertis, E. (2006). Spemann's organizer and self-regulation in amphibian embryos. Nature Reviews Molecular Cell Biology 7, 296-302.

De Robertis, E. (2008). The molecular ancestry of segmentation mechanisms. Proceedings of the National Academy of Sciences of the United States of America 105, 16411-16412.

De Robertis, E., and Kuroda, H. (2004). Dorsal-ventral patterning and neural induction in Xenopus embryos. Annual Review of Cell and Developmental Biology 20, 285-308.

Dennler, S., Itoh, S., Vivien, D., ten Dijke, P., Huet, S., and Gauthier, J. (1998). Direct binding of Smad3 and Smad4 to critical TGF beta-inducible elements in the promoter of human plasminogen activator inhibitor-type 1 gene. Embo Journal 17, 3091-3100.

DeRobertis, E., and Sasai, Y. (1996). A common plan for dorsoventral patterning in Bilateria. Nature 380, 37-40.

Derynck, R., and Zhang, Y. (2003). Smad-dependent and Smad-independent pathways in TGF-beta family signalling. Nature 425, 577-584.

Ding, Z., Wu, C., Chu, G., Xiao, Y., Ho, D., Zhang, J., Perry, S., Labrot, E., Wu, X., Lis, R., et al. (2011). SMAD4-dependent barrier constrains prostate cancer growth and metastatic progression. Nature 470, 269-+.

Dominguez, M., and Hafen, E. (1997). Hedgehog directly controls initiation and propagation of retinal differentiation in the Drosophila eye. Genes & Development 11, 3254-3264.

Dorfman, R., and Shilo, B. (2001). Biphasic activation of the BMP pathway patterns the Drosophila embryonic dorsal region. Development 128, 965-972.

Duan, X., Liang, Y., Feng, X., and Lin, X. (2006). Protein serine/threonine phosphatase PPM1A dephosphorylates Smad1 in the bone morphogenetic protein signaling pathway. Journal of Biological Chemistry 281, 36526-36532.

Duncan, D., Burgess, E., and Duncan, I. (1998). Control of distal antennal identity and tarsal development in Drosophila by spineless-aristapedia, a homolog of the mammalian dioxin receptor. Genes & Development 12, 1290-1303.

Duong, H., Wang, C., Sun, Y., and Courey, A. (2008). Transformation of eye to antenna by misexpression of a single gene. Mechanisms of Development 125, 130-141.

Dupont, S., Mamidi, A., Cordenonsi, M., Montagner, M., Zacchigna, L., Adorno, M., Martello, G., Stinchfield, M., Soligo, S., Morsut, L., et al. (2009). FAM/USP9x, a Deubiquitinating Enzyme Essential for TGF beta Signaling, Controls Smad4 Monoubiquitination. Cell 136, 123-135.

Dupont, S., Zacchigna, L., Cordenonsi, M., Soligo, S., Adorno, M., Rugge, M., and Piccolo, S. (2005). Germ-layer specification and control of cell growth by ectodermin, a Smad4 ubiquitin ligase. Cell 121, 87-99.

Ebisawa, T., Fukuchi, M., Murakami, G., Chiba, T., Tanaka, K., Imamura, T., and Miyazono, K. (2001). Smurf1 interacts with transforming growth factor-beta type I receptor through Smad7 and induces receptor degradation. Journal of Biological Chemistry 276, 12477-12480.

Eivers, E., Fuentealba, L., and De Robertis, E. (2008). Integrating positional information at the level of Smad1/5/8. Current Opinion in Genetics & Development 18, 304-310.

Eivers, E., Fuentealba, L., Sander, V., Clemens, J., Hartnett, L., and Robertis, E. (2009). Mad Is Required for Wingless Signaling in Wing Development and Segment Patterning in Drosophila. Plos One 4.

Eivers, E., McCarthy, K., Glynn, C., Nolan, C., and Byrnes, L. (2004). Insulin-like growth factor (IGF) signalling is required for early dorso-anterior development of the zebrafish embryo. International Journal of Developmental Biology 48, 1131-1140.

Estella, C., McKay, D., and Mann, R. (2008). Molecular integration of wingless, decapentaplegic, and autoregulatory inputs into Distalless during Drosophila leg development. Developmental Cell 14, 86-96.

Fedi, P., Bafico, A., Soria, A., Burgess, W., Miki, T., Bottaro, D., Kraus, M., and Aaronson, S. (1999). Isolation and biochemical characterization of the human Dkk-1 homologue, a novel inhibitor of mammalian Wnt signaling. Journal of Biological Chemistry 274, 19465-19472.

Feng, X., and Derynck, R. (2005). Specificity and versatility in TGF-beta signaling through Smads. Annual Review of Cell and Developmental Biology 21, 659-693.

Feng, X., Zhang, Y., Wu, R., and Derynck, R. (1998). The tumor suppressor Smad4/DPC4 and transcriptional adaptor CBP/p300 are coactivators for Smad3 in TGF-beta-induced transcriptional activation. Genes & Development 12, 2153-2163.

Fuchs, S., Spiegelman, V., and Kumar, K. (2004). The many faces of beta-TrCP E3 ubiquitin ligases: reflections in the magic mirror of cancer. Oncogene 23, 2028-2036.

Fuentealba, L., Eivers, E., Geissert, D., Taelman, V., and De Robertis, E. (2008). Asymmetric mitosis: Unequal segregation of proteins destined for degradation. Proceedings of the National Academy of Sciences of the United States of America 105, 7732-7737.

Fuentealba, L., Eivers, E., Ikeda, A., Hurtado, C., Kuroda, H., Pera, E., and De Robertis, E. (2007). Integrating patterning signals: Wnt/GSK3 regulates the duration of the BMP/Smad1 signal. Cell 131, 980-993.

Gao, S., Alarcon, C., Sapkota, G., Rahman, S., Chen, P., Goerner, N., Macias, M., Erdjument-Bromage, H., Tempst, P., and Massague, J. (2009). Ubiquitin Ligase Nedd4L Targets Activated Smad2/3 to Limit TGF-beta Signaling. Molecular Cell 36, 457-468.

Gao, S., and Laughon, A. (2007). Flexible interaction of Drosophila Smad complexes with bipartite binding sites. Biochimica Et Biophysica Acta-Gene Structure and Expression 1769, 484-496.

Glinka, A., Wu, W., Delius, H., Monaghan, A., Blumenstock, C., and Niehrs, C. (1998). Dickkopf-1 is a member of a new family of secreted proteins and functions in head induction. Nature 391, 357-362.

Glinka, A., Wu, W., Onichtchouk, D., Blumenstock, C., and Niehrs, C. (1997). Head induction by simultaneous repression of Bmp and Wnt signalling in Xenopus. Nature 389, 517-519.

Grimm, O., and Gurdon, J. (2002). Nuclear exclusion of Smad2 is a mechanism leading to loss of competence. Nature Cell Biology 4, 519-522.

Guardavaccaro, D., Kudo, Y., Boulaire, J., Barchi, M., Busino, L., Donzelli, M., Margottin-Goguet, F., Jackson, P., Yamasaki, L., and Pagano, M. (2003). Control of meiotic and mitotic progression by the F box protein beta-Trcp1 in vivo. Developmental Cell 4, 799-812.

Guo, X., Ramirez, A., Waddell, D., Li, Z., Liu, X., and Wang, X. (2008). Axin and GSK3-beta control Smad3 protein stability and modulate TGF-beta signaling. Genes & Development 22, 106-120.

Gurley, K., Rink, J., and Alvarado, A. (2008). beta-catenin defines head versus tail identity during planarian regeneration and Homeostasis. Science 319, 323-327.

Halder, S., Beauchamp, R., and Datta, P. (2005). A specific inhibitor of TGF-beta receptor kinase, SB-431542, as a potent antitumor agent for human cancers. Neoplasia 7, 509-521.

Hanahan, D., and Weinberg, R. (2011). Hallmarks of Cancer: The Next Generation. Cell 144, 646-674.

Hashimoto, H., Itoh, M., Yamanaka, Y., Yamashita, S., Shimizu, T., Solnica-Krezel, L., Hibi, M., and Hirano, T. (2000). Zebrafish Dkk1 functions in forebrain specification and axial mesendoderm formation. Developmental Biology 217, 138-152.

Hata, A., Lagna, G., Massague, J., and Hemmati-Brivanlou, A. (1998). Smad6 inhibits BMP/Smad1 signaling by specifically competing with the Smad4 tumor suppressor. Genes & Development 12, 186-197.

Hata, A., Lo, R., Wotton, D., Lagna, G., and Massague, J. (1997). Mutations increasing autoinhibition inactivate tumour suppressors Smad2 and Smad4. Nature 388, 82-87.

Hayashi, H., Abdollah, S., Qiu, Y., Cai, J., Xu, Y., Grinnell, B., Richardson, M., Topper, J., Gimbrone, M., Wrana, J., et al. (1997). The MAD-related protein Smad7 associates with the TGF beta receptor and functions as an antagonist of TGF beta signaling. Cell 89, 1165-1173.

Holley, S., Neul, J., Attisano, L., Wrana, J., Sasai, Y., OConnor, M., DeRobertis, E., and Ferguson, E. (1996). The Xenopus dorsalizing factor noggin ventralizes Drosophila embryos by preventing DPP from activating its receptor. Cell 86, 607-617.

Hoodless, P., Haerry, T., Abdollah, S., Stapleton, M., OConnor, M., Attisano, L., and Wrana, J. (1996). MADR1, a MAD-related protein that functions in BMP2 signaling pathways. Cell 85, 489-500.

Hoverter, N., Ting, J., Sundaresh, S., Baldi, P., and Waterman, M. (2012). A WNT/p21 Circuit Directed by the C-Clamp, a Sequence-Specific DNA Binding Domain in TCFs. Molecular and Cellular Biology 32, 3648-3662.

Hu, M., and Rosenblum, N. (2005). Smad1, beta-catenin and Tcf4 associate in a molecular complex with the Myc promoter in dysplastic renal tissue and cooperate to control Myc transcription. Development 132, 215-225.

Huse, M., Chen, Y., Massague, J., and Kuriyan, J. (1999). Crystal structure of the cytoplasmic domain of the type I TGF beta receptor in complex with FKBP12. Cell 96, 425-436.

Huse, M., Muir, T., Xu, L., Chen, Y., Kuriyan, J., and Massague, J. (2001). The TGF beta receptor activation process: An inhibitor- to substrate-binding switch. Molecular Cell 8, 671-682.

Imamura, T., Takase, M., Nishihara, A., Oeda, E., Hanai, J., Kawabata, M., and Miyazono, K. (1997). Smad6 inhibits signalling by the TGF-beta superfamily. Nature 389, 622-626.

Inman, G., and Hill, C. (2002). Stoichiometry of active Smad-transcription factor complexes on DNA. Journal of Biological Chemistry 277, 51008-51016.

Inoue, H., Imamura, T., Ishidou, Y., Takase, M., Udagawa, Y., Oka, Y., Tsuneizumi, K., Tabata, T., Miyazono, K., and Kawabata, M. (1998). Interplay of signal mediators of decapentaplegic (Dpp): Molecular characterization of mothers against dpp, Medea, and daughters against dpp. Molecular Biology of the Cell 9, 2145-2156.

Janknecht, R., Wells, N., and Hunter, T. (1998). TGF-beta-stimulated cooperation of Smad proteins with the coactivators CBP/p300. Genes & Development 12, 2114-2119.

Jayaraman, L., and Massague, J. (2000). Distinct oligomeric states of SMAD proteins in the transforming growth factor-beta pathway. Journal of Biological Chemistry 275, 40710-40717.

Kao, K., Masui, Y., and Elinson, R. (1986). Lithium-induced respecification of pattern in xenopus-laevis embryos. Nature 322, 371-373.

Kavsak, P., Rasmussen, R., Causing, C., Bonni, S., Zhu, H., Thomsen, G., and Wrana, J. (2000). Smad7 binds to Smurf2 to form an E3 ubiquitin ligase that targets the TGF beta receptor for degradation. Molecular Cell 6, 1365-1375.

Kawabata, M., Imamura, T., and Miyazono, K. (1998). Signal transduction by bone morphogenetic proteins. Cytokine & Growth Factor Reviews 9, 49-61.

Khokha, M., Yeh, J., Grammer, T., and Harland, R. (2005). Depletion of three BMP antagonists from Spemann's organizer leads to a catastrophic loss of dorsal structures. Developmental Cell 8, 401-411.

Kiecker, C., and Niehrs, C. (2001). A morphogen gradient of Wnt/beta-catenin signalling regulates anteroposterior neural patterning in Xenopus. Development 128, 4189-4201.

Kim, J., Johnson, K., Chen, H., Carroll, S., and Laughon, A. (1997). Drosophila MAD binds to DNA and directly mediates activation of vestigial by decapentaplegic. Nature 388, 304-308.

Kim, N., Xu, C., and Gumbiner, B. (2009). Identification of targets of the Wnt pathway destruction complex in addition to beta-catenin. Proceedings of the National Academy of Sciences of the United States of America 106, 5165-5170.

Kinoshita, E., Kinoshita-Kikuta, E., Takiyama, K., and Koike, T. (2006). Phosphate-binding tag, a new tool to visualize phosphorylated proteins. Molecular & Cellular Proteomics 5, 749-757.

Kishimoto, Y., Lee, K., Zon, L., Hammerschmidt, M., and Schulte-Merker, S. (1997). The molecular nature of zebrafish swirl: BMP2 function is essential during early dorsoventral patterning. Development 124, 4457-4466.

Knockaert, M., Sapkota, G., Alarcon, C., Massague, J., and Brivanlou, A. (2006). Unique players in the BMP pathway: Small C-terminal domain phosphatases dephosphorylate Smad1 to attenuate BMP signaling. Proceedings of the National Academy of Sciences of the United States of America 103, 11940-11945.

Korchynskyi, O., and ten Dijke, P. (2002). Identification and functional characterization of distinct critically important bone morphogenetic protein-

specific response elements in the Id1 promoter. Journal of Biological Chemistry 277, 4883-4891.

Kouhara, H., Hadari, Y., SpivakKroizman, T., Schilling, J., BarSagi, D., Lax, I., and Schlessinger, J. (1997). A lipid-anchored Grb2-binding protein that links FGF-receptor activation to the Ras/MAPK signaling pathway. Cell 89, 693-702.

Kretzschmar, M., Doody, J., and Massague, J. (1997a). Opposing BMP and EGF signalling pathways converge on the TGF-beta family mediator Smad1. Nature 389, 618-622.

Kretzschmar, M., Doody, J., Timokhina, I., and Massague, J. (1999). A mechanism of repression of TGF beta/Smad signaling by oncogenic Ras. Genes & Development 13, 804-816.

Kretzschmar, M., Liu, F., Hata, A., Doody, J., and Massague, J. (1997b). The TGF-P family mediator Smad1 is phosphorylated directly and activated functionally by the BMP receptor kinase. Genes & Development 11, 984-995.

Kuroda, H., Fuentealba, L., Ikeda, A., Reversade, B., and De Robertis, E. (2005). Default neural induction: neuralization of dissociated Xenopus cells is mediated by Ras/MAPK activation. Genes & Development 19, 1022-1027.

Labbe, E., Letamendia, A., and Attisano, L. (2000). Association of Smads with lymphoid enhancer binding factor 1/T cell-specific factor mediates cooperative signaling by the transforming growth factor-beta and Wnt pathways. Proceedings of the National Academy of Sciences of the United States of America 97, 8358-8363.

Lagna, G., Hata, A., HemmatiBrivanlou, A., and Massague, J. (1996). Partnership between DPC4 and SMAD proteins in TGF-beta signalling pathways. Nature 383, 832-836.

Lee, Y., and Carthew, R. (2003). Making a better RNAi vector for Drosophila: use of intron spacers. Methods 30, 322-329.

Lehmann, K., Janda, E., Pierreux, C., Rytomaa, M., Schulze, A., McMahon, M., Hill, C., Beug, H., and Downward, J. (2000). Raf induces TGF beta production

while blocking its apoptotic but not invasive responses: a mechanism leading to increased malignancy in epithelial cells. Genes & Development 14, 2610-2622.

Lei, S., Dubeykovskiy, A., Chakladar, A., Wojtukiewicz, L., and Wang, T. (2004). The murine gastrin promoter is synergistically activated by transforming growth factor-beta/Smad and Wnt signaling pathways. Journal of Biological Chemistry 279, 42492-42502.

Levy, L., and Hill, C. (2006). Alterations in components of the TGF-beta superfamily signaling pathways in human cancer. Cytokine & Growth Factor Reviews 17, 41-58.

Li, L., Xin, H., Xu, X., Huang, M., Zhang, X., Chen, Y., Zhang, S., Fu, X., and Chang, Z. (2004). CHIP mediates degradation of smad proteins and potentially regulates smad-induced transcription. Molecular and Cellular Biology 24, 856-864.

Lin, H., Bergmann, S., and Pandolfi, P. (2004). Cytoplasmic PML function in TGF-beta signalling. Nature 431, 205-211.

Lin, X., Duan, X., Liang, Y., Su, Y., Wrighton, K., Long, J., Hu, M., Davis, C., Wang, J., Brunicardi, F., et al. (2006). PPM1A functions as a Smad phosphatase to terminate TGF beta signaling. Cell 125, 915-928.

Lin, X., Liang, M., and Feng, X. (2000). Smurf2 is a ubiquitin E3 ligase mediating proteasome-dependent degradation of Smad2 in transforming growth factor-beta signaling. Journal of Biological Chemistry 275, 36818-36822.

Little, S., and Mullins, M. (2009). Bone morphogenetic protein heterodimers assemble heteromeric type I receptor complexes to pattern the dorsoventral axis. Nature Cell Biology 11, 637-U439.

Liu, F., Hata, A., Baker, J., Doody, J., Carcamo, J., Harland, R., and Massague, J. (1996). A human Mad protein acting as a BMP-regulated transcriptional activator. Nature 381, 620-623.

Liu, X., Sun, Y., Constantinescu, S., Karam, E., Weinberg, R., and Lodish, H. (1997). Transforming growth factor beta-induced phosphorylation of Smad3 is required for growth inhibition and transcriptional induction in epithelial cells.

Proceedings of the National Academy of Sciences of the United States of America 94, 10669-10674.

Lo, R., Chen, Y., Shi, Y., Pavletich, N., and Massague, J. (1998). The L3 loop: a structural motif determining specific interactions between SMAD proteins and TGF-beta receptors. Embo Journal 17, 996-1005.

Logan, C., and Nusse, R. (2004). The Wnt signaling pathway in development and disease. Annual Review of Cell and Developmental Biology 20, 781-810.

MaciasSilva, M., Abdollah, S., Hoodless, P., Pirone, R., Attisano, L., and Wrana, J. (1996). MADR2 is a substrate of the TGF beta receptor and its phosphorylation is required for nuclear accumulation and signaling. Cell 87, 1215-1224.

Massague, J. (1998). TGF-beta signal transduction. Annual Review of Biochemistry 67, 753-791.

Massague, J. (2000). How cells read TGF-beta signals. Nature Reviews Molecular Cell Biology 1, 169-178.

Massague, J. (2012). TGF beta signalling in context. Nature Reviews Molecular Cell Biology 13, 616-630.

Matsuura, I., Denissova, N., Wang, G., He, D., Long, J., and Liu, F. (2004). Cyclin-dependent kinases regulate the antiproliferative function of Smads. Nature 430, 226-231.

McGrew, L., Hoppler, S., and Moon, R. (1997). Wnt and FGF pathways cooperatively pattern anteroposterior neural ectoderm in Xenopus. Mechanisms of Development 69, 105-114.

Meijer, L., Skaltsounis, A., Magiatis, P., Polychronopoulos, P., Knockaert, M., Leost, M., Ryan, X., Vonica, C., Brivanlou, A., Dajani, R., et al. (2003). GSK-3-selective inhibitors derived from Tyrian purple indirubins. Chemistry & Biology 10, 1255-1266.

Metcalfe, C., Mendoza-Topaz, C., Mieszczanek, J., and Bienz, M. (2010). Stability elements in the LRP6 cytoplasmic tail confer efficient signalling upon DIX-dependent polymerization. Journal of Cell Science 123, 1588-1599.

Millet, C., Yamashita, M., Heller, M., Yu, L., Veenstra, T., and Zhang, Y. (2009). A Negative Feedback Control of Transforming Growth Factor-beta Signaling by Glycogen Synthase Kinase 3-mediated Smad3 Linker Phosphorylation at Ser-204. Journal of Biological Chemistry 284, 19808-19816.

Miyanaga, Y., Torregroza, I., and Evans, T. (2002). A maternal smad protein regulates early embryonic apoptosis in Xenopus laevis. Molecular and Cellular Biology 22, 1317-1328.

Molenaar, M., vandeWetering, M., Oosterwegel, M., PetersonMaduro, J., Godsave, S., Korinek, V., Roose, J., Destree, O., and Clevers, H. (1996). XTcf-3 transcription factor mediates beta-catenin-induced axis formation in Xenopus embryos. Cell 86, 391-399.

Moon, R., and Christian, J. (1992). Competence modifiers synergize with growth-factors during mesoderm induction and patterning in Xenopus. Cell 71, 709-712.

Moren, A., Imamura, T., Miyazono, K., Heldin, C., and Moustakas, A. (2005). Degradation of the tumor suppressor Smad4 by WW and HECT domain ubiquitin ligases. Journal of Biological Chemistry 280, 22115-22123.

Morimura, S., Maves, L., Chen, Y., and Hoffmann, F. (1996). decapentaplegic overexpression affects Drosophila wing and leg imaginal disc development and wingless expression. Developmental Biology 177, 136-151.

Muller, B., Hartmann, B., Pyrowolakis, G., Affolter, M., and Basler, K. (2003). Conversion of an extracellular Dpp/BMP morphogen gradient into an inverse transcriptional gradient. Cell 113, 221-233.

Murakami, G., Watabe, T., Takaoka, K., Miyazono, K., and Imamura, T. (2003). Cooperative inhibition of bone morphogenetic protein signaling by Smurf1 and inhibitory Smads. Molecular Biology of the Cell 14, 2809-2817.

Muzzopappa, M., and Wappner, P. (2005). Multiple roles of the F-box protein Slimb in Drosophila egg chamber development. Development 132, 2561-2571.

Nakao, A., Afrakhte, M., Moren, A., Nakayama, T., Christian, J., Heuchel, R., Itoh, S., Kawabata, N., Heldin, N., Heldin, C., et al. (1997). Identification of Smad7, a TGF beta-inducible antagonist of TGF-beta signalling. Nature 389, 631-635.

Nakayama, T., Snyder, M., Grewal, S., Tsuneizumi, K., Tabata, T., and Christian, J. (1998). Xenopus Smad8 acts downstream of BMP-4 to modulate its activity during vertebrate embryonic patterning. Development 125, 857-867.

Nentwich, O., Dingwell, K., Nordheim, A., and Smith, J. (2009). Downstream of FGF during mesoderm formation in Xenopus: The roles of Elk-1 and Egr-1. Developmental Biology 336, 313-326.

Neubuser, A., Peters, H., Balling, R., and Martin, G. (1997). Antagonistic interactions between FGF and BMP signaling pathways: A mechanism for positioning the sites of tooth formation. Cell 90, 247-255.

Neumann, C., and Cohen, S. (1997). Long-range action of Wingless organizes the dorsal-ventral axis of the Drosophila wing. Development 124, 871-880.

Nguyen, V., Schmid, B., Trout, J., Connors, S., Ekker, M., and Mullins, M. (1998). Ventral and lateral regions of the zebrafish gastrula, including the neural crest progenitors, are established by a bmp2b/swirl pathway of genes. Developmental Biology 199, 93-110.

Niehrs, C. (2004). Regionally specific induction by the Spemann-Mangold organizer. Nature Reviews Genetics 5, 425-434.

Nishimura, R., Kato, Y., Chen, D., Harris, S., Mundy, G., and Yoneda, T. (1998). Smad5 and DPC4 are key molecules in mediating BMP-2-induced osteoblastic differentiation of the pluripotent mesenchymal precursor cell fine C2C12. Journal of Biological Chemistry 273, 1872-1879.

Nishita, M., Hashimoto, M., Ogata, S., Laurent, M., Ueno, N., Shibuya, H., and Cho, K. (2000). Interaction between Wnt and TGF-beta signalling pathways during formation of Spemann's organizer. Nature 403, 781-785.

Niswander, L., and Martin, G. (1993). FGF-4 and BMP-2 have opposite effects on limb growth. Nature 361, 68-71.

Noordermeer, J., Klingensmith, J., Perrimon, N., and Nusse, R. (1994). Dishevelled and armadillo act in the wingless signaling pathway in Drosophila. Nature 367, 80-83.

Nussleinvolhard, C., and Wieschaus, E. (1980). Mutations affecting segment number and polarity in Drosophila. Nature 287, 795-801.

O'Connor, M., Umulis, D., Othmer, H., and Blair, S. (2006). Shaping BMP morphogen gradients in the Drosophila embryo and pupal wing. Development 133, 183-193.

Ong, S., Guy, G., Hadari, Y., Laks, S., Gotoh, N., Schlessinger, J., and Lax, I. (2000). FRS2 proteins recruit intracellular signaling pathways by binding to diverse targets on fibroblast growth factor and nerve growth factor receptors. Molecular and Cellular Biology 20, 979-989.

Orian, A., Gonen, H., Bercovich, B., Fajerman, I., Eytan, E., Israel, A., Mercurio, F., Iwai, K., Schwartz, A., and Ciechanover, A. (2000). SCF beta-TrcP ubiquitin ligase-mediated processing of NF-kappa B p105 requires phosphorylation of its C-terminus by I kappa B kinase. Embo Journal 19, 2580-2591.

Pearson, K., Hunter, T., and Janknecht, R. (1999). Activation of Smad1-mediated transcription by p300/CBP. Biochimica Et Biophysica Acta-Gene Structure and Expression 1489, 354-364.

Pera, E., Ikeda, A., Eivers, E., and De Robertis, E. (2003). Integration of IGF, FGF, and anti-BMP signals via Smad1 phosphorylation in neural induction. Genes & Development 17, 3023-3028.

Pera, E., Wessely, O., Li, S., and De Robertis, E. (2001). Neural and head induction by insulin-like growth factor signals. Developmental Cell 1, 655-665.

Persson, U., Izumi, H., Souchelnytskyi, S., Itoh, S., Grimsby, S., Engstrom, U., Heldin, C., Funa, K., and ten Dijke, P. (1998). The L45 loop in type I receptors for TGF-beta family members is a critical determinant in specifying Smad isoform activation. Febs Letters 434, 83-87.

Petersen, C., and Reddien, P. (2008). Smed-beta-catenin-1 is required for anteroposterior blastema polarity in planarian regeneration. Science 319, 327-330.

Piccolo, S., Agius, E., Leyns, L., Bhattacharyya, S., Grunz, H., Bouwmeester, T., and De Robertis, E. (1999). The head inducer Cerberus is a multifunctional antagonist of Nodal, BMP and Wnt signals. Nature 397, 707-710.

Piccolo, S., Sasai, Y., Lu, B., and DeRobertis, E. (1996). Dorsoventral patterning in xenopus: Inhibition of ventral signals by direct binding of Chordin to BMP-4. Cell 86, 589-598.

Plouhinec, J., and De Robertis, E. (2009). Systems Biology of the Self-regulating Morphogenetic Gradient of the Xenopus Gastrula. Cold Spring Harbor Perspectives in Biology 1.

Podos, S., Hanson, K., Wang, Y., and Ferguson, E. (2001). The DSmurf ubiquitin-protein ligase restricts BMP signaling spatially and temporally during Drosophila embryogenesis. Developmental Cell 1, 567-578.

Pouponnot, C., Jayaraman, L., and Massague, J. (1998). Physical and functional interaction of SMADs and p300/CBP. Journal of Biological Chemistry 273, 22865-22868.

Pourquie, O. (2003). The segmentation clock: Converting embryonic time into spatial pattern. Science 301, 328-330.

Prokova, V., Mavridou, S., Papakosta, P., and Kardassis, D. (2005). Characterization of a novel transcriptionally active domain in the transforming growth factor beta-regulated Smad3 protein. Nucleic Acids Research 33, 3708-3721.

Pueyo, J., Lanfear, R., and Couso, J. (2008). Ancestral Notch-mediated segmentation revealed in the cockroach Periplaneta americana. Proceedings of the National Academy of Sciences of the United States of America 105, 16614-16619.

Qin, B., Chacko, B., Lam, S., de Caestecker, M., Correia, J., and Lin, K. (2001). Structural basis of Smad1 activation by receptor kinase phosphorylation. Molecular Cell 8, 1303-1312.

Qin, B., Lam, S., and Lin, K. (1999). Crystal structure of a transcriptionally active Smad4 fragment. Structure With Folding & Design 7, 1493-1503.

Raftery, L., Twombly, V., Wharton, K., and Gelbart, W. (1995). Genetic screens to identify elements of the decapentaplegic signaling pathway in Drosophila. Genetics 139, 241-254.

Randi, A., Sperone, A., Dryden, N., and Birdsey, G. (2009). Regulation of angiogenesis by ETS transcription factors. Biochemical Society Transactions 37, 1248-1253.

Reid, C., Zhang, Y., Sheets, M., and Kessler, D. (2012). Transcriptional integration of Wnt and Nodal pathways in establishment of the Spemann organizer. Developmental Biology 368, 231-241.

Reversade, B., and De Robertis, E. (2005). Regulation of ADMP and BMP2/4/7 at opposite embryonic poles generates a self-regulating morphogenetic field. Cell 123, 1147-1160.

Richard-Parpaillon, L., Heligon, C., Chesnel, F., Boujard, D., and Philpott, A. (2002). The IGF pathway regulates head formation by inhibiting Wnt signaling in Xenopus. Developmental Biology 244, 407-417.

Roelen, B., Cohen, O., Raychowdhury, M., Chadee, D., Zhang, Y., Kyriakis, J., Alessandrini, A., and Lin, H. (2003). Phosphorylation of threonine 276 in Smad4 is involved in transforming growth factor-beta-induced nuclear accumulation. American Journal of Physiology-Cell Physiology 285, C823-C830.

Saha, D., Datta, P., and Beauchamp, R. (2001). Oncogenic Ras represses transforming growth factor-beta/Smad signaling by degrading tumor suppressor Smad4. Journal of Biological Chemistry 276, 29531-29537.

Sapkota, G., Alarcon, C., Spagnoli, F., Brivanlou, A., and Massague, J. (2007). Balancing BMP signaling through integrated inputs into the Smad1 linker. Molecular Cell 25, 441-454.

Sapkota, G., Knockaert, M., Alarcon, C., Montalvo, E., Brivanlou, A., and Massague, J. (2006). Dephosphorylation of the linker regions of Smad1 and Smad2/3 by small C-terminal domain phosphatases has distinct outcomes for bone morphogenetic protein and transforming growth factor-beta pathways. Journal of Biological Chemistry 281, 40412-40419.

Sasai, Y., Lu, B., Steinbeisser, H., Geissert, D., Gont, L., and Derobertis, E. (1994). Xenopus Chordin - a novel dorsalizing factor-activated by organizer-specific homeobox genes. Cell 79, 779-790.

Sater, A., El-Hodiri, H., Goswami, M., Alexander, T., Al-Sheikh, O., Etkin, L., and Uzman, J. (2003). Evidence for antagonism of BMP-4 signals by MAP kinase during Xenopus axis determination and neural specification. Differentiation 71, 434-444.

Savage, C., Das, P., Finelli, A., Townsend, S., Sun, C., Baird, S., and Padgett, R. (1996). Caenorhabditis elegans genes sma2, sma-3, and sma-4 define a conserved family of transforming growth factor beta pathway components. Proceedings of the National Academy of Sciences of the United States of America 93, 790-794.

Schmid, B., Furthauer, M., Connors, S., Trout, J., Thisse, B., Thisse, C., and Mullins, M. (2000). Equivalent genetic roles for bmp7/snailhouse and bmp2b/swirl in dorsoventral pattern formation. Development 127, 957-967.

Schohl, A., and Fagotto, F. (2002). beta-catenin, MAPK and Smad signaling during early Xenopus development. Development 129, 37-52.

Schubbert, S., Shannon, K., and Bollag, G. (2007). Hyperactive Ras in developmental disorders and cancer. Nature Reviews Cancer 7, 295-308.

Schubiger, M., Sustar, A., and Schubiger, G. (2010). Regeneration and transdetermination: The role of wingless and its regulation. Developmental Biology 347, 315-324.

Schwank, G., and Basler, K. (2010). Regulation of Organ Growth by Morphogen Gradients. Cold Spring Harbor Perspectives in Biology 2.

Schwappacher, R., Weiske, J., Heining, E., Ezerski, V., Marom, B., Henis, Y., Huber, O., and Knaus, P. (2009). Novel crosstalk to BMP signalling: cGMP-dependent kinase I modulates BMP receptor and Smad activity. Embo Journal 28, 1537-1550.

Sekelsky, J., Newfeld, S., Raftery, L., Chartoff, E., and Gelbart, W. (1995). Genetic-characterization and cloning of mothers against dpp, a gene required for decapentaplegic function in Drosophila-melanogaster. Genetics 139, 1347-1358.

Shen, X., Hu, P., Liberati, N., Datto, M., Frederick, J., and Wang, X. (1998). TGF-beta-induced phosphorylation of Smad3 regulates its interaction with coactivator p300/CREB-binding protein. Molecular Biology of the Cell 9, 3309-3319.

Shi, W., Chen, H., Sun, J., Chen, C., Zhao, J., Wang, Y., Anderson, K., and Warburton, D. (2004). Overexpression of Smurf1 negatively regulates mouse embryonic lung branching morphogenesis by specifically reducing Smad1 and Smad5 proteins. American Journal of Physiology-Lung Cellular and Molecular Physiology 286, L293-L300.

Shi, Y., Hata, A., Lo, R., Massague, J., and Pavletich, N. (1997). A structural basis for mutational inactivation of the tumour suppressor Smad4. Nature 388, 87-93.

Shi, Y., and Massague, J. (2003). Mechanisms of TGF-beta signaling from cell membrane to the nucleus. Cell 113, 685-700.

Shi, Y., Wang, Y., Jayaraman, L., Yang, H., Massague, J., and Pavletich, N. (1998). Crystal structure of a Smad MH1 domain bound to DNA: Insights on DNA binding in TGF-beta signaling. Cell 94, 585-594.

Smith, W., and Harland, R. (1992). Expression cloning of noggin, a new dorsalizing factor localized to the spemann organizer in xenopus embryos. Cell 70, 829-840.

Sokol, S., and Melton, D. (1992). Interaction of wnt and activin in dorsal mesoderm induction in xenopus. Developmental Biology 154, 348-355.

Song, C., Siok, T., and Gelehrter, T. (1998). Smad4/DPC4 and Smad3 mediate transforming growth factor-beta (TGF-beta) signaling through direct binding to a novel TGF-beta-responsive element in the human plasminogen activator inhibitor-1 promoter. Journal of Biological Chemistry 273, 29287-29290.

Souchelnytskyi, S., Tamaki, K., Engstrom, U., Wernstedt, C., tenDijke, P., and Heldin, C. (1997). Phosphorylation of Ser(465) and Ser(467) in the C terminus of Smad2 mediates interaction with Smad4 and is required for transforming growth factor-beta signaling. Journal of Biological Chemistry 272, 28107-28115.

Streit, A., Berliner, A., Papanayotou, C., Sirulnik, A., and Stern, C. (2000). Initiation of neural induction by FGF signalling before gastrulation. Nature 406, 74-78.

Struhl, G., and Basler, K. (1993). Organizing activity of wingless protein in Drosophila. Cell 72, 527-540.

Sutherland, D., Li, M., Liu, X., Stefancsik, R., and Raftery, L. (2003). Stepwise formation of a SMAD activity gradient during dorsal-ventral patterning of the Drosophila embryo. Development 130, 5705-5716.

Taelman, V., Dobrowolski, R., Plouhinec, J., Fuentealba, L., Vorwald, P., Gumper, I., Sabatini, D., and De Robertis, E. (2010). Wnt Signaling Requires Sequestration of Glycogen Synthase Kinase 3 inside Multivesicular Endosomes. Cell 143, 1136-1148.

Takaesu, N., Bulanin, D., Johnson, A., Orenic, T., and Newfeld, S. (2008). A combinatorial enhancer recognized by Mad, TCF and Brinker first activates then represses dpp expression in the posterior spiracles of Drosophila. Developmental Biology 313, 829-843.

Takaku, K., Oshima, M., Miyoshi, H., Matsui, M., Seldin, M., and Taketo, M. (1998). Intestinal tumorigenesis in compound mutant mice of both Dpc4 (Smad4) and Apc genes. Cell 92, 645-656.

Takase, M., Imamura, T., Sampath, T., Takeda, K., Ichijo, H., Miyazono, K., and Kawabata, M. (1998). Induction of Smad6 mRNA by bone morphogenetic proteins. Biochemical and Biophysical Research Communications 244, 26-29.

Theisen, H., Haerry, T., OConnor, M., and Marsh, J. (1996). Developmental territories created by mutual antagonism between wingless and decapentaplegic. Development 122, 3939-3948.

Tsukazaki, T., Chiang, T., Davison, A., Attisano, L., and Wrana, J. (1998). SARA, a FYVE domain protein that recruits Smad2 to the TGF beta receptor. Cell 95, 779-791.

Tucker, J., Mintzer, K., and Mullins, M. (2008). The BMP signaling gradient patterns dorsoventral tissues in a temporally progressive manner along the anteroposterior axis. Developmental Cell 14, 108-119.

van Beest, M., Dooijes, D., van de Wetering, M., Kjaerulff, S., Bonvin, A., Nielsen, O., and Clevers, H. (2000). Sequence-specific high mobility group box factors recognize 10-12-base pair minor groove motifs. Journal of Biological Chemistry 275, 27266-27273.

vandeWetering, M., Cavallo, R., Dooijes, D., vanBeest, M., vanEs, J., Loureiro, J., Ypma, A., Hursh, D., Jones, T., Bejsovec, A., et al. (1997). Armadillo coactivates transcription driven by the product of the Drosophila segment polarity gene dTCF. Cell 88, 789-799.

Varelas, X., Sakuma, R., Samavarchi-Tehrani, P., Peerani, R., Rao, B., Dembowy, J., Yaffe, M., Zandstra, P., and Wrana, J. (2008). TAZ controls Smad nucleocytoplasmic shuttling and regulates human embryonic stem-cell self-renewal. Nature Cell Biology 10, 837-848.

Varelas, X., Samavarchi-Tehrani, P., Narimatsu, M., Weiss, A., Cockburn, K., Larsen, B., Rossant, J., and Wrana, J. (2010). The Crumbs Complex Couples Cell Density Sensing to Hippo-Dependent Control of the TGF-beta-SMAD Pathway. Developmental Cell 19, 831-844.

Veeman, M., Slusarski, D., Kaykas, A., Louie, S., and Moon, R. (2003). Zebrafish prickle, a modulator of noncanonical Wnt/Fz signaling, regulates gastrulation movements. Current Biology 13, 680-685.

Vinyoles, M., Del Valle-Perez, B., Curto, J., Vinas-Castells, R., Alba-Castellon, L., de Herreros, A., and Dunach, M. (2014). Multivesicular GSK3 Sequestration upon Wnt Signaling Is Controlled by p120-Catenin/Cadherin Interaction with LRP5/6. Molecular Cell 53, 444-457.

Vogelstein, B., Papadopoulos, N., Velculescu, V., Zhou, S., Diaz, L., and Kinzler, K. (2013). Cancer Genome Landscapes. Science 339, 1546-1558.

Wan, M., Huang, J., Jhala, N., Tytler, E., Yang, L., Vickers, S., Tang, Y., Lu, C., Wang, N., and Cao, X. (2005). SCF ss-TrCP1 controls Smad4 protein stability in pancreatic cancer cells. American Journal of Pathology 166, 1379-1392.

Wan, M., Tang, Y., Tytler, E., Lu, C., Jin, B., Vickers, S., Yang, L., Shi, X., and Cao, X. (2004). Smad4 protein stability is regulated by ubiquitin ligase SCF beta-TrCP1. Journal of Biological Chemistry 279, 14484-14487.

Warmflash, A., Zhang, Q., Sorre, B., Vonica, A., Siggia, E., and Brivanlou, A. (2012). Dynamics of TGF-beta signaling reveal adaptive and pulsatile behaviors reflected in the nuclear localization of transcription factor Smad4. Proceedings of

the National Academy of Sciences of the United States of America 109, E1947-E1956.

Watanabe, M., Masuyama, N., Fukuda, M., and Nishida, E. (2000). Regulation of intracellular dynamics of Smad4 by its leucine-rich nuclear export signal. Embo Reports 1, 176-182.

Willert, K., Brown, J., Danenberg, E., Duncan, A., Weissman, I., Reya, T., Yates, J., and Nusse, R. (2003). Wnt proteins are lipid-modified and can act as stem cell growth factors. Nature 423, 448-452.

Wilson, S., Graziano, E., Harland, R., Jessell, T., and Edlund, T. (2000). An early requirement for FGF signalling in the acquisition of neural cell fate in the chick embryo. Current Biology 10, 421-429.

Wisotzkey, R., Johnson, A., Takaesu, N., and Newfeld, S. (2003). alpha/beta hydrolase2, a predicated gene adjacent to Mad in Drosophila melanogaster, belongs to a new global multigene family and is associated with obesity. Journal of Molecular Evolution 56, 351-361.

Wrighton, K., Willis, D., Long, J., Liu, F., Lin, X., and Feng, X. (2006). Small C-terminal domain phosphatases dephosphorylate the regulatory linker regions of Smad2 and Smad3 to enhance transforming growth factor-beta signaling. Journal of Biological Chemistry 281, 38365-38375.

Wu, G., Chen, Y., Ozdamar, B., Gyuricza, C., Chong, P., Wrana, J., Massague, J., and Shi, Y. (2000). Structural basis of Smad2 recognition by the Smad anchor for receptor activation. Science 287, 92-97.

Wu, J., Fairman, R., Penry, J., and Shi, Y. (2001a). Formation of a stable heterodimer between Smad2 and Smad4. Journal of Biological Chemistry 276, 20688-20694.

Wu, J., Hu, M., Chai, J., Seoane, J., Huse, M., Li, C., Rigotti, D., Kyin, S., Muir, T., Fairman, R., et al. (2001b). Crystal structure of a phosphorylated Smad2: Recognition of phosphoserine by the MH2 domain and insights on Smad function in TGF-beta signaling. Molecular Cell 8, 1277-1289.

Xiao, Z., Latek, R., and Lodish, H. (2003). An extended bipartite nuclear localization signal in Smad4 is required for its nuclear import and transcriptional activity. Oncogene 22, 1057-1069.

Xiao, Z., Liu, X., Henis, Y., and Lodish, H. (2000). A distinct nuclear localization signal in the N terminus of Smad 3 determines its ligand-induced nuclear translocation. Proceedings of the National Academy of Sciences of the United States of America 97, 7853-7858.

Xiao, Z., Watson, N., Rodriguez, C., and Lodish, H. (2001). Nucleocytoplasmic shuttling of Smad1 conferred by its nuclear localization and nuclear export signals. Journal of Biological Chemistry 276, 39404-39410.

Xu, C., Kim, N., and Gumbiner, B. (2009). Regulation of protein stability by GSK3 mediated phosphorylation. Cell Cycle 8, 4032-4039.

Xu, J., and Attisano, L. (2000). Mutations in the tumor suppressors Smad2 and Smad4 inactivate transforming growth factor beta signaling by targeting Smads to the ubiquitin-proteasome pathway. Proceedings of the National Academy of Sciences of the United States of America 97, 4820-4825.

Xu, L., Alarcon, X., Col, S., and Massague, J. (2003). Distinct domain utilization by Smad3 and Smad4 for nucleoporin interaction and nuclear import. Journal of Biological Chemistry 278, 42569-42577.

Xu, L., Kang, Y., Col, S., and Massague, J. (2002). Smad2 nucleocytoplasmic shuttling by nucleoporins CAN/Nup214 and Nup153 feeds TGF beta signaling complexes in the cytoplasm and nucleus. Molecular Cell 10, 271-282.

Xu, L., and Massague, A. (2004). Nucleocytoplasmic shuttling of signal transducers. Nature Reviews Molecular Cell Biology 5, 209-219.

Yaffe, M., and Elia, A. (2001). Phosphoserine/threonine-binding domains. Current Opinion in Cell Biology 13, 131-138.

Yamamoto, N., Akiyama, S., Katagiri, T., Namiki, M., Kurokawa, T., and Suda, T. (1997). Smad1 and Smad5 act downstream of intracellular signalings of BMP-2 that inhibits myogenic differentiation and induces osteoblast differentiation in

C2C12 myoblasts. Biochemical and Biophysical Research Communications 238, 574-580.

Yang, L., Wang, N., Tang, Y., Cao, X., and Wan, M. (2006). Acute myelogenous leukemia-derived SMAD4 mutations target the protein ubiquitin-proteasome degradation. Human Mutation 27, 897-905.

Yost, C., Farr, G., Pierce, S., Ferkey, D., Chen, M., and Kimelman, D. (1998). GBP, an inhibitor of GSK-3, is implicated in Xenopus development and oncogenesis. Cell 93, 1031-1041.

Yu, J., Satou, Y., Holland, N., Shin-I, T., Kohara, Y., Satoh, N., Bronner-Fraser, M., and Holland, L. (2007). Axial patterning in cephalochordates and the evolution of the organizer. Nature 445, 613-617.

Zawel, L., Dai, J., Buckhaults, P., Zhou, S., Kinzler, K., Vogelstein, B., and Kern, S. (1998). Human Smad3 and Smad4 are sequence-specific transcription activators. Molecular Cell 1, 611-617.

Zeng, X., Huang, H., Tamai, K., Zhang, X., Harada, Y., Yokota, C., Almeida, K., Wang, J., Doble, B., Woodgett, J., et al. (2008a). Initiation of Wnt signaling: control of Wnt coreceptor Lrp6 phosphorylation/activation via frizzled, dishevelled and axin functions. Development 135, 367-375.

Zeng, Y., Rahnama, M., Wang, S., Lee, W., and Verheyen, E. (2008b). Inhibition of Drosophila Wg Signaling Involves Competition between Mad and Armadillo/beta-Catenin for dTcf Binding. Plos One 3.

Zeng, Y., Rahnama, M., Wang, S., Sosu-Sedzorme, W., and Verheyen, E. (2007). Drosophila Nemo antagonizes BMP signaling by phosphorylation of Mad and inhibition of its nuclear accumulation. Development 134, 2061-2071.

Zhang, Y., Chang, C., Gehling, D., Hemmati-Brivanlou, A., and Delynck, R. (2001). Regulation of Smad degradation and activity by Smurf2, an E3 ubiquitin ligase. Proceedings of the National Academy of Sciences of the United States of America 98, 974-979.

Zhang, Y., Musci, T., and Derynck, R. (1997). The tumor suppressor Smad4 DPC 4 as a central mediator of Smad function. Current Biology 7, 270-276.

Zhu, H., Kavsak, P., Abdollah, S., Wrana, J., and Thomsen, G. (1999). A SMAD ubiquitin ligase targets the BMP pathway and affects embryonic pattern formation. Nature 400, 687-693.

Zimmerman, L., DeJesus-Escobar, J., and Harland, R. (1996). The Spemann organizer signal noggin binds and inactivates bone morphogenetic protein 4. Cell 86, 599-606.